ISSN 1007-9327 (print)
ISSN 2219-2840 (online)

World Journal of *Gastroenterology*

World J Gastroenterol 2023 August 21; 29(31): 4706-4814

Published by Baishideng Publishing Group Inc

World Journal of Gastroenterology

Contents

Weekly Volume 29 Number 31 August 21, 2023

ABOUT COVER

Editorial Board Member of *World Journal of Gastroenterology*, De-Liang Fu, MD, PhD, Chief Doctor, Professor, Department of Pancreatic Surgery, Pancreatic Disease Institute, Huashan Hospital, Shanghai 200040, China. surgeonfu@163.com

AIMS AND SCOPE

The primary aim of *World Journal of Gastroenterology* (*WJG*, *World J Gastroenterol*) is to provide scholars and readers from various fields of gastroenterology and hepatology with a platform to publish high-quality basic and clinical research articles and communicate their research findings online. *WJG* mainly publishes articles reporting research results and findings obtained in the field of gastroenterology and hepatology and covering a wide range of topics including gastroenterology, hepatology, gastrointestinal endoscopy, gastrointestinal surgery, gastrointestinal oncology, and pediatric gastroenterology.

INDEXING/ABSTRACTING

The *WJG* is now abstracted and indexed in Science Citation Index Expanded (SCIE, also known as SciSearch®), Current Contents/Clinical Medicine, Journal Citation Reports, Index Medicus, MEDLINE, PubMed, PubMed Central, Scopus, Reference Citation Analysis, China National Knowledge Infrastructure, China Science and Technology Journal Database, and Superstar Journals Database. The 2023 edition of Journal Citation Reports® cites the 2022 impact factor (IF) for *WJG* as 4.3; IF without journal self cites: 4.1; 5-year IF: 5.3; Journal Citation Indicator: 0.82; Ranking: 33 among 93 journals in gastroenterology and hepatology; and Quartile category: Q2. The *WJG*'s CiteScore for 2021 is 8.3 and Scopus CiteScore rank 2022: Gastroenterology is 22/149.

RESPONSIBLE EDITORS FOR THIS ISSUE

Production Editor: *Yi-Xuan Cai*; **Production Department Director:** *Xiang Li*; **Editorial Office Director:** *Jia-Ru Fan.*

NAME OF JOURNAL
World Journal of Gastroenterology

ISSN
ISSN 1007-9327 (print) ISSN 2219-2840 (online)

LAUNCH DATE
October 1, 1995

FREQUENCY
Weekly

EDITORS-IN-CHIEF
Andrzej S Tarnawski

EDITORIAL BOARD MEMBERS
http://www.wjgnet.com/1007-9327/editorialboard.htm

PUBLICATION DATE
August 21, 2023

INSTRUCTIONS TO AUTHORS
https://www.wjgnet.com/bpg/gerinfo/204

GUIDELINES FOR ETHICS DOCUMENTS
https://www.wjgnet.com/bpg/GerInfo/287

GUIDELINES FOR NON-NATIVE SPEAKERS OF ENGLISH
https://www.wjgnet.com/bpg/gerinfo/240

PUBLICATION ETHICS
https://www.wjgnet.com/bpg/GerInfo/288

PUBLICATION MISCONDUCT
https://www.wjgnet.com/bpg/gerinfo/208

ARTICLE PROCESSING CHARGE
https://www.wjgnet.com/bpg/gerinfo/242

STEPS FOR SUBMITTING MANUSCRIPTS
https://www.wjgnet.com/bpg/GerInfo/239

ONLINE SUBMISSION
https://www.f6publishing.com

World Journal of Gastroenterology

Submit a Manuscript: https://www.f6publishing.com

World J Gastroenterol 2023 August 21; 29(31): 4706-4735

DOI: 10.3748/wjg.v29.i31.4706

ISSN 1007-9327 (print) ISSN 2219-2840 (online)

REVIEW

Dysregulated microRNAs as a biomarker for diagnosis and prognosis of hepatitis B virus-associated hepatocellular carcinoma

Ming-He Zhang, Yu-Feng Yuan, Li-Juan Liu, Yu-Xin Wei, Wan-Yue Yin, Lan-Zhuo-Yin Zheng, Ying-Ying Tang, Zhao Lv, Fan Zhu

Specialty type: Gastroenterology and hepatology

Provenance and peer review: Invited article; Externally peer reviewed.

Peer-review model: Single blind

Peer-review report's scientific quality classification

Grade A (Excellent): A
Grade B (Very good): 0
Grade C (Good): C
Grade D (Fair): D
Grade E (Poor): 0

P-Reviewer: Korkmaz P, Turkey; Oura S, Japan; Quarleri J, Argentina

Received: March 28, 2023
Peer-review started: March 28, 2023
First decision: June 17, 2023
Revised: June 29, 2023
Accepted: August 1, 2023
Article in press: August 1, 2023
Published online: August 21, 2023

Ming-He Zhang, Yu-Feng Yuan, Department of Hepatobiliary & Pancreatic Surgery, Zhongnan Hospital of Wuhan University, Wuhan 430071, Hubei Province, China

Ming-He Zhang, Li-Juan Liu, Yu-Xin Wei, Wan-Yue Yin, Lan-Zhuo-Yin Zheng, Ying-Ying Tang, Zhao Lv, Fan Zhu, State Key Laboratory of Virology, Department of Medical Microbiology, School of Basic Medical Sciences, Wuhan University, Wuhan 430071, Hubei Province, China

Yu-Xin Wei, Department of Neurosurgery, Renmin Hospital of Wuhan University, Wuhan 430060, Hubei Province, China

Lan-Zhuo-Yin Zheng, Department of Cardiology, Zhongnan Hospital of Wuhan University, Wuhan 430071, Hubei Province, China

Ying-Ying Tang, Department of Neurology, Zhongnan Hospital of Wuhan University, Wuhan 430071, Hubei Province, China

Fan Zhu, Hubei Province Key Laboratory of Allergy & Immunology, Wuhan University, Wuhan 430071, Hubei Province, China

Corresponding author: Fan Zhu, PhD, Professor, State Key Laboratory of Virology, Department of Medical Microbiology, School of Basic Medical Sciences, Wuhan University, No. 185 Donghu Road, Wuhan 430071, Hubei Province, China. fanzhu@whu.edu.cn

Abstract

Hepatocellular carcinoma (HCC) is a malignancy with a high incidence and fatality rate worldwide. Hepatitis B virus (HBV) infection is one of the most important risk factors for its occurrence and development. Early detection of HBV-associated HCC (HBV-HCC) can improve clinical decision-making and patient outcomes. Biomarkers are extremely helpful, not only for early diagnosis, but also for the development of therapeutics. MicroRNAs (miRNAs), a subset of non-coding RNAs approximately 22 nucleotides in length, have increasingly attracted scientists' attention due to their potential utility as biomarkers for cancer detection and therapy. HBV profoundly impacts the expression of miRNAs potentially involved in the development of hepatocarcinogenesis. In this review, we summarize the current progress on the role of miRNAs in the diagnosis and treatment of HBV-HCC. From a molecular standpoint, we discuss the mechanism by which HBV regulates miRNAs and investigate the exact effect of miRNAs on the promotion of HCC. In the near future, miRNA-based diagnostic, prognostic,

and therapeutic applications will make their way into the clinical routine.

Key Words: Hepatitis B virus; Hepatocellular carcinoma; MicroRNA; Diagnosis; Prognosis; Biomarker

Core Tip: Hepatocellular carcinoma (HCC) is one of the most common malignancies worldwide. Hepatitis B virus (HBV) infection is one of the predominant risk factors for developing HCC. Early diagnosis and prognosis prediction are pivotal for patients with HBV-associated HCC (HBV-HCC) in their clinical management. MicroRNAs (miRNAs), a subset of non-coding RNAs, play an essential role in human diseases including HBV-HCC. Here, we summarize the role of miRNAs in the diagnosis and prognosis prediction of patients with HBV-HCC. Furthermore, we discuss the underlying mechanism by which HBV dysregulates miRNAs, and the potential role of dysregulated miRNAs in promoting hepatocarcinogenesis, laying the foundation for applying potential therapeutic targets.

Citation: Zhang MH, Yuan YF, Liu LJ, Wei YX, Yin WY, Zheng LZY, Tang YY, Lv Z, Zhu F. Dysregulated microRNAs as a biomarker for diagnosis and prognosis of hepatitis B virus-associated hepatocellular carcinoma. *World J Gastroenterol* 2023; 29(31): 4706-4735
URL: https://www.wjgnet.com/1007-9327/full/v29/i31/4706.htm
DOI: https://dx.doi.org/10.3748/wjg.v29.i31.4706

INTRODUCTION

According to World Health Organization (WHO) reports, in 2020, primary liver cancer is the sixth most frequently occurring cancer worldwide, with mortality ranking third among all cancers. Hepatocellular carcinoma (HCC) accounted for about 75%-85% of cases. Chronic hepatitis B virus (HBV) infection is one of the major known risk factors[1]. Although the HBV-vaccination program has greatly reduced the incidence of HBV infection, it is estimated that nearly 292 million people are living with chronic hepatitis B (CHB) globally, and approximately 900000 people die annually because of HBV-induced liver cirrhosis and HCC, according to WHO estimates[2]. Liver surgery, including liver resection and liver transplantation, has become an established therapy for HCC and cirrhosis. Early diagnosis is a key factor for liver resection. Biomarkers are widely used for the early diagnosis of several cancers. But HCC biomarkers cannot be clinically useful for early HCC diagnosis due to their low sensitivity[3]. Similarly essential is the construction of prognosis of HBV-associated HCC (HBV-HCC), which can help make treatment decisions[3]. At present, circulating nucleic acid biomarkers, including microRNAs (miRNA), are identified as possible biomarkers for the diagnosis, prognosis, and therapeutics of liver diseases, especially HBV-HCC[4].

miRNA, a subset of non-coding RNAs, possess 19-25 nucleotides in length and play crucial biological roles in the process of gene silencing. Given that up to 60% of human protein-coding genes have conserved miRNA target sites, it is not surprising that dysregulated miRNAs can disrupt homeostasis and cause diseases including cancer[5]. miRNAs play a vital role in different stages of the HBV-HCC continuum, including early HBV infection, chronic inflammation, fibrosis/cirrhosis, and the emergence of HCC[6].

Although most miRNAs are located within cells, circulating miRNAs are present in body fluids and may reflect the pathophysiology of tissues. Several desirable characteristics of circulating miRNAs, such as their high stability in biological samples, non-invasive methods for sampling, and high sensitivity and accuracy, make them suitable as biomarker candidates for cancer diagnosis, prognosis, and therapeutic response prediction[7]. In this review, we summarize the application of miRNAs as diagnostic, prognostic, and therapeutic markers in HBV-HCC. We further discuss the mechanism by which HBV affects miRNA transcription and stability. We also try to understand the mechanisms by which miRNAs participate in the development of HCC. This will provide an in-depth understanding to identify promising biomarkers in HBV-HCC diagnosis, prognosis, and treatment.

DYSREGULATED MIRNAS IN THE DIAGNOSIS OF HBV-HCC

miRNAs are expressed with high tissue and cell selectivity. For example, some miRNAs, such as miR-122-5p, are particularly abundant in the liver, suggesting that certain miRNAs participate in HCC carcinogenesis and progression[8]. After tumor resection in HCC patients, some serum circulating miRNAs exhibit significant changes[9-13], indicating that circulating miRNAs may be specific non-invasive and diagnostic markers for HBV-HCC.

In clinical diagnostic tests, area under the receiver operating characteristic curve (AUC) is widely used to judge the diagnostic accuracy. Generally, an AUC between 0.7 and 0.8 is considered clinically useful, between 0.8 and 0.9 is deemed excellent, and greater than 0.9 is considered outstanding discrimination[14]. Numerous individual miRNAs have shown good diagnostic efficacy, with miR-93-5p[15], miR-122[16], miR-125b[17], miR-150[13], miR-487b[18,19], miR-768-3p[20],

and miR-5193[21] achieving AUC > 0.9 in discriminating HBV-HCC patients from healthy controls (HC) (Table 1), miR-122[22], miR-125b[23], and miR-192[22] in differentiating HBV-HCC from CHB patients (Table 2), and miR-101[24] and miR-125b[17,23] in discriminating HBV-HCC from HBV related liver cirrhosis (HBV-LC) patients (Table 2). Additionally, some HBV dysregulated miRNAs show different expression profiles in the serum or plasma of HBV-HCC patients compared to control populations[25-29], suggesting a potential value of these miRNAs in diagnosing HBV-HCC. In addition, one study reveals that urine miR-93-5p demonstrates diagnostic performance comparable to plasma miR-93-5p for diagnosing early HBV-HCC. Urine sample is non-invasive and simple to perform on humans. Therefore, urine miRNAs may have more clinical application potential than plasma miRNAs[15]. However, individual miRNAs may have limitations in sensitivity and specificity due to HBV-associated chronic liver disease. In addition, despite the fact that numerous miRNAs were highly effective at distinguishing HBV-HCC patients from healthy populations or all control populations, the efficacy used to differentiate HBV-HCC from CHB or HBV-LC is nonspecific. Hence, new methods are required to improve the diagnostic efficacy of miRNAs in diagnosing HBV-HCC patients, particularly in distinguishing them from CHB and LC populations.

Individual miRNAs are altered in different infectious diseases, nonspecific inflammation, and acute lesions in addition to cancer, revealing their lack of specificity. Forming a miRNA panel may help serve as diagnostic biomarkers for HBV-HCC (Table 3). Several miRNA panels, such as miR-21 + miR-122 + miR-192[22], miR-125b + miR-223 + miR-27a + miR-26a[30], and miR-23b + miR-423 + miR-375 + miR-23a + miR-342-3p[31] reach a high value in differentiating HBV-HCC from HC, CHB and HBV-LC patients. However, the good diagnostic efficiency of miRNA profiles does not necessitate the combination of as many miRNAs as feasible to improve diagnostic accuracy, due to the complexity of the method necessary to detect miRNAs and the lengthy timeframes involved. In some cases, the combination of multiple biomarkers showed no additive effect on HBV-HCC diagnosis[32]. Several studies demonstrate that panels with only two miRNAs can also reach a high AUC as panels with more miRNAs, such as miR-10a + miR-125b[31] and miR-15b + miR-130b[9]. Consequently, additional research is required to determine the optimal combination of the fewest possible number of miRNAs and to reduce the cost of diagnosis as much as possible, all while attaining a good diagnostic capacity.

It will be better to combine miRNAs with other biomarkers in HBV-HCC diagnosis (Table 4). The most prevalent combination biomarker is alpha fetoprotein (AFP), a traditional biomarker in HCC. Obviously, the combination of most miRNAs with AFP demonstrates a high AUC and diagnostic accuracy for discriminating HBV-HCC from HC or patients with CHB, HBV-CLD, and HBV-LC, such as miR-24-3p[33], miR-96[34], miR-101[24], miR-122[35], miR-126[32], miR-142-3p[32], miR-205[36] and miR-224[11]. Another study combines miR-122 with AFP and TERT gene promoter mutations in cfDNA. The results show that it reaches a 0.98 and 0.88 AUC in discriminating HBV-HCC patients from CHB and HBV-LC patients, respectively, demonstrating a high diagnostic value in HBV-HCC[35]. Similarly, the combination of miR-122 with AFP and prothrombin induced by vitamin K deficiency or antagonist- II (PIVKA-II) reaches a 0.918 AUC in separating HBV-HCC from HBV-LC patients[37]. Consequently, the combination of single miRNA with other biomarkers may improve the diagnostic accuracy for HBV-HCC from other HBV-related diseases. Moreover, some miRNAs panels show a better diagnostic value than AFP[38], and combination of these miRNA panels with AFP further increased the efficacy[22,30,32]. Therefore, the use of miRNA profiles paired with AFP may be the optimum modality for the diagnosis of HBV-HCC.

In addition, miRNAs may be of particular value in the diagnosis of HBV-HCC with low AFP levels. Despite the fact that AFP is the most often utilized biomarker for HCC worldwide, serum AFP levels stay normal in 15%-30% of advanced HCC. Meanwhile, approximately 30% of early-stage HCC cannot be diagnosed *via* AFP measurement, which delays therapy. Therefore, it is crucial to establish biomarkers capable of identifying HCC patients with negative AFP levels[39]. Different miRNAs and miRNA panels have shown good capacity for separating HBV-HCC patients with negative AFP expression from HC and CHB patients (Table 5), such as miR-125b[23], miR-15b + miR-130b[9] miR-21 + miR-122 + miR-192[22], and miR-125b + miR-223 + miR-27a + miR-26a[30]. A meta-analysis suggests that circulating miRNAs have a relatively high diagnostic accuracy in distinguishing HBV-HCC patients with low AFP levels from non-HCC controls[40]. Therefore, circulating miRNAs may be an ideal potential diagnostic biomarker for HBV-HCC patients with low AFP levels. Notably, these miRNAs or miRNAs panels only show ordinary effects when differentiating HBV-HCC with HBV-LC, and thus, more research is needed to improve the value of miRNA in differentiating HBV-LC and HBV-HCC patients with negative AFP expression.

Overall, miRNAs have great potential for use in the diagnosis of HBV-HCC. Two meta-analyses also show that miRNAs attain a level between moderate and high in terms of diagnostic evaluation criteria, and also demonstrate superior diagnostic performance than AFP[41,42]. According to both studies, miR-125b demonstrates a stronger diagnostic value for HBV-related HCC than other single miRNAs[41,42]. The subgroup analysis further concludes that downregulated miRNAs, miRNA panels, and serum-type miRNAs provide the most accurate diagnostic function for HBV-HCC[42]. Notably, the majority of patients with HCC are frequently diagnosed at an advanced stage, with a 1-year survival rate of less than 50% and a 5-year survival rate of only 10%[43]. This is due to the lack of accurate early diagnostic biomarkers. Several other studies also evaluate the ability of miRNAs to discriminate between early-stage HBV-HCC and controls. In one study, the combination of AFP and miR-125b, miR-223, miR-27a, and miR-26a has the highest diagnostic accuracy for early-stage HBV-HCC[30]. Another study finds that one miRNA panel consisting of seven miRNAs shows significant diagnostic accuracy for HBV-HCC, particularly in patients with early Barcelona Clinic Liver Cancer (BCLC) stages (0/A)[44]. Consequently, these miRNA profiles may serve as possible early diagnostic markers for HBV-HCC.

Notably, in addition to circulating miRNAs, exosome miRNAs may also have diagnostic and prognostic value in HBV-HCC. Exosome miRNAs are miRNAs contained within exosomes and released by various cells. Exosome miRNAs are frequently more stable in bodily fluids than other circulating miRNAs because the exosome membrane protects them from degradation, indicating a higher value as cancer biomarkers[45]. As HBV can impact the production of exosomes

Table 1 Efficacy of single microRNAs used in diagnosing hepatitis B virus-associated hepatocellular carcinoma patients from healthy control

miRNA	AUC	Sensitivity	Specificity	Ref.
miR-18a	0.881	0.861	0.750	[228]
miR-26a	0.711	0.876	0.600	[30]
miR-26a[1]	0.685	0.907	0.600	[30]
miR-26a-5p	0.762	0.689	0.744	[38]
miR-27a	0.859	0.933	0.733	[30]
miR-27a[1]	0.809	0.926	0.733	[30]
miR-34a	0.736	0.920	0.600	[21]
miR-93-5p	0.906	0.859	0.954	[15]
miR-93-5p	0.903	0.879	0.938	[15]
miR-93-5p	0.905	0.862	0.954	[15]
miR-101	0.788	0.761	0.700	[24]
miR-122	0.984	0.960	0.940	[16]
miR-122	0.869	0.816	0.833	[10]
miR-122-5p	0.697	0.489	0.822	[38]
miR-125b	0.835	0.798	0.867	[30]
miR-125b	0.891	0.859	0.786	[23]
miR-125b	0.940	0.830	0.960	[17]
miR-125b[1]	0.822	0.815	0.867	[30]
miR-141-3p	0.758	0.681	0.833	[38]
miR-143	0.813	0.776	0.860	[229]
miR-145	0.852	0.882	0.780	[229]
miR-150	0.931	0.825	0.837	[13]
miR-192-5p	0.695	0.719	0.756	[38]
miR-199a-5p	0.638	0.593	0.667	[38]
miR-205	0.885	0.969	0.679	[36]
miR-206	0.615	0.481	0.788	[38]
miR-212	0.886	0.696	0.950	[230]
miR-214	0.747	0.760	0.740	[21]
miR-223	0.736	0.921	0.633	[30]
miR-223[1]	0.822	0.907	0.633	[30]
miR-433-5p	0.736	0.793	0.644	[38]
miR-487b	0.946	0.888	0.909	[18]
miR-487b	0.929	0.839	0.928	[19]
miR-768-3p	0.908	0.873	0.800	[20]
miR-1228-5p	0.552	0.793	0.278	[38]
miR-5193	0.993	0.960	1.000	[21]
miR-6510	0.839	0.720	0.910	[21]

[1]Comparing early-stage hepatitis B virus-associated hepatocellular carcinoma patients to patients with other stages.
AUC: Area under the receiver operating characteristic curve; miRNAs: MicroRNAs.

Table 2 Efficacy of single microRNAs used in diagnosing hepatitis B virus-associated hepatocellular carcinoma patients from hepatitis B virus-positive patients

Comparison	miRNA	AUC	Sensitivity	Specificity	Ref.
HBV-carriers	miR-20a-5p	0.770	0.866	0.573	[231]
HBV-carriers	miR-25-3p	0.718	0.553	0.793	[231]
HBV-carriers	miR-30a-5p	0.681	0.642	0.683	[231]
HBV-carriers	miR-92a-3p	0.765	0.761	0.683	[231]
HBV-carriers	miR-132-3p	0.722	0.910	0.366	[231]
HBV-carriers	miR-185-5p	0.788	0.910	0.390	[231]
HBV-carriers	miR-320a	0.678	0.388	0.878	[231]
HBV-carriers	miR-324-3p	0.656	0.746	0.500	[231]
CHB	miR-26a	0.650	0.533	0.833	[30]
CHB	miR-26a[1]	0.411	0.582	0.500	[30]
CHB	miR-27a	0.761	0.677	0.833	[30]
CHB	miR-27a[1]	0.690	0.527	0.833	[30]
CHB	miR-34a	0.619	0.400	0.870	[21]
CHB	miR-96	0.803	0.779	0.753	[34]
CHB	miR-99a[2]	0.694	0.844	0.567	[232]
CHB	miR-101	0.777	0.881	0.620	[24]
CHB	miR-122	0.190	0.250	0.250	[16]
CHB	miR-122	0.630	0.776	0.578	[10]
CHB	miR-125b	0.675	0.522	0.867	[30]
CHB	miR-125b	0.958	0.938	0.857	[23]
CHB	miR-125b	0.792	0.906	0.567	[232]
CHB	miR-125b	0.800	0.810	0.870	[17]
CHB	miR-125b[1]	0.631	0.400	0.870	[30]
CHB	miR-126	0.670	0.630	0.580	[32]
CHB	miR-142-3p	0.550	0.320	0.910	[32]
CHB	miR-150	0.881	0.791	0.765	[13]
CHB	miR-214	0.520	0.850	0.430	[21]
CHB	miR-223	0.737	0.544	0.933	[30]
CHB	miR-223[1]	0.656	0.782	0.533	[30]
CHB	miR-224	0.846	0.865	0.745	[11]
CHB	miR-487b	0.815	0.836	0.667	[18]
CHB	miR-487b	0.856	0.759	0.897	[19]
CHB	miR-768-3p	0.819	0.850	0.727	[20]
CHB	miR-5193	0.817	0.798	0.820	[21]
CHB	miR-6510	0.531	0.810	0.390	[21]
HBV-DN	let-7b	0.633	0.825	0.467	[233]
HBV-DN	miR-122	0.648	0.667	0.567	[233]
HBV-LC	miR-26a-5p	0.744	0.607	0.909	[38]
HBV-LC	miR-99a[2]	0.696	0.967	0.563	[232]
HBV-LC	miR-101	0.976	0.955	0.902	[24]

HBV-LC	miR-122	0.675	0.610	0.760	[37]
HBV-LC	miR-122-5p	0.751	0.489	0.902	[38]
HBV-LC	miR-125b	0.958	0.891	0.881	[23]
HBV-LC	miR-125b	0.910	0.780	0.960	[17]
HBV-LC	miR-126	0.578	0.550	0.580	[32]
HBV-LC	miR-141-3p	0.663	0.607	0.727	[38]
HBV-LC	miR-142-3p	0.566	0.550	0.630	[32]
HBV-LC	miR-192-5p	0.687	0.548	0.833	[38]
HBV-LC	miR-199a-5p	0.589	0.593	0.576	[38]
HBV-LC	miR-205	0.781	0.969	0.542	[36]
HBV-LC	miR-206	0.693	0.778	0.689	[38]
HBV-LC	miR-224	0.832	0.865	0.667	[11]
HBV-LC	miR-433-5p	0.644	0.564	0.674	[38]
HBV-LC	miR-1228-5p	0.542	0.667	0.470	[38]
CHB + HBV-LC	miR-18a	0.775	0.772	0.700	[228]
CHB + HBV-LC	miR-224	0.840	0.865	0.711	[11]
CHB + HBV-LC	miR-375	0.768	0.938	0.639	[234]

[1]Comparing early-stage hepatitis B virus (HBV)-associated hepatocellular carcinoma (HCC) patients to patients with other stages.
[2]Comparing advanced HBV-HCC to patients with other stages.
CHB: Chronic hepatitis B patient, HBV-DN: Hepatitis B virus-related dysplastic nodule patient; HBV-LC: Hepatitis B virus-related liver cirrhosis patient; AUC: Area under the receiver operating characteristic curve; miRNAs: MicroRNAs.

and their cargos to promote HBV replication and diseases progression[46], exosomes derived from HBV-infected cells may be useful biomarkers for HBV-related diseases[47,48]. Several studies have validated and reviewed exosome-encapsulated miRNAs as circulating diagnostic markers for HCC[49,50], which may be beneficial for monitoring CHB progression and for detecting HBV-HCC at an early stage[51,52].

DYSREGULATED MIRNAS IN THE PROGNOSIS OF HBV-HCC

miRNAs, whose expression level is correlated with disease severity and survival rate in HCC patients, have shown good prognostic value for HCC[53]. For HBV-HCC patients, several miRNAs from HCC tissues or blood are found to be significantly correlated with overall survival, diseases-free survival (DFS) and progression-free survival (Table 6). For tissue miRNAs, higher expression of miR-122[54,55], miR-143[55], miR-145[56], miR-193b[57], miR-203a[58], miR-216b [59], miR-375[55,60], and miR-384[61] is associated with a better prognosis, and higher expression of miR-9-3[62], miR-10b [62], miR-21[56], miR-29a-5p[63], miR-31[62], miR-106b[64], miR-224[55], miR-371a-5p[27], miR-519c[62], miR-522[62,65], miR-523[65], miR-3188[28], miR-3682-3p[66], miR-3660[62], miR-4784[62], miR-5188[67], and miR-6883[62] is associated with a significantly poorer long-term prognosis. For circulating miRNAs, higher expression of miR-150[13], miR-223-3p [68], and miR-768-3p[20] is associated with a better prognosis, higher expression of miR-24-3p[33], miR-29a-3p[69], miR-96[34], miR-155[70], miR-192-5p[69], and miR-487b[18,19] is associated with a significantly poorer long-term prognosis. Therefore, tissues or circulating miRNAs can be a promising tool in predicting the prognosis of HBV-HCC patients. Specifically, due to the fact that miRNAs are abundant in serum exosomes, serum exosomal miRNAs can be used to predict the outcome of HCC patients. In addition, tissue miR-21[56], miR-203a[58], miR-375[60], and miR-5188[67], and serum miR-26a[30], miR-27a[30], miR-29a-3p[69], miR-125b[30], miR-150[13], miR-192-5p[69], miR-223[30,68], miR-487b [18,19], and miR-768-3p[20] are independent prognostic factors of HBV-HCC patients.

Researchers also develop different models to predict HBV-HCC survival. One study constructs a multivariate risk model that incorporates BCLC stage, miR-192-5p, and miR-29-3p. This risk model is significantly correlated with patient survival and has a good prognostic value. Consequently, the serum miRNA signature can offer predictive value for the BCLC stage classification. In addition, one random forests model made with miRNAs can predict HBV-HCC survival well[62].

It is worthy of note that miRNAs are also correlated with the probability of HBV-HCC recurrence. Several miRNAs may serve as a potential predictor for early tumor recurrence after HCC resection. For instance, the amount of miR-29a-5p in HCC tissues is strongly linked with early HCC recurrence following surgery, including in early-stage HCCs. Stages 0 and A of BCLC are regarded as the early stages, it implies that these HCC patients may have a better prognosis. However, in clinical practice, some patients still have a bad prognosis. Predicting the prognosis of these individuals is a

Table 3 Efficacy of microRNAs panels used in diagnosing hepatitis B virus-associated hepatocellular carcinoma

Comparison	miRNA	AUC	Sensitivity	Specificity	Ref.
HC	miR-125b + miR-223[1]	0.881	0.891	0.833	[30]
HC	miR-125b + miR-26a[1]	0.884	0.873	0.867	[30]
HC	miR-223 + miR-27a[1]	0.892	0.909	0.833	[30]
HC	miR-223 + miR-26a[1]	0.828	0.927	0.667	[30]
HC	miR-27a + miR-26a[1]	0.895	0.945	0.833	[30]
HC	miR-125b + miR-223 + miR-27a + miR-26a	0.932	0.865	0.933	[30]
HC	miR-125b + miR-223 + miR-27a + miR-26a[1]	0.910	0.852	0.933	[30]
HC	miR-375 + miR-25 + and let-7f	0.997	0.979	0.991	[31]
HC	miR-23b + miR-423 + miR-375 + miR-23a + miR-342-3p	0.999	0.969	0.994	[31]
HC	miR-122 + miR-192 + miR-21 + miR-223 + miR-26a + miR-27a + miR-801	0.941	0.832	0.939	[44]
HC	miR-27b-3p + miR-192-5p	0.823	0.685	0.952	[235]
HC	miR-206 + miR-141-3p + miR-433-5p + miR-1228-5p + miR-199a-5p + miR-122-5p + miR-192-5p + miR-26a-5p	0.893	0.828	0.833	[38]
HBV-carriers	miR-20a-5p + miR-25-3p + miR-30a-5p + miR-92a-3p + miR-132-3p + miR-185-5p + miR-320a + miR-324-3p	0.802	0.866	0.646	[231]
HBV-carriers	miR-20a-5p + miR-320a + miR-324-3p + miR-375	0.768	0.650	0.775	[231]
HBV-carriers	miR-20a-5p + miR-320a + miR-324-3p + miR-375	0.706	0.560	0.838	[231]
CHB	miR-125b + miR-223[1]	0.680	0.473	0.867	[30]
CHB	miR-125b + miR-26a[1]	0.668	0.509	0.833	[30]
CHB	miR-223 + miR-27a[1]	0.714	0.582	0.833	[30]
CHB	miR-223 + miR-26a[1]	0.708	0.509	0.900	[30]
CHB	miR-27a + miR-26a[1]	0.741	0.873	0.533	[30]
CHB	miR-125b + miR-223 + miR-27a + miR-26a	0.761	0.622	0.867	[30]
CHB	miR-125b + miR-223 + miR-27a + miR-26a[1]	0.687	0.818	0.533	[30]
CHB	miR-10a + miR-125b	0.992	0.985	0.985	[31]
CHB	miR-122 + miR-192 + miR-21 + miR-223 + miR-26a + miR-27a + miR-801	0.842	0.791	0.764	[44]
HBV-LC	miR-122 + miR-192 + miR-21 + miR-223 + miR-26a + miR-27a + miR-801	0.884	0.750	0.911	[44]
HBV-LC	miR-27b-3p + miR-192-5p	0.859	0.785	0.793	[235]
HBV-LC	miR-206 + miR-141-3p + miR-433-5p + miR-1228-5p + miR-199a-5p + miR-122-5p + miR-192-5p + miR-26a-5p	0.892	0.816	0.846	[38]

[1]Comparing early-stage hepatitis B virus-associated hepatocellular carcinoma patients to patients with other stages.
HC: Healthy control, CHB: Chronic hepatitis B patient; HBV-LC: Hepatitis B virus-related liver cirrhosis patient; AUC: Area under the receiver operating characteristic curve; miRNAs: MicroRNAs.

huge challenge for clinicians. As miR-29a-5p sensitivity and specificity may reach approximately 70% for HCC patients with BCLC 0/A stage, their miR-29a-5p expression level may provide a visual aid to distinguish them from other early-stage patients[63]. In addition, it has been discovered that the recurrence of HBV-HCC is closely associated with dysregulation of miR-21 and miR-145[56].

In addition, one study reveals that miRNAs are related with the development risk of HCC in CHB. In CHB patients who do not develop HCC, nucleos(t)ide analogue (NA) treatment restores expression of these miRNAs to near-normal levels, whereas the expression profile is not fully restored in individuals who ultimately develop HCC. Therefore, in CHB patients treated with NA, the changes in miRNAs expression may help identify HCC development risks[71].

MECHANISMS OF HBV-INDUCED DYSREGULATION OF MIRNA

In HCC, HBV and its proteins [HBV surface antigen (HBs), HBV core antigen (HBc), HBV envelope antigen (HBe), HBV x

Table 4 Efficacy of microRNAs combined with other biomarkers used in diagnosing hepatitis B virus-associated hepatocellular carcinoma

Comparison	miRNA	AUC	Sensitivity	Specificity	Ref.
HC	miR-125b + miR-27a + AFP[1]	0.937	0.909	0.933	[30]
HC	miR-125b + miR-223 + miR-27a + miR-26a + AFP	0.945	0.910	0.933	[30]
HC	miR-125b + miR-223 + miR-27a + miR-26a + AFP[2]	0.972	0.944	0.900	[30]
HC	miR-125b + miR-223 + miR-27a + miR-26a + AFP[1]	0.936	0.907	0.933	[30]
HC	miR-125b + miR-223 + miR-27a + miR-26a + AFP[1,2]	0.956	0.800	1.000	[30]
HBV-carriers	miR-20a-5p + miR-320a + miR-324-3p + miR-375 + AFP	0.789	0.700	0.775	[231]
HBV-carriers	miR-20a-5p + miR-320a + miR-324-3p + miR-375 + AFP	0.767	0.640	0.838	[231]
CHB	miR-96 + AFP	0.889	0.836	0.824	[34]
CHB	miR-126 + AFP	0.920	0.840	0.920	[32]
CHB	miR-142-3p + AFP	0.910	0.860	0.940	[32]
CHB	miR-224 + AFP	0.867	0.875	0.765	[11]
CHB	miR-125b + miR-27a + AFP[1]	0.722	0.600	0.833	[30]
CHB	miR-125b + miR-223 + miR-27a + miR-26a + AFP	0.790	0.689	0.867	[30]
CHB	miR-125b + miR-223 + miR-27a + miR-26a + AFP[2]	0.833	0.820	0.767	[30]
CHB	miR-125b + miR-223 + miR-27a + miR-26a + AFP[1]	0.728	0.582	0.867	[30]
CHB	miR-125b + miR-223 + miR-27a + miR-26a + AFP[1,2]	0.812	0.704	0.833	[30]
CHB	miR-126 + miR-142-3p + AFP	0.930	0.880	0.970	[32]
HBV-DN	let-7b + AFP	0.706	0.508	0.767	[233]
HBV-DN	miR-122 + AFP	0.714	0.792	0.533	[233]
HBV-LC	miR-99a + AFP	0.780	0.719	0.828	[232]
HBV-LC	miR-101 + AFP	0.973	0.966	0.879	[24]
HBV-LC	miR-122 + AFP + PIVKA-II	0.918	0.910	0.880	[37]
HBV-LC	miR-126 + AFP	0.897	0.800	0.790	[32]
HBV-LC	miR-142-3p + AFP	0.899	0.850	1.000	[32]
HBV-LC	miR-205 + AFP	0.893	0.750	0.860	[36]
HBV-LC	miR-224 + AFP	0.844	0.969	0.641	[11]
HBV-LC	miR-126 + miR-142-3p + AFP	0.939	0.850	0.840	[32]
CHB + HBV-LC	miR-224 + AFP	0.857	0.875	0.722	[11]

[1]Comparing early-stage hepatitis B virus-associated hepatocellular carcinoma patients to patients with other stages.
[2]Adjusting for gender and age differences.
HC: Healthy control; CHB: Chronic hepatitis B patient; HBV: Hepatitis B virus; HBV-DN: Hepatitis B virus-related dysplastic nodule patient; HBV-LC: Hepatitis B virus-related liver cirrhosis patient; AFP: Alpha fetoprotein; PIVKA-II: Prothrombin induced by vitamin K deficiency or antagonist- II; AUC: Area under the receiver operating characteristic curve; miRNAs: MicroRNAs.

protein (HBx), and HBV polymerase protein (HBp)] dysregulate miRNAs to promote hepatocarcinogenesis. In this part, we summarize the available studies deciphering the way in which HBV regulates the expression profiles of miRNAs through modulating miRNA processing genes and proteins and influencing transcriptional, posttranscriptional, and epigenetic mechanisms, as well as the factors affecting the regulation process, which may help to identify the novel

Table 5 Efficacy of microRNAs used in diagnosing hepatitis B virus-associated hepatocellular carcinoma with low alpha fetoprotein expression

AFP level in HBV-HCC patients	Comparison	miRNA	AUC	Sensitivity	Specificity	Ref.
< 15 ng/mL	HBV-DN	let-7b	0.645	0.848	0.500	[233]
< 15 ng/mL	HBV-DN	miR-122	0.629	0.712	0.577	[233]
< 15 ng/mL	HBV-DN	miR-122 + let-7b	0.646	0.848	0.500	[233]
≤ 20 ng/mL	CHB + HC	miR-26a	0.733	0.868	0.574	[30]
≤ 20 ng/mL	CHB + HC	miR-26a[1]	0.701	0.880	0.574	[30]
≤ 20 ng/mL	CHB + HC	miR-27a	0.832	0.838	0.723	[30]
≤ 20 ng/mL	CHB + HC	miR-27a[1]	0.771	0.800	0.723	[30]
≤ 20 ng/mL	CHB + HC	miR-125b	0.778	0.760	0.790	[30]
≤ 20 ng/mL	CHB + HC	miR-125b[1]	0.775	0.800	0.787	[30]
≤ 20 ng/mL	CHB + HC	miR-223	0.759	0.789	0.702	[30]
≤ 20 ng/mL	CHB + HC	miR-223[1]	0.715	0.720	0.723	[30]
< 20 ng/mL	CHB + HC	miR-15b + miR-130b	0.980	0.967	0.915	[9]
≤ 20 ng/mL	CHB + HC	miR-125b + miR-223 + miR-27a + and miR-26a	0.874	0.842	0.851	[30]
≤ 20 ng/mL	CHB + HC	miR-125b + miR-223 + miR-27a + miR-26a[1]	0.849	0.800	0.894	[30]
< 200 ng/mL	CHB	miR-125b	0.943	1.000	0.755	[23]
< 250 ng/mL	CHB	miR-126	0.765	0.610	0.690	[32]
< 250 ng/mL	HBV-LC	miR-126	0.643	0.610	0.580	[32]
< 400 ng/mL	HBV-LC	miR-205	0.815	1.000	0.560	[36]
20-400 ng/mL	CHB + HC	miR-15b + miR-130b	0.976	1.000	0.915	[9]
< 400 ng/mL	CHB + HBV-LC + HC	miR-122 + miR-192 + miR-21 + miR-223 + miR-26a + miR-27a + miR-801	0.879	0.777	0.845	[44]

[1]Comparing early-stage hepatitis B virus-associated hepatocellular carcinoma patients to patients with other stages.
HBV-DN: Hepatitis B virus-related dysplastic nodule patient; CHB: Chronic hepatitis B patient; HC: Healthy control; HBV: Hepatitis B virus; HCC: Hepatocellular carcinoma; HBV-LC: Hepatitis B virus-related liver cirrhosis patient; AFP: Alpha fetoprotein; AUC: Area under the receiver operating characteristic curve; miRNAs: MicroRNAs.

therapeutic pathways (Figure 1).

HBV modulates miRNA processing proteins to affect the biogenesis of miRNAs

It takes a complex process to form mature miRNAs. Firstly, miRNA genes, encoded by introns of noncoding or coding regions, are transcribed to pri-miRNAs by RNA polymerase II (Pol II) in the nucleus. Then, pri-miRNAs are spliced to pre-miRNAs by the Microprocessor complex (composed by the nuclear RNase III Drosha and DGCR8). Depending on the protein exportin 5 (EXP5), pre-miRNAs are exported to the cytosol, and are cleaved to a small RNA duplex by Dicer. The duplex is subsequently sorted and loaded onto Ago proteins, of which the guide strand is selected and preserved to form the RNA-induced silencing complex and silence gene expression[72].

There is evidence that HBV contributes to pre-miRNA production. Rather than pri-miR-18a levels, pre-miR-18a levels are associated with miR-18a elevation in HBV-HCC cases, indicating increased processing of pri- to pre-miR-18a[73]. Another study demonstrates that ectopic expression of HBx stimulates the transcription of pri-miR-1269b and hence induces the expression of pre-miR-1269b in HCC cell lines[74]. Therefore, HBV may affect miRNA expression through modulating its synthesis process.

Studies have verified a strong correlation between HBV and miRNA processing proteins. CHB patients with high HBV loads have lower mRNA and protein levels of Drosha, Dicer and Ago2 compared with patients with low viral loads[75]. In HBV-positive HCC patients, Drosha, DGCR8, Ago1, and Ago2 are significantly overexpressed[76], whereas Dicer and Ago3 are significantly downregulated in HCC tissues than that in adjacent nontumor tissues[76,77].

Table 6 Efficacy of microRNAs used to predict the prognosis of hepatitis B virus-associated hepatocellular carcinoma

Tissues/serum	miRNA panels	Risk/protective factors	Outcome	HR	CI	Ref.
Tissues	miR-9-3[a]	Risk	OS	-	-	[62]
Tissues	miR-10b[a]	Risk	OS	-	-	[62]
Tissues	miR-21[b]	Risk	DFS	3.019	0.219-6.939	[56]
Tissues	miR-29a-5p[b]	Risk	TTR	0.5	0.3-0.8	[63]
Tissues	miR-29a-5p[b]	Risk	OS	-	-	[63]
Tissues	miR-31[a]	Risk	OS	-	-	[62]
Tissues	miR-106b[a]	Risk	OS, DFS	-	-	[64]
Tissues	miR-122[a]	Protect	OS	-	-	[54]
Tissues	miR-122[b]	Protect	OS	-	-	[55]
Tissues	miR-143[b]	Protect	OS	-	-	[55]
Tissues	miR-145[a]	Protect	DFS	1.12	0.293-2.958	[56]
Tissues	miR-193b[c]	Protect	OS	-	-	[57]
Tissues	miR-203a	Protect	OS	0.63	0.41-0.97	[58]
Tissues	miR-216b[c]	Protect	OS, DFS	-	-	[59]
Tissues	miR-224[b]	Risk	OS	-	-	[55]
Tissues	miR-371a-5p[b]	Risk	OS	-	-	[27]
Tissues	miR-375	Protect	DFS	-	-	[60]
Tissues	miR-375[b]	Protect	OS	-	-	[55]
Tissues	miR-384[a]	Protect	OS	-	-	[61]
Tissues	miR-519c[a]	Risk	OS	-	-	[62]
Tissues	miR-522[a]	Risk	OS	-	-	[62]
Tissues	miR-522[b]	Risk	OS	2.19	1.33-3.6	[65]
Tissues	miR-523[b]	Risk	OS	1.5	1-2.44	[65]
Tissues	miR-3188[c]	Risk	OS, DFS	-	-	[28]
Tissues	miR-3660[a]	Risk	OS	-	-	[62]
Tissues	miR-3682-3p[c]	Risk	OS	-	-	[66]
Tissues	miR-4784[a]	Risk	OS	-	-	[62]
Tissues	miR-5188[b]	Risk	OS	-	-	[67]
Tissues	miR-6883[a]	Risk	OS	-	-	[62]
Serum	miR-24-3p[b]	Risk	OS	2.141	1.158-3.960	[33]
Serum	miR-24-3p[b]	Risk	DFS	2.055	1.114-3.792	[33]
Serum	miR-29a-3p[b]	Risk	OS	4.0	1.2-13.9	[69]
Serum	miR-29a-3p[a]	Risk	PFS	-	-	[69]
Serum	miR-96[a]	Risk	OS	-	-	[34]
Serum	miR-150[c]	Protect	OS	0.446	0.233-0.854	[13]
Serum	miR-192-5p[b]	Risk	OS	-	-	[69]
Serum	miR-192-5p[b]	Risk	PFS	2.2	1.1-4.2	[69]
Serum	miR-487b[a]	Risk	OS	2.846	1.139-7.114	[19]
Serum	miR-487b[c]	Risk	OS	2.115	1.083-4.132	[18]
Serum	miR-768-3p[b]	Protect	OS	3.057	1.136-8.225	[20]
Plasma	miR-155	Risk	OS	-	-	[70]

[a]*P* < 0.05.
[b]*P* < 0.01.
[c]*P* < 0.001.
OS: Overall survival; DFS: Disease-free survival; TTR: Time to tumor recurrence; PFS: Progression-free survival; HR: Hazard ratio; CI: Confidence interval; miRNAs: MicroRNAs.

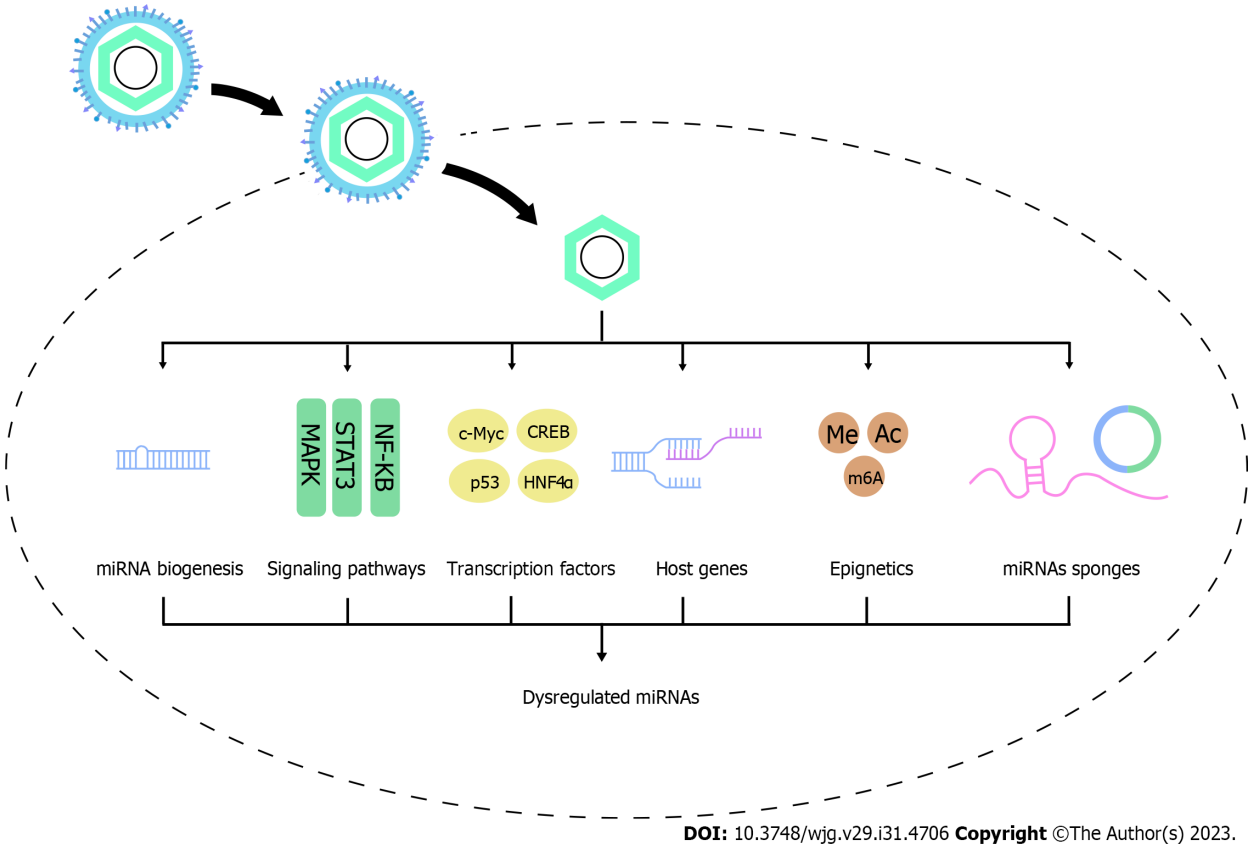

DOI: 10.3748/wjg.v29.i31.4706

Figure 1 Mechanisms of hepatitis B virus-induced dysregulation of microRNAs. miRNAs: MicroRNAs.

For Drosha protein, researchers find that HBV inhibits Drosha promoter activity to downregulate its expression. HBx are inferred to interact with SP1 and AP-2a to downregulate Drosha expression[78]. HBV can downregulate DGCR8 expression *via* suppressing its promoter activity through upregulating transcription factor YY-1, in which HBs and HBx may play a role[79]. No study has provided direct evidence that the EXP5 protein is controlled by HBV. PIN1 decreases mature miRNA expression by catalyzing EXP5's conformational change and reducing its ability to export pre-miRNAs from the nucleus to the cytoplasm[80]. It is reported that PIN1 can bind specifically to the HBx to synergistically increase cell proliferation[81], indicating that HBx interacts with PIN1 and may affect pre-miRNAs export. Upon export to the cytoplasm, pre-miRNA is cleaved by Dicer in Drosophila. MiRNAs and siRNAs share a similar step in splicing and partitioning[82]. Considering that HBx can inhibit the Dicer-mediated processing of dsRNAs into siRNAs[75], HBV may also modulate miRNA through inhibiting Dicer and Dicer-mediated splicing of pre-miRNAs. Researchers discover that Ago2 mRNA is repressed by miR-99a in Huh7 and Hep3B cells[83], whereas miR-99a is found to be up-regulated in serum of HBV patients[84], indicating that there may be an HBV/miR-99a/Ago2 regulatory axis.

Overall, there is still no evidence directly indicating that HBV affects miRNA expression by altering miRNA processing proteins. But due to the crucial role of these proteins in miRNA biogenesis, it is reasonable to infer that this is possible. It's worth noting that in a study with non-viral-associated HCC samples, DGCR8, Dicer, Ago3 and Ago4 are also significantly downregulated, in which epigenetic regulation may be implicated[77]. Therefore, the regulatory role and mechanisms of HBV on miRNA machinery components still need further investigation (Figure 2).

HBV alters signaling pathways to modulate miRNAs

Although miRNAs share a common synthesis machinery, specific miRNA is regulated by different transcriptional and posttranscriptional mechanisms. HBV generally leads to a range of aberration of signaling pathways, Sartorius *et al*[6] summarize the miRNAs that are dysregulated by HBV and are involved in regulating these signaling pathways. However, miRNAs are also regulated by these signaling pathways induced by HBV infection (Table 7).

Table 7 Dysregulated signaling pathways mediates hepatitis B virus-induced microRNAs dysregulation

Upstream signaling pathway	miRNA	HBV protein	Expression	Ref.
ERK1/2/CREB	miR-212-3p	HBe	Up	[85]
MAPK/Ap1	miR-21	HBx	Up	[87,88]
MAPK/YY1	miR-129-2	HBV	Down	[89]
MAPK/YY1	miR-203	HBV	Down	[89]
MAPK/YY1	miR-335	HBV	Down	[89]
IL-6/STAT3	miR-21	HBx	Up	[91]
STAT3	miR-328-3p	HBV, HBx, HBc	Up	[90]
STAT3	miR-34a	HBx	Down	[95]
STAT3/SALL4	miR-200c	HBV	Down	[94]
STAT3	miR-204	HBV	Down	[93]
STAT3	miR-539	HBx	Up	[92]
NF-κB	miR-23a	HBV	Up	[103]
NF-κB	miR-143	HBx	Up	[98,99]
NF-κB	miR-146a	HBx	Up	[100]
NF-κB	miR-146a-5p	HBx, HBc	Up	[97]
NF-κB	miR-1269b	HBx	Up	[74]
PI3K, NF-κB	miR-155	HBe	Up	[101]
IKKα/NF-κB	miR-7	HBx	Up	[104]
IKKα/NF-κB	miR-21	HBx	Up	[104]
IKKα/NF-κB	miR-103	HBx	Up	[104]
IKKα/NF-κB	miR-107	HBx	Up	[104]
Androgen pathway	miR-216a	HBx	Up	[111]
TLR7/NF-κB	miR-155	HBV	Down	[106]
LEF-1	miR-371a-5p	HBV	Up	[27]
PPARγ/NF-κB/p65	miR-130a	HBV	Down	[105]

HBV: Hepatitis B virus; HBe: Hepatitis B virus envelope antigen; HBx: Hepatitis B virus x protein, HBc: Hepatitis B virus core antigen; miRNAs: MicroRNAs.

MAPK pathway plays a crucial role during the innate immune response. HBeAg is able to activate ERK, one of the MAP kinases, to induce the expression of phosphorylated CREB, which is able to bind to the promoter of miR-212-3p and subsequently enhance miR-212-3p expression[85]. In addition, several AP-1 components including Fra-1, c-Jun, and JunB are found to be recruited on a miR-21 50-flanking region, thus promoting miR-21 transcription. HBx has been previously shown to activate Ap-1, which is activated predominately by MAPK signaling cascade[86]. Therefore, there is a potential HBx/MAPK/Ap1/miR-21 regulatory pathway[87,88]. Meanwhile, HBV also induces YY1 expression through MAPK signaling, and negatively regulates the expression of miR-335, miR-129-2, and miR-203[89].

STAT3 is crucial for transducing signals and regulating the expression of a wide range of genes to promote tumor progression. Studies have found that HBV, HBc and HBx but not HBs and HBp increase STAT3 phosphorylation[90], suggesting that HBV and its viral proteins underline a role in STAT3 activation. STAT3 has been proved to directly bind to several miRNAs' promotors, increase the promotors activity, and subsequently activate miRNAs transcription. STAT3 mediates upregulation of miR-21[91], miR-328-3p[90] and miR-539[92], which are dysregulated by HBV infection. However, Huang *et al*[93] found that STAT3 mediates HBV-induced miR-204 suppression. HBV also activates STAT3 to induce SALL4 expression, while SALL4 suppresses miR-200c expression through directly binding to miR-200c promoter [94]. In addition, STAT3 may mediate the suppression of miR-34a caused by HBx[95].

NF-κB is a transcription factor with broad roles in gene induction in a variety of cellular responses, particularly throughout the immune system. HBV and its proteins have been shown to increase NF-κB content and facilitate its translocation from the cytoplasm to the nucleus[74,96]. Researches show that multiple miRNAs are dysregulated by HBV through modulating NF-κB signaling. For example, HBx and HBc upregulate miR-146a-5p through activating NF-κB signaling[97]. HBx upregulates miR-143[98,99], miR-146a[100] and miR-1269b[74] by activating NF-κB binding to the

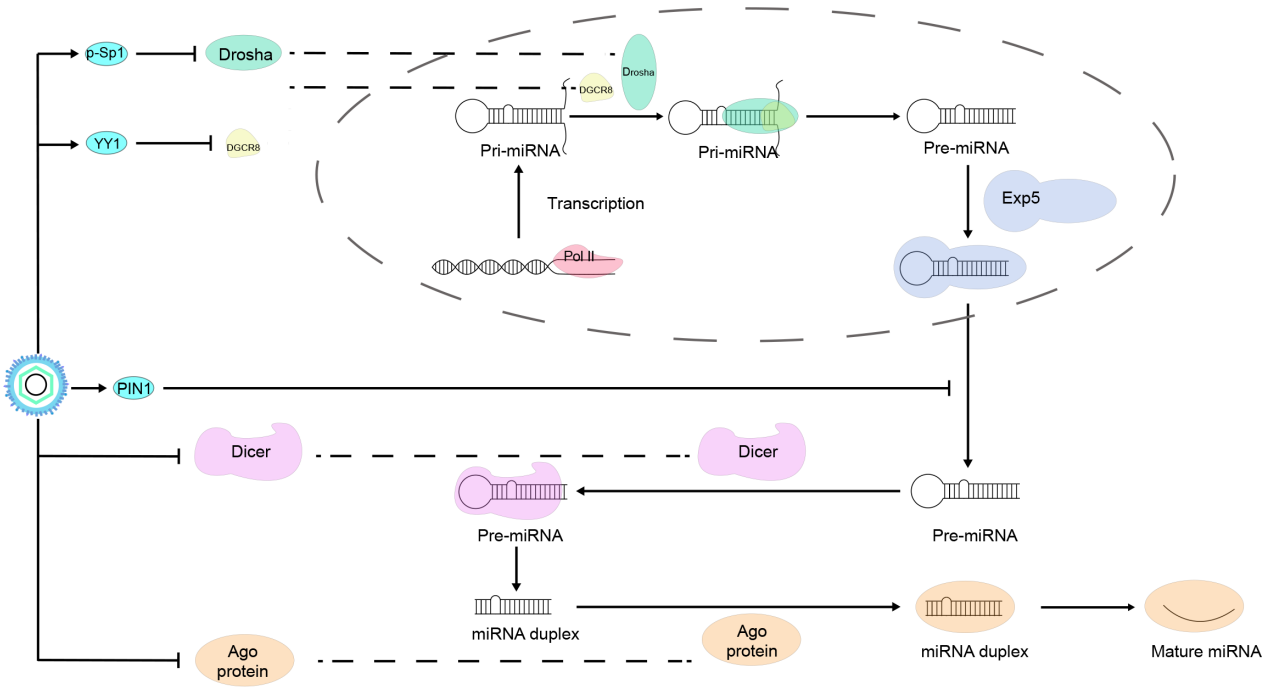

DOI: 10.3748/wjg.v29.i31.4706

Figure 2 Hepatitis B virus modulates microRNAs processing proteins to affect the biogenesis of microRNAs. miRNAs: MicroRNAs.

miRNAs promotor. Meanwhile, inhibitors of NF-κB and PI3K decrease miR-155 in HBeAg-stimulated macrophages, suggesting NF-κB and PI3K mediate HBeAg-induced miR-155 upregulation in macrophages[101]. In addition, NF-κB subunit p50 but not p65 mediates upregulation of miR-942 by LPS through binding to miR-942 promotor, and miR-942 expression is increased with progression of HBV-mediated liver fibrosis, implying a putative regulation of HBV on miR-942[102]. As a consensus p65-binding sequence (AGGGATTTCC) is located in the miR-23a promoter region, p65 dominantly represses miR-23a promoter activity, and suppresses miR-23a transcription[103]. Therefore, HBV has the potential to upregulate miR-23a by suppressing p65 expression. In addition, nuclear IKKα coordinates the transcriptional activity of NF-κB to mediate the expression of miR-7, miR-21, miR-103, and miR-107 caused by HBx[104]. Intriguingly, HBV induced PPARγ to negatively control NF-κB/p65 protein *via* ubiquitination and degradation. Repressed NF-κB/p65 then reduces the endogenous miR-130a expression[105]. The discrepancy in the NF-κB results may be due to the different HBV viral proteins.

Toll-like receptors (TLRs), the main cellular innate immune cell receptor, play crucial roles in immune responses against viral infections, including HBV. Sarkar *et al*[106] find that TLR7 expression is reduced by HBV infection, while TLR7 is able to induce miR-155 through the NF-κB pathway. Considering that HBV suppresses TLR7 and its subsequent signaling pathway including MAPK/Ap-1, NF-κB, IRF3 and IRF7[107], HBV may impact miRNAs expression through regulating TLR proteins and their signaling pathways. In addition, one study finds that HBV upregulates LEF-1, a key component of the Wnt signaling pathway, to induce miR-371a-5p expression through binding with miR-371a-5p promoter[27].

Membrane-initiated estrogen receptor (ER) and androgen receptor (AR) signaling participate significantly in physiology and disease[108]. HBx enhances AR-responsive gene expression[109], and represses ERα responsive gene transcription[110]. Therefore, HBV has the potential to regulate the miRNAs that act as AR or ERα responsive elements. HBx amplified the transcription of pri-miR-216a which is activated as a result of ligand-stimulated AR binding to the ARE site at the 5′ promoter region. However, when applied to AR-negative cells, HBx failed to stimulate an increase in pri-miR-216a[111].

HBV modulates transcription factors to regulate miRNAs

HBV protein and its RNA can modulate the expression of some transcription factors or other proteins, which in turn regulate miRNAs expression (Table 8).

HBV promotes the expression of oncogenic proteins to regulate miRNAs. c-Myc oncoprotein is a transcription factor that regulates numerous physiological processes. Chang *et al*[112] identify 13 miRNAs which are prominently repressed by c-Myc through binding to miRNA promotors. HBV can directly interact with c-Myc and stimulate its expression, thereby affecting the expression of miRNAs. For example, HBx induces c-Myc, and then c-Myc is recruited to a region of miR-192 promotor, which leads to decreased promotor activity, and subsequently downregulates miR-192-3p expression [113]. Similarly, HBx also downregulates miR-15a/16 expression[114], and suppresses let-7 family through c-Myc[115]. In addition, Jung *et al*[116] find that c-Myc mediates HBV-induced miR-17-92 overexpression. c-Myc also binds to the miR-3682-3p promoter, thus HBx may also induce miR-3682-3p expression *via* c-Myc[66]. CREB is an essential subset of phosphorylation-dependent transcription factors. HBx promotes CREB-mediated activation of miR-3188[28]. Similarly,

Table 8 Dysregulated transcription factors or upstream regulatory elements mediates hepatitis B virus-induced microRNAs dysregulation

Transcription factors or upstream regulatory elements	miRNA	HBV protein	Expression	Ref.
c-Myc	let-7	HBx	Down	[115]
c-Myc	miR-15a/16	HBx	Down	[114]
c-Myc	miR-17-92	HBV	Up	[116]
c-Myc	miR-192	HBx	Down	[113]
c-Myc	miR-3682-3p	HBx	Up	[66]
CREB1	miR-520c-3p	HBx	Up	[117]
CREB	miR-3188	HBx	Up	[28]
Survivin, Sp1	miR-520b	HBx	Up	[118]
FOXO3	miR-30b-5p	HBp	Up	[119]
URG11	miR-148a	HBx	Up	[126]
JNK/c-Jun	miR-199a-3p	HBx	Up	[120]
p53	miR-216b	HBx	Down	[59]
p53	miR-148a	HBx	Down	[122]
Hnf4α	miR-122	HBV	Down	[123]
Hnf4α	miR-548p	HBx	Down	[124]
DDX3	miR-34	HBx	Down	[127]

HBV: Hepatitis B virus; HBx: Hepatitis B virus x protein; HBp: Hepatitis B virus polymerase protein; miRNAs: MicroRNAs.

HBx promotes miR-520c transcription through CREB1[117]. Meanwhile, HBx, survivin and Sp1 form a complex in the promotor of miR-520b, and the interaction between HBx and survivin or Sp1 is indispensable for the regulation of miR-520b[118]. FOXO3 is a transcriptional factor that promotes oncogenesis, HBp can promote the expression of miR-30b-5p through its interaction with FOXO3[119]. Moreover, HBx and TGF-1 induce JNK-dependent activation of c-Jun, which is then recruited to the miR-199a-3p promoter to stimulate its transcription[120].

HBV inhibits the expression of tumor suppressor proteins to regulate miRNAs. Acting as an important tumor suppressor gene, TP53 is the most frequently mutated gene in HBV-related HCC[121]. HBx can decrease the recruitment of p53 to the miR-216b promoter, and then inhibit miR-216b transcription[59]. Another research indicates that HBx can also repress miR-148a *via* suppressing p53-mediated activation[122]. Hepatocyte nuclear factor 4α (Hnf4α), a liver-enriched transcription factor that activates miR-122 gene transcription by binding to its promotor, is found to be repressed by HBV infection in both mRNA and protein levels[123]. Similarly, Hnf4α mediates HBx induced downregulation of miR-548p, possibly through direct binding to the miR-548p promoter[124].

In addition to these transcription factors, HBV also regulates some other proteins to affect miRNAs expression. URG4/URGCP, up-regulated by HBx, can up-regulate 77 miRNAs and down-regulate 9 miRNAs in HepG2 cells[125]. Yuan *et al* [126] find that HBx-induced miR-148a is dependent on oncogenic URG11. HBx also downregulates DDX3, which upregulates miR-34 expression[127]. Meanwhile, one study also identifies 75 miRNAs by ChIP-Seq whose promotor regions are putatively targeted by HBx protein, some of which have been implicated in hepatocarcinogenesis[128].

HBV affects production of miRNAs from their host genes

As the majority of miRNA genes are encoded in the introns of either noncoding or coding regions, multiple studies have demonstrated that only one-third of intronic miRNAs are transcribed from their own promoters. The coregulation of intronic miRNAs with their host genes can be further illustrated by their tissue- or disease-specific co-expression patterns [129].

Some miRNAs are derived from lncRNA precursors, which have the potential to be affected by HBV. LncRNA H19 has been proved to harbor a miRNA containing hairpin in its exon 1, which serves as the precursor for miRNA-675[130]. HBx upregulates H19 expression, leading to a corresponding increase of miR-675[131,132]. Therefore, HBV may affect the LncRNA-derived miRNAs. However, HBx can positively regulate miR-545/374a cluster in the Ftx lncRNA, but fails to regulate miR-421/374b cluster which is also encoded in Ftx introns. Even though miR-374a and miR-545 are transcribed off the same promoter, their abundances are not always correlated[12].

In addition, intronic miRNAs may be coupled with their host genes. miR-26b gene resides in an intron of CTDSP1. They share the same transcription start sites (TSS). miR-26b is therefore transcribed as part of its host transcription unit [133,134]. HBV downregulates miR-26b expression, partly because of the suppression of CTDSP1 mRNA transcription. Notably, the extent of the decrease in miR-26b level was greater than that of CTDSP1 mRNA, implying the other putative

regulatory pathway[135]. Similarly, HBx promotes miR-106b, miR-93, and miR-25 transcription in HCC cells, whose host gene MCM7 is also co-transcribed and upregulated, suggesting that MCM7 activation may be involved in the regulation of these miRNAs by HBV[64].

Notably, despite the fact that some miRNA genes share the promoter of their host gene, the vast majority of miRNA genes have multiple TSS, and the promoters of intronic miRNAs are sometimes distinct from the promoters of their host genes.

HBV participants in epigenetic regulation of miRNAs

Epigenetic mechanisms mainly include DNA methylation, posttranslational histone modifications, chromatin remodeling, ncRNA interactions and RNA modification. Despite the significant involvement of miRNAs in epigenetic regulation, miRNAs are also regulated by epigenetic modifications and involved in diverse human diseases[136]. HBV can regulate epigenetics of miRNAs, leading to the functional disruption of miRNAs and consequently promoting HCC.

HBx has been found to increase the DNA methyltransferase (DNMT) activities and promote regional hypermethylation of specific tumor suppressor genes (TSG)[137]. It has been elucidated that HBx induces DNA hypermethylation of CpG islands in miR-18b[138], miR-30e[139], miR-132[140], and miR-205 promoter[141] to affect their expression. Shang *et al*[89] identify that miR-335, miR-129-2, and miR-203 are repressed by HBV, but are significantly activated by 5-azacytidine, the DNMT inhibitor, indicating that HBV regulates these miRNAs through DNMT-mediated methylation. Meanwhile, Tsang *et al*[142] find that knockdown of HBV-upregulated YY1[89] significantly decreases DNA methylation levels in the miR-9 Loci, leading to an increased miR-9 in HCC cells. Thus, YY1 may mediate the suppression of miRNAs caused by HBV through inducing DNA methylation. Conversely, although HBx leads to overall hypomethylation, HBx highly interferes methylation levels of -550 CpG site in the miR-125a promoter, and therefore triggers miR-125 expression[143]. Further study is needed to elaborate this phenomenon.

As for the histone modification, Guerrieri *et al*[128] verify that HBx decreases H4 acetylation level in the promoter regions of miR-138-2, miR-224, miR-302e, miR-576-3p and miR-596, which may explain their downregulation. Conversely, HBx increases H4 acetylation at the miR-26b promoter. These imply HBx ability to regulate miRNAs by modulating the histone modification of miRNAs promotors[128]. In addition, H3K27me3 is an epigenetic modification to the DNA packaging protein Histone H3[144]. The genomic regions enriched for H3K27me3 can function as silencers to repress gene expression *via* chromatin interactions[145]. Knockdown of HBV-upregulated YY1 reduced not only global H3K27me3 levels, but also EZH2 and H3K27me3 promoter occupancy, leading to the increased miR-9 in HCC cells. It is also found that HBV-upregulated YY1 Leads to EZH2 recruitment for H3K27me3-mediated silencing of tumor-suppressing miRNAs[142], supporting the idea that HBV may indirectly regulate miRNAs through impacting H3K27me3 Levels mediated by EZH2 and YY1.

PPARγ, a ligand-activated transcription factor, is able to form a heterodimer with RXRα. The complex binds to DR1 and DR2 motifs in the miR-122 gene promoter to enhance miR-122 gene transcription, which will be amplified by 5-Aza-CdR (DNA methylation inhibitor) and PBA (histone deacetylation inhibitor). However, this positive regulation is abrogated by HBx which suppresses PPARγ-mediated transactivation through binding to the PPARγ DNA binding domain[146], indicating HBx may affect miR-122 epigenetics through binding and inhibiting PPARγ.

N6methyladenosine (m6A) modification is the most widespread post-transcriptional modification in mammalian mRNAs. MiRNAs can control the expression of m6A regulator, but they are also frequently modified with m6A[147]. HBV infection enhances the expression of METTL3, promotes miR-146a-5p maturation in an m6A-dependent manner [148]. In addition, Gld2 is a cytoplasmic non-canonical poly(A) RNA polymerase that adds successive AMP monomers to the 3'-end of specific RNAs. It can directly monoadenylate specific miRNAs, including miR-122, to stabilize and prolong the activity of miRNAs[149]. HBx also downregulates Gld2 expression, decreasing miR-122 3’ monoadenylation and ultimately suppressing mature miR-122 expression[150].

A variety of endogenous RNAs are able to bind to miRNAs to reduce the number of free miRNAs. These competitive endogenous RNAs (ceRNAs) mainly include lncRNAs and circRNAs, showing an increasing significance in multiple diseases[151]. HBV has been shown to regulate miRNAs through lncRNAs or circRNAs (Table 9). HBV-induced lncRNA-Unigene56159 directly targets miR-140-5p and suppresses its expression[152]. HBV infection also elevates lncRNA PCNAP1 to target miR-154[153]. HBV also enhances LncRNA n335586 to competitively bind with miR-924[154]. Meanwhile, HBx is found to stimulate lncRNA H19 to directly target to miR-138[131] and miR-22[155] through endogenous competition. HBx upregulates TRERNA1, which functions as a ceRNA sponge for miR-22-3p[156]. Additionally, HBx upregulates lncRNA MALAT1 and downregulates miR-124 expression. Further study indicates that MALAT1 directly binds to miR-124[157]. HBx also upregulates HMMR-AS1 and downregulates miR-627-3p expression. And HMMR-AS1 directly targets miR-627-3p[158]. Conversely, HBx inhibits LINC01352, which functions as a tumor suppressor by sponging miR-135b, through binding to the site where ERα binds[159]. HBx also downregulates lncRNA F11-AS1 expression and elevates expression of miR-211-5p, while lncRNA F11-AS1 is capable of binding to miR-211-5p [160]. In HBV-positive HCC cells, LncRNA XIST[161], LINC01232[162] are markedly increased and TFAP2A-AS1[163] are significantly decreased. Further studies show that XIST targets miR-192[161], LINC01232 targets miR-708-5p[162] and TFAP2A-AS1 targets miR-933[163] in HCC, suggesting HBV may dysregulate these miRNAs through lncRNAs. Similarly, HBV may downregulate LINC00924 expression, while LINC00924 interacts with miR-6755-5p, suggesting a potential HBV/ LINC00924/ miR-6755-5p regulatory axis[164]. HBx also promotes the progression of HCC through translocation and secretion of HMGB1, as a sponge to competitively bind the miR-200 family, *via* calcium dependent cascades[165,166]. Therefore, HBx may affect miR-200 expression through HMGB1.

HBV also regulates circRNAs to affect miRNAs (Table 9). HBx upregulates METTL3 expression to increase the m6A modification of circ-ARL3, and further favors circ-ARL3 reverse splicing and biogenesis. circ-ARL3 binds to miR-1305, antagonizing the inhibitory effects of miR-1305 on target oncogenes[167]. HBV also upregulated Circ-RNF13, as a sponge

Table 9 MicroRNAs sponges dysregulated by hepatitis B virus to induce microRNAs dysregulation

	miRNAs sponges	miRNA	Expression	Ref.
LncRNA	LncRNA Unigene56159	miR-140-5p	Down	[152]
	LncRNA PCNAP1	miR-154	Down	[153]
	LncRNA n335586	miR-924	Down	[154]
	LncRNA H19	miR-138	Down	[131]
	LncRNA H19	miR-22	Down	[155]
	LncRNA TRERNA1	miR-22-3p	Down	[156]
	LncRNA MALAT1	miR-124	Down	[157]
	LncRNA HMMR-AS1	miR-627-3p	Down	[158]
	LncRNA LINC01352	miR-135b	Up	[159]
	LncRNA F11-AS1	miR-211-5p	Up	[160]
	LncRNA XIST	miR-192	Down	[161]
	LncRNA LINC01232	miR-708-5p	Down	[162]
	LncRNA TFAP2A-AS1	miR-933	Up	[163]
	LncRNA LINC00924	miR-6755-5p	Up	[164]
	LncRNA HMGB1	miR-200	Down	[165,166]
CircRNA	CircRNA ARL3	miR-1305	Down	[167]
	CircRNA RNF13	miR-424-5p	Down	[168]
	CircRNA BACH1	miR-200a-3p	Down	[169]
	CircRNA ATP5H	miR-138-5p	Down	[170]
	CircRNA 0027089	miR-136-5p	Down	[171]
HBV mRNAs	HBx mRNA	miR-15a/miR-16-1	Down	[172]
	HBV mRNAs	miR-15a/miR-16	Down	[173]
	HBV mRNAs	miR-122	Down	[174]
	HBV mRNAs	let-7a	Down	[175]
	HBs mRNA	let-7g	Down	[176]
	HBx mRNA	miR-129-5p	Down	[177]
	HBx-LINE1	miR-122	Down	[179]

HBV: Hepatitis B virus; HBx: Hepatitis B virus x protein; HBs: Hepatitis B virus surface protein; miRNAs: MicroRNAs.

for miR-424-5p[168]. HBV upregulates Circ-BACH1, which sponges miR-200a-3p to reduce its expression[169]. Meanwhile, HBV upregulates Circ-ATP5H expression, while Circ-ATP5H directly targets miR-138-5p[170]. In HBV-positive HCC cells compared to HBV-negative HCC cells, circ_0027089 is markedly increased and specifically binds to miR-136-5p[171].

HBV sponges miRNAs to inhibits miRNAs' function

In addition to the lncRNAs and circRNAs, ceRNAs also include viral RNAs and host mRNAs[151]. HBV RNA could function as sponges to directly bind with miRNAs. Studies have implicated that HBV RNA may dysregulate miRNAs by binding to the complementary binding sites of miRNAs and depletion of miRNAs (Table 9).

HBV mRNAs, including pre-C/C (pgRNA), pre-S, S 3'-UTR, and X mRNAs, act as sponges to bind and sequester miR-15a/16-1, subsequently resulting in a depletion of miR-15a/16-1[172,173]. Li *et al*[174] validate that HBV mRNAs (pre-C/C (or pgRNA), pre-S, S 3'-UTR, and X mRNAs) can sponge miR-122 to inhibit its expression and function. Deng *et al*[175] identify that there is a let-7a complementary region in the HBV genome in HBV pre-C/C, pre-S, and S mRNAs. Notably, HBV regulates downstream targets of let-7a in a sequence-dependent manner. In addition, HBV transcripts harboring the preS2 region, such as HBV large S mRNA, can almost entirely interact with let-7g and subsequently promote HCC[176]. Ochi *et al*[177] find that HBx mRNA has complementary sequences with the central region of miR-129-5p, HBx mRNA interacts with the responsive element in the 3' UTR of miR-129-5p and sequesters it from forming a complex with Ago2. It is noted that the abundances of viral RNAs may affect their regulation on miRNAs. Although HCV 5'UTR may be able to

bind miR-122, it fails to change miR-122 expression like HBV mRNAs do. This discrepancy may be due to the fact that HCV mRNAs copy numbers are much less than miR-122, while HBV mRNAs copy numbers are more than miR-122[174]. Besides, HBV RNA copies per cell are much higher than those of let-7a[175], which may be essential for HBV RNA sequestration.

Of note, HBV genome gene is frequently inserted to host genes, which may lead to the transcription of the integrated virus-human chimeric fusion. It is exemplified by the discovery of a novel chimeric HBx-LINE1 RNA, which is generated from a normally silenced region of chromosome 8p11.21 after HBV integration[178]. Functioning as a long noncoding RNA (lncRNA)-like transcript, HBx-LINE1 sequesters cellular miR-122 by directly absorbing it, which ultimately leads to the depletion of miR-122[178,179].

HBV affects miRNAs through autophagy

Autophagy is the major intracellular degradation system and plays a pivotal role in multiple physiological processes [180], some of which have been delineated to function through modulating specific miRNAs. Majority of existing works have shown that HBV is able to induce autophagy. However, Lan *et al*[181] find that HBx transgenesis leads to a lower autophagic level, and miR-224 is preferentially recruited and degraded through autophagic progression. In addition, the selective autophagy receptor NDP52 targets Dicer and Ago2 proteins for the degradation. Autophagy is required for miRNA homeostasis and activity. Moreover, autophagy participates in the posttranscriptional regulation of Dicer mRNA, and chronic autophagy deficits impair miRNA stability after pre-miRNA processing[182]. Therefore, HBV has the potential to affect autophagy to disrupt the homeostasis of miRNAs biogenesis.

C-terminal truncated HBx and HBV integration may affect the ability of HBV in inducing dysregulation of miRNA

Carboxyl-terminal truncated HBx proteins (Ct-HBx, also called HBxΔC or trHBx) are variants transcribed from the mutant HBV X gene whose 3′-end are deleted during HBV genome integration into the host cells. Ct-HBx plays a pivotal role in hepatocarcinogenesis[183,184]. Ct-HBx regulates specific miRNAs more effectively than full-length HBx (HBx-FL). For instance, HBx-D35 enhances miR-21 promoter occupancy and upregulates miR-21 expression compared to HBx-FL [91]. HBxD127 also remarkably increases miR-215 expression relative to HBx[185]. A possible explanation is that C-terminal truncation may affect the binding of HBx to cellular proteins, resulting in altered miRNA gene expression patterns in cells[184]. Notably, Ct-HBx directly binds to some miRNAs promotors, such as miR-26a and miR-29c, resulting in direct transcriptional suppression which HBx-FL is unable to induce. The reason for this discrepancy may be that HBx-FL and Ct-HBx bind to different chromatin binding regions of miRNAs[186]. However, not all miRNAs are under this regulation. miR-23a and miR-27a are concordantly regulated by both HBx-FL and Ct-HBx, and their binding regions are similar[186]. For miR-146a, Ct-HBx does not lead to the same elevation as HBx-FL does[187].

HBV pre-S2 mutant protein may also play a role in the dysregulation of miRNA. HBV pre-S2 mutant induces endoplasmic reticulum stress and the mTOR signal cascade in transgenic livers and HCC tissues[188,189]. Meanwhile, Mdm^2-dependent ubiquitinoylation of Drosha by mTOR activates miRNA synthesis and controls many cancer-related miRNAs[190]. Since PreS/S proteins initiate a cascade of events that lead to malignancy[189], it's worth to investigate whether PreS mutant dysregulates miRNAs.

Considering HBV integration severely disrupts host cellular gene expression, genomic loci containing miRNA sequences inserted by HBV may impact miRNA expression. It has been found that HBV DNA integration into fragile sites may alter the expression of a couple of miRNAs which are located in or near fragile sites, including miR-200a near FRA1A, miR-143, miR-145 and miR-224 near FRA5C, miRNA-17–92 cluster near FRA13D, miR-195 near FRA17A, miR-99b, miR-125a and let-7e near FRA19A, and miR-199a-1 near FRA19B[191-193]. These miRNAs have been documented in HCC[191], and there are still a great many miRNAs that are potentially dysregulated by HBV integration[192].

In addition, Yang *et al*[194] also find miR-602 is upregulated by HBV or HBx, and they speculate that the chromosome 9q34.3 containing miR-602 sequence is commonly integrated by HBV, which may lead to increased miR-602 expression. Similarly, Guo *et al*[195] speculate that HBV-induced chromosome instability caused by HBV integration may play a role in promoting the miRNAs-371-3 gene cluster expression. Further study is needed to support this hypothesis. Therefore, HBV DNA integration may alter miRNA expression, but the underlying mechanism requires additional study.

MECHANISMS OF HBV DYSREGULATED MIRNAS IN PROMOTING HCC

By dysregulating miRNAs, HBV exacerbates its function in the oncogenesis of HCC. Currently, multiple reviews have summarized the essential role of HBV-dysregulated miRNAs in affecting tumor cell cycle, cell proliferation, cell apoptosis, cell migration and invasion, and epithelial-mesenchymal transition (EMT)[6,196-199]. Therefore, we provided an updated supplementary list of miRNAs dysregulated by HBV and involved in these processes (Supplementary Tables 1 and 2), which will not be elaborated here. In this section, we discuss the role of HBV-dysregulated miRNAs in the tumor stemness, metabolic reprogramming, anti-tumor immunity, and tumor drug resistance of HCC, which may shed light on potential treatment approaches (Table 10 and Figure 3).

Dysregulated miRNAs promote tumor stemness

Liver cancer stem cells (CSCs) are a distinct population of HCC cells with stem cell characteristics, defining a hierarchical structure and contributing to treatment resistance and tumor recurrence. HBV is one of the most prominent players in liver CSCs. miRNAs partially mediate the stemness progression[200] (Table 11).

Table 10 Functions of hepatitis B virus-dysregulated microRNAs in promoting hepatocellular carcinoma

miRNA	HBV protein	Expression	Target genes	Abnormal function in HBV-HCC	Ref.
miR-7	HBV, HBx	Up	Mapsin	Conferring HBx-mediated anoikis resistance and doxorubicin resistance	[213]
miR-15a/16	HBV mRNA	Down	-	Inducing etoposide-induced apoptosis	[173]
miR-21	HBV, HBx	Up	Mapsin	Conferring HBx-mediated anoikis resistance and doxorubicin resistance	[213]
miR-23a	HBV	Down	CCL22	Inhibiting Tregs recruitment	[103]
miR-30b-5p	HBp	Up	MINPP1	Promoting tumor growth, enhancing cell proliferation, promoting cell migration and invasion, regulating glycolytic bypass metabolism	[119]
miR-34a	HBV	Down	CCL22	Inhibiting Tregs recruitment	[209]
miR-103	HBV, HBx	Up	Mapsin	Conferring HBx-mediated anoikis resistance and doxorubicin resistance	[213]
miR-107	HBV, HBx	Up	Mapsin	Conferring HBx-mediated anoikis resistance and doxorubicin resistance	[213]
miR-124	HBx	Down	PI3K/Akt	Suppressing CSC differentiation	[157]
miR-135a-5p	HBc	Up	VAMP2	Preventing Doxorubicin hydrochloride-induced apoptosis	[212]
miR-138	HBV	Down	PD-1	Regulating cytokine secretion of T cells and improving T-cell immune responses	[208]
miR-146a	HBV	Up	STAT1	Suppressing IFN-induced anti-HBV effect	[187]
miR-152	HBV	Down	HLA-G	Enhanced NK cytolysis against hepatoma cells	[210]
miR-193b	HBV	Down	Mcl-1	Sensitizing sorafenib-induced apoptosis	[57]
miR-200a/200b/429	HBx	Down	RICTOR	Impairing HCC stem cell properties, regulating glutamine metabolism, sensitizing the response to anti-PD-L1 immuno-therapy	[165, 166]
miR-203a	HBs	Down	BMI1	Sensitizing 5-FU-induced apoptosis, impairing HCC stem cell properties	[58]
miR-205	HBx	Down	ACSL1	May promote lipogenesis	[141] [206]
miR-325-3p	HBV	Down	DPAGT1	Sensitizing the response to Doxorubicin chemotherapy	[201, 202]
miR-329	HBV, HBx	Down	AFP	Sensitizing chemotherapy induced apoptosis	[214]
miR-384	HBV, HBx	Down	PTN/PI3K/AKT/mTORC1	Inhibiting high glucose-induced lipogenesis	[61]
miR-429	HBx	Down	Rab18	Inhibiting dysregulation of lipogenesis	[205]
miR-1236	HBV, HBx	Down	AFP	Sensitizing chemotherapy induced apoptosis	[214]
miR-3682-3p	HBx	Up	FOXO3/PI3K/AKT1/β-catenin/c-Myc	Promoting HCC stemness	[66]
miR-5188	HBx	Up	FOXO1/β-catenin	Resisting the effects of chemotherapy 5-FU, CDDP and EPI, promoting HCC stemness	[67]

HBV: Hepatitis B virus; HBx: Hepatitis B virus x protein; HBp: Hepatitis B virus polymerase protein; HBc: Hepatitis B virus core antigen; HBs: Hepatitis B virus surface antigen; HCC: Hepatocellular carcinoma; miRNAs: MicroRNAs.

In HCC cells, the expression of CD44, CD133, and EpCAM is markedly reduced by miR-124, indicating the pivotal effects of miR-124 in suppressing CSCs differentiation. HBx downregulates miR-124, and may therefore interfere CSCs differentiation[157]. In one research, HBx supports the progression of HCC *via* translocation and secretion of HMGB1, which regulates RICTOR expression in HCC by competitively binding to the miR-200 family[166]. Both HMGB1 and RICTOR mRNAs can augment HCC stemness characteristics in HCC[165]. HBsAg inhibits the expression of miR-203a in HCC cells. miR-203a decreases the proportion of CD133-positive HCC cells but not CD90, and it also significantly lowers

Table 11 Hepatitis B virus-dysregulated microRNAs that play different roles in hepatitis B virus-associated hepatocellular carcinoma

Process	HBV-dysregulated miRNAs
Tumor stemness	miR-124[157], miR-200a/200b/429[165], miR-203[58], miR-325-3p[201], miR-3682-3p[66], miR-5188[67]
Metabolic reprogramming	miR-30b-5p[119], miR-200[165], miR-205[141,206], miR-384[61], miR-429[205]
Anti-tumor immunity	miR-23a[103], miR-34a[209], miR-138[208], miR-146a[187], miR-152[210], miR-200[165,166]
Drug resistance	miR-7[213], miR-21[213], miR-103[213], miR-107[213], miR-135a-5p[212], miR-5188[67], miR-15a/16[173], miR-193b[57], miR-203a[58], miR-325-3p[201,202], miR-329[214], miR-1236[214]

HBV: Hepatitis B virus; miRNAs: MicroRNAs.

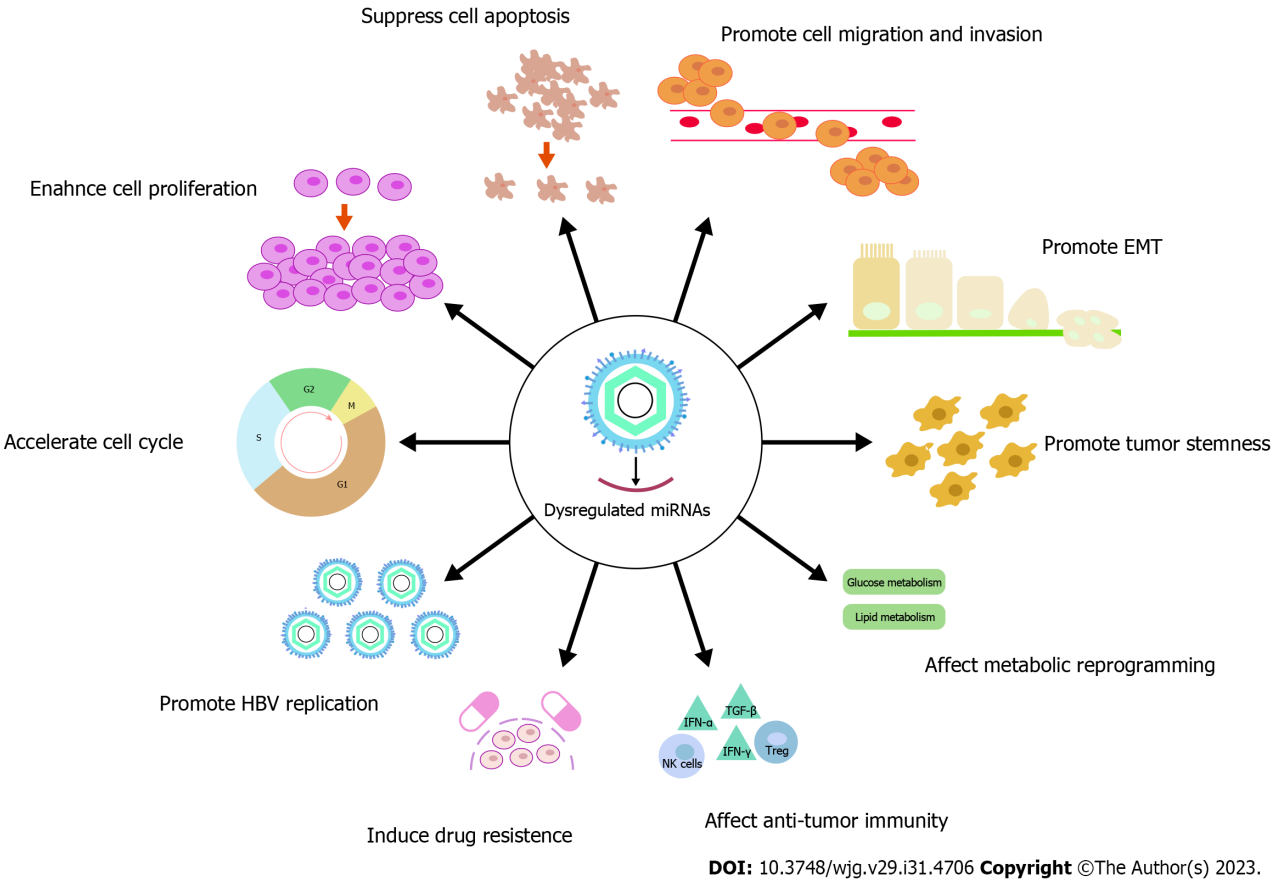

Figure 3 Mechanisms of hepatitis B virus dysregulated microRNAs in promoting hepatocellular carcinoma. miRNAs: MicroRNAs; HBV: Hepatitis B virus; EMT: Epithelial-mesenchymal transition.

the average percentage of ALDH-positive malignant stem cells. Therefore, HBV infection may promote the stemness of HCC *via* regulating miR-203a[58]. HBV also inhibits miR-325-3p[201], which suppresses the expression of critical stemness markers, including SOX-2, Nestin, Notch-1, OCT4, and Nanog. miR-325-3p/DPAGT1 may presumably have a role in HBV-induced HCC stemness[202]. In addition, miR-3682-3p mediates the oncogenic consequences of HBx-induced PI3K/AKT/c-Myc signaling. HBx increases stemness by elevating miR-3682-3p expression[66]. Meanwhile, miR-5188 directly targets FOXO1, which inhibits the nuclear translocation of β-catenin and promotes Wnt signaling activation and downstream tumor stemness. HBx modulates the miR-5188/FOXO1/β-catenin/c-Jun feedback loop to drive Wnt/β-catenin activation, subsequently promoting HCC stemness[67].

Dysregulated miRNAs affect metabolic reprogramming

Metabolic reprogramming plays a crucial role in the initiation and progression of cancer. A few studies have revealed that HBV affects the process of HCC by regulating metabolism (Table 11). Aerobic glycolysis is a distinguishing feature of HCC and is responsible for regulating proliferation, immune evasion, invasion, metastasis, and drug resistance in HCC [203]. The miR-30b-5p/MINPP1 axis is capable of accelerating the conversion of glucose to lactate and 2,3-bisphosphoglycerate (2,3-BPG), as well as regulating the glycolytic bypass to generate more 2-PG for energy supplementation. HBV

protein P (HBp) regulates the miR-30b-5p/MINPP1 axis, contributing to the development of HBV-positive HCC cells *via* glycolytic bypass[119]. RICTOR regulates glutamine metabolism *via* mTOR signaling[165]. HBx stimulates the translocation and secretion of HMGB1[166], which regulates RICTOR expression in HCC by binding competitively to the miR-200 family. Therefore, HBx may affect miR-200 to dysregulate glutamine metabolism. As for lipid metabolism, changes in fatty acid synthesis, β-oxidation, and cellular lipidic composition contribute to hepatocarcinogenesis[204]. HBx inhibits miR-384 and upregulates its target PTN expression, while PTN promotes hepatoma cell lipogenesis[61]. Knockdown of Rab18b decreases the lipogenesis. HBx activates Rab18 through downregulating miR-429. Therefore, HBx could enhance hepatocarcinogenesis by leading to the dysregulation of lipogenesis *via* the miR-429/Rab18 axis[205]. Meanwhile, HBx inhibits miR-205 expression[141], and miR-205 inhibits lipogenesis in hepatoma cells dependent on ACSL1, suggesting that HBx inhibits miR-205 to promote lipogenesis[206].

Dysregulated miRNAs affect anti-tumor immunity

It is widely acknowledged that HBV causes chronic liver damage through aberrant immunological reactions. During chronic HBV infection in humans, adaptive immunity transitions may be immune pathogenic factors for the development of HCC[207]. A number of research have revealed the function of miRNAs in HBV-induced immunological dysregulation (Table 11). HBV infection increases the expression of miR-146a, which impairs the IFN-induced anti-HBV immune response. Additionally, inhibition of miR-146a improves IFN-α-mediated anti-HBV efficacy[187]. In HBV-HCC patients, miR-138 is significantly higher than in asymptomatic carriers. By targeting the 3'-UTR region of PD-1, miR-138 alters its expression directly. miR-138 exerts its regulatory effects on T-cell cytokine production by suppressing PD-1 expression [208].

HBV also represses some miRNAs to affect anti-tumor immunity. One study finds that HBV-elevated CCL22 induction is mediated by transcriptionally repressing miR-23a. It is hypothesized that the axis of p65/miR-23a/CCL22 is present in the HCC cells and may drive tumor progression by recruiting Tregs, particularly when HBV infection was involved[103]. In HBV-expressing HepG2.215 cells, miR-34a is downregulated, while suppressed miR-34a leads to enhanced production of chemokine CCL22, which recruits Tregs to facilitate immune escape[209]. In addition, HLA-G, which inhibits different kinds of immune cells directly, such as NK, is downregulated by miR-152 in hepatoma cells. HBV inhibits miR-152 and increases the expression of its target HLA-G, which may further suppress NK against cancer cells[210]. Additionally, mRNAs of HMGB1 regulated by HBV and RICTOR regulated by HMGB1 mediated by miR-200[166] inhibit the response to anti-PD-L1 immunotherapy in HCC by elevating PD-L1+ exosomes[165].

Dysregulated miRNAs promote tumor drug resistance

Chemoresistance, resulting in cancer relapse and spread, is frequently mentioned as the largest cause of cancer therapeutic failure. In HCC, HBV commonly drives chemoresistance[211]. Accumulating evidence implicates the role of miRNAs in HBV-driven chemoresistance of HCC (Table 11).

HBc upregulates miR-135a-5p to suppress VAMP2 expression, blocking doxorubicin hydrochloride-induced apoptosis in HCC[212]. Similarly, HBV-upregulated miR-5188 Leads to an increase in resistance to the chemotherapy drugs 5-FU, cisplatin, and pharmorubicin[67]. Meanwhile, it is inferred that HBx elevates miR-7, -103, -107, and -21 expression to downregulate their target mapsin. Silencing maspin boosts HCC resistance to doxorubicin and other chemotherapeutic drugs[213]. These miRNAs may contribute to HBV-induced resistance to chemotherapy.

For some anti-tumor miRNAs, HBV suppresses their expression to promote HCC drug resistance. HBV mRNA can directly sponge miR-15a/16 and inhibit the subsequent cascade of etoposide-induced apoptosis in hepatoma cells[173]. miR-193b is downregulated in HBV-positive cells and tissues. Recent research shows that it increases the sensitivity of HCC cells to sorafenib by suppressing the expression of the anti-apoptotic protein Mcl-1[57]. miR-203a reduces HCC cell viability after 5-fluorouracil (5-FU) treatment and also increases the apoptosis rate of HCC cells in response to 5-FU[58]. HBV suppresses miR-203a expression, and subsequently renders HCC cells resistant to chemotherapy drug-induced apoptosis. HBV inhibits miR-325-3p[201], which remarkably increases chemosensitivity to doxorubicin in HCC cells[202]. Similarly, HBV negatively regulates miR-329 and miR-1236 to elevate their target AFP expression, while AFP further attenuates the proapoptotic effect of chemotherapy agents cisplatinum[214].

At present, the research on HBV-dysregulated miRNAs to enhance drug resistance in HCC is in its infancy. It has been discovered that miRNA promotes tumor treatment resistance through targeted regulation of multiple drug-related genes and DNA damage repair-related genes[215]. Therefore, more in-depth studies are needed.

Dysregulated miRNAs promote HBV replication to perpetuate its infection

The majority of HBV-infected patients have strong viral replication. By promoting self-replication, HBV maintains a high titer and promotes hepatocarcinogenesis. The complex relationship between HBV replication and miRNA has been described in a number of reviews[53,199,216]. We have enumerated the currently known miRNAs dysregulated by HBV that regulate HBV replication in the Supplementary Tables 1 and 2. Intriguingly, HBx upregulates miR-125a-5p expression[217], which interferes with expression of HBV surface antigen[218]. HBV may modulate miRNAs to restrict self-replication, therefore maintaining a long period of existence.

Others

DNA hypermethylation is responsible for suppressing TSGs in hepatocarcinogenesis. The inhibition of miR-101 by HBx leads to an increase in DNMT3A expression, while miR-101 inhibition or overexpression drastically affects the mRNA expression of different TSGs, demonstrating that miR-101 operates upstream to enhance TSG expression[219].

During the process of metastasis, cancer cells detaching from extracellular matrix (ECM) acquire the ability to persist in circulation by evading anoikis-induced cell death[220]. It is found that HBx induces miR-7, -103, -107, and -21 to suppress maspin expression, while maspin downregulation conferes HBx-mediated anoikis resistance in HCC cells[213]. Therefore, it can be speculated that these miRNAs may similarly confer HBx-mediated anoikis resistance.

In addition to directly affecting tumor cells, miRNA can indirectly accelerate the development of HCC *via* acting on other liver cells. Exosomal miR-142-3p from HBV-positive cells induces ferroptosis in HBV-infected M1-type macrophages *via* SLC3A2[221]. Similarly, exosomal miR-222 from HBV-infected hepatic cells boosts LX-2 cell activation by suppressing TFRC-induced ferroptosis, which ultimately exacerbates liver fibrosis[222]. Besides that, HBx-elevated P4HA2 enhances the collagen deposition in the liver *in vivo* and *in vitro* by inhibiting miR-30e, leading to liver fibrosis and liver cancer progression[139]. Moreover, HBx and TGF-β1 exposure induces the upregulation of miR-199a-3p, which contributes to the malignant transformation of hepatic progenitor cells (HPCs)[120]. As HPCs have the capacity to generate HCC with the cooperation of HBx and AFB1 in the liver microenvironment, this may provide new insight of HBV promoting HCC[223].

FUTURE PROSPECTS - CHALLENGES AND POTENTIAL CLINICAL USE OF MIRNAS IN DIAGNOSIS AND TREATMENT OF HBV-HCC

Due to the significant changes of miRNA in bodily fluid and tissues of HBV-HCC, its utility as a biomarker for the diagnosis of HCC incidence and prognostic risk has been extensively evaluated. However, since the PLR of miRNAs diagnosing HBV-HCC is less than 10 and the NLR is greater than 0.1[41,42], the clinical use of miRNAs for detecting HBV-HCC may still be limited. Traditional techniques for detecting miRNAs include Northern blotting, quantitative reverse transcription polymerase chain reaction (qRT-PCR), next-generation sequencing, and microarray-based hybridization[7,224]. However, quantifying miRNA in a dependable and robust manner can be challenging, and these methods may involve significant trade-offs between cost, complexity, and efficacy[7,224]. Therefore, using standardized measurements with unified standards will facilitate the collection of trustworthy miRNA data that can be compared across institutions[7]. It is crucial to minimize the influence of confounding factors, such as measurement technical characteristics, when detecting miRNA. Additionally, novel miRNA detection assays, such as miRacles which utilize conformationally responsive DNA nanoswitches, have been proved to be a simple, inexpensive, and accurate method for detecting miRNAs[224]. With the continuous development of new materials, it is anticipated that the miRNAs detection technology will increase in precision and sensitivity while decreasing in cost and operational complexity.

In addition to their use as diagnostics, miRNAs have significant promise for prognostication. Current relevant research has focused on miRNAs to predict the risk of recurrence, OS, and DFS in patients with HBV-HCC. There are few studies and insufficient data on circulating miRNAs. As circulating miRNAs offer numerous advantages, such as being convenient, safe, and noninvasive, their potential as biomarkers can be exploited further. For instance, miRNAs can be used to predict or evaluate the efficacy of neoadjuvant chemotherapy[225], radiotherapy[226], and immunotherapy[227] in cancer patients. Hence, miRNAs have the potential to anticipate therapeutic efficacy in HBV-HCC, which warrants further investigation.

Since HBV-dysregulated miRNAs play a significant role in hepatocarcinogenesis, miRNAs can be used as viable alternative therapeutic targets. Despite the fact that miRNA delivery to specific locations is hampered by many challenges, several techniques, such as conjugation, virus-associated delivery, and nanoparticles, have been researched to improve the efficacy of miRNA delivery[8]. In fact, multiple miRNA-based therapeutics have entered the clinical phase of cancer therapy. The combination of miRNAs therapy with chemotherapy, radiotherapy, and immunotherapy has shown encouraging outcomes against different malignancies[215]. Unfortunately, there is no relevant clinical research on the use of miRNAs in the treatment of HCC. Given that miRNAs play a crucial part in the occurrence and progression of HBV-HCC, the approaches of combining diverse strategies, applying complementary miRNAs together, or inventing new forms of miRNAs may bring considerable clinical benefits for HBV-HCC patients. To reach the ultimate objective of enhancing patient OS and DFS, additional research is required in this area.

CONCLUSION

HBV dysregulates miRNAs in multiple ways, thereby contributing to the occurrence and progression of HCC. Consequently, miRNAs are anticipated to become HBV-HCC biomarkers for diagnosis and prognosis. miRNAs-based therapies may also improve the efficacy of HBV-HCC. More research is required for miRNA clinical transformation.

FOOTNOTES

Author contributions: Zhang MH gathered the pertinent literature, drafted the initial manuscript, and conceptualized the tables and figures; Yuan YF, Liu LJ, Wei YX, Yin WY, Zheng LZY, Tang YY, Lv Z, and Zhu F conceptualized the text's structure and revised it for significant intellectual content; all authors have viewed and approved the final manuscript version.

Supported by the Translational Medicine and Interdisciplinary Research Joint Fund of Zhongnan Hospital of Wuhan University, No.

ZNLH201902.

Conflict-of-interest statement: Authors declare no conflict of interests for this article.

Country/Territory of origin: China

ORCID number: Ming-He Zhang 0009-0000-4161-2204; Yu-Feng Yuan 0000-0003-3924-3803; Li-Juan Liu 0000-0002-2549-5463; Yu-Xin Wei 0009-0005-7930-2662; Wan-Yue Yin 0009-0004-6034-8014; Lan-Zhuo-Yin Zheng 0000-0002-0616-7990; Ying-Ying Tang 0009-0005-1122-2906; Zhao Lv 0009-0008-6499-213X; Fan Zhu 0000-0001-7031-2956.

S-Editor: Yan JP
L-Editor: A
P-Editor: Zhao S

REFERENCES

1 **Sung H**, Ferlay J, Siegel RL, Laversanne M, Soerjomataram I, Jemal A, Bray F. Global Cancer Statistics 2020: GLOBOCAN Estimates of Incidence and Mortality Worldwide for 36 Cancers in 185 Countries. *CA Cancer J Clin* 2021; **71**: 209-249 [PMID: 33538338 DOI: 10.3322/caac.21660]
2 **World Health Organization**. Global hepatitis report 2017. Geneva: World Health Organization; 2017
3 **Piñero F**, Dirchwolf M, Pessôa MG. Biomarkers in Hepatocellular Carcinoma: Diagnosis, Prognosis and Treatment Response Assessment. *Cells* 2020; **9** [PMID: 32492896 DOI: 10.3390/cells9061370]
4 **Johnson P**, Zhou Q, Dao DY, Lo YMD. Circulating biomarkers in the diagnosis and management of hepatocellular carcinoma. *Nat Rev Gastroenterol Hepatol* 2022; **19**: 670-681 [PMID: 35676420 DOI: 10.1038/s41575-022-00620-y]
5 **Ha M**, Kim VN. Regulation of microRNA biogenesis. *Nat Rev Mol Cell Biol* 2014; **15**: 509-524 [PMID: 25027649 DOI: 10.1038/nrm3838]
6 **Sartorius K**, Makarova J, Sartorius B, An P, Winkler C, Chuturgoon A, Kramvis A. The Regulatory Role of MicroRNA in Hepatitis-B Virus-Associated Hepatocellular Carcinoma (HBV-HCC) Pathogenesis. *Cells* 2019; **8** [PMID: 31771261 DOI: 10.3390/cells8121504]
7 **Valihrach L**, Androvic P, Kubista M. Circulating miRNA analysis for cancer diagnostics and therapy. *Mol Aspects Med* 2020; **72**: 100825 [PMID: 31635843 DOI: 10.1016/j.mam.2019.10.002]
8 **Ho PTB**, Clark IM, Le LTT. MicroRNA-Based Diagnosis and Therapy. *Int J Mol Sci* 2022; **23** [PMID: 35806173 DOI: 10.3390/ijms23137167]
9 **Liu AM**, Yao TJ, Wang W, Wong KF, Lee NP, Fan ST, Poon RT, Gao C, Luk JM. Circulating miR-15b and miR-130b in serum as potential markers for detecting hepatocellular carcinoma: a retrospective cohort study. *BMJ Open* 2012; **2**: e000825 [PMID: 22403344 DOI: 10.1136/bmjopen-2012-000825]
10 **Qi P**, Cheng SQ, Wang H, Li N, Chen YF, Gao CF. Serum microRNAs as biomarkers for hepatocellular carcinoma in Chinese patients with chronic hepatitis B virus infection. *PLoS One* 2011; **6**: e28486 [PMID: 22174818 DOI: 10.1371/journal.pone.0028486]
11 **Lin L**, Lu B, Yu J, Liu W, Zhou A. Serum miR-224 as a biomarker for detection of hepatocellular carcinoma at early stage. *Clin Res Hepatol Gastroenterol* 2016; **40**: 397-404 [PMID: 26724963 DOI: 10.1016/j.clinre.2015.11.005]
12 **Zhao Q**, Li T, Qi J, Liu J, Qin C. The miR-545/374a cluster encoded in the Ftx lncRNA is overexpressed in HBV-related hepatocellular carcinoma and promotes tumorigenesis and tumor progression. *PLoS One* 2014; **9**: e109782 [PMID: 25299640 DOI: 10.1371/journal.pone.0109782]
13 **Yu F**, Lu Z, Chen B, Dong P, Zheng J. microRNA-150: a promising novel biomarker for hepatitis B virus-related hepatocellular carcinoma. *Diagn Pathol* 2015; **10**: 129 [PMID: 26215970 DOI: 10.1186/s13000-015-0369-y]
14 **Mandrekar JN**. Receiver operating characteristic curve in diagnostic test assessment. *J Thorac Oncol* 2010; **5**: 1315-1316 [PMID: 20736804 DOI: 10.1097/JTO.0b013e3181ec173d]
15 **Zhou G**, Zeng Y, Luo Y, Guo S, Bao L, Zhang Q. Urine miR-93-5p is a promising biomarker for early detection of HBV-related hepatocellular carcinoma. *Eur J Surg Oncol* 2022; **48**: 95-102 [PMID: 34175168 DOI: 10.1016/j.ejso.2021.06.015]
16 **Quoc NB**, Phuong NDN, Ngan TK, Linh NTM, Cuong PH, Chau NNB. Expression of Plasma hsa-miR122 in HBV-Related Hepatocellular Carcinoma (HCC) in Vietnamese Patients. *Microrna* 2018; **7**: 92-99 [PMID: 29701140 DOI: 10.2174/2211536607666180427165114]
17 **Xu L**, Wei B, Hui H, Liu Y. Association of serum microRNA-125b and HBV-related hepatocellular carcinoma in Chinese Han patients. *Int J Clin Exp Med* 2018; **11**: 3699-3703
18 **Li X**, Guo Y, Wang X, Ge A, Wang H, Fan K, Guo C. Clinical significance of serum miR-487b in HBV-related hepatocellular carcinoma and its potential mechanism. *Infect Dis (Lond)* 2021; **53**: 546-554 [PMID: 33783293 DOI: 10.1080/23744235.2021.1901981]
19 **Cao X**, Yang Q, Yu Q. Increased Expression of miR-487b Is Associated With Poor Prognosis and Tumor Progression of HBV-Related Hepatocellular Carcinoma. *Open Forum Infect Dis* 2020; **7**: ofaa498 [PMID: 33364257 DOI: 10.1093/ofid/ofaa498]
20 **Cao C**, Wang C. Clinical significance of serum miR-768-3p in HBV-related hepatocellular carcinoma and its potential mechanism. *Clin Exp Med* 2020; **20**: 569-576 [PMID: 32712720 DOI: 10.1007/s10238-020-00646-z]
21 **Moradi N**, Paryan M, Khansarinejad B, Sarmadian H, Mondanizadeh M. Plasma Level of miR-5193 As a Novel Biomarker for Diagnosis of HBV-Related Hepatocellular Carcinoma. *Hepat Mon* 2019; In Press [DOI: 10.5812/hepatmon.84455]
22 **Tat Trung N**, Duong DC, Tong HV, Hien TTT, Hoan PQ, Bang MH, Binh MT, Ky TD, Tung NL, Thinh NT, Sang VV, Thao LTP, Bock CT,

Velavan TP, Meyer CG, Song LH, Toan NL. Optimisation of quantitative miRNA panels to consolidate the diagnostic surveillance of HBV-related hepatocellular carcinoma. *PLoS One* 2018; **13**: e0196081 [PMID: 29672637 DOI: 10.1371/journal.pone.0196081]

23 **Chen S**, Chen H, Gao S, Qiu S, Zhou H, Yu M, Tu J. Differential expression of plasma microRNA-125b in hepatitis B virus-related liver diseases and diagnostic potential for hepatitis B virus-induced hepatocellular carcinoma. *Hepatol Res* 2017; **47**: 312-320 [PMID: 27152955 DOI: 10.1111/hepr.12739]

24 **Xie Y**, Yao Q, Butt AM, Guo J, Tian Z, Bao X, Li H, Meng Q, Lu J. Expression profiling of serum microRNA-101 in HBV-associated chronic hepatitis, liver cirrhosis, and hepatocellular carcinoma. *Cancer Biol Ther* 2014; **15**: 1248-1255 [PMID: 24971953 DOI: 10.4161/cbt.29688]

25 **Mjelle R**, Dima SO, Bacalbasa N, Chawla K, Sorop A, Cucu D, Herlea V, Sætrom P, Popescu I. Comprehensive transcriptomic analyses of tissue, serum, and serum exosomes from hepatocellular carcinoma patients. *BMC Cancer* 2019; **19**: 1007 [PMID: 31660891 DOI: 10.1186/s12885-019-6249-1]

26 **Xia G**, Xie Y, He Q. Hepatitis B Virus Affected Serum MicroRNA-203a Level in Hepatocellular Carcinoma. *Clin Lab* 2021; **67** [PMID: 33739050 DOI: 10.7754/Clin.Lab.2020.200748]

27 **Bai PS**, Hou P, Kong Y. Hepatitis B virus promotes proliferation and metastasis in male Chinese hepatocellular carcinoma patients through the LEF-1/miR-371a-5p/SRCIN1/pleiotrophin/Slug pathway. *Exp Cell Res* 2018; **370**: 174-188 [PMID: 29928866 DOI: 10.1016/j.yexcr.2018.06.020]

28 **Zhou SJ**, Deng YL, Liang HF, Jaoude JC, Liu FY. Hepatitis B virus X protein promotes CREB-mediated activation of miR-3188 and Notch signaling in hepatocellular carcinoma. *Cell Death Differ* 2017; **24**: 1577-1587 [PMID: 28574502 DOI: 10.1038/cdd.2017.87]

29 **Riazalhosseini B**, Mohamed R, Apalasamy YD, Langmia IM, Mohamed Z. Circulating microRNA as a marker for predicting liver disease progression in patients with chronic hepatitis B. *Rev Soc Bras Med Trop* 2017; **50**: 161-166 [PMID: 28562750 DOI: 10.1590/0037-8682-0416-2016]

30 **Zuo D**, Chen L, Liu X, Wang X, Xi Q, Luo Y, Zhang N, Guo H. Combination of miR-125b and miR-27a enhances sensitivity and specificity of AFP-based diagnosis of hepatocellular carcinoma. *Tumour Biol* 2016; **37**: 6539-6549 [PMID: 26637228 DOI: 10.1007/s13277-015-4545-1]

31 **Li LM**, Hu ZB, Zhou ZX, Chen X, Liu FY, Zhang JF, Shen HB, Zhang CY, Zen K. Serum microRNA profiles serve as novel biomarkers for HBV infection and diagnosis of HBV-positive hepatocarcinoma. *Cancer Res* 2010; **70**: 9798-9807 [PMID: 21098710 DOI: 10.1158/0008-5472.CAN-10-1001]

32 **Ghosh A**, Ghosh A, Datta S, Dasgupta D, Das S, Ray S, Gupta S, Chowdhury A, Chatterjee R, Mohapatra SK, Banerjee S. Hepatic miR-126 is a potential plasma biomarker for detection of hepatitis B virus infected hepatocellular carcinoma. *Int J Cancer* 2016; **138**: 2732-2744 [PMID: 26756996 DOI: 10.1002/ijc.29999]

33 **Meng FL**, Wang W, Jia WD. Diagnostic and prognostic significance of serum miR-24-3p in HBV-related hepatocellular carcinoma. *Med Oncol* 2014; **31**: 177 [PMID: 25129312 DOI: 10.1007/s12032-014-0177-3]

34 **Chen Y**, Dong X, Yu D, Wang X. Serum miR-96 is a promising biomarker for hepatocellular carcinoma in patients with chronic hepatitis B virus infection. *Int J Clin Exp Med* 2015; **8**: 18462-18468 [PMID: 26770453]

35 **Trung NT**, Hoan NX, Trung PQ, Binh MT, Van Tong H, Toan NL, Bang MH, Song LH. Clinical significance of combined circulating TERT promoter mutations and miR-122 expression for screening HBV-related hepatocellular carcinoma. *Sci Rep* 2020; **10**: 8181 [PMID: 32424223 DOI: 10.1038/s41598-020-65213-8]

36 **Chen SS**, Chen H, Gao SS, Zhou H, Qiu SL, Yu MX, Tu JC. Differential expression of plasma miR-205 in HBV-related liver diseases and diagnostic potential for HBV-induced hepatocellular carcinoma. *Wuhan Daxue Xuebao (Yixueban)* 2016; **37**: 445-450

37 **Caviglia GP**, Abate ML, Gaia S, Petrini E, Bosco C, Olivero A, Rosso C, Ciancio A, Pellicano R, Saracco GM, Rizzetto M, Smedile A. Risk of hepatocellular carcinoma in HBV cirrhotic patients assessed by the combination of miR-122, AFP and PIVKA-II. *Panminerva Med* 2017; **59**: 283-289 [PMID: 28650134 DOI: 10.23736/S0031-0808.17.03353-5]

38 **Tan Y**, Ge G, Pan T, Wen D, Chen L, Yu X, Zhou X, Gan J. A serum microRNA panel as potential biomarkers for hepatocellular carcinoma related with hepatitis B virus. *PLoS One* 2014; **9**: e107986 [PMID: 25238238 DOI: 10.1371/journal.pone.0107986]

39 **Luo P**, Wu S, Yu Y, Ming X, Li S, Zuo X, Tu J. Current Status and Perspective Biomarkers in AFP Negative HCC: Towards Screening for and Diagnosing Hepatocellular Carcinoma at an Earlier Stage. *Pathol Oncol Res* 2020; **26**: 599-603 [PMID: 30661224 DOI: 10.1007/s12253-019-00585-5]

40 **Peng C**, Li Z, Xie Z, Wang Z, Ye Y, Li B, Li W. The role of circulating microRNAs for the diagnosis of hepatitis B virus-associated hepatocellular carcinoma with low alpha-fetoprotein level: a systematic review and meta-analysis. *BMC Gastroenterol* 2020; **20**: 249 [PMID: 32736604 DOI: 10.1186/s12876-020-01345-5]

41 **Zhang WT**, Gil-Gómez A, Liu CH, Gao SS, Romero-Gómez M. Diagnostic accuracy of circulating microRNA in hepatitis B virus-related hepatocellular carcinoma: a meta-analysis based on Asian data. *Rev Esp Enferm Dig* 2022; **114**: 280-288 [PMID: 34423645 DOI: 10.17235/reed.2021.8139/2021]

42 **Jin X**, Cai C, Qiu Y. Diagnostic Value of Circulating microRNAs in Hepatitis B Virus-Related Hepatocellular Carcinoma: A Systematic Review and Meta-Analysis. *J Cancer* 2019; **10**: 4754-4764 [PMID: 31598147 DOI: 10.7150/jca.32833]

43 **Shi J**, Liu J, Tu X, Li B, Tong Z, Wang T, Zheng Y, Shi H, Zeng X, Chen W, Yin W, Fang W. Single-cell immune signature for detecting early-stage HCC and early assessing anti-PD-1 immunotherapy efficacy. *J Immunother Cancer* 2022; **10** [PMID: 35101942 DOI: 10.1136/jitc-2021-003133]

44 **Zhou J**, Yu L, Gao X, Hu J, Wang J, Dai Z, Wang JF, Zhang Z, Lu S, Huang X, Wang Z, Qiu S, Wang X, Yang G, Sun H, Tang Z, Wu Y, Zhu H, Fan J. Plasma microRNA panel to diagnose hepatitis B virus-related hepatocellular carcinoma. *J Clin Oncol* 2011; **29**: 4781-4788 [PMID: 22105822 DOI: 10.1200/JCO.2011.38.2697]

45 **Sanz-Rubio D**, Martin-Burriel I, Gil A, Cubero P, Forner M, Khalyfa A, Marin JM. Stability of Circulating Exosomal miRNAs in Healthy Subjects. *Sci Rep* 2018; **8**: 10306 [PMID: 29985466 DOI: 10.1038/s41598-018-28748-5]

46 **Karamichali E**, Foka P, Papadopoulou G, Loukaki-Gkountara D, Andresaki K, Koskinas I, Georgopoulou U. Hepatitis Viruses Control Host Immune Responses by Modifying the Exosomal Biogenesis Pathway and Cargo. *Int J Mol Sci* 2022; **23** [PMID: 36142773 DOI: 10.3390/ijms231810862]

47 **Liu Z**, Li Y, Wang Y, Bai X, Zhang Y. Exosomes in HBV infection. *Clin Chim Acta* 2023; **538**: 65-69 [PMID: 36375524 DOI: 10.1016/j.cca.2022.11.012]

48 **Li S**, Li S, Wu S, Chen L. Exosomes Modulate the Viral Replication and Host Immune Responses in HBV Infection. *Biomed Res Int* 2019; **2019**: 2103943 [PMID: 31275965 DOI: 10.1155/2019/2103943]

49 **Ghosh S**, Bhowmik S, Majumdar S, Goswami A, Chakraborty J, Gupta S, Aggarwal S, Ray S, Chatterjee R, Bhattacharyya S, Dutta M, Datta

S, Chowdhury A, Dhali GK, Banerjee S. The exosome encapsulated microRNAs as circulating diagnostic marker for hepatocellular carcinoma with low alpha-fetoprotein. *Int J Cancer* 2020; **147**: 2934-2947 [PMID: 32441313 DOI: 10.1002/ijc.33111]

50 **Wei XC**, Liu LJ, Zhu F. Exosomes as potential diagnosis and treatment for liver cancer. *World J Gastrointest Oncol* 2022; **14**: 334-347 [PMID: 35116120 DOI: 10.4251/wjgo.v14.i1.334]

51 **Pandyarajan V**, Govalan R, Yang JD. Risk Factors and Biomarkers for Chronic Hepatitis B Associated Hepatocellular Carcinoma. *Int J Mol Sci* 2021; **22** [PMID: 33418899 DOI: 10.3390/ijms22020479]

52 **Bandopadhyay M**, Bharadwaj M. Exosomal miRNAs in hepatitis B virus related liver disease: a new hope for biomarker. *Gut Pathog* 2020; **12**: 23 [PMID: 32346400 DOI: 10.1186/s13099-020-00353-w]

53 **Xu J**, An P, Winkler CA, Yu Y. Dysregulated microRNAs in Hepatitis B Virus-Related Hepatocellular Carcinoma: Potential as Biomarkers and Therapeutic Targets. *Front Oncol* 2020; **10**: 1271 [PMID: 32850386 DOI: 10.3389/fonc.2020.01271]

54 **Yuan LT**, Lee WJ, Yang YC, Chen BR, Yang CY, Chen MW, Chen JQ, Hsiao M, Chien MH, Hua KT. Histone Methyltransferase G9a-Promoted Progression of Hepatocellular Carcinoma Is Targeted by Liver-Specific Hsa-miR-122. *Cancers (Basel)* 2021; **13** [PMID: 34069116 DOI: 10.3390/cancers13102376]

55 **Zhang Q**, Xu HF, Song WY, Zhang PJ, Song YB. Potential microRNA panel for the diagnosis and prediction of overall survival of hepatocellular carcinoma with hepatitis B virus infection. *World J Gastrointest Oncol* 2020; **12**: 383-393 [PMID: 32368317 DOI: 10.4251/wjgo.v12.i4.383]

56 **Dundar HZ**, Aksoy F, Aksoy SA, Tasar P, Ugras N, Tunca B, Egeli U, Cecener G, Yerci O, Kaya E. Overexpression of miR-21 Is Associated With Recurrence in Patients With Hepatitis B Virus-Mediated Hepatocellular Carcinoma Undergoing Liver Transplantation. *Transplant Proc* 2019; **51**: 1157-1161 [PMID: 31101191 DOI: 10.1016/j.transproceed.2019.01.089]

57 **Mao K**, Zhang J, He C, Xu K, Liu J, Sun J, Wu G, Tan C, Zeng Y, Wang J, Xiao Z. Restoration of miR-193b sensitizes Hepatitis B virus-associated hepatocellular carcinoma to sorafenib. *Cancer Lett* 2014; **352**: 245-252 [PMID: 25034398 DOI: 10.1016/j.canlet.2014.07.004]

58 **Qin YF**, Zhou ZY, Fu HW, Lin HM, Xu LB, Wu WR, Liu C, Xu XL, Zhang R. Hepatitis B Virus Surface Antigen Promotes Stemness of Hepatocellular Carcinoma through Regulating MicroRNA-203a. *J Clin Transl Hepatol* 2023; **11**: 118-129 [PMID: 36406317 DOI: 10.14218/JCTH.2021.00373]

59 **Liu FY**, Zhou SJ, Deng YL, Zhang ZY, Zhang EL, Wu ZB, Huang ZY, Chen XP. MiR-216b is involved in pathogenesis and progression of hepatocellular carcinoma through HBx-miR-216b-IGF2BP2 signaling pathway. *Cell Death Dis* 2015; **6**: e1670 [PMID: 25741595 DOI: 10.1038/cddis.2015.46]

60 **Zhou N**, Wu J, Wang X, Sun Z, Han Q, Zhao L. Low-level expression of microRNA-375 predicts poor prognosis in hepatocellular carcinoma. *Tumour Biol* 2016; **37**: 2145-2152 [PMID: 26349912 DOI: 10.1007/s13277-015-3841-0]

61 **Bai PS**, Xia N, Sun H, Kong Y. Pleiotrophin, a target of miR-384, promotes proliferation, metastasis and lipogenesis in HBV-related hepatocellular carcinoma. *J Cell Mol Med* 2017; **21**: 3023-3043 [PMID: 28557334 DOI: 10.1111/jcmm.13213]

62 **Zhen Y**, Xinghui Z, Chao W, Yi Z, Jinwen C, Ruifang G, Chao Z, Min Z, Chunlei G, Yan F, Lingfang D, Long S, Wenzhi S, Xiaohe L, Rong X. Several microRNAs could predict survival in patients with hepatitis B-related liver cancer. *Sci Rep* 2017; **7**: 45195 [PMID: 28322348 DOI: 10.1038/srep45195]

63 **Zhu HT**, Dong QZ, Sheng YY, Wei JW, Wang G, Zhou HJ, Ren N, Jia HL, Ye QH, Qin LX. MicroRNA-29a-5p is a novel predictor for early recurrence of hepatitis B virus-related hepatocellular carcinoma after surgical resection. *PLoS One* 2012; **7**: e52393 [PMID: 23285022 DOI: 10.1371/journal.pone.0052393]

64 **Yen CS**, Su ZR, Lee YP, Liu IT, Yen CJ. miR-106b promotes cancer progression in hepatitis B virus-associated hepatocellular carcinoma. *World J Gastroenterol* 2016; **22**: 5183-5192 [PMID: 27298561 DOI: 10.3748/wjg.v22.i22.5183]

65 **Dai X**, Huang R, Hu S, Zhou Y, Sun X, Gui P, Yu Z, Zhou P. A novel miR-0308-3p revealed by miRNA-seq of HBV-positive hepatocellular carcinoma suppresses cell proliferation and promotes G1/S arrest by targeting double CDK6/Cyclin D1 genes. *Cell Biosci* 2020; **10**: 24 [PMID: 32128112 DOI: 10.1186/s13578-020-00382-7]

66 **Chen Q**, Yang SB, Zhang YW, Han SY, Jia L, Li B, Zhang Y, Zuo S. miR-3682-3p directly targets FOXO3 and stimulates tumor stemness in hepatocellular carcinoma *via* a positive feedback loop involving FOXO3/PI3K/AKT/c-Myc. *World J Stem Cells* 2022; **14**: 539-555 [PMID: 36157524 DOI: 10.4252/wjsc.v14.i7.539]

67 **Lin X**, Zuo S, Luo R, Li Y, Yu G, Zou Y, Zhou Y, Liu Z, Liu Y, Hu Y, Xie Y, Fang W. HBX-induced miR-5188 impairs FOXO1 to stimulate β-catenin nuclear translocation and promotes tumor stemness in hepatocellular carcinoma. *Theranostics* 2019; **9**: 7583-7598 [PMID: 31695788 DOI: 10.7150/thno.37717]

68 **Pratedrat P**, Chuaypen N, Nimsamer P, Payungporn S, Pinjaroen N, Sirichindakul B, Tangkijvanich P. Diagnostic and prognostic roles of circulating miRNA-223-3p in hepatitis B virus-related hepatocellular carcinoma. *PLoS One* 2020; **15**: e0232211 [PMID: 32330203 DOI: 10.1371/journal.pone.0232211]

69 **Zhu HT**, Hasan AM, Liu RB, Zhang ZC, Zhang X, Wang J, Wang HY, Wang F, Shao JY. Serum microRNA profiles as prognostic biomarkers for HBV-positive hepatocellular carcinoma. *Oncotarget* 2016; **7**: 45637-45648 [PMID: 27317768 DOI: 10.18632/oncotarget.10082]

70 **Niu LJ**, Huang T, Wang L, Sun XF, Zhang YM. HBX suppresses PTEN to promote the malignant progression of hepatocellular carcinoma through mi-R155 activation. *Ann Hepatol* 2022; **27**: 100688 [PMID: 35196550 DOI: 10.1016/j.aohep.2022.100688]

71 **Wakasugi H**, Takahashi H, Niinuma T, Kitajima H, Oikawa R, Matsumoto N, Takeba Y, Otsubo T, Takagi M, Ariizumi Y, Suzuki M, Okuse C, Iwabuchi S, Nakano M, Akutsu N, Kang JH, Matsui T, Yamada N, Sasaki H, Yamamoto E, Kai M, Sasaki Y, Sasaki S, Tanaka Y, Yotsuyanagi H, Tsutsumi T, Yamamoto H, Tokino T, Nakase H, Suzuki H, Itoh F. Dysregulation of miRNA in chronic hepatitis B is associated with hepatocellular carcinoma risk after nucleos(t)ide analogue treatment. *Cancer Lett* 2018; **434**: 91-100 [PMID: 30026054 DOI: 10.1016/j.canlet.2018.07.019]

72 **Kim VN**. MicroRNA biogenesis: coordinated cropping and dicing. *Nat Rev Mol Cell Biol* 2005; **6**: 376-385 [PMID: 15852042 DOI: 10.1038/nrm1644]

73 **Li CL**, Yeh KH, Liu WH, Chen CL, Chen DS, Chen PJ, Yeh SH. Elevated p53 promotes the processing of miR-18a to decrease estrogen receptor-α in female hepatocellular carcinoma. *Int J Cancer* 2015; **136**: 761-770 [PMID: 24975878 DOI: 10.1002/ijc.29052]

74 **Kong XX**, Lv YR, Shao LP, Nong XY, Zhang GL, Zhang Y, Fan HX, Liu M, Li X, Tang H. HBx-induced MiR-1269b in NF-κB dependent manner upregulates cell division cycle 40 homolog (CDC40) to promote proliferation and migration in hepatoma cells. *J Transl Med* 2016; **14**: 189 [PMID: 27349221 DOI: 10.1186/s12967-016-0949-y]

75 **Chinnappan M**, Singh AK, Kakumani PK, Kumar G, Rooge SB, Kumari A, Varshney A, Rastogi A, Sarin SK, Malhotra P, Mukherjee SK, Bhatnagar RK. Key elements of the RNAi pathway are regulated by hepatitis B virus replication and HBx acts as a viral suppressor of RNA

silencing. *Biochem J* 2014; **462**: 347-358 [PMID: 24902849 DOI: 10.1042/BJ20140316]

76 **Liu AM**, Zhang C, Burchard J, Fan ST, Wong KF, Dai H, Poon RT, Luk JM. Global regulation on microRNA in hepatitis B virus-associated hepatocellular carcinoma. *OMICS* 2011; **15**: 187-191 [PMID: 21319996 DOI: 10.1089/omi.2010.0098]

77 **Kitagawa N**, Ojima H, Shirakihara T, Shimizu H, Kokubu A, Urushidate T, Totoki Y, Kosuge T, Miyagawa S, Shibata T. Downregulation of the microRNA biogenesis components and its association with poor prognosis in hepatocellular carcinoma. *Cancer Sci* 2013; **104**: 543-551 [PMID: 23398123 DOI: 10.1111/cas.12126]

78 **Ren M**, Qin D, Li K, Qu J, Wang L, Wang Z, Huang A, Tang H. Correlation between hepatitis B virus protein and microRNA processor Drosha in cells expressing HBV. *Antiviral Res* 2012; **94**: 225-231 [PMID: 22554933 DOI: 10.1016/j.antiviral.2012.04.004]

79 **Shan X**, Ren M, Chen K, Huang A, Tang H. Regulation of the microRNA processor DGCR8 by hepatitis B virus proteins *via* the transcription factor YY1. *Arch Virol* 2015; **160**: 795-803 [PMID: 25427980 DOI: 10.1007/s00705-014-2286-x]

80 **Li J**, Pu W, Sun HL, Zhou JK, Fan X, Zheng Y, He J, Liu X, Xia Z, Liu L, Wei YQ, Peng Y. Pin1 impairs microRNA biogenesis by mediating conformation change of XPO5 in hepatocellular carcinoma. *Cell Death Differ* 2018; **25**: 1612-1624 [PMID: 29445125 DOI: 10.1038/s41418-018-0065-z]

81 **Pang R**, Lee TK, Poon RT, Fan ST, Wong KB, Kwong YL, Tse E. Pin1 interacts with a specific serine-proline motif of hepatitis B virus X-protein to enhance hepatocarcinogenesis. *Gastroenterology* 2007; **132**: 1088-1103 [PMID: 17383430 DOI: 10.1053/j.gastro.2006.12.030]

82 **Förstemann K**, Horwich MD, Wee L, Tomari Y, Zamore PD. Drosophila microRNAs are sorted into functionally distinct argonaute complexes after production by dicer-1. *Cell* 2007; **130**: 287-297 [PMID: 17662943 DOI: 10.1016/j.cell.2007.05.056]

83 **Zhang J**, Jin H, Liu H, Lv S, Wang B, Wang R, Ding M, Yang Y, Li L, Zhang J, Fu S, Xie D, Wu M, Zhou W, Qian Q. MiRNA-99a directly regulates AGO2 through translational repression in hepatocellular carcinoma. *Oncogenesis* 2014; **3**: e97 [PMID: 24732044 DOI: 10.1038/oncsis.2014.11]

84 **Hayes CN**, Akamatsu S, Tsuge M, Miki D, Akiyama R, Abe H, Ochi H, Hiraga N, Imamura M, Takahashi S, Aikata H, Kawaoka T, Kawakami Y, Ohishi W, Chayama K. Hepatitis B virus-specific miRNAs and Argonaute2 play a role in the viral life cycle. *PLoS One* 2012; **7**: e47490 [PMID: 23091627 DOI: 10.1371/journal.pone.0047490]

85 **Chen W**, Bian H, Xie X, Yang X, Bi B, Li C, Zhang Y, Zhu Q, Song J, Qin C, Qi J. Negative feedback loop of ERK/CREB/miR-212-3p inhibits HBeAg-induced macrophage activation. *J Cell Mol Med* 2020; **24**: 10935-10945 [PMID: 32767729 DOI: 10.1111/jcmm.15723]

86 **Atsaves V**, Leventaki V, Rassidakis GZ, Claret FX. AP-1 Transcription Factors as Regulators of Immune Responses in Cancer. *Cancers (Basel)* 2019; **11** [PMID: 31340499 DOI: 10.3390/cancers11071037]

87 **Talotta F**, Cimmino A, Matarazzo MR, Casalino L, De Vita G, D'Esposito M, Di Lauro R, Verde P. An autoregulatory loop mediated by miR-21 and PDCD4 controls the AP-1 activity in RAS transformation. *Oncogene* 2009; **28**: 73-84 [PMID: 18850008 DOI: 10.1038/onc.2008.370]

88 **Tanaka Y**, Kanai F, Ichimura T, Tateishi K, Asaoka Y, Guleng B, Jazag A, Ohta M, Imamura J, Ikenoue T, Ijichi H, Kawabe T, Isobe T, Omata M. The hepatitis B virus X protein enhances AP-1 activation through interaction with Jab1. *Oncogene* 2006; **25**: 633-642 [PMID: 16247477 DOI: 10.1038/sj.onc.1209093]

89 **Shang J**, Zheng Y, Guo X, Mo J, Xie X, Xiong Y, Liu Y, Wu K, Wu J. Hepatitis B virus replication and sex-determining region Y box 4 production are tightly controlled by a novel positive feedback mechanism. *Sci Rep* 2015; **5**: 10066 [PMID: 25970172 DOI: 10.1038/srep10066]

90 **Fu X**, Ouyang Y, Mo J, Li R, Fu L, Peng S. Upregulation of microRNA-328-3p by hepatitis B virus contributes to THLE-2 cell injury by downregulating FOXO4. *J Transl Med* 2020; **18**: 143 [PMID: 32228643 DOI: 10.1186/s12967-020-02299-8]

91 **Li CH**, Xu F, Chow S, Feng L, Yin D, Ng TB, Chen Y. Hepatitis B virus X protein promotes hepatocellular carcinoma transformation through interleukin-6 activation of microRNA-21 expression. *Eur J Cancer* 2014; **50**: 2560-2569 [PMID: 25087183 DOI: 10.1016/j.ejca.2014.07.008]

92 **Liu Y**, Feng J, Sun M, Yang G, Yuan H, Wang Y, Bu Y, Zhao M, Zhang S, Zhang X. Long non-coding RNA HULC activates HBV by modulating HBx/STAT3/miR-539/APOBEC3B signaling in HBV-related hepatocellular carcinoma. *Cancer Lett* 2019; **454**: 158-170 [PMID: 30981758 DOI: 10.1016/j.canlet.2019.04.008]

93 **Huang JY**, Chen HL, Shih C. MicroRNA miR-204 and miR-1236 inhibit hepatitis B virus replication *via* two different mechanisms. *Sci Rep* 2016; **6**: 34740 [PMID: 27734898 DOI: 10.1038/srep34740]

94 **Sun C**, Lan P, Han Q, Huang M, Zhang Z, Xu G, Song J, Wang J, Wei H, Zhang J, Sun R, Zhang C, Tian Z. Oncofetal gene SALL4 reactivation by hepatitis B virus counteracts miR-200c in PD-L1-induced T cell exhaustion. *Nat Commun* 2018; **9**: 1241 [PMID: 29593314 DOI: 10.1038/s41467-018-03584-3]

95 **Zhang Y**, Ren H, Li J, Xue R, Liu H, Zhu Z, Pan C, Lin Y, Hu A, Gou P, Cai J, Zhou J, Zhu W, Shi X. Elevated HMGB1 expression induced by hepatitis B virus X protein promotes epithelial-mesenchymal transition and angiogenesis through STAT3/miR-34a/NF-κB in primary liver cancer. *Am J Cancer Res* 2021; **11**: 479-494 [PMID: 33575082]

96 **Yi H**, Zhang Y, Yang X, Li M, Hu H, Xiong J, Wang N, Jin J, Song Y, Wang X, Chen L, Lian J. Hepatitis B Core Antigen Impairs the Polarization While Promoting the Production of Inflammatory Cytokines of M2 Macrophages *via* the TLR2 Pathway. *Front Immunol* 2020; **11**: 535 [PMID: 32292408 DOI: 10.3389/fimmu.2020.00535]

97 **Fu L**, Fu X, Mo J, Li X, Li R, Peng S. miR-146a-5p enhances hepatitis B virus replication through autophagy to promote aggravation of chronic hepatitis B. *IUBMB Life* 2019; **71**: 1336-1346 [PMID: 31018043 DOI: 10.1002/iub.2044]

98 **Zhang X**, Liu S, Hu T, He Y, Sun S. Up-regulated microRNA-143 transcribed by nuclear factor kappa B enhances hepatocarcinoma metastasis by repressing fibronectin expression. *Hepatology* 2009; **50**: 490-499 [PMID: 19472311 DOI: 10.1002/hep.23008]

99 **Yin X**, Sun S, Zhao J, Yang J, Lei X, Xu C, Li K. Rs4705342 polymorphism is involved in the tumorigenesis of HBV positive HCC by altering the binding affinity of HBV induced NF-kB with the promoter region of microRNA-143. *J Cell Biochem* 2018; **119**: 5233-5242 [PMID: 29236306 DOI: 10.1002/jcb.26581]

100 **Li JF**, Dai XP, Zhang W, Sun SH, Zeng Y, Zhao GY, Kou ZH, Guo Y, Yu H, Du LY, Jiang SB, Zhou YS. Upregulation of microRNA-146a by hepatitis B virus X protein contributes to hepatitis development by downregulating complement factor H. *mBio* 2015; **6** [PMID: 25805734 DOI: 10.1128/mBio.02459-14]

101 **Wang W**, Bian H, Li F, Li X, Zhang D, Sun S, Song S, Zhu Q, Ren W, Qin C, Qi J. HBeAg induces the expression of macrophage miR-155 to accelerate liver injury *via* promoting production of inflammatory cytokines. *Cell Mol Life Sci* 2018; **75**: 2627-2641 [PMID: 29349567 DOI: 10.1007/s00018-018-2753-8]

102 **Tao L**, Xue D, Shen D, Ma W, Zhang J, Wang X, Zhang W, Wu L, Pan K, Yang Y, Nwosu ZC, Dooley S, Seki E, Liu C. MicroRNA-942 mediates hepatic stellate cell activation by regulating BAMBI expression in human liver fibrosis. *Arch Toxicol* 2018; **92**: 2935-2946 [PMID: 30097701 DOI: 10.1007/s00204-018-2278-9]

103 **Li ZQ**, Wang HY, Zeng QL, Yan JY, Hu YS, Li H, Yu ZJ. p65/miR-23a/CCL22 axis regulated regulatory T cells recruitment in hepatitis B virus positive hepatocellular carcinoma. *Cancer Med* 2020; **9**: 711-723 [PMID: 31769216 DOI: 10.1002/cam4.2611]

104 **Chen WS**, Liu LC, Yen CJ, Chen YJ, Chen JY, Ho CY, Liu SH, Chen CC, Huang WC. Nuclear IKKα mediates microRNA-7/-103/107/21 inductions to downregulate maspin expression in response to HBx overexpression. *Oncotarget* 2016; **7**: 56309-56323 [PMID: 27409165 DOI: 10.18632/oncotarget.10462]

105 **Huang JY**, Chou SF, Lee JW, Chen HL, Chen CM, Tao MH, Shih C. MicroRNA-130a can inhibit hepatitis B virus replication *via* targeting PGC1α and PPARγ. *RNA* 2015; **21**: 385-400 [PMID: 25595716 DOI: 10.1261/rna.048744.114]

106 **Sarkar N**, Panigrahi R, Pal A, Biswas A, Singh SP, Kar SK, Bandopadhyay M, Das D, Saha D, Kanda T, Sugiyama M, Chakrabarti S, Banerjee A, Chakravarty R. Expression of microRNA-155 correlates positively with the expression of Toll-like receptor 7 and modulates hepatitis B virus *via* C/EBP-β in hepatocytes. *J Viral Hepat* 2015; **22**: 817-827 [PMID: 25720442 DOI: 10.1111/jvh.12390]

107 **Sepehri Z**, Kiani Z, Alavian SM, Arababadi MK, Kennedy D. The link between TLR7 signaling and hepatitis B virus infection. *Life Sci* 2016; **158**: 63-69 [PMID: 27373425 DOI: 10.1016/j.lfs.2016.06.026]

108 **Mauvais-Jarvis F**, Lange CA, Levin ER. Membrane-Initiated Estrogen, Androgen, and Progesterone Receptor Signaling in Health and Disease. *Endocr Rev* 2022; **43**: 720-742 [PMID: 34791092 DOI: 10.1210/endrev/bnab041]

109 **Yang WJ**, Chang CJ, Yeh SH, Lin WH, Wang SH, Tsai TF, Chen DS, Chen PJ. Hepatitis B virus X protein enhances the transcriptional activity of the androgen receptor through c-Src and glycogen synthase kinase-3beta kinase pathways. *Hepatology* 2009; **49**: 1515-1524 [PMID: 19205031 DOI: 10.1002/hep.22833]

110 **Han J**, Ding L, Yuan B, Yang X, Wang X, Li J, Lu Q, Huang C, Ye Q. Hepatitis B virus X protein and the estrogen receptor variant lacking exon 5 inhibit estrogen receptor signaling in hepatoma cells. *Nucleic Acids Res* 2006; **34**: 3095-3106 [PMID: 16757575 DOI: 10.1093/nar/gkl389]

111 **Chen PJ**, Yeh SH, Liu WH, Lin CC, Huang HC, Chen CL, Chen DS, Chen PJ. Androgen pathway stimulates microRNA-216a transcription to suppress the tumor suppressor in lung cancer-1 gene in early hepatocarcinogenesis. *Hepatology* 2012; **56**: 632-643 [PMID: 22392644 DOI: 10.1002/hep.25695]

112 **Chang TC**, Yu D, Lee YS, Wentzel EA, Arking DE, West KM, Dang CV, Thomas-Tikhonenko A, Mendell JT. Widespread microRNA repression by Myc contributes to tumorigenesis. *Nat Genet* 2008; **40**: 43-50 [PMID: 18066065 DOI: 10.1038/ng.2007.30]

113 **Wang J**, Chen J, Liu Y, Zeng X, Wei M, Wu S, Xiong Q, Song F, Yuan X, Xiao Y, Cao Y, Li C, Chen L, Guo M, Shi YB, Sun G, Guo D. Hepatitis B Virus Induces Autophagy to Promote its Replication by the Axis of miR-192-3p-XIAP Through NF kappa B Signaling. *Hepatology* 2019; **69**: 974-992 [PMID: 30180281 DOI: 10.1002/hep.30248]

114 **Wu G**, Yu F, Xiao Z, Xu K, Xu J, Tang W, Wang J, Song E. Hepatitis B virus X protein downregulates expression of the miR-16 family in malignant hepatocytes in vitro. *Br J Cancer* 2011; **105**: 146-153 [PMID: 21629246 DOI: 10.1038/bjc.2011.190]

115 **Wu G**, Huang P, Ju X, Li Z, Wang Y. Lin28B over-expression mediates the repression of let-7 by hepatitis B virus X protein in hepatoma cells. *Int J Clin Exp Med* 2015; **8**: 15108-15116 [PMID: 26628994]

116 **Jung YJ**, Kim JW, Park SJ, Min BY, Jang ES, Kim NY, Jeong SH, Shin CM, Lee SH, Park YS, Hwang JH, Kim N, Lee DH. c-Myc-mediated overexpression of miR-17-92 suppresses replication of hepatitis B virus in human hepatoma cells. *J Med Virol* 2013; **85**: 969-978 [PMID: 23532756 DOI: 10.1002/jmv.23534]

117 **Liu Y**, Wang J, Chen J, Wu S, Zeng X, Xiong Q, Guo Y, Sun J, Song F, Xu J, Yuan S, Li C, He Y, Wang M, Chen L, Shi YB, Guo M, Guo D, Sun G. Upregulation of miR-520c-3p *via* hepatitis B virus drives hepatocellular migration and invasion by the PTEN/AKT/NF-κB axis. *Mol Ther Nucleic Acids* 2022; **29**: 47-63 [PMID: 35795482 DOI: 10.1016/j.omtn.2022.05.031]

118 **Zhang W**, Lu Z, Kong G, Gao Y, Wang T, Wang Q, Cai N, Wang H, Liu F, Ye L, Zhang X. Hepatitis B virus X protein accelerates hepatocarcinogenesis with partner survivin through modulating miR-520b and HBXIP. *Mol Cancer* 2014; **13**: 128 [PMID: 24886421 DOI: 10.1186/1476-4598-13-128]

119 **Chen W**, Jiang J, Gong L, Shu Z, Xiang D, Zhang X, Bi K, Diao H. Hepatitis B virus P protein initiates glycolytic bypass in HBV-related hepatocellular carcinoma *via* a FOXO3/miRNA-30b-5p/MINPP1 axis. *J Exp Clin Cancer Res* 2021; **40**: 1 [PMID: 33390177 DOI: 10.1186/s13046-020-01803-8]

120 **Dong KS**, Chen Y, Yang G, Liao ZB, Zhang HW, Liang HF, Chen XP, Dong HH. TGF-β1 accelerates the hepatitis B virus X-induced malignant transformation of hepatic progenitor cells by upregulating miR-199a-3p. *Oncogene* 2020; **39**: 1807-1820 [PMID: 31740785 DOI: 10.1038/s41388-019-1107-9]

121 **Gao Q**, Zhu H, Dong L, Shi W, Chen R, Song Z, Huang C, Li J, Dong X, Zhou Y, Liu Q, Ma L, Wang X, Zhou J, Liu Y, Boja E, Robles AI, Ma W, Wang P, Li Y, Ding L, Wen B, Zhang B, Rodriguez H, Gao D, Zhou H, Fan J. Integrated Proteogenomic Characterization of HBV-Related Hepatocellular Carcinoma. *Cell* 2019; **179**: 561-577.e22 [PMID: 31585088 DOI: 10.1016/j.cell.2019.08.052]

122 **Xu X**, Fan Z, Kang L, Han J, Jiang C, Zheng X, Zhu Z, Jiao H, Lin J, Jiang K, Ding L, Zhang H, Cheng L, Fu H, Song Y, Jiang Y, Liu J, Wang R, Du N, Ye Q. Hepatitis B virus X protein represses miRNA-148a to enhance tumorigenesis. *J Clin Invest* 2013; **123**: 630-645 [PMID: 23321675 DOI: 10.1172/JCI64265]

123 **Wu Q**, Liu HO, Liu YD, Liu WS, Pan D, Zhang WJ, Yang L, Fu Q, Xu JJ, Gu JX. Decreased expression of hepatocyte nuclear factor 4α (Hnf4α)/microRNA-122 (miR-122) axis in hepatitis B virus-associated hepatocellular carcinoma enhances potential oncogenic GALNT10 protein activity. *J Biol Chem* 2015; **290**: 1170-1185 [PMID: 25422324 DOI: 10.1074/jbc.M114.601203]

124 **Hu XM**, Yan XH, Hu YW, Huang JL, Cao SW, Ren TY, Tang YT, Lin L, Zheng L, Wang Q. miRNA-548p suppresses hepatitis B virus X protein associated hepatocellular carcinoma by downregulating oncoprotein hepatitis B x-interacting protein. *Hepatol Res* 2016; **46**: 804-815 [PMID: 26583881 DOI: 10.1111/hepr.12618]

125 **Dodurga Y**, Yonguc GN, Avci CB, Bagci G, Gunduz C, Satiroglu-Tufan NL. Investigation of microRNA expression changes in HepG2 cell line in presence of URG4/URGCP and in absence of URG4/URGCP suppressed by RNA interference. *Mol Biol Rep* 2012; **39**: 11119-11124 [PMID: 23053999 DOI: 10.1007/s11033-012-2019-8]

126 **Yuan K**, Lian Z, Sun B, Clayton MM, Ng IO, Feitelson MA. Role of miR-148a in hepatitis B associated hepatocellular carcinoma. *PLoS One* 2012; **7**: e35331 [PMID: 22496917 DOI: 10.1371/journal.pone.0035331]

127 **Mishra AK**, Hossain MM, Umar M, Sata TN, Yadav AK, Sah AK, Ismail M, Nayak B, Shalimar, Venugopal SK. DDX3-mediated miR-34 expression inhibits autophagy and HBV replication in hepatic cells. *J Viral Hepat* 2023; **30**: 327-334 [PMID: 36597176 DOI: 10.1111/jvh.13799]

128 **Guerrieri F**, Belloni L, D'Andrea D, Pediconi N, Le Pera L, Testoni B, Scisciani C, Floriot O, Zoulim F, Tramontano A, Levrero M. Genome-wide identification of direct HBx genomic targets. *BMC Genomics* 2017; **18**: 184 [PMID: 28212627 DOI: 10.1186/s12864-017-3561-5]

129 **Kwok ZH**, Zhang B, Chew XH, Chan JJ, Teh V, Yang H, Kappei D, Tay Y. Systematic Analysis of Intronic miRNAs Reveals Cooperativity within the Multicomponent FTX Locus to Promote Colon Cancer Development. *Cancer Res* 2021; **81**: 1308-1320 [PMID: 33172934 DOI: 10.1158/0008-5472.CAN-20-1406]

130 **Keniry A**, Oxley D, Monnier P, Kyba M, Dandolo L, Smits G, Reik W. The H19 lincRNA is a developmental reservoir of miR-675 that suppresses growth and Igf1r. *Nat Cell Biol* 2012; **14**: 659-665 [PMID: 22684254 DOI: 10.1038/ncb2521]

131 **Ge L**, Zhang X, Hu S, Song Y, Kong J, Zhang B, Yang X. H19 suppresses the growth of hepatoblastoma cells by promoting their apoptosis *via* the signaling pathways of miR-675/FADD and miR-138/PTK2. *J Cell Biochem* 2019; **120**: 5218-5231 [PMID: 30367502 DOI: 10.1002/jcb.27797]

132 **Liu Y**, Xu L, Lu B, Zhao M, Li L, Sun W, Qiu Z, Zhang B. LncRNA H19/microRNA-675/PPARα axis regulates liver cell injury and energy metabolism remodelling induced by hepatitis B X protein *via* Akt/mTOR signalling. *Mol Immunol* 2019; **116**: 18-28 [PMID: 31574452 DOI: 10.1016/j.molimm.2019.09.006]

133 **Zhu Y**, Lu Y, Zhang Q, Liu JJ, Li TJ, Yang JR, Zeng C, Zhuang SM. MicroRNA-26a/b and their host genes cooperate to inhibit the G1/S transition by activating the pRb protein. *Nucleic Acids Res* 2012; **40**: 4615-4625 [PMID: 22210897 DOI: 10.1093/nar/gkr1278]

134 **Wang H**, Luo J, He Q, Yao D, Wu J, Loor JJ. miR-26b promoter analysis reveals regulatory mechanisms by lipid-related transcription factors in goat mammary epithelial cells. *J Dairy Sci* 2017; **100**: 5837-5849 [PMID: 28527797 DOI: 10.3168/jds.2016-12440]

135 **Zhao F**, Xu G, Zhou Y, Wang L, Xie J, Ren S, Liu S, Zhu Y. MicroRNA-26b inhibits hepatitis B virus transcription and replication by targeting the host factor CHORDC1 protein. *J Biol Chem* 2014; **289**: 35029-35041 [PMID: 25342750 DOI: 10.1074/jbc.M114.589978]

136 **Piletič K**, Kunej T. MicroRNA epigenetic signatures in human disease. *Arch Toxicol* 2016; **90**: 2405-2419 [PMID: 27557899 DOI: 10.1007/s00204-016-1815-7]

137 **Park IY**, Sohn BH, Yu E, Suh DJ, Chung YH, Lee JH, Surzycki SJ, Lee YI. Aberrant epigenetic modifications in hepatocarcinogenesis induced by hepatitis B virus X protein. *Gastroenterology* 2007; **132**: 1476-1494 [PMID: 17408664 DOI: 10.1053/j.gastro.2007.01.034]

138 **Yang Z**, Li J, Feng G, Wang Y, Yang G, Liu Y, Zhang S, Feng J, Zhang X. Hepatitis B virus X protein enhances hepatocarcinogenesis by depressing the targeting of NUSAP1 mRNA by miR-18b. *Cancer Biol Med* 2019; **16**: 276-287 [PMID: 31516748 DOI: 10.20892/j.issn.2095-3941.2018.0283]

139 **Feng GX**, Li J, Yang Z, Zhang SQ, Liu YX, Zhang WY, Ye LH, Zhang XD. Hepatitis B virus X protein promotes the development of liver fibrosis and hepatoma through downregulation of miR-30e targeting P4HA2 mRNA. *Oncogene* 2017; **36**: 6895-6905 [PMID: 28846110 DOI: 10.1038/onc.2017.291]

140 **Wei X**, Tan C, Tang C, Ren G, Xiang T, Qiu Z, Liu R, Wu Z. Epigenetic repression of miR-132 expression by the hepatitis B virus x protein in hepatitis B virus-related hepatocellular carcinoma. *Cell Signal* 2013; **25**: 1037-1043 [PMID: 23376496 DOI: 10.1016/j.cellsig.2013.01.019]

141 **Zhang T**, Zhang J, Cui M, Liu F, You X, Du Y, Gao Y, Zhang S, Lu Z, Ye L, Zhang X. Hepatitis B virus X protein inhibits tumor suppressor miR-205 through inducing hypermethylation of miR-205 promoter to enhance carcinogenesis. *Neoplasia* 2013; **15**: 1282-1291 [PMID: 24339740 DOI: 10.1593/neo.131362]

142 **Tsang DP**, Wu WK, Kang W, Lee YY, Wu F, Yu Z, Xiong L, Chan AW, Tong JH, Yang W, Li MS, Lau SS, Li X, Lee SD, Yang Y, Lai PB, Yu DY, Xu G, Lo KW, Chan MT, Wang H, Lee TL, Yu J, Wong N, Yip KY, To KF, Cheng AS. Yin Yang 1-mediated epigenetic silencing of tumour-suppressive microRNAs activates nuclear factor-κB in hepatocellular carcinoma. *J Pathol* 2016; **238**: 651-664 [PMID: 26800240 DOI: 10.1002/path.4688]

143 **Zhang H**, Huang C, Wang Y, Lu Z, Zhuang N, Zhao D, He J, Shi L. Hepatitis B Virus X Protein Sensitizes TRAIL-Induced Hepatocyte Apoptosis by Inhibiting the E3 Ubiquitin Ligase A20. *PLoS One* 2015; **10**: e0127329 [PMID: 25993287 DOI: 10.1371/journal.pone.0127329]

144 **Ferrari KJ**, Scelfo A, Jammula S, Cuomo A, Barozzi I, Stützer A, Fischle W, Bonaldi T, Pasini D. Polycomb-dependent H3K27me1 and H3K27me2 regulate active transcription and enhancer fidelity. *Mol Cell* 2014; **53**: 49-62 [PMID: 24289921 DOI: 10.1016/j.molcel.2013.10.030]

145 **Cai Y**, Zhang Y, Loh YP, Tng JQ, Lim MC, Cao Z, Raju A, Lieberman Aiden E, Li S, Manikandan L, Tergaonkar V, Tucker-Kellogg G, Fullwood MJ. H3K27me3-rich genomic regions can function as silencers to repress gene expression *via* chromatin interactions. *Nat Commun* 2021; **12**: 719 [PMID: 33514712 DOI: 10.1038/s41467-021-20940-y]

146 **Song K**, Han C, Zhang J, Lu D, Dash S, Feitelson M, Lim K, Wu T. Epigenetic regulation of MicroRNA-122 by peroxisome proliferator activated receptor-gamma and hepatitis b virus X protein in hepatocellular carcinoma cells. *Hepatology* 2013; **58**: 1681-1692 [PMID: 23703729 DOI: 10.1002/hep.26514]

147 **Feng H**, Yuan X, Wu S, Yuan Y, Cui L, Lin D, Peng X, Liu X, Wang F. Effects of writers, erasers and readers within miRNA-related m6A modification in cancers. *Cell Prolif* 2023; **56**: e13340 [PMID: 36162823 DOI: 10.1111/cpr.13340]

148 **Cheng D**, Wu C, Li Y, Liu Y, Mo J, Fu L, Peng S. METTL3 inhibition ameliorates liver damage in mouse with hepatitis B virus-associated acute-on-chronic liver failure by regulating miR-146a-5p maturation. *Biochim Biophys Acta Gene Regul Mech* 2022; **1865**: 194782 [PMID: 34968770 DOI: 10.1016/j.bbagrm.2021.194782]

149 **D'Ambrogio A**, Gu W, Udagawa T, Mello CC, Richter JD. Specific miRNA stabilization by Gld2-catalyzed monoadenylation. *Cell Rep* 2012; **2**: 1537-1545 [PMID: 23200856 DOI: 10.1016/j.celrep.2012.10.023]

150 **Peng F**, Xiao X, Jiang Y, Luo K, Tian Y, Peng M, Zhang M, Xu Y, Gong G. HBx down-regulated Gld2 plays a critical role in HBV-related dysregulation of miR-122. *PLoS One* 2014; **9**: e92998 [PMID: 24667324 DOI: 10.1371/journal.pone.0092998]

151 **Thomson DW**, Dinger ME. Endogenous microRNA sponges: evidence and controversy. *Nat Rev Genet* 2016; **17**: 272-283 [PMID: 27040487 DOI: 10.1038/nrg.2016.20]

152 **Lv J**, Fan HX, Zhao XP, Lv P, Fan JY, Zhang Y, Liu M, Tang H. Long non-coding RNA Unigene56159 promotes epithelial-mesenchymal transition by acting as a ceRNA of miR-140-5p in hepatocellular carcinoma cells. *Cancer Lett* 2016; **382**: 166-175 [PMID: 27597739 DOI: 10.1016/j.canlet.2016.08.029]

153 **Feng J**, Yang G, Liu Y, Gao Y, Zhao M, Bu Y, Yuan H, Yuan Y, Yun H, Sun M, Gao H, Zhang S, Liu Z, Yin M, Song X, Miao Z, Lin Z, Zhang X. LncRNA PCNAP1 modulates hepatitis B virus replication and enhances tumor growth of liver cancer. *Theranostics* 2019; **9**: 5227-5245 [PMID: 31410212 DOI: 10.7150/thno.34273]

154 **Fan H**, Lv P, Mu T, Zhao X, Liu Y, Feng Y, Lv J, Liu M, Tang H. LncRNA n335586/miR-924/CKMT1A axis contributes to cell migration and invasion in hepatocellular carcinoma cells. *Cancer Lett* 2018; **429**: 89-99 [PMID: 29753758 DOI: 10.1016/j.canlet.2018.05.010]

155 **Li L**, Han T, Liu K, Lei CG, Wang ZC, Shi GJ. LncRNA H19 promotes the development of hepatitis B related hepatocellular carcinoma through regulating microRNA-22 *via* EMT pathway. *Eur Rev Med Pharmacol Sci* 2019; **23**: 5392-5401 [PMID: 31298392 DOI: 10.26355/eurrev_201906_18208]

156 **Song W**, Zheng C, Liu M, Xu Y, Qian Y, Zhang Z, Su H, Li X, Wu H, Gong P, Li Y, Fan H. TRERNA1 upregulation mediated by HBx promotes sorafenib resistance and cell proliferation in HCC *via* targeting NRAS by sponging miR-22-3p. *Mol Ther* 2021; **29**: 2601-2616 [PMID: 33839325 DOI: 10.1016/j.ymthe.2021.04.011]

157 **He B**, Peng F, Li W, Jiang Y. Interaction of lncRNA-MALAT1 and miR-124 regulates HBx-induced cancer stem cell properties in HepG2 through PI3K/Akt signaling. *J Cell Biochem* 2019; **120**: 2908-2918 [PMID: 30500989 DOI: 10.1002/jcb.26823]

158 **Zhuang H**, Ma X, Liu X, Li C, Li X, Wu L, Wen M, Shi W, Yang X. Hyaluronan-mediated motility receptor antisense RNA 1 promotes hepatitis B virus-related hepatocellular carcinoma progression by regulating miR-627-3p/High Mobility Group AT-hook 2 axis. *Bioengineered* 2022; **13**: 8617-8630 [PMID: 35322735 DOI: 10.1080/21655979.2022.2054151]

159 **Huang P**, Xu Q, Yan Y, Lu Y, Hu Z, Ou B, Zhang H, Mao K, Zhang J, Wang J, Xiao Z. HBx/ERα complex-mediated LINC01352 downregulation promotes HBV-related hepatocellular carcinoma *via* the miR-135b-APC axis. *Oncogene* 2020; **39**: 3774-3789 [PMID: 32157216 DOI: 10.1038/s41388-020-1254-z]

160 **Deng Y**, Wei Z, Huang M, Xu G, Wei W, Peng B, Nong S, Qin H. Long non-coding RNA F11-AS1 inhibits HBV-related hepatocellular carcinoma progression by regulating NR1I3 *via* binding to microRNA-211-5p. *J Cell Mol Med* 2020; **24**: 1848-1865 [PMID: 31880390 DOI: 10.1111/jcmm.14881]

161 **Wang J**, Yin G, Bian H, Yang J, Zhou P, Yan K, Liu C, Chen P, Zhu J, Li Z, Xue T. LncRNA XIST upregulates TRIM25 *via* negatively regulating miR-192 in hepatitis B virus-related hepatocellular carcinoma. *Mol Med* 2021; **27**: 41 [PMID: 33858324 DOI: 10.1186/s10020-021-00278-3]

162 **Guo L**, Gao S, Sun W, Wang Y, Zhao J. Elevated LINC01232 is associated with poor prognosis and HBV infection in hepatocellular carcinoma patients and contributes to tumor progression in vitro. *Clin Res Hepatol Gastroenterol* 2022; **46**: 101813 [PMID: 34583064 DOI: 10.1016/j.clinre.2021.101813]

163 **Cheng Y**, Shi W, Cui X, Sun L, Nan Y, Yao H, Fan J, Zhu L, Yu L. Long Noncoding RNA TFAP2A-AS1 Suppressed Hepatitis B Virus Replication by Modulating miR-933/HDAC11. *Dis Markers* 2022; **2022**: 7733390 [PMID: 35478990 DOI: 10.1155/2022/7733390]

164 **Yu K**, Mei Y, Wang Z, Liu B, Deng M. LncRNA LINC00924 upregulates NDRG2 to inhibit epithelial-mesenchymal transition *via* sponging miR-6755-5p in hepatitis B virus-related hepatocellular carcinoma. *J Med Virol* 2022; **94**: 2702-2713 [PMID: 34997970 DOI: 10.1002/jmv.27578]

165 **Wei Y**, Tang X, Ren Y, Yang Y, Song F, Fu J, Liu S, Yu M, Chen J, Wang S, Zhang K, Tan Y, Han Z, Wei L, Zhang B, Cheng Z, Li L, Wang H. An RNA-RNA crosstalk network involving HMGB1 and RICTOR facilitates hepatocellular carcinoma tumorigenesis by promoting glutamine metabolism and impedes immunotherapy by PD-L1+ exosomes activity. *Signal Transduct Target Ther* 2021; **6**: 421 [PMID: 34916485 DOI: 10.1038/s41392-021-00801-2]

166 **Chen S**, Dong Z, Yang P, Wang X, Jin G, Yu H, Chen L, Li L, Tang L, Bai S, Yan H, Shen F, Cong W, Wen W, Wang H. Hepatitis B virus X protein stimulates high mobility group box 1 secretion and enhances hepatocellular carcinoma metastasis. *Cancer Lett* 2017; **394**: 22-32 [PMID: 28216372 DOI: 10.1016/j.canlet.2017.02.011]

167 **Rao X**, Lai L, Li X, Wang L, Li A, Yang Q. N(6) -methyladenosine modification of circular RNA circ-ARL3 facilitates Hepatitis B virus-associated hepatocellular carcinoma *via* sponging miR-1305. *IUBMB Life* 2021; **73**: 408-417 [PMID: 33372396 DOI: 10.1002/iub.2438]

168 **Chen Y**, Li S, Wei Y, Xu Z, Wu X. Circ-RNF13, as an oncogene, regulates malignant progression of HBV-associated hepatocellular carcinoma cells and HBV infection through ceRNA pathway of circ-RNF13/miR-424-5p/TGIF2. *Bosn J Basic Med Sci* 2021; **21**: 555-568 [PMID: 33714261 DOI: 10.17305/bjbms.2020.5266]

169 **Du N**, Li K, Wang Y, Song B, Zhou X, Duan S. CircRNA circBACH1 facilitates hepatitis B virus replication and hepatoma development by regulating the miR-200a-3p/MAP3K2 axis. *Histol Histopathol* 2022; **37**: 863-877 [PMID: 35352818 DOI: 10.14670/HH-18-452]

170 **Jiang W**, Wang L, Zhang Y, Li H. Circ-ATP5H Induces Hepatitis B Virus Replication and Expression by Regulating miR-138-5p/TNFAIP3 Axis. *Cancer Manag Res* 2020; **12**: 11031-11040 [PMID: 33173336 DOI: 10.2147/CMAR.S272983]

171 **He W**, Zhu X, Tang X, Xiang X, Yu J, Sun H. Circ_0027089 regulates NACC1 by targeting miR-136-5p to aggravate the development of hepatitis B virus-related hepatocellular carcinoma. *Anticancer Drugs* 2022; **33**: e336-e348 [PMID: 34419960 DOI: 10.1097/CAD.0000000000001211]

172 **Wang Y**, Jiang L, Ji X, Yang B, Zhang Y, Fu XD. Hepatitis B viral RNA directly mediates down-regulation of the tumor suppressor microRNA miR-15a/miR-16-1 in hepatocytes. *J Biol Chem* 2013; **288**: 18484-18493 [PMID: 23649629 DOI: 10.1074/jbc.M113.458158]

173 **Liu N**, Zhang J, Jiao T, Li Z, Peng J, Cui Z, Ye X. Hepatitis B virus inhibits apoptosis of hepatoma cells by sponging the MicroRNA 15a/16 cluster. *J Virol* 2013; **87**: 13370-13378 [PMID: 24089558 DOI: 10.1128/JVI.02130-13]

174 **Li C**, Wang Y, Wang S, Wu B, Hao J, Fan H, Ju Y, Ding Y, Chen L, Chu X, Liu W, Ye X, Meng S. Hepatitis B virus mRNA-mediated miR-122 inhibition upregulates PTTG1-binding protein, which promotes hepatocellular carcinoma tumor growth and cell invasion. *J Virol* 2013; **87**: 2193-2205 [PMID: 23221562 DOI: 10.1128/JVI.02831-12]

175 **Deng M**, Hou J, Hu J, Wang S, Chen M, Chen L, Ju Y, Li C, Meng S. Hepatitis B virus mRNAs functionally sequester let-7a and enhance hepatocellular carcinoma. *Cancer Lett* 2016; **383**: 62-72 [PMID: 27693636 DOI: 10.1016/j.canlet.2016.09.028]

176 **Takata A**, Otsuka M, Ohno M, Kishikawa T, Yoshikawa T, Koike K. Mutual antagonism between hepatitis B viral mRNA and host microRNA let-7. *Sci Rep* 2016; **6**: 23237 [PMID: 26979389 DOI: 10.1038/srep23237]

177 **Ochi M**, Otsuka M, Maruyama R, Koike K. HBx increases EGFR expression by inhibiting miR129-5p function. *Biochem Biophys Res Commun* 2020; **529**: 198-203 [PMID: 32703411 DOI: 10.1016/j.bbrc.2020.06.018]

178 **Lau CC**, Sun T, Ching AK, He M, Li JW, Wong AM, Co NN, Chan AW, Li PS, Lung RW, Tong JH, Lai PB, Chan HL, To KF, Chan TF, Wong N. Viral-human chimeric transcript predisposes risk to liver cancer development and progression. *Cancer Cell* 2014; **25**: 335-349 [PMID: 24582836 DOI: 10.1016/j.ccr.2014.01.030]

179 **Liang HW**, Wang N, Wang Y, Wang F, Fu Z, Yan X, Zhu H, Diao W, Ding Y, Chen X, Zhang CY, Zen K. Hepatitis B virus-human chimeric transcript HBx-LINE1 promotes hepatic injury *via* sequestering cellular microRNA-122. *J Hepatol* 2016; **64**: 278-291 [PMID: 26409216 DOI: 10.1016/j.jhep.2015.09.013]

180 **Levine B**, Kroemer G. Biological Functions of Autophagy Genes: A Disease Perspective. *Cell* 2019; **176**: 11-42 [PMID: 30633901 DOI: 10.1016/j.cell.2018.09.048]

181 **Lan SH**, Wu SY, Zuchini R, Lin XZ, Su IJ, Tsai TF, Lin YJ, Wu CT, Liu HS. Autophagy suppresses tumorigenesis of hepatitis B virus-associated hepatocellular carcinoma through degradation of microRNA-224. *Hepatology* 2014; **59**: 505-517 [PMID: 23913306 DOI: 10.1002/hep.26659]

182 **Gibbings D**, Mostowy S, Jay F, Schwab Y, Cossart P, Voinnet O. Selective autophagy degrades DICER and AGO2 and regulates miRNA

activity. *Nat Cell Biol* 2012; **14**: 1314-1321 [DOI: 10.1038/ncb2611]

183 **Ma NF**, Lau SH, Hu L, Xie D, Wu J, Yang J, Wang Y, Wu MC, Fung J, Bai X, Tzang CH, Fu L, Yang M, Su YA, Guan XY. COOH-terminal truncated HBV X protein plays key role in hepatocarcinogenesis. *Clin Cancer Res* 2008; **14**: 5061-5068 [PMID: 18698024 DOI: 10.1158/1078-0432.CCR-07-5082]

184 **Minarovits J**, Niller HH. Truncated oncoproteins of retroviruses and hepatitis B virus: A lesson in contrasts. *Infect Genet Evol* 2019; **73**: 342-357 [PMID: 31152910 DOI: 10.1016/j.meegid.2019.05.020]

185 **Liu F**, You X, Chi X, Wang T, Ye L, Niu J, Zhang X. Hepatitis B virus X protein mutant HBxΔ127 promotes proliferation of hepatoma cells through up-regulating miR-215 targeting PTPRT. *Biochem Biophys Res Commun* 2014; **444**: 128-134 [PMID: 24434140 DOI: 10.1016/j.bbrc.2014.01.004]

186 **Yip WK**, Cheng AS, Zhu R, Lung RW, Tsang DP, Lau SS, Chen Y, Sung JG, Lai PB, Ng EK, Yu J, Wong N, To KF, Wong VW, Sung JJ, Chan HL. Carboxyl-terminal truncated HBx regulates a distinct microRNA transcription program in hepatocellular carcinoma development. *PLoS One* 2011; **6**: e22888 [PMID: 21829663 DOI: 10.1371/journal.pone.0022888]

187 **Hou ZH**, Han QJ, Zhang C, Tian ZG, Zhang J. miR146a impairs the IFN-induced anti-HBV immune response by downregulating STAT1 in hepatocytes. *Liver Int* 2014; **34**: 58-68 [PMID: 23890093 DOI: 10.1111/liv.12244]

188 **Su IJ**, Wang LH, Hsieh WC, Wu HC, Teng CF, Tsai HW, Huang W. The emerging role of hepatitis B virus pre-S2 deletion mutant proteins in HBV tumorigenesis. *J Biomed Sci* 2014; **21**: 98 [PMID: 25316153 DOI: 10.1186/s12929-014-0098-7]

189 **Levrero M**, Zucman-Rossi J. Mechanisms of HBV-induced hepatocellular carcinoma. *J Hepatol* 2016; **64**: S84-S101 [PMID: 27084040 DOI: 10.1016/j.jhep.2016.02.021]

190 **Zhang Y**, Huang B, Wang HY, Chang A, Zheng XFS. Emerging Role of MicroRNAs in mTOR Signaling. *Cell Mol Life Sci* 2017; **74**: 2613-2625 [PMID: 28238105 DOI: 10.1007/s00018-017-2485-1]

191 **Murakami Y**, Yasuda T, Saigo K, Urashima T, Toyoda H, Okanoue T, Shimotohno K. Comprehensive analysis of microRNA expression patterns in hepatocellular carcinoma and non-tumorous tissues. *Oncogene* 2006; **25**: 2537-2545 [PMID: 16331254 DOI: 10.1038/sj.onc.1209283]

192 **Feitelson MA**, Lee J. Hepatitis B virus integration, fragile sites, and hepatocarcinogenesis. *Cancer Lett* 2007; **252**: 157-170 [PMID: 17188425 DOI: 10.1016/j.canlet.2006.11.010]

193 **Calin GA**, Sevignani C, Dumitru CD, Hyslop T, Noch E, Yendamuri S, Shimizu M, Rattan S, Bullrich F, Negrini M, Croce CM. Human microRNA genes are frequently located at fragile sites and genomic regions involved in cancers. *Proc Natl Acad Sci U S A* 2004; **101**: 2999-3004 [PMID: 14973191 DOI: 10.1073/pnas.0307323101]

194 **Yang L**, Ma Z, Wang D, Zhao W, Chen L, Wang G. MicroRNA-602 regulating tumor suppressive gene RASSF1A is overexpressed in hepatitis B virus-infected liver and hepatocellular carcinoma. *Cancer Biol Ther* 2010; **9**: 803-808 [PMID: 20364114 DOI: 10.4161/cbt.9.10.11440]

195 **Guo H**, Liu H, Mitchelson K, Rao H, Luo M, Xie L, Sun Y, Zhang L, Lu Y, Liu R, Ren A, Liu S, Zhou S, Zhu J, Zhou Y, Huang A, Wei L, Guo Y, Cheng J. MicroRNAs-372/373 promote the expression of hepatitis B virus through the targeting of nuclear factor I/B. *Hepatology* 2011; **54**: 808-819 [PMID: 21608007 DOI: 10.1002/hep.24441]

196 **Zhang B**, Han S, Feng B, Chu X, Chen L, Wang R. Hepatitis B virus X protein-mediated non-coding RNA aberrations in the development of human hepatocellular carcinoma. *Exp Mol Med* 2017; **49**: e293 [PMID: 28186085 DOI: 10.1038/emm.2016.177]

197 **Sartorius K**, Swadling L, An P, Makarova J, Winkler C, Chuturgoon A, Kramvis A. The Multiple Roles of Hepatitis B Virus X Protein (HBx) Dysregulated MicroRNA in Hepatitis B Virus-Associated Hepatocellular Carcinoma (HBV-HCC) and Immune Pathways. *Viruses* 2020; **12** [PMID: 32664401 DOI: 10.3390/v12070746]

198 **Sartorius K**, An P, Winkler C, Chuturgoon A, Li X, Makarova J, Kramvis A. The Epigenetic Modulation of Cancer and Immune Pathways in Hepatitis B Virus-Associated Hepatocellular Carcinoma: The Influence of HBx and miRNA Dysregulation. *Front Immunol* 2021; **12**: 661204 [PMID: 33995383 DOI: 10.3389/fimmu.2021.661204]

199 **Xie KL**, Zhang YG, Liu J, Zeng Y, Wu H. MicroRNAs associated with HBV infection and HBV-related HCC. *Theranostics* 2014; **4**: 1176-1192 [PMID: 25285167 DOI: 10.7150/thno.8715]

200 **Lee TK**, Guan XY, Ma S. Cancer stem cells in hepatocellular carcinoma - from origin to clinical implications. *Nat Rev Gastroenterol Hepatol* 2022; **19**: 26-44 [PMID: 34504325 DOI: 10.1038/s41575-021-00508-3]

201 **Zhang Z**, Han Y, Sun G, Liu X, Jia X, Yu X. MicroRNA-325-3p inhibits cell proliferation and induces apoptosis in hepatitis B virus-related hepatocellular carcinoma by down-regulation of aquaporin 5. *Cell Mol Biol Lett* 2019; **24**: 13 [PMID: 30805015 DOI: 10.1186/s11658-019-0137-1]

202 **Li R**, Xu T, Wang H, Wu N, Liu F, Jia X, Mi J, Lv J, Gao H. Dysregulation of the miR-325-3p/DPAGT1 axis supports HBV-positive HCC chemoresistance. *Biochem Biophys Res Commun* 2019; **519**: 358-365 [PMID: 31519321 DOI: 10.1016/j.bbrc.2019.08.116]

203 **Feng J**, Li J, Wu L, Yu Q, Ji J, Wu J, Dai W, Guo C. Emerging roles and the regulation of aerobic glycolysis in hepatocellular carcinoma. *J Exp Clin Cancer Res* 2020; **39**: 126 [PMID: 32631382 DOI: 10.1186/s13046-020-01629-4]

204 **Sangineto M**, Villani R, Cavallone F, Romano A, Loizzi D, Serviddio G. Lipid Metabolism in Development and Progression of Hepatocellular Carcinoma. *Cancers (Basel)* 2020; **12** [PMID: 32486341 DOI: 10.3390/cancers12061419]

205 **You X**, Liu F, Zhang T, Li Y, Ye L, Zhang X. Hepatitis B virus X protein upregulates oncogene Rab18 to result in the dysregulation of lipogenesis and proliferation of hepatoma cells. *Carcinogenesis* 2013; **34**: 1644-1652 [PMID: 23471881 DOI: 10.1093/carcin/bgt089]

206 **Cui M**, Wang Y, Sun B, Xiao Z, Ye L, Zhang X. MiR-205 modulates abnormal lipid metabolism of hepatoma cells *via* targeting acyl-CoA synthetase long-chain family member 1 (ACSL1) mRNA. *Biochem Biophys Res Commun* 2014; **444**: 270-275 [PMID: 24462768 DOI: 10.1016/j.bbrc.2014.01.051]

207 **Chen Y**, Tian Z. HBV-Induced Immune Imbalance in the Development of HCC. *Front Immunol* 2019; **10**: 2048 [PMID: 31507621 DOI: 10.3389/fimmu.2019.02048]

208 **Liu W**, Zheng X, Wang J, He Q, Li J, Zhang Z, Liu H. MicroRNA-138 Regulates T-Cell Function by Targeting PD-1 in Patients with Hepatitis B Virus-Related Liver Diseases. *Lab Med* 2021; **52**: 439-451 [PMID: 33410459 DOI: 10.1093/labmed/lmaa110]

209 **Yang P**, Li QJ, Feng Y, Zhang Y, Markowitz GJ, Ning S, Deng Y, Zhao J, Jiang S, Yuan Y, Wang HY, Cheng SQ, Xie D, Wang XF. TGF-β-miR-34a-CCL22 signaling-induced Treg cell recruitment promotes venous metastases of HBV-positive hepatocellular carcinoma. *Cancer Cell* 2012; **22**: 291-303 [PMID: 22975373 DOI: 10.1016/j.ccr.2012.07.023]

210 **Bian X**, Si Y, Zhang M, Wei R, Yang X, Ren H, Zheng G, Wang C, Zhang Y. Down-expression of miR-152 lead to impaired anti-tumor effect of NK *via* upregulation of HLA-G. *Tumour Biol* 2016; **37**: 3749-3756 [PMID: 26468017 DOI: 10.1007/s13277-015-3669-7]

211 **Sadri Nahand J**, Rabiei N, Fathazam R, Taghizadieh M, Ebrahimi MS, Mahjoubin-Tehran M, Bannazadeh Baghi H, Khatami A, Abbasi-Kolli M, Mirzaei HR, Rahimian N, Darvish M, Mirzaei H. Oncogenic viruses and chemoresistance: What do we know? *Pharmacol Res* 2021; **170**: 105730 [PMID: 34119621 DOI: 10.1016/j.phrs.2021.105730]

212 **Wei XC**, Xia YR, Zhou P, Xue X, Ding S, Liu LJ, Zhu F. Hepatitis B core antigen modulates exosomal miR-135a to target vesicle-associated membrane protein 2 promoting chemoresistance in hepatocellular carcinoma. *World J Gastroenterol* 2021; **27**: 8302-8322 [PMID: 35068871 DOI: 10.3748/wjg.v27.i48.8302]

213 **Chen WS**, Yen CJ, Chen YJ, Chen JY, Wang LY, Chiu SJ, Shih WL, Ho CY, Wei TT, Pan HL, Chien PH, Hung MC, Chen CC, Huang WC. miRNA-7/21/107 contribute to HBx-induced hepatocellular carcinoma progression through suppression of maspin. *Oncotarget* 2015; **6**: 25962-25974 [PMID: 26296971 DOI: 10.18632/oncotarget.4504]

214 **Zhang C**, Liu P, Zhang C. Hepatitis B virus X protein upregulates alpha-fetoprotein to promote hepatocellular carcinoma by targeting miR-1236 and miR-329. *J Cell Biochem* 2020; **121**: 2489-2499 [PMID: 31680299 DOI: 10.1002/jcb.29471]

215 **He B**, Zhao Z, Cai Q, Zhang Y, Zhang P, Shi S, Xie H, Peng X, Yin W, Tao Y, Wang X. miRNA-based biomarkers, therapies, and resistance in Cancer. *Int J Biol Sci* 2020; **16**: 2628-2647 [PMID: 32792861 DOI: 10.7150/ijbs.47203]

216 **Lamontagne J**, Steel LF, Bouchard MJ. Hepatitis B virus and microRNAs: Complex interactions affecting hepatitis B virus replication and hepatitis B virus-associated diseases. *World J Gastroenterol* 2015; **21**: 7375-7399 [PMID: 26139985 DOI: 10.3748/wjg.v21.i24.7375]

217 **Mosca N**, Castiello F, Coppola N, Trotta MC, Sagnelli C, Pisaturo M, Sagnelli E, Russo A, Potenza N. Functional interplay between hepatitis B virus X protein and human miR-125a in HBV infection. *Biochem Biophys Res Commun* 2014; **449**: 141-145 [PMID: 24824183 DOI: 10.1016/j.bbrc.2014.05.009]

218 **Potenza N**, Papa U, Mosca N, Zerbini F, Nobile V, Russo A. Human microRNA hsa-miR-125a-5p interferes with expression of hepatitis B virus surface antigen. *Nucleic Acids Res* 2011; **39**: 5157-5163 [PMID: 21317190 DOI: 10.1093/nar/gkr067]

219 **Wei X**, Xiang T, Ren G, Tan C, Liu R, Xu X, Wu Z. miR-101 is down-regulated by the hepatitis B virus x protein and induces aberrant DNA methylation by targeting DNA methyltransferase 3A. *Cell Signal* 2013; **25**: 439-446 [PMID: 23124077 DOI: 10.1016/j.cellsig.2012.10.013]

220 **Liu Y**, Lou G, Wu W, Zheng M, Shi Y, Zhao D, Chen Z. Involvement of the NF-κB pathway in multidrug resistance induced by HBx in a hepatoma cell line. *J Viral Hepat* 2011; **18**: e439-e446 [PMID: 21914061 DOI: 10.1111/j.1365-2893.2011.01463.x]

221 **Hu Z**, Yin Y, Jiang J, Yan C, Wang Y, Wang D, Li L. Exosomal miR-142-3p secreted by hepatitis B virus (HBV)-hepatocellular carcinoma (HCC) cells promotes ferroptosis of M1-type macrophages through SLC3A2 and the mechanism of HCC progression. *J Gastrointest Oncol* 2022; **13**: 754-767 [PMID: 35557596 DOI: 10.21037/jgo-21-916]

222 **Zhang Q**, Qu Y, Zhang Q, Li F, Li B, Li Z, Dong Y, Lu L, Cai X. Exosomes derived from hepatitis B virus-infected hepatocytes promote liver fibrosis *via* miR-222/TFRC axis. *Cell Biol Toxicol* 2023; **39**: 467-481 [PMID: 34978008 DOI: 10.1007/s10565-021-09684-z]

223 **Li CH**, Wang YJ, Dong W, Xiang S, Liang HF, Wang HY, Dong HH, Chen L, Chen XP. Hepatic oval cell lines generate hepatocellular carcinoma following transfection with HBx gene and treatment with aflatoxin B1 in vivo. *Cancer Lett* 2011; **311**: 1-10 [PMID: 21821357 DOI: 10.1016/j.canlet.2011.05.035]

224 **Chandrasekaran AR**, MacIsaac M, Dey P, Levchenko O, Zhou L, Andres M, Dey BK, Halvorsen K. Cellular microRNA detection with miRacles: microRNA- activated conditional looping of engineered switches. *Sci Adv* 2019; **5**: eaau9443 [PMID: 30891499 DOI: 10.1126/sciadv.aau9443]

225 **Guo T**, Tang XH, Gao XY, Zhou Y, Jin B, Deng ZQ, Hu Y, Xing XF, Li ZY, Ji JF. A liquid biopsy signature of circulating exosome-derived mRNAs, miRNAs and lncRNAs predict therapeutic efficacy to neoadjuvant chemotherapy in patients with advanced gastric cancer. *Mol Cancer* 2022; **21**: 216 [PMID: 36510184 DOI: 10.1186/s12943-022-01684-9]

226 **To NH**, Nguyen HQ, Thiolat A, Liu B, Cohen J, Radosevic-Robin N, Belkacemi Y; TransAtlantic Radiation Oncology Network (TRONE) & Association of Radiotherapy, and Oncology of the Mediterranean Area (AROME). Radiation therapy for triple-negative breast cancer: emerging role of microRNAs as biomarkers and radiosensitivity modifiers. A systematic review. *Breast Cancer Res Treat* 2022; **193**: 265-279 [PMID: 35397079 DOI: 10.1007/s10549-022-06533-3]

227 **Peng XX**, Yu R, Wu X, Wu SY, Pi C, Chen ZH, Zhang XC, Gao CY, Shao YW, Liu L, Wu YL, Zhou Q. Correlation of plasma exosomal microRNAs with the efficacy of immunotherapy in EGFR/ALK wild-type advanced non-small cell lung cancer. *J Immunother Cancer* 2020; **8** [PMID: 31959728 DOI: 10.1136/jitc-2019-000376]

228 **Li L**, Guo Z, Wang J, Mao Y, Gao Q. Serum miR-18a: a potential marker for hepatitis B virus-related hepatocellular carcinoma screening. *Dig Dis Sci* 2012; **57**: 2910-2916 [PMID: 22865399 DOI: 10.1007/s10620-012-2317-y]

229 **Zhao Q**, Sun X, Liu C, Li T, Cui J, Qin C. Expression of the microRNA-143/145 cluster is decreased in hepatitis B virus-associated hepatocellular carcinoma and may serve as a biomarker for tumorigenesis in patients with chronic hepatitis B. *Oncol Lett* 2018; **15**: 6115-6122 [PMID: 29616093 DOI: 10.3892/ol.2018.8117]

230 **Zhang Y**, Xi H, Nie X, Zhang P, Lan N, Lu Y, Liu J, Yuan W. Assessment of miR-212 and Other Biomarkers in the Diagnosis and Treatment of HBV-infection-related Liver Diseases. *Curr Drug Metab* 2019; **20**: 785-798 [PMID: 31608838 DOI: 10.2174/1389200220666191011120434]

231 **Wen Y**, Han J, Chen J, Dong J, Xia Y, Liu J, Jiang Y, Dai J, Lu J, Jin G, Wei Q, Shen H, Sun B, Hu Z. Plasma miRNAs as early biomarkers for detecting hepatocellular carcinoma. *Int J Cancer* 2015; **137**: 1679-1690 [PMID: 25845839 DOI: 10.1002/ijc.29544]

232 **Xiong F**, Ma H, Qu Y, Wen F, Bao X, Han D, Lu J. Profiles of serum miR-99a, let-7c and miR-125b in hepatitis B virus (HBV)-associated chronic hepatitis, liver cirrhosis and hepatocellular carcinoma. *Int J Clin Exp Pathol* 2016; **9**: 7087-7095

233 **Hung CH**, Hu TH, Lu SN, Kuo FY, Chen CH, Wang JH, Huang CM, Lee CM, Lin CY, Yen YH, Chiu YC. Circulating microRNAs as biomarkers for diagnosis of early hepatocellular carcinoma associated with hepatitis B virus. *Int J Cancer* 2016; **138**: 714-720 [PMID: 26264553 DOI: 10.1002/ijc.29802]

234 **Zhang W**, Fu T, Guo Z, Zhang Y, Zhang L, Su H, Long Y, Ji Z, Yan Y, Shao Z. Serum miR-375 Levels Are Closely Related to Disease Progression from HBV Infection to HBV-Related Hepatocellular Carcinoma. *Biomed Res Int* 2020; **2020**: 5819385 [PMID: 32382558 DOI: 10.1155/2020/5819385]

235 **Zhu HT**, Liu RB, Liang YY, Hasan AME, Wang HY, Shao Q, Zhang ZC, Wang J, He CY, Wang F, Shao JY. Serum microRNA profiles as diagnostic biomarkers for HBV-positive hepatocellular carcinoma. *Liver Int* 2017; **37**: 888-896 [PMID: 28061012 DOI: 10.1111/liv.13356]

World Journal of Gastroenterology

Submit a Manuscript: https://www.f6publishing.com

World J Gastroenterol 2023 August 21; 29(31): 4736-4743

DOI: 10.3748/wjg.v29.i31.4736

ISSN 1007-9327 (print) ISSN 2219-2840 (online)

MINIREVIEWS

Diabetes as a consequence of acute pancreatitis

Ericka Charley, Brett Dinner, Kimberly Pham, Neil Vyas

Specialty type: Gastroenterology and hepatology

Provenance and peer review: Unsolicited article; Externally peer reviewed.

Peer-review model: Single blind

Peer-review report's scientific quality classification

Grade A (Excellent): 0
Grade B (Very good): B
Grade C (Good): C
Grade D (Fair): 0
Grade E (Poor): 0

P-Reviewer: Mao EQ, China; Xiao B, China

Received: June 26, 2023
Peer-review started: June 26, 2023
First decision: July 5, 2023
Revised: July 17, 2023
Accepted: July 28, 2023
Article in press: July 28, 2023
Published online: August 21, 2023

Ericka Charley, Department of Gastroenterology, Creighton University - St. Joseph's Hospital and Medical Center Phoenix, AZ 85013, United States

Brett Dinner, Kimberly Pham, Department of Internal Medicine, Creighton University St. Joseph's Hospital and Medical Center, Phoenix, AZ 85013, United States

Neil Vyas, Department of Gastroenterology, Creighton University St. Joseph's Hospital and Medical Center, Phoenix, AZ 85013, United States

Corresponding author: Ericka Charley, MD, Gastroenterology Fellow Department of Gastroenterology, Creighton University - Phoenix, 350 W Thomas Road, Phoenix, AZ 85013, United States. erickaziggycharley@gmail.com

Abstract

Diabetes is a highly prevalent disease that was initially simplified into three major types: Type 1, type 2 and gestational diabetes. With the global rise in incidence of acute pancreatitis (AP), a lesser-known type of diabetes referred to as diabetes of the exocrine pancreas (DEP) is becoming more recognized. However, there is a poor understanding of the inherent relationship between diabetes and AP. There is established data about certain diseases affecting the exocrine function of the pancreas which can lead to diabetes. More specifically, there are well established guidelines for diagnosis and management of DEP caused be chronic pancreatitis. Conversely, the sequelae of AP leading to diabetes has limited recognition and data. The purpose of this review is to provide a comprehensive summary of the prevalence, epidemiology, pathophysiology and future research aims of AP-related diabetes. In addition, we propose a screening and diagnostic algorithm to aid clinicians in providing better care for their patients.

Key Words: Acute pancreatitis; Type 3c diabetes; Diabetes of the exocrine pancreas; Sequelae of acute pancreatitis; Screening and diagnostic algorithm

Core Tip: Acute pancreatitis (AP)-related diabetes has limited recognition and data. The disease occurs more often than previously recognized and patients are often misdiagnosed with type 2 diabetes. The purpose of this review is to provide a comprehensive summary of the prevalence, epidemiology, pathophysiology and future research aims of AP-related diabetes. In addition, we propose a screening and diagnostic algorithm to aid clinicians in providing better care for their patients.

Citation: Charley E, Dinner B, Pham K, Vyas N. Diabetes as a consequence of acute pancreatitis. *World J Gastroenterol* 2023; 29(31): 4736-4743
URL: https://www.wjgnet.com/1007-9327/full/v29/i31/4736.htm
DOI: https://dx.doi.org/10.3748/wjg.v29.i31.4736

INTRODUCTION

Acute pancreatitis (AP) is a condition defined by rapid onset pancreatic inflammation that is short-lived and may be associated with local and systemic complications[1]. Alcohol use and gallstones are the most common etiologies, which may explain its standing as one of the leading gastrointestinal diseases requiring hospitalization in the United States[2]. The severity of AP is graded based on the presence or absence of local complications, systemic complications, and persistent organ failure. Patients with mild disease recover with supportive care alone while those with severe disease may experience prolonged hospitalization and require procedural interventions to treat various complications. The severe form of the disease occurs in 20% of all patients with AP and carries a mortality rate as high as 30%-40%[1,3]. Following a single episode of AP, all patients are susceptible to the potential sequela of the injury sustained by the pancreas regardless of the severity of the episode[4]. The complication acquiring interest of late is new-onset diabetes mellitus (DM) after AP.

Diabetes is a term used to classify a group of diseases characterized by persistent hyperglycemia that afflicts 37 million adults in the United States alone. Type I diabetes (T1D) accounts for 5%-10% of the total prevalence of diabetes and is hypothesized to be a consequence of autoimmune destruction of beta cells, resulting in inadequate insulin levels[5]. The most common form of diabetes, type II DM (T2DM), is caused by insufficient insulin secretion by pancreatic beta cells and progressive development of insulin resistance (IR). Persistent impairment in glucose control may also be promoted by diseases of the exocrine pancreas, including AP[6]. This form of diabetes has been referred to as type 3c diabetes or diabetes of the exocrine pancreas (DEP)[6,7].

Hyperglycemia during AP was previously speculated to be a transient event that resolved as the inflammatory process improved[4]. Recent meta-analyses have questioned this notion by showing evidence of a high incidence of AP-related DM[4]. Two meta-analyses found 15%-23% of patients developed new-onset diabetes following a single episode of AP and the remaining patients had greater than a two-fold risk of diabetes over five years[8,9].

The various pancreatic diseases known to potentially cause DEP are often grouped together despite this collection encompassing multiple distinct conditions that should be further investigated on an individual basis. The unique mechanisms in which these conditions cause damage to the pancreas is important to take into consideration as they may allow for specific therapeutic options, change screening recommendations, and affect the length of time to diabetes. AP in particular, the most common disease of the exocrine pancreas, warrants further discussion. The goal of this review is to summarize the prevalence and pathophysiology of DEP after episode(s) of AP, elucidate diagnostic criteria for AP-related DM and identify risk factors of those at highest risk of developing the complication. We will also suggest management and screening recommendations, including the emergence of potential new ways to diagnose AP-related DM and identify areas for further study.

PREVALENCE OF DM AFTER AP

In the United States, AP is estimated to account for approximately 275000 hospital admissions and $2.5 billion in healthcare costs annually[10]. A meta-analysis of the global incidence of AP from 1961 to 2016 found the incidence of AP has been increasing over time. Select populations were noted to have disproportionate rises in incidence especially throughout the majority of countries within the Western world, including North America, Europe, and Oceania[3]. One study aimed at determining the global incidence of AP reported the countries with the greatest incidence of AP in 2019 were India, China, and the United States. Alcohol was found to be an important cause of increased morbidity and mortality. The study also uncovered the existence of significant differences in the burden of AP across geographic regions and differences in outcomes based on socioeconomic factors. For example, patients admitted to smaller hospitals with fewer resources were noted to have a higher risk of pancreatitis-related mortality[10].

The lesser-known sequelae of AP are the development of endocrine and exocrine insufficiency, which in turn can contribute to the development of diabetes. All patients are susceptible to these effects, even those with a mild case of AP and after a first-time episode[11]. In one cohort study, exocrine pancreatic dysfunction was associated with significantly increased risk for new-onset DM, including when the analysis was limited to mild AP[12]. A systematic review and meta-analysis from May 2019 found the incidence of AP-related DM was 23% and new onset insulin dependent DM (IDDM) was 15%. The incidence of DM was higher for severe AP (SAP) compared to mild AP, pancreatic necrosis compared to without, and alcoholic compared to biliary AP. The incidence of IDDM after SAP was 21% and 18% following an episode

of alcohol-related AP. Within five years of the initial episode of AP, the rate of DM and IDDM was 20% and 14%, respectively. The rate of DM and IDDM after AP increased to 37% and 25%, respectively[9]. Another study demonstrated similar findings of the development of endocrine and exocrine insufficiency despite severity of AP, number of or time from episodes of AP, gender, and etiology. However, there was a statistically significant difference in the prevalence of DM when patients with SAP were compared with non-SAP[12].

PATHOPHYSIOLOGY

Ongoing investigations have proposed multiple mechanisms believed to contribute to the development of AP-related DM. These mechanisms presumably occur in parallel and it is unknown which mechanism has the greatest impact. Prior to further discussing the theories it is important to understand the roles of the individual cell types of the pancreas and where they reside. This will aid in demonstrating the clinical implications of their malfunction or loss.

The pancreas consists of two tissue types which give rise to the distinct actions of the pancreas, the exocrine and endocrine functions. Exocrine tissue makes up an estimated 95% of the pancreas and produces enzymes necessary for digestion. The remaining tissue is made up of special endocrine cells embedded within the exocrine pancreas that are collectively known as the islets of Langerhans[13]. This collection consists of four cell types that play exclusive roles in regulating glucose levels and pancreatic secretions: Alpha cells, beta cells, pancreatic polypeptide (PP) cells and delta cells. Alpha cells release glucagon and make up 15% of the total islet cell volume in the anterior portions of the pancreas (head, body and tail). Glucagon is important in preventing hypoglycemia through several well-known mechanisms. Insulin-releasing beta cells make up 80% of the islet volume in the anterior pancreas and 20% of the volume in the posterior head. Insulin regulates glucose by promoting uptake and storage of glucose in the liver, muscle and adipose tissue. The hormone also regulates the action of alpha cells through paracrine inhibition. PP cells make up 80% of the islet volume in the posterior head and have a small presence (< 1%) in the anterior portions of the pancreas. They produce PP, which enhances the effect of insulin on the liver. Delta cells have a small overall existence, contributing to < 1% of islet volume in the posterior head and 5% in the anterior pancreas. Nevertheless, they are essential for their release of somatostatin which has multiple functions throughout the body. In the gastrointestinal system, somatostatin is important for regulating the release of glucagon and insulin through paracrine inhibition. The hormone also slows both gastric emptying and nutrient absorption from the intestinal tract[7].

MECHANICAL DESTRUCTION OF THE PANCREAS *VS* LOSS OF ISLET MASS

Unlike T1D and T2DM, DEP is a consequence of damage to the pancreas that affects all of the highly specialized cells of the organ. Based on this observation and previous data showing a higher incidence of DEP in patients suffering from necrotizing pancreatitis compared to those without necrosis, a correlation between the extent of loss of islet cells and the risk of developing AP-related DM has been suggested[9]. This inference has been further substantiated by evidence that patients with T1D and T2DM have decreased pancreatic volume compared to non-diabetics[14]. Nevertheless, emerging evidence indicates the overall pathogenesis is likely more complicated and requires more investigation. One systematic review examining the risk of developing DM after partial pancreatectomy found the incidence of new-onset DM was significantly different between various types of resection. Those who underwent a distal pancreatectomy had the highest incidence of developing DEP followed by patients who underwent a Whipple. Patients who underwent a central pancreatectomy had the smallest incidence[15]. A study by Tu *et al*[16] reports that in comparison to necrosis in the head and body of the pancreas, necrosis in the tail was associated with a greater risk of developing diabetes. Others also report that surgical resection of up to 50% of the pancreas did not necessarily lead to diabetes[14]. These new findings may explain why the severity of AP does not necessarily positively correlate with the risk of developing AP-related DM.

DYSFUNCTION OF THE EXOCRINE PANCREAS

Damage to the exocrine pancreas may contribute to endocrine dysfunction through mechanisms still undergoing analysis. When chronic pancreatic exocrine disease occurs, findings of decreased pancreatic endocrine function including islet function and insulin secretion can be seen. For example, one of the results of chronic pancreatitis is damage to nerve bundles, specifically vagal afferents, which are necessary for PP secretion. Volume loss within the posterior head of the pancreas, in which resides the majority of PP cells, further exacerbates the reduction in insulin secretion. Significant pancreatic endocrine dysfunction can thereby lead to DEP[14].

In a recent cohort study, Cho *et al*[12] found that patients with exocrine pancreatic dysfunction requiring pancreatic enzyme replacement therapy (PERT) after their initial attack of pancreatitis were at increased risk of new-onset DM. New-onset DM was defined as diagnostic coding of DM and/or receiving a new oral hypoglycemic medication. This association remained even when the analysis was limited to mild AP. Patients with exocrine dysfunction are prone to deficiencies in fat-soluble vitamins.

In the past, vitamin D was found to play a role in glucose control. Mirhosseini *et al*[17] describe the mechanism in a meta-analysis, reporting that the active form of vitamin D regulates the expression of the insulin receptor gene and facilitates the transport of glucose into muscle cells. The authors conclude that vitamin D supplementation may

significantly reduce serum fasting plasma glucose (FPG) and hemoglobin A1c (HbA1c)[17]. However, study results regarding the association of vitamin D and glucose control have been inconsistent. One randomized placebo-controlled trial found that daily vitamin D and calcium supplementation did not have a significant effect on insulin sensitivity, insulin secretion, or β-cell function in vitamin D deficient individuals at risk of T2DM[18]. An important point to note is that the authors classified patients "at risk of T2DM" based on a diabetes risk questionnaire. In a *post hoc* analysis restricted to patients with clinically diagnosed prediabetes, they found a significant beneficial effect of vitamin D and calcium supplementation on insulin sensitivity. There were no changes in insulin secretion or beta cell function.

In a more recent study, Norbitt *et al*[19] investigated potential connections between the intake of fat- and water-soluble vitamins with markers of glucose metabolism in patients after AP. They found a significant association between three fat-soluble vitamins (α-carotene, β-carotene, and total carotene) and homeostasis model assessment of β-cell function (HOMA-β) in patients with new-onset prediabetes/diabetes after AP[19]. Despite this association, there were no significant associations with FPG or HOMA-IR index. Although more studies are needed to help uncover the role of vitamin deficiencies in oxidative stress-driven disorders, it appears that optimizing the exocrine function of the pancreas plays an important role in glucose control. This may provide a key opportunity for intervention to prevent AP-related DM.

RISK FACTORS

An important component of understanding the etiology of AP-related DM is identifying risk factors linked with heightened endocrine dysfunction after AP. One case-controlled study with multivariable analysis found AP-related DM occurred more often in patients with components of metabolic syndrome such as hypertension, obesity and hyperlipidemia[20]. The potential explanation is that this particular population has an underlying predisposition toward T2DM and the additional insult of AP accelerates the progression to sustained hyperglycemia[21,22]. In another study, Lv *et al* [23] found similar results but also discovered non-alcoholic fatty liver disease (NAFLD) was an additional independent risk factor. Until now, most studies have focused on the effect of the exocrine pancreas on endocrine function yet the liver also plays a critical role in regulating and maintaining glucose levels. Those with NAFLD have underlying IR due to chronic inflammation from the release of inflammatory mediators by adipose tissue. These mediators which include leucine-rich alpha-2-glycoprotein 1 and interleukin-6 have been found to inhibit insulin receptors and the action of insulin through different signaling pathways[23]. The authors suggest chronic inflammation combined with inflammation-induced lipolysis contribute to the process of IR. Investigations to further characterize risk factors for AP-related DM are needed to help identify patients who will benefit from closer follow-up and earlier interventions to control glucose levels following an episode of AP.

DIAGNOSIS

Diagnostic criteria for T1D and T2DM have been well established and have undergone very minor revision over the last decades. The diagnosis of DEP has been more challenging to standardize as it shares clinical features that overlap with T1D and T2DM. The development of standardized criteria is also complicated by the fact that DEP is the result of multiple clinically distinct diseases and/or mechanisms. These individual etiologies lead to variable levels of pancreatic dysfunction and have varying rates of progression to diabetes, making the timing of the initiation of screening difficult to determine[7,24]. Previously, Ewald and Bretzel[25] suggested the following to diagnose DEP: Major criteria (all must be fulfilled): Presence of exocrine pancreatic insufficiency (according to the monoclonal fecal elastase-1 test or direct function tests); pathological pancreatic imaging (endoscopic ultrasound, magnetic resonance imaging, computed tomography); absence of T1DM associated autoimmune markers. Minor criteria: Impaired beta cell function (*e.g.*, HOMA-B, C-peptide/glucose-ratio); no excessive IR (*e.g.*, HOMA-IR); impaired incretin secretion [*e.g.*, glucagon-like peptide 1 (GLP-1), PP]; low serum levels of lipid-soluble vitamins (A, D, E, and K).

Although cited in numerous articles over the years, the criteria were never universally accepted. As we learn more about the underlying mechanisms of each disease process and how they may lead to DEP, most of the above criteria have become invalid. For example, pancreatic insufficiency is not a specific characteristic of any of the diseases of the exocrine pancreas. Pancreatic insufficiency is a risk factor for the development of DEP and therefore should not be considered a defining characteristic. Additionally, pathological pancreatic imaging varies among the different diseases and is not a reliable marker of pancreatic function. Not all patients with imaging findings consistent with necrotizing pancreatitis develop DEP. Patients with mild pancreatitis may lack significant radiographic findings yet are still at risk of developing DEP. Furthermore, patients with pancreatic adenocarcinoma are commonly diagnosed with diabetes prior to developing cancer visible on cross-sectional imaging[26].

Here, we will focus on screening and diagnosis of AP-related diabetes (Figure 1). The first step should be to rule out undiagnosed diabetes/prediabetes by obtaining an HbA1c on admission for AP. We recommend screening for diabetes three months after hospital discharge by obtaining an HbA1c and an oral glucose tolerance test (OGTT). The timing of screening at three months post-hospitalization was selected to limit confounding by stress-related hyperglycemia and to help ensure that the HbA1c is an accurate reflection of changes in glucose levels after AP. Recommendations to use an OGTT are based on several observations. First, studies have shown poor test performance of HbA1c in diagnosing diabetes in patients with cystic fibrosis, another well-known disease affecting the exocrine pancreas. As a result, screening guidelines for cystic fibrosis-related diabetes recommend use of OGTT over HbA1c, and the committee concluded HbA1c

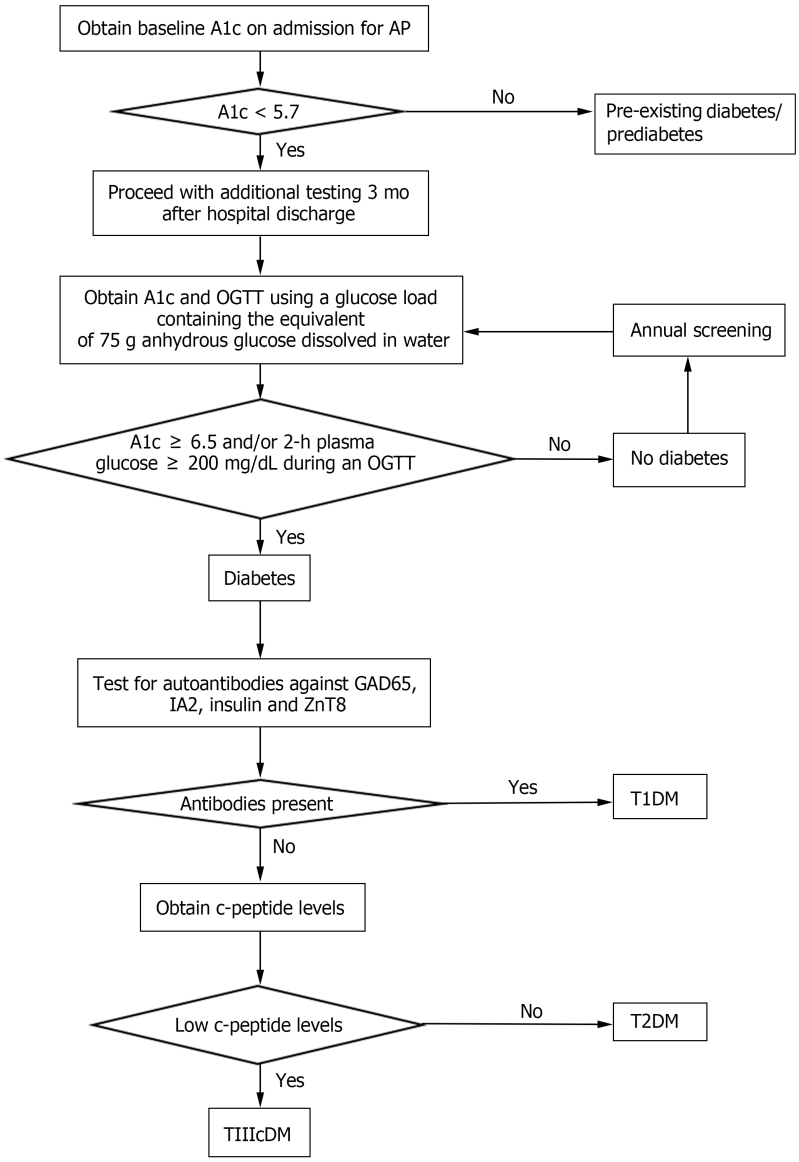

DOI: 10.3748/wjg.v29.i31.4736

Figure 1 Diagnostic algorithm for acute pancreatitis related diabetes. OGTT: Oral glucose tolerance test; GAD65: Glutamic acid decarboxylase; IA2: Tyrosine phosphatase; ZnT8: Zinc transporter 8; T1DM: Type 1 diabetes mellitus; AP: Acute pancreatitis.

was not sufficiently sensitive for diagnosis of diabetes in this patient population[27]. Similarly, Meier and Giese[28] advocate for the use of OGTT for earlier detection of diabetes in those with pancreatic disease. They found the OGTT diagnosed diabetes when the beta cell area was reduced by 64% compared to a more sizeable beta cell area loss of 89% when diabetes was diagnosed by HbA1c. A more recent study found that fasting glucose and HbA1c underestimate the prevalence of DEP and also recommend use of OGTT[29]. In this study, the diagnosis of over half of the new cases of diabetes after SAP were only possible by using the OGTT.

Once a diagnosis of diabetes is established, the next steps involve ruling out T1D and T2DM. The exclusion of T1D is more straightforward and can be performed by demonstrating the absence of autoantibodies. Duggan *et al*[29] suggest that c-peptide levels may be used to differentiate DEP and T2DM. Levels of c-peptide are typically used to distinguish T1D from T2DM, as levels are low in T1D and high in T2DM. They found that SAP patients with diabetes demonstrated a lower insulin response to glucose ingestion and had lower c-peptide secretion. This suggests the diagnosis of AP-related DM/DEP should be made in the setting of low c-peptide levels and the absence of autoantibodies[29]. More studies are needed to confirm the correlation, but it is a reasonable place to start. As studies showed risk of developing DEP up to five years after a single attack, it would be reasonable to consider continuing annual screening with HbA1c and OGTT *vs* more frequently depending on the presence of other risk factors.

MANAGEMENT

While the overall pathophysiology of DEP is far more complex than the more common types of diabetes, the treatment

algorithms for T2DM are often applied for management of DEP. This may be problematic on several fronts. Studies have shown that patients with CP have an increased risk of developing pancreatic adenocarcinoma through a mechanism potentiated by hyperinsulinemia[2,7,30]. As a result, interventions that reduce ambient insulin levels (*i.e.*, exercise, weight loss, low-carb diet) coupled with the anti-neoplastic properties of Metformin has become the preferred first-line treatment option. If glucose levels remain elevated it is reasonable to consider the addition of oral agents from the thiazolidinedione and/or alpha-glucosidase inhibitor classes. Clinical trials evaluating the safety of sulfonylureas, GLP-1 analogs, and dipeptidyl peptidase-IV inhibitors are lacking and these medications should be avoided due to possible association with pancreatitis[7,30]. All patients should also be counseled on the importance of abstinence from alcohol and tobacco use.

Screening for malabsorption and fat-soluble vitamin deficiencies can help guide the initiation of PERT and vitamin supplementation. The response and release of incretins, such as GLP-1, to fat hydrolysis may even be impaired with subclinical fat-soluble vitamin deficiency and thereby promote post-prandial hyperglycemia. PERT may augment the post-prandial incretin response and has been demonstrated to stabilize glucose levels in patients with alcoholic pancreatitis and cystic fibrosis. Additionally, some believe that PERT may help improve pain associated with pancreatitis.

Every effort should be made to detect AP-related DM before the development of critical insulin deficiency. If insulin therapy is necessary, it is important to remember that DEP may cause enhanced peripheral sensitivity to insulin, increasing the risk of hypoglycemia[7,30]. Dosing calculations similar to those used for T1D should be used rather than those used for T2DM[7]. Additionally, patients with DEP may require more frequent dose adjustments compared to patients with T2DM.

FUTURE RESEARCH

Further investigation should focus on how to use IR and insufficient insulin production to distinguish T2DM from DEP. Although we have proposed a set of diagnostic criteria, further research is needed to confirm whether the absence of autoantibodies in conjunction with low c-peptide levels is enough to diagnose DEP. Additionally, exploration into the possible contribution of PP cell tracking and other biomarkers to characterize DEP is necessary[4].

Improved characterization of alpha cells, beta cells, PP cells and delta cells may also have implications on the diagnosis and treatment of DEP[4]. Methods to do so may include new radiological techniques as well as neural networks. Newer advanced magnetic resonance techniques, including diffusion-weighted imaging, T1 mapping, and T2 mapping, provide quantifiable imaging features to gain additional understanding of underlying irregularities in AP. This goes beyond the traditional magnetic resonance sequences' qualitative imaging features to detect morphological changes in AP[31]. Further, these newer radiological techniques may be able to improve the detection of islet volume changes involved in DEP. Advanced analytic techniques, including radiomics and artificial neural networks, may be able to uncover imaging biomarkers to enable further risk stratification of DEP secondary to AP.

Artificial intelligence (AI) offers risk stratification and prognostication information for AP, including DEP secondary to AP. Machine learning through large data sets may be able to better determine an association between AP disease severity and DEP. An ongoing clinical trial is investigating whether AI machine learning can be used to estimate the disease severity in AP according to the revised Atlanta criteria, which may have implications on DEP[32]. Similarly, while parameters used in handcrafted AP severity prediction scores, such as APACHE II and Ranson, are typically unavailable until 24 to 72 h after hospitalization, the early achievable severity index prediction score which was developed using machine learning, can identify patients at high risk for SAP within 24 h of hospital admission[33]. Early identification of patients at risk of SAP allows for early interventions to decrease mortality, which may also be critical in preventing the development of DEP.

As deficiency of fat-soluble vitamins associated with exocrine pancreatic dysfunction may be linked to new-onset DM, early administration of fat-soluble vitamins needs to be further studied as a possible preventative measure against the development of DEP[12]. Additionally, serum levels of fat-soluble vitamins (vitamin D in particular) may have the potential to be used as markers of risk of AP-related DM, as mentioned by Norbitt *et al*[19]. The connection comes from previous findings that vitamin D levels negatively correlated with AP severity indexes[19,34].

Based on the data mentioned earlier, the incidence of AP continues to rise and we should anticipate an increasing incidence of AP-related DM. This escalates the importance of needing to screen for, monitor, and treat DEP[3]. The next major step in research should also include investigating the reasons for the increased incidence of AP to prevent the disease and DEP by extension.

CONCLUSION

AP is the most common disease of the exocrine pancreas and places a significant strain on healthcare costs as the incidence continues to rise. While many studies have focused on treatment during hospitalization, the sequela of the disease are becoming more important as more patients develop AP and recover from the disease. AP-related diabetes, a type of DEP, is likely more prevalent than initially thought as it is often misclassified as T2DM and treated as such. As new studies emerge, we have learned that the diagnostic criteria for AP-related diabetes needs to be better defined in order to improve management of this unique type of diabetes. Through common knowledge of the pathophysiology of T1D and T2DM and the review of newer studies attempting to find biomarkers to help characterize DEP, we were able to propose a set of diagnostic criteria for AP-related DM. Although studies are needed to test the utility, this may at least provide a starting point. Furthermore, we have identified specific areas in need of further research in hopes that it may

help lead to the development of guidelines for the diagnosis and management of AP-related DM.

FOOTNOTES

Author contributions: Charley E contributed to the final review; Charley E and Dinner B composed the paper; Dinner B added to the literature review and created the included figure; Charley E and Pham K conducted the literature review; Pham K made critical revisions; Vyas N provided mentorship, contributed to the overall concept and made critical revisions; and all authors have read and approve the final manuscript.

Conflict-of-interest statement: All the authors report no relevant conflicts of interest for this article.

Country/Territory of origin: United States

ORCID number: Ericka Charley 0009-0004-3647-2971; Neil Vyas 0000-0002-0166-3928.

S-Editor: Wang JJ
L-Editor: A
P-Editor: Cai YX

REFERENCES

1 **Garg PK**, Singh VP. Organ Failure Due to Systemic Injury in Acute Pancreatitis. *Gastroenterology* 2019; **156**: 2008-2023 [PMID: 30768987 DOI: 10.1053/j.gastro.2018.12.041]
2 **Gapp J**, Tariq A, Chandra S. Acute Pancreatitis. 2023 Feb 9. In: StatPearls [Internet]. Treasure Island (FL): StatPearls Publishing; 2023 Jan- [PMID: 29494075]
3 **Iannuzzi JP**, King JA, Leong JH, Quan J, Windsor JW, Tanyingoh D, Coward S, Forbes N, Heitman SJ, Shaheen AA, Swain M, Buie M, Underwood FE, Kaplan GG. Global Incidence of Acute Pancreatitis Is Increasing Over Time: A Systematic Review and Meta-Analysis. *Gastroenterology* 2022; **162**: 122-134 [PMID: 34571026 DOI: 10.1053/j.gastro.2021.09.043]
4 **Hart PA**, Bradley D, Conwell DL, Dungan K, Krishna SG, Wyne K, Bellin MD, Yadav D, Andersen DK, Serrano J, Papachristou GI. Diabetes following acute pancreatitis. *Lancet Gastroenterol Hepatol* 2021; **6**: 668-675 [PMID: 34089654 DOI: 10.1016/S2468-1253(21)00019-4]
5 **Centers for Disease Control and Prevention**. What Is Diabetes? [cited 26 November 2022]. Available from: https://www.cdc.gov/diabetes/basics/diabetes.html
6 **Hart PA**, Bellin MD, Andersen DK, Bradley D, Cruz-Monserrate Z, Forsmark CE, Goodarzi MO, Habtezion A, Korc M, Kudva YC, Pandol SJ, Yadav D, Chari ST; Consortium for the Study of Chronic Pancreatitis, Diabetes, and Pancreatic Cancer(CPDPC). Type 3c (pancreatogenic) diabetes mellitus secondary to chronic pancreatitis and pancreatic cancer. *Lancet Gastroenterol Hepatol* 2016; **1**: 226-237 [PMID: 28404095 DOI: 10.1016/S2468-1253(16)30106-6]
7 **Wynne K**, Devereaux B, Dornhorst A. Diabetes of the exocrine pancreas. *J Gastroenterol Hepatol* 2019; **34**: 346-354 [PMID: 30151918 DOI: 10.1111/jgh.14451]
8 **Das SL**, Singh PP, Phillips AR, Murphy R, Windsor JA, Petrov MS. Newly diagnosed diabetes mellitus after acute pancreatitis: a systematic review and meta-analysis. *Gut* 2014; **63**: 818-831 [PMID: 23929695 DOI: 10.1136/gutjnl-2013-305062]
9 **Zhi M**, Zhu X, Lugea A, Waldron RT, Pandol SJ, Li L. Incidence of New Onset Diabetes Mellitus Secondary to Acute Pancreatitis: A Systematic Review and Meta-Analysis. *Front Physiol* 2019; **10**: 637 [PMID: 31231233 DOI: 10.3389/fphys.2019.00637]
10 **Li CL**, Jiang M, Pan CQ, Li J, Xu LG. The global, regional, and national burden of acute pancreatitis in 204 countries and territories, 1990-2019. *BMC Gastroenterol* 2021; **21**: 332 [PMID: 34433418 DOI: 10.1186/s12876-021-01906-2]
11 **Mederos MA**, Reber HA, Girgis MD. Acute Pancreatitis: A Review. *JAMA* 2021; **325**: 382-390 [PMID: 33496779 DOI: 10.1001/jama.2020.20317]
12 **Cho J**, Scragg R, Pandol SJ, Petrov MS. Exocrine Pancreatic Dysfunction Increases the Risk of New-Onset Diabetes Mellitus: Results of a Nationwide Cohort Study. *Clin Transl Sci* 2021; **14**: 170-178 [PMID: 32692901 DOI: 10.1111/cts.12837]
13 **Columbia Surgery**. The pancreas and its functions. [cited 15 November 2022]. Available from: https://columbiasurgery.org/pancreas/pancreas-and-its-functions
14 **Rickels MR**, Norris AW, Hull RL. A tale of two pancreases: exocrine pathology and endocrine dysfunction. *Diabetologia* 2020; **63**: 2030-2039 [PMID: 32894313 DOI: 10.1007/s00125-020-05210-8]
15 **Wu L**, Nahm CB, Jamieson NB, Samra J, Clifton-Bligh R, Mittal A, Tsang V. Risk factors for development of diabetes mellitus (Type 3c) after partial pancreatectomy: A systematic review. *Clin Endocrinol (Oxf)* 2020; **92**: 396-406 [PMID: 32017157 DOI: 10.1111/cen.14168]
16 **Tu J**, Zhang J, Ke L, Yang Y, Yang Q, Lu G, Li B, Tong Z, Li W, Li J. Endocrine and exocrine pancreatic insufficiency after acute pancreatitis: long-term follow-up study. *BMC Gastroenterol* 2017; **17**: 114 [PMID: 29078749 DOI: 10.1186/s12876-017-0663-0]
17 **Mirhosseini N**, Vatanparast H, Mazidi M, Kimball SM. The Effect of Improved Serum 25-Hydroxyvitamin D Status on Glycemic Control in Diabetic Patients: A Meta-Analysis. *J Clin Endocrinol Metab* 2017; **102**: 3097-3110 [PMID: 28957454 DOI: 10.1210/jc.2017-01024]
18 **Gagnon C**, Daly RM, Carpentier A, Lu ZX, Shore-Lorenti C, Sikaris K, Jean S, Ebeling PR. Effects of combined calcium and vitamin D supplementation on insulin secretion, insulin sensitivity and β-cell function in multi-ethnic vitamin D-deficient adults at risk for type 2

diabetes: a pilot randomized, placebo-controlled trial. *PLoS One* 2014; **9**: e109607 [PMID: 25299668 DOI: 10.1371/journal.pone.0109607]

19 **Norbitt CF**, Kimita W, Bharmal SH, Ko J, Petrov MS. Relationship between Habitual Intake of Vitamins and New-Onset Prediabetes/Diabetes after Acute Pancreatitis. *Nutrients* 2022; **14** [PMID: 35406092 DOI: 10.3390/nu14071480]

20 **Firkins SA**, Hart PA, Papachristou GI, Lara LF, Cruz-Monserrate Z, Hinton A, Conwell DL, Bradley DP, Krishna SG. Identification of a Risk Profile for New-Onset Diabetes After Acute Pancreatitis. *Pancreas* 2021; **50**: 696-703 [PMID: 34016890 DOI: 10.1097/MPA.0000000000001818]

21 **Goodarzi MO**, Petrov MS, Andersen DK, Hart PA. Diabetes in chronic pancreatitis: risk factors and natural history. *Curr Opin Gastroenterol* 2021; **37**: 526-531 [PMID: 34074860 DOI: 10.1097/MOG.0000000000000756]

22 **Woodmansey C**, McGovern AP, McCullough KA, Whyte MB, Munro NM, Correa AC, Gatenby PAC, Jones SA, de Lusignan S. Incidence, Demographics, and Clinical Characteristics of Diabetes of the Exocrine Pancreas (Type 3c): A Retrospective Cohort Study. *Diabetes Care* 2017; **40**: 1486-1493 [PMID: 28860126 DOI: 10.2337/dc17-0542]

23 **Lv Y**, Zhang J, Yang T, Sun J, Hou J, Chen Z, Yu X, Yuan X, Lu X, Xie T, Yu T, Su X, Liu G, Zhang C, Li L. Non-Alcoholic Fatty Liver Disease (NAFLD) Is an Independent Risk Factor for Developing New-Onset Diabetes After Acute Pancreatitis: A Multicenter Retrospective Cohort Study in Chinese Population. *Front Endocrinol (Lausanne)* 2022; **13**: 903731 [PMID: 35692404 DOI: 10.3389/fendo.2022.903731]

24 **Richardson A**, Park WG. Acute pancreatitis and diabetes mellitus: a review. *Korean J Intern Med* 2021; **36**: 15-24 [PMID: 33147904 DOI: 10.3904/kjim.2020.505]

25 **Ewald N**, Bretzel RG. Diabetes mellitus secondary to pancreatic diseases (Type 3c)--are we neglecting an important disease? *Eur J Intern Med* 2013; **24**: 203-206 [PMID: 23375619 DOI: 10.1016/j.ejim.2012.12.017]

26 **Petrov MS**, Basina M. DIAGNOSIS OF ENDOCRINE DISEASE: Diagnosing and classifying diabetes in diseases of the exocrine pancreas. *Eur J Endocrinol* 2021; **184**: R151-R163 [PMID: 33460395 DOI: 10.1530/EJE-20-0974]

27 **Moran A**, Brunzell C, Cohen RC, Katz M, Marshall BC, Onady G, Robinson KA, Sabadosa KA, Stecenko A, Slovis B; CFRD Guidelines Committee. Clinical care guidelines for cystic fibrosis-related diabetes: a position statement of the American Diabetes Association and a clinical practice guideline of the Cystic Fibrosis Foundation, endorsed by the Pediatric Endocrine Society. *Diabetes Care* 2010; **33**: 2697-2708 [PMID: 21115772 DOI: 10.2337/dc10-1768]

28 **Meier JJ**, Giese A. Diabetes associated with pancreatic diseases. *Curr Opin Gastroenterol* 2015; **31**: 400-406 [PMID: 26125315 DOI: 10.1097/MOG.0000000000000199]

29 **Duggan SN**, O'Connor DB, Antanaitis A, Campion JR, Lawal O, Ahmed M, Tisdall AR, Sherlock M, Boran G, le Roux C, Gibney J, Conlon KC. Metabolic dysfunction and diabetes mellitus during long-term follow-up of severe acute pancreatitis: A case-matched study. *Pancreatology* 2020; **20**: 813-821 [PMID: 32522508 DOI: 10.1016/j.pan.2020.03.016]

30 **Cui Y**, Andersen DK. Pancreatogenic diabetes: special considerations for management. *Pancreatology* 2011; **11**: 279-294 [PMID: 21757968 DOI: 10.1159/000329188]

31 **Ghandili S**, Shayesteh S, Fouladi DF, Blanco A, Chu LC. Emerging imaging techniques for acute pancreatitis. *Abdom Radiol (NY)* 2020; **45**: 1299-1307 [PMID: 31428811 DOI: 10.1007/s00261-019-02192-z]

32 **İnce AT**. Artificial Intelligence Prediction for the Severity of Acute Pancreatitis. [accessed 2023 Jan 24]. In: ClinicalTrials.gov [Internet]. Bethesda (MD): U.S. National Library of Medicine. Available from: https://clinicaltrials.gov/study/NCT04735055 ClinicalTrials.gov Identifier: NCT04735055

33 **Kui B**, Pintér J, Molontay R, Nagy M, Farkas N, Gede N, Vincze Á, Bajor J, Gódi S, Czimmer J, Szabó I, Illés A, Sarlós P, Hágendorn R, Pár G, Papp M, Vitális Z, Kovács G, Fehér E, Földi I, Izbéki F, Gajdán L, Fejes R, Németh BC, Török I, Farkas H, Mickevicius A, Sallinen V, Galeev S, Ramírez-Maldonado E, Párniczky A, Erőss B, Hegyi PJ, Márta K, Váncsa S, Sutton R, Szatmary P, Latawiec D, Halloran C, de-Madaria E, Pando E, Alberti P, Gómez-Jurado MJ, Tantau A, Szentesi A, Hegyi P; Hungarian Pancreatic Study Group. EASY-APP: An artificial intelligence model and application for early and easy prediction of severity in acute pancreatitis. *Clin Transl Med* 2022; **12**: e842 [PMID: 35653504 DOI: 10.1002/ctm2.842]

34 **Huh JH**, Kim JW, Lee KJ. Vitamin D deficiency predicts severe acute pancreatitis. *United European Gastroenterol J* 2019; **7**: 90-95 [PMID: 30788120 DOI: 10.1177/2050640618811489]

World Journal of Gastroenterology

Submit a Manuscript: https://www.f6publishing.com

World J Gastroenterol 2023 August 21; 29(31): 4744-4762

DOI: 10.3748/wjg.v29.i31.4744

ISSN 1007-9327 (print) ISSN 2219-2840 (online)

ORIGINAL ARTICLE

Basic Study

Huangqin decoction alleviates lipid metabolism disorders and insulin resistance in nonalcoholic fatty liver disease by triggering Sirt1/NF-κB pathway

Bao-Fei Yan, Lan-Fen Pan, Yi-Fang Quan, Qian Sha, Jing-Zheng Zhang, Yi-Feng Zhang, Li-Bing Zhou, Xi-Long Qian, Xiao-Mei Gu, Feng-Tao Li, Ting Wang, Jia Liu, Xian Zheng

Specialty type: Gastroenterology and hepatology

Provenance and peer review: Unsolicited article; Externally peer reviewed.

Peer-review model: Single blind

Peer-review report's scientific quality classification

Grade A (Excellent): 0
Grade B (Very good): B, B
Grade C (Good): 0
Grade D (Fair): 0
Grade E (Poor): 0

P-Reviewer: Bugaj AM, Poland; Dietrich CG, Germany

Received: April 27, 2023
Peer-review started: April 27, 2023
First decision: July 9, 2023
Revised: July 23, 2023
Accepted: July 31, 2023
Article in press: July 31, 2023
Published online: August 21, 2023

Bao-Fei Yan, Jing-Zheng Zhang, Feng-Tao Li, Jia Liu, College of Pharmacy, Jiangsu Health Vocational College, Nanjing 211800, Jiangsu Province, China

Lan-Fen Pan, Department of Pathology, Affiliated Kunshan Hospital of Jiangsu University, Kunshan 215300, Jiangsu Province, China

Yi-Fang Quan, Department of Education and Science, The First People's Hospital of Taicang, Kunshan 215400, Jiangsu Province, China

Qian Sha, Department of Pharmacy, Affiliated Hospital of Xuzhou Medical University, Xuzhou 221006, Jiangsu Province, China

Yi-Feng Zhang, School of Pharmacy, Nantong University, Nantong 226019, Jiangsu Province, China

Li-Bing Zhou, Xiao-Mei Gu, Ting Wang, Xian Zheng, Department of Pharmacy, Affiliated Kunshan Hospital of Jiangsu University, Kunshan 215300, Jiangsu Province, China

Xi-Long Qian, School of Pharmacy, Nanjing University of Chinese Medicine, Nanjing 210023, Jiangsu Province, China

Corresponding author: Xian Zheng, PhD, Pharmacist, Postdoc, Department of Pharmacy, Affiliated Kunshan Hospital of Jiangsu University, No. 566 Qianjin East Road, Development Zone, Kunshan 215300, Jiangsu Province, China. zhengxiannew@163.com

Abstract

BACKGROUND

Nonalcoholic fatty liver disease (NAFLD) is a clinicopathological entity characterized by intrahepatic ectopic steatosis. As a consequence of increased consumption of high-calorie diet and adoption of a sedentary lifestyle, the incidence of NAFLD has surpassed that of viral hepatitis, making it the most common cause of chronic liver disease globally. Huangqin decoction (HQD), a Chinese medicinal formulation that has been used clinically for thousands of years, has beneficial outcomes in patients with liver diseases, including NAFLD. However, the role and mechanism of action of HQD in lipid metabolism disorders

and insulin resistance in NAFLD remain poorly understood.

AIM
To evaluate the ameliorative effects of HQD in NAFLD, with a focus on lipid metabolism and insulin resistance, and to elucidate the underlying mechanism of action.

METHODS
High-fat diet-induced NAFLD rats and palmitic acid (PA)-stimulated HepG2 cells were used to investigate the effects of HQD and identify its potential mechanism of action. Phytochemicals in HQD were analyzed by high-performance liquid chromatography (HPLC) to identify the key components.

RESULTS
Ten primary chemical components of HQD were identified by HPLC analysis. *In vivo*, HQD effectively prevented rats from gaining body and liver weight, improved the liver index, ameliorated hepatic histological aberrations, decreased transaminase and lipid profile disorders, and reduced the levels of pro-inflammatory factors and insulin resistance. *In vitro* studies revealed that HQD effectively alleviated PA-induced lipid accumulation, inflammation, and insulin resistance in HepG2 cells. In-depth investigation revealed that HQD triggers Sirt1/NF-κB pathway-modulated lipogenesis and inflammation, contributing to its beneficial actions, which was further corroborated by the addition of the Sirt1 antagonist EX-527 that compromised the favorable effects of HQD.

CONCLUSION
In summary, our study confirmed that HQD mitigates lipid metabolism disorders and insulin resistance in NAFLD by triggering the Sirt1/NF-κB pathway.

Key Words: Nonalcoholic fatty liver disease; Huangqin decoction; Lipid metabolism disorders; Insulin resistance; Sirt1/NF-κB pathway

Core Tip: Huangqin decoction (HQD) has substantial therapeutic effects in liver diseases. We previously showed that HQD mitigates hepatic inflammation in a rat model of High-fat diet (HFD)-induced Nonalcoholic fatty liver disease (NAFLD) by inhibiting the TLR4/NF-κB/NLRP3 pathway. Here, we investigated the effects of HQD on lipid metabolism disorders and insulin resistance in NAFLD. Our results demonstrated that HQD effectively antagonizes hepatocyte steatosis and insulin resistance in HFD-fed rats and palmitic acid-challenged HepG2 cells by triggering Sirt1/NF-κB pathway-modulated lipogenesis and inflammation. These data will significantly promote the clinical application of HQD in the treatment of NAFLD.

Citation: Yan BF, Pan LF, Quan YF, Sha Q, Zhang JZ, Zhang YF, Zhou LB, Qian XL, Gu XM, Li FT, Wang T, Liu J, Zheng X. Huangqin decoction alleviates lipid metabolism disorders and insulin resistance in nonalcoholic fatty liver disease by triggering Sirt1/NF-κB pathway. *World J Gastroenterol* 2023; 29(31): 4744-4762
URL: https://www.wjgnet.com/1007-9327/full/v29/i31/4744.htm
DOI: https://dx.doi.org/10.3748/wjg.v29.i31.4744

INTRODUCTION

As lifestyles have been increasingly shifting to "eat more, move less", overweight and obese cohorts is on a monumental rise. Consequently, the incidence of obesity-related chronic diseases, such as type 2 diabetes, cardiovascular disease, and nonalcoholic fatty liver disease (NAFLD) is on the rise. NAFLD is the most common liver disease characterized by excessive hepatocellular lipid build-up, which is caused by factors other than alcohol intake, drugs, viral infections, and autoimmunity[1]. The initial signs and symptoms of NAFLD are limited to benign steatosis[2]. However, if not managed, approximately 30% of NAFLD cases will progress to nonalcoholic steatohepatitis (NASH). Subsequently approximately 30%–40% of NASH cases will further progress to fibrosis and cirrhosis, and approximately 5%–25% of NASH patients will die from advanced liver diseases within ten years[2-5]. Additionally, epidemiological studies suggest that NAFLD patients are more prone to develop heart disease and die from heart attacks compared to healthy individuals[6]. Currently, NAFLD affects approximately 25% of the general population worldwide, and the associated morbidity in China has increased substantially from 18% to approximately 30% in recent decades[7]. It is estimated that more than 300 million cases of NAFLD will emerge in China by 2030, causing a tremendous strain on its healthcare and economy[8]. Unfortunately, no specific drug has been approved by the Food and Drug Administration for NAFLD; invasive bariatric surgery and lifestyle modifications are thought to be effective strategies[9]. Therefore, there is an urgent need to identify more efficacious agents for NAFLD treatment.

NAFLD is driven by multiple factors and its etiology remains complex and elusive. Several hypotheses have been proposed over the past few decades to explain its pathogenesis. According to the canonical "two-hit" hypothesis originally proposed by Day and James[10], obesity and insulin resistance-evoked excessive intrahepatic lipid accumulation constitutes the "first hit," and ensuing oxidative stress and inflammation constitute the "second hit". Subsequent studies found that hepatocyte regeneration and proliferation were impeded during the progression of NAFLD, which was termed as the "third-hit"[11]. Following further in-depth investigations, a more precise "multiple-hit" hypothesis was proposed that deems that hepatic steatosis increases the susceptibility of the liver to intra- and extrahepatic offenders, such as hepatic oxidative stress and inflammation, gut dysbiosis, and disturbed adipokines, and the multiple insults simultaneously and synergistically induce and advance NAFLD[12]. However, in both the hypotheses, hepatic steatosis is considered to be the paramount driver of NAFLD, and numerous studies have focused on lipid metabolism-associated targets (*e.g.*, Sirt1) in an attempt to reduce intrahepatic fat[9]. Sirt1, a nicotinamide adenine dinucleotide-dependent lysine deacetylase, is a metabolic sensor that is highly expressed in metabolically active organs (*e.g.*, the liver and skeletal muscles) and is extensively involved in glucose and lipid metabolism[9,13,14]. Clinical evidence indicates that patients with NAFLD exhibit defective Sirt1 expression in the liver[15]. Additionally, inhibition of Sirt1 exacerbated high-fat diet (HFD)-induced hepatic steatosis in mice, whereas activation of Sirt1 exerted anti-steatotic effect[16]. Importantly, it was reported that Sirt1 deacetylates lysine residues of NF-κB (RelA/p65 subunit), thereby affecting its transcriptional activity and restricting the expression of pro-inflammatory target genes[17]. Curative effects including anti-steatosis, anti-inflammation, and anti-apoptosis were noted when Sirt1/NF-κB pathway was triggered in methionine-choline-deficient diet-induced NASH mice, indicating the vital role of Sirt1/NF-κB pathway in defense against NAFLD[18]. In addition, recent studies suggest that NF-κB-stimulated pro-inflammatory factors activate hepatic insulin resistance, and thereby aggravate hepatic steatosis[17,19]. Therefore, triggering the Sirt1/NF-κB pathway represents a potential strategy for counteracting insulin resistance and hepatic steatosis in NAFLD.

Huangqin decoction (HQD) is a classical traditional Chinese medicine (TCM) formulation that was first mentioned in "Treatise on Febrile Diseases" by the medical sage Zhong-Jing Zhang. According to records, HQD harbors the efficacy of "clearing away heat and treating dysentery" and "regulating the stomach and relieving pain," and has long been utilized to treat inflammatory diseases. It has a positive reputation as "the ancestral agent for curing dysentery in all ages" and "the first decoction for febrile diseases"[20]. Notably, HQD has been used to treat liver disorders (*e.g.*, NAFLD) at the First Affiliated Hospital of Nanjing University of Chinese Medicine for decades with positive outcomes. HQD is composed of four botanical herbs, *Scutellariae Radix* (Huangqin in Chinese), *Paeoniae Radix Alba* (Baishao in Chinese), *Glycyrrhizae Radix et Rhizome* (Gancao in Chinese), and *Jujubae Fructus* (Dazao in Chinese), which are clinically combined in a 3:2:2:2 ratio. Previous studies reported that these herbs can alleviate NAFLD when used independently[21-23]. More importantly, in our recent study, the anti-hepatitis effects of HQD in HFD-induced NAFLD rats were found to be mediated *via* inhibition of the TLR4/NF-κB/NLRP3 pathway[24]. However, the regulatory mechanisms of HQD in hepatic steatosis and its ameliorative effects in insulin resistance remain undefined.

To address this gap, we used HFD-induced NAFLD rats and palmitic acid (PA)-induced HepG2 cells to investigate the ameliorative effects of HQD in lipid metabolism disorders and insulin resistance, and identify the potential molecular mechanisms by focusing on the Sirt1/NF-κB pathway.

MATERIALS AND METHODS

Plant materials and reagents

Scutellariae Radix, *Paeoniae Radix Alba*, Glycyrrhizae Radix et Rhizome, and *Jujubae Fructus* were obtained from Wansheng Herbal Decoction Pieces Co. Ltd. (Bozhou, China) and authenticated by Professor Sheng-Jin Liu of the Nanjing University of Chinese Medicine (Nanjing, China). All voucher specimens (Voucher No. 220301, 220302, 220303, and 220304) were deposited at the Central Laboratory of Jiangsu Health Vocational College (Nanjing, China). Gallic acid, paeoniflorin, scutellarin, liquiritin, baicalin, scutellarein, wogonoside, baicalein, wogonin, and chrysin (purity ≥ 98%) were purchased from Yuanye Biotechnology Co. Ltd. (Shanghai, China). Fenofibrate (Fen) was obtained from SPGC Sine Pharmaceutical Co. Ltd. (Shanghai, China). Enzyme-linked immunosorbent assay (ELISA) kits for insulin, tumor necrosis factor (TNF)-α, interleukin (IL)-6, and IL-1β were obtained from Solarbio (Beijing, China). Commercial biochemical kits for triacylglycerol (TG), total cholesterol (TC), free fatty acids (FFA), low-density lipoprotein cholesterol (LDL-c), high-density lipoprotein cholesterol (HDL-c), alanine transaminase (ALT), and aspartate transaminase (AST) were obtained from the Nanjing Jiancheng Bioengineering Institute (Nanjing, China). Hematoxylin and eosin (H&E) and Oil Red O staining kits were supplied by Beyotime (Shanghai, China). Dulbecco's modified Eagle's medium (DMEM), fetal bovine serum (FBS), bovine serum albumin (BSA), and PA were purchased from Sigma-Aldrich (St. Louis, MO, United States). Penicillin-streptomycin solution was obtained from Thermo Fisher Scientific (Waltham, MA, United States). EX-527 was purchased from Selleck Chemicals (Houston, TX, United States). A colorimetric 2-deoxydglucose (2DG) uptake assay kit and antibodies against IL-1β, sterol regulatory element-binding protein (SREBP)-1, fatty acid synthase (FAS), cluster of differentiation 36 (CD36), Sirt1, NF-κB, p-NF-κB, IRS-2, p-IRS-2, and glyceraldehyde-3-phosphate dehydrogenase (GAPDH) were purchased from Abcam (Cambridge, MA, United Kingdom). All the chemicals used were of analytical grade.

Preparation of HQD

HQD was prepared using established protocols. Briefly, 300 g *Scutellariae Radix*, 200 g *Paeoniae Radix Alba*, 200 g *Glycyrrhizae Radix et Rhizome*, and 200 g *Jujubae Fructus* were combined in 10-fold volume of double-distilled water and extracted in boiling water for 1 h. Following filtration through gauze, the herbal residue was extracted again for 1 h at 100

°C with 8-fold volume of double-distilled water. Subsequently, the two extracts were pooled, concentrated under reduced pressure, and lyophilized to yield 173.1 g of the extract powder. The extract ratio of HQD was 19.23% (w/w). The lyophilized extract powder was stored at -80 °C for subsequent experiments.

High-performance liquid chromatography analysis of HQD

An Agilent 1260 high-performance liquid chromatography (HPLC) separation system (Agilent, Santa Clara, CA, United States) equipped with a diode array detector was used to analyze the chemical composition of HQD. Briefly, the lyophilized powder (0.5 g) was dissolved in 20 mL of ultrapure water using ultrasonication. Following filtration through a 0.22 μm syringe filter, 20 μL of the supernatant was injected into the HPLC system and separated chromatographically through an Agilent ZORBAX SB-C18 column (4.6 mm × 150 mm, 5 μm). The mobile phase comprised of linear gradients of 0.1% (v/v) formic acid in water and acetonitrile. Gradient elution was performed as follows: 0–10 min, 5%–8% acetonitrile; 10–20 min, 8%–16% acetonitrile; 20–40 min, 16%–22% acetonitrile; 40–50 min, 22%–25% acetonitrile; 50–60 min, 25%–40% acetonitrile; 60–70 min, 40%–60% acetonitrile; 70–75 min, 60%–5% acetonitrile; 75–80 min, 5% acetonitrile. Programmable parameters for flow rate, injection volume, and detector wavelength were 1 mL/min, 5 μL, and 270 nm, respectively.

Animals

Male Sprague-Dawley rats (seven weeks old, weighing 180–200 g) were obtained from the Hangzhou Medical College (Hangzhou, China). The rats were housed in a conventional habitat (40%–50% humidity, 25 ± 1 °C, and 12 h light/dark) at the Laboratory Animal Center of the Jiangsu Health Vocational College. The experimental protocols strictly complied with the European Community criteria and were authorized by the Animal Ethics Committee of the Jiangsu Health Vocational College (Permission No. JHVC-IACUC-2022-B007).

Animal grouping and treatment

Following one week of acclimatization, the rats were randomly allocated to five groups (n = 8/group): Normal, HFD, HFD plus Fen (30 mg/kg), and HFD plus HQD (400 and 800 mg/kg). Rats in the normal group were fed a normal chow diet (10% calories from fat), whereas the rats in the other groups were fed a HFD (60% calories from fat) for 16 wk to establish the NAFLD model[25]. Both diets were provided by Jiangsu Xietong Pharmaceutical Bioengineering Co. Ltd. (Nanjing, China). Starting from the 8th week, the rats were orally administered Fen or HQD once daily for intervention, whereas the rats in the normal and HFD groups received an equal volume of 0.5% sodium carboxymethylcellulose (CMC-Na) orally as the control. Body weights of the animals were monitored weekly during the experimental period. At the end of the experiment, the rats were fasted overnight prior to being anesthetized with 1% pentobarbital sodium. To obtain serum, blood samples were collected from the abdominal aorta and centrifuged at 3500 rpm for 15 min. The rat livers were swiftly resected and flushed with phosphate buffered saline. Liver weights were measured and the liver indices (liver weight/body weight) were calculated. Portions of the liver were fixed in 4% paraformaldehyde for histological analysis and the remaining liver specimen was snap-frozen and stored at -80 °C for future molecular biology analyses.

Evaluation of insulin sensitivity

Two days prior to the termination of the experiment, the mice were fasted for 12 h and then orally administered 2 g/kg glucose. Blood was drawn from the tail vein before or at the indicated time points (30, 60, 90, and 120 min) after gavage. Blood glucose levels were measured using a glucometer (Yuwell, Inc., Zhenjiang, China). The oral glucose tolerance test (OGTT) curve and area under the curve (AUC) of the OGTT were drawn and calculated using GraphPad Prism 8.0. At the end of the experiment, fasting blood glucose (FBG) and serum insulin levels were determined using a glucometer and an insulin ELISA kit, respectively. The homeostasis model assessment of insulin resistance (HOMA-IR) was calculated as follows: (FBG × fasting serum insulin)/22.5.

Cell culture and treatment

HepG2 cells were purchased from the Chinese Academy of Cell Resource Center (Shanghai, China) and cultured in DMEM (supplemented with 10% FBS and 1% penicillin-streptomycin) at 37 °C in a humid environment containing 5% CO_2. PA stock solution (5 mmol/L) was dissolved in 5% BSA by incubating at 55 °C for 15 min. Subsequently, the PA-BSA solution was incorporated into the medium at a final concentration of 125 μM. HQD-mediated cytotoxicity was determined using the 3-(4,5-dimethylthiazol-2-yl)-2,5-diphenyltetrazolium bromide (MTT) assay. For the interventions, HepG2 cells (70% confluent and serum-starved for 12 h) were treated with insulin (1 IU/mL), various doses of HQD (0, 25, 75, or 125 μg/mL) or a combination of HQD (100 μg/mL) and EX-527 (10 μM) under PA (125 μM) challenge for 24 h. HepG2 cells grown in serum-free media with 5% BSA served as the blank control.

MTT assay

HepG2 cells were seeded in 96-well plates (1×10^4 cells/well) and cultured overnight, followed by exposure to different concentrations of HQD (0, 25, 50, 75, 100, 120, 150, 175, and 200 μg/mL) with or without 125 μM PA for 24 h. MTT solution (10 μL of 5 mg/mL) was added to each well and incubated at 37 °C for 4 h. Dimethyl sulfoxide (150 μL) was added to dissolve the formazan crystals with vigorously shaking for 5 min. Finally, a Multiskan MK3 microplate reader (Thermo Fisher Scientific) was used to measure the absorbance at 490 nm. Cell viability (% of control) was calculated using the following formula: [Optical density (OD) 490 (sample-blank)/OD 490 (control-blank)] × 100%.

Glucose uptake assay

HepG2 cells were cultured overnight in 96-well plates (5 × 10^3 cells/well) and then starved for 12 h. The cells were stimulated without or with 1 μM insulin for 20 min to activate the glucose transporters. A colorimetric 2DG uptake test was performed according to the manufacturer's protocol to evaluate glucose absorption by HepG2 cells in response to insulin.

ELISA and biochemical analyses

TNF-β, IL-6, and IL-1β levels in the liver and cell supernatants, as well as serum insulin levels, were measured using the corresponding ELISA kits following the manufacturer's instructions. Biochemical parameters in the serum, liver, and HepG2 cells, including TG, TC, LDL-c, HDL-c, FFA, ALT, and AST were determined using commercial kits following the manufacturer's instructions.

Histological and immunohistochemistrical/immunofluorescent analyses

Fixed liver tissues were embedded in paraffin, cut into 5 μm slices, and stained with H&E according to the standard procedure. Immunohistochemical analyses were performed as described previously[25]. Briefly, primary antibodies against IL-1β, SREBP-1, Sirt1, and p-NF-κB were diluted 200-fold and then incubated with the tissue samples overnight at 4 °C. Following that, 100 μL of secondary antibody (diluted 400-fold) was added dropwise to each section. Horseradish peroxidase (HRP)-conjugated goat anti-rabbit IgG (H + L) was used for IL-1β and SREBP-1. HRP- or Alexa Fluor594-conjugated goat anti-rabbit IgG (H + L) was used for Sirt1 and p-NF-κB. Subsequently, 4',6-diamidino-2-phenylindole (DAPI) or 3,3'-diaminobenzidine substrate solution was sequentially added to each section. Images were captured using either a DM2500 optical microscope (Leica, Wetzlar, Germany) or an LSM 700 confocal laser microscope (Zeiss, Oberkochen, Germany). Finally, the data were quantified using the Image-Pro Plus software (version 6.0; Media Cybernetics, Rockville, MD, United States). For immunofluorescence analysis, HepG2 cells were immobilized in 4% paraformaldehyde solution for 10 min, blocked with 5% BSA, and incubated overnight with primary antibodies against Sirt1 and NF-κB (both diluted 200-fold). Thereafter, the cells were probed with Alexa Fluor 488-conjugated secondary antibodies (diluted 500-fold) and counterstained with DAPI to visualize the nuclei. Fluorescence images were acquired using an LSM 700 confocal laser microscope (Zeiss).

Oil Red O staining

Paraffin-embedded liver tissues were cut into 5 μm sections, followed by staining with Oil Red O dye according to standard procedure. HepG2 cells were fixed in 4% paraformaldehyde for 15 min, rinsed with distilled water, and stained with Oil Red O dye. Images were captured using a DM2500 optical microscope (Leica).

Western blotting

Pre-chilled radio immunoprecipitation assay buffer (containing a protease inhibitor cocktail) was used to lyse liver samples. A commercial bicinchoninic acid assay kit was used to quantify total proteins. Immunoblot analysis was performed as previously described[25]. Specific primary antibodies against SREBP-1c, FAS, CD36, Sirt1, NF-κB, p-NF-κB, IRS-2, p-IRS-2, and GAPDH were used at 1000-fold dilution. The protein bands were visualized and semi-quantified using Azure Biosystems C600 (Azure Biosystems Inc., Dublin, CA, United States) and ImageJ software (NIH, Bethesda, MD, United States), respectively.

Statistical analysis

Data were analyzed using IBM SPSS software (version 21.0; Armonk, NY, United States) and expressed as mean ± SD. One-way analysis of variance followed by a least significant difference test for multiple comparisons was used to assess significant differences among groups. Statistical significance was set at $P \leq 0.05$.

RESULTS

Phytochemical analysis of HQD

The multifaceted effectiveness of TCMs stem from their multi-component trait. First, we sought to identify the primary chemical components of HQD using HPLC analysis. As shown in Figure 1, ten major monomeric components were identified in HQD by comparing the retention times of the standards. Based on the standards, the concentrations of: (1) Gallic acid, (2) paeoniflorin, (3) scutellarin, (4) liquiritin, (5) baicalin, (6) scutellarein, (7) wogonoside, (8) baicalein, (9) wogonin, and (10) chrysin were determined to be 0.709, 2.005, 1.417, 1.626, 60.092, 0.916, 13.471, 1.905, 2.088, and 0.559 mg/g, respectively.

HQD alleviated adiposity and hepatic histological abnormalities in HFD-induced NAFLD rats

Patients with NAFLD frequently present with increased body and liver weight. Fen, a lipid-lowering medication that is clinically used for NAFLD treatment, was chosen as the positive control drug. The experimental scheme is indicated in Figure 2A. As shown in Figure 2B-E, HQD treatment (400 and 800 mg/kg) significantly attenuated HFD-induced increase in body and liver weight, as well as the liver index. As hepatic steatosis is the primary hallmark of NAFLD, we performed histological analysis to assess the effect of HQD on hepatic steatosis. H&E staining indicated that rats in the HFD group presented with severe structural disruption of the hepatic lobules, steatosis, and hepatocellular ballooning degeneration,

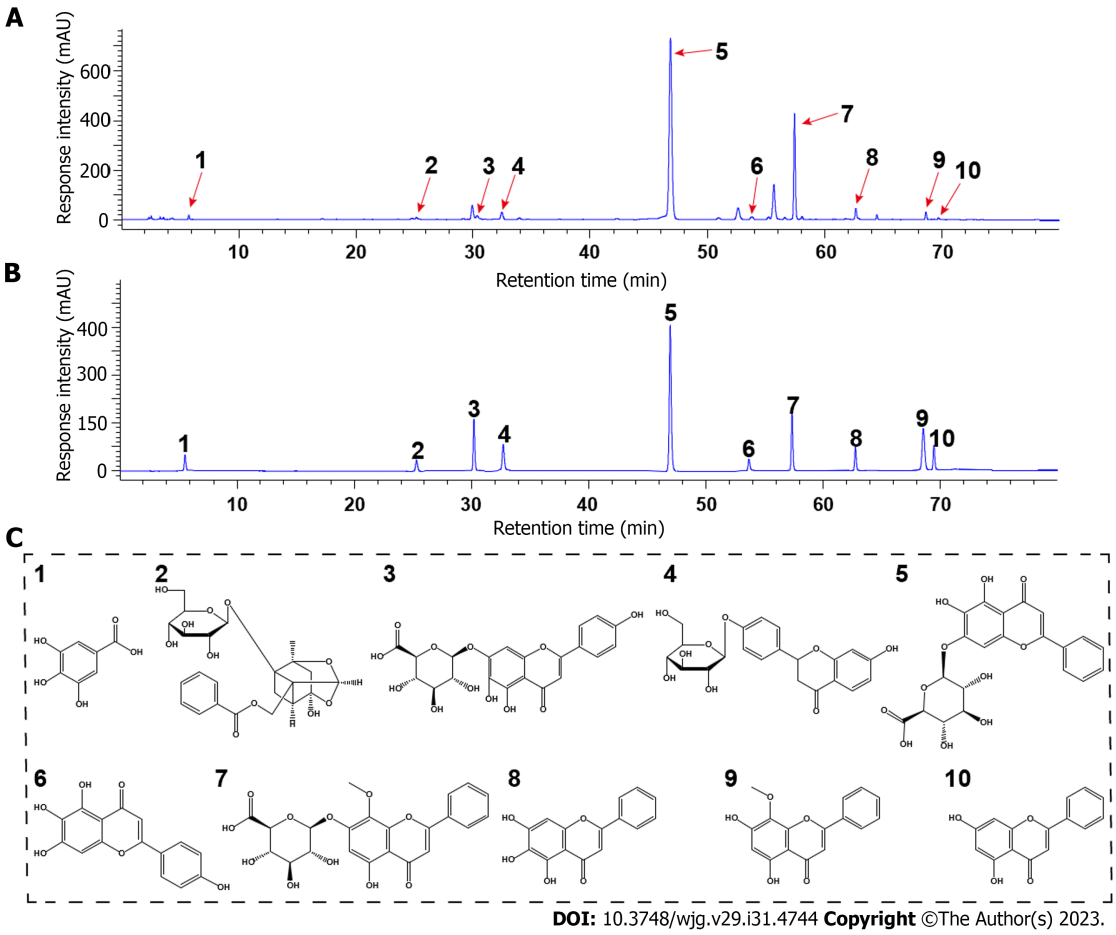

DOI: 10.3748/wjg.v29.i31.4744

Figure 1 High-performance liquid chromatography fingerprint spectrum of Huangqin decoction and structures of the major phytochemicals in Huangqin decoction. A and B: High-performance liquid chromatography profiles of Huangqin decoction (HQD) and the standard mixture: (1) Gallic acid, (2) paeoniflorin, (3) scutellarin, (4) liquiritin, (5) baicalin, (6) scutellarein, (7) wogonoside, (8) baicalein, (9) wogonin, and (10) chrysin; C: Structures of the major phytochemicals in HQD.

whereas oral administration of HQD mitigated these pathological alterations in a dose-dependent manner, as evidenced by relatively intact hepatic lobules and smaller fat vacuoles (Figure 2F). Additionally, Oil Red O staining showed numerous lipid droplets in the HFD group that reduced significantly following HQD treatment (Figure 2G and H). Notably, high-dose HQD exerted anti-steatosis effects comparable to those of Fen.

HQD mitigated liver damage and lipid metabolism disorders in HFD-induced NAFLD rats

Biochemical parameters of liver damage and lipid metabolism disorders, including ALT, AST, TC, TG, FFA, LDL-c, and HDL-c, are robust diagnostic markers for NAFLD. As shown in Figure 3, serum levels of ALT, AST, TC, TG, FFA, and LDL-c, as well as hepatic TC, TG, and FFA in the HFD group were noticeably higher than those in the control group. These levels were markedly reduced following HQD treatment. In contrast, the HFD-challenged group exhibited lower serum HDL-c level than the normal group, which was markedly restored following HQD treatment. In addition, the therapeutic efficacy of a high dose of HQD was equivalent to that of Fen.

HQD relieved hepatic inflammation and insulin resistance in HFD-induced NAFLD rats

Liver inflammation and insulin resistance are pivotal concomitant factors that facilitate NAFLD progression. Inflammation exacerbates insulin resistance, and both form a vicious cycle with each promoting the other and accelerating NAFLD progression[26]. As shown in Figure 4A and B, IL-1β-positive area in the liver of the HFD group was significantly higher relative to that in the control group, indicating extensive inflammatory response in the liver, which was further supported by markedly elevated levels of IL-6, IL-1β, and TNF-α in the liver (Figure 4C-E). However, all these alterations were reversed following HQD interventions. To ascertain the effect of HQD on glucose tolerance, an OGTT was performed. As shown in Figure 4F and G, higher levels of blood glucose (0–120 min) were noted in the HFD group following intragastric administration of glucose, which was robustly attenuated by HQD treatment. This was quantitatively verified by the AUC of the OGTT. Moreover, the HFD-induced elevation in serum insulin levels also decreased markedly following HQD treatment (Figure 4H). As shown in Figure 4I, the HOMA-IR value in HFD-challenged rats was significantly higher than that in normal rats, and was effectively reduced following HQD intervention. Notably, high-dose HQD showed curative efficacy similar to that of Fen.

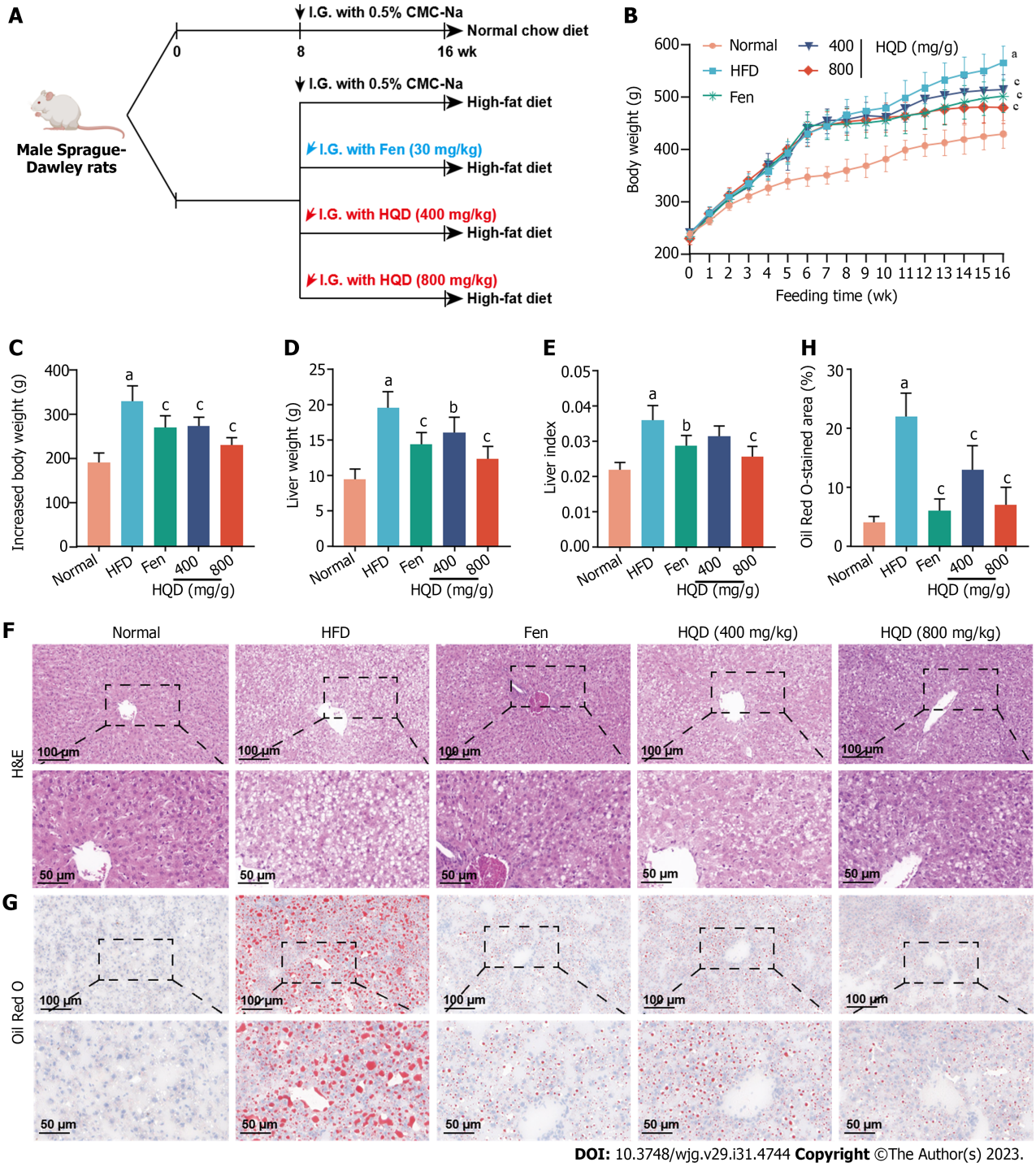

DOI: 10.3748/wjg.v29.i31.4744

Figure 2 Huangqin decoction improves adiposity and hepatic histological abnormalities in high-fat diet-induced nonalcoholic fatty liver disease rats. Data are presented as mean ± SD (n = 4–8). $^{a}P < 0.01$ *vs* the normal group, $^{b}P < 0.05$ and $^{c}P < 0.01$ *vs* the high-fat diet group. A: Workflow of the experimental design; B: Dynamic curve of the body weight; C-E: Barcharts showing the effects of different treatments on body weight (C), liver weight at the termination of the experiment (D), and liver index (liver weight/body weight) (E) at the termination of the experiment; F and G: Representative micrographs of Hematoxylin and eosin and Oil Red O stained liver sections; H: Quantitative analysis of positive areas in Oil Red O staining. CMC-Na: Sodium carboxymethylcellulose; Fen: fenofibrate; HQD: Huangqin decoction; I.G.: Intragastric administration.

HQD triggered the Sirt1/NF-κB pathway in HFD-induced NAFLD rats

Sirt1/NF-κB pathway-modulated insulin resistance and hepatic steatosis play an important role in the progression of NAFLD. Therefore, protein levels of Sirt1, NF-κB, p-NF-κB, and the downstream insulin signal transduction- and lipid metabolism-related proteins (*i.e.*, IRS-2, p-IRS-2, SREBP-1, FAS, and CD36) in the liver were examined. As shown in Figure 5A-G, Sirt1 and p-IRS-2 protein levels were significantly lower in the HFD group relative to that in the normal group, whereas those of p-NF-κB, SREBP-1, FAS, and CD36 were clearly elevated in response to HFD challenge. Oral supplementation with HQD markedly reversed these changes in a dose-dependent manner. To further validate these findings, the levels of Sirt1, p-NF-κB, and SREBP-1 were evaluated immunohistochemically. Consistent with the previous

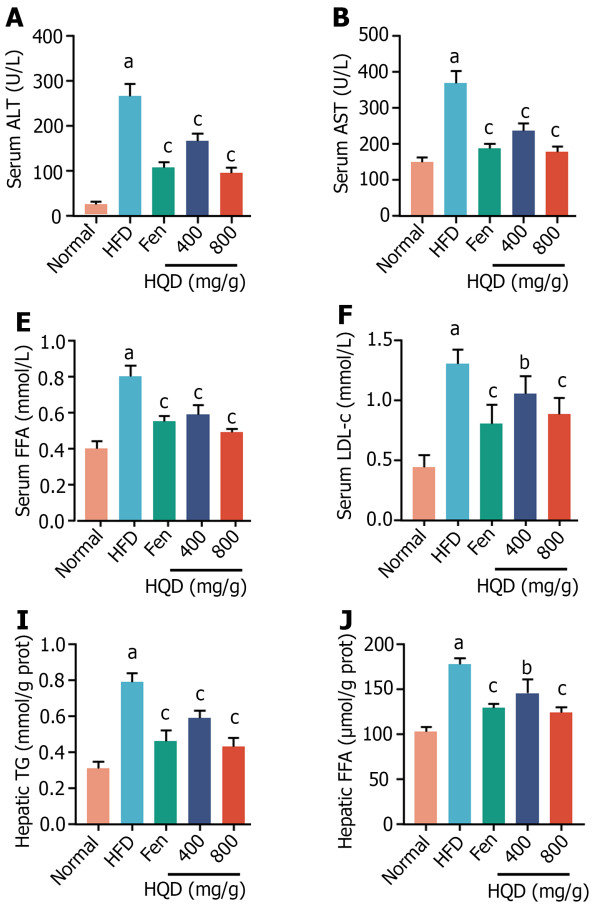

DOI: 10.3748/wjg.v29.i31.4744

Figure 3 Huangqin decoction alleviates liver damage and lipid metabolism disorders in high-fat diet-induced nonalcoholic fatty liver disease rats. Data are presented as mean ± SD (n = 8). $^{a}P < 0.01$ *vs* the normal group, $^{b}P < 0.05$ and $^{c}P < 0.01$ *vs* high-fat diet group. A-J: Effects of different treatments on levels of alanine transaminase (A); aspartate transaminase (B); total cholesterol (TC) (C); triacylglycerol (TG) (D); free fatty acid (FFA) (E); low-density lipoprotein cholesterol (F); high-density lipoprotein cholesterol (G); TC (H); TG (I); FFA (J) levels in rats are shown. ALT: Alanine transaminase; AST: Aspartate transaminase; Fen: Fenofibrate; FFA: Free fatty acid; HDL-c: High-density lipoprotein cholesterol; HFD: High-fat diet; HQD: Huangqin decoction; LDL-c: Low-density lipoprotein cholesterol; TC: Total cholesterol; TG: Triacylglycerol.

data, mild staining intensity of Sirt1 (brown/fluorescence) and strong staining intensities of p-NF-κB (brown/fluorescence) and SREBP-1 (brown) were observed in the HFD group, indicating the up-regulation of these proteins and activation of Sirt1/NF-κB pathway (Figure 5H-P). However, HQD administration substantially reduced the increased expression noted in immunohistochemical analyses. Overall, these findings suggest that the therapeutic effects of HQD on HFD-induced disorders in insulin signaling and lipid metabolism are closely associated with the Sirt1/NF-κB pathway.

HQD improved steatosis, inflammation, and insulin resistance in PA-induced HepG2 cells

The direct exposure of HepG2 cells to PA is a commonly used approach to mimic the symptoms of NAFLD *in vitro*[27, 28]. PA-induced HepG2 cells were used to investigate the therapeutic effects of HQD in NAFLD *in vitro*. Initially, MTT assay was used to examine the cytotoxicity of HQD in HepG2 cells. As shown in Figure 6A and B, HQD presented no obvious cytotoxic effect in HepG2 cells at doses ≤ 150 μg/mL, and the safe concentration of HQD when co-incubated with PA (125 μM) was determined to be ≤ 125 μg/mL. Accordingly, HQD at doses of 25, 75, and 125 μg/mL were selected for the treatment of PA-induced HepG2 cells in subsequent experiments. As shown in Figure 6C and D, the levels of neutral lipids (TC and TG) in PA-challenged HepG2 cells were noticeably increased relative to that in the control cells, but markedly reduced following HQD intervention. This was further supported by the results of Oil Red O staining, which showed reduced lipid droplets in the HQD-treated groups (Figure 6E). As inflammation is a major cause of NAFLD and is strongly associated with insulin resistance, we examined the effects of HQD on the release of inflammatory factors in PA-challenged HepG2 cells. Figure 6F-H shows that HQD attenuated the PA-induced increase in the levels of IL-6, IL-1β, and TNF-β in a dose-dependent manner. A 2DG assay was performed to assess insulin resistance. The results showed that 2DG uptake was significantly lower in PA-treated HepG2 cells, whereas it increased markedly following HQD treatment (Figure 6I), indicative of the ameliorative effect of HQD on insulin resistance.

HQD exerted hepatocyte protection by triggering Sirt1/NF-κB pathway in PA-induced HepG2 cells

Consistent with the *in vivo* results, we noted that PA-stimulated HepG2 cells showed markedly decreased expression of

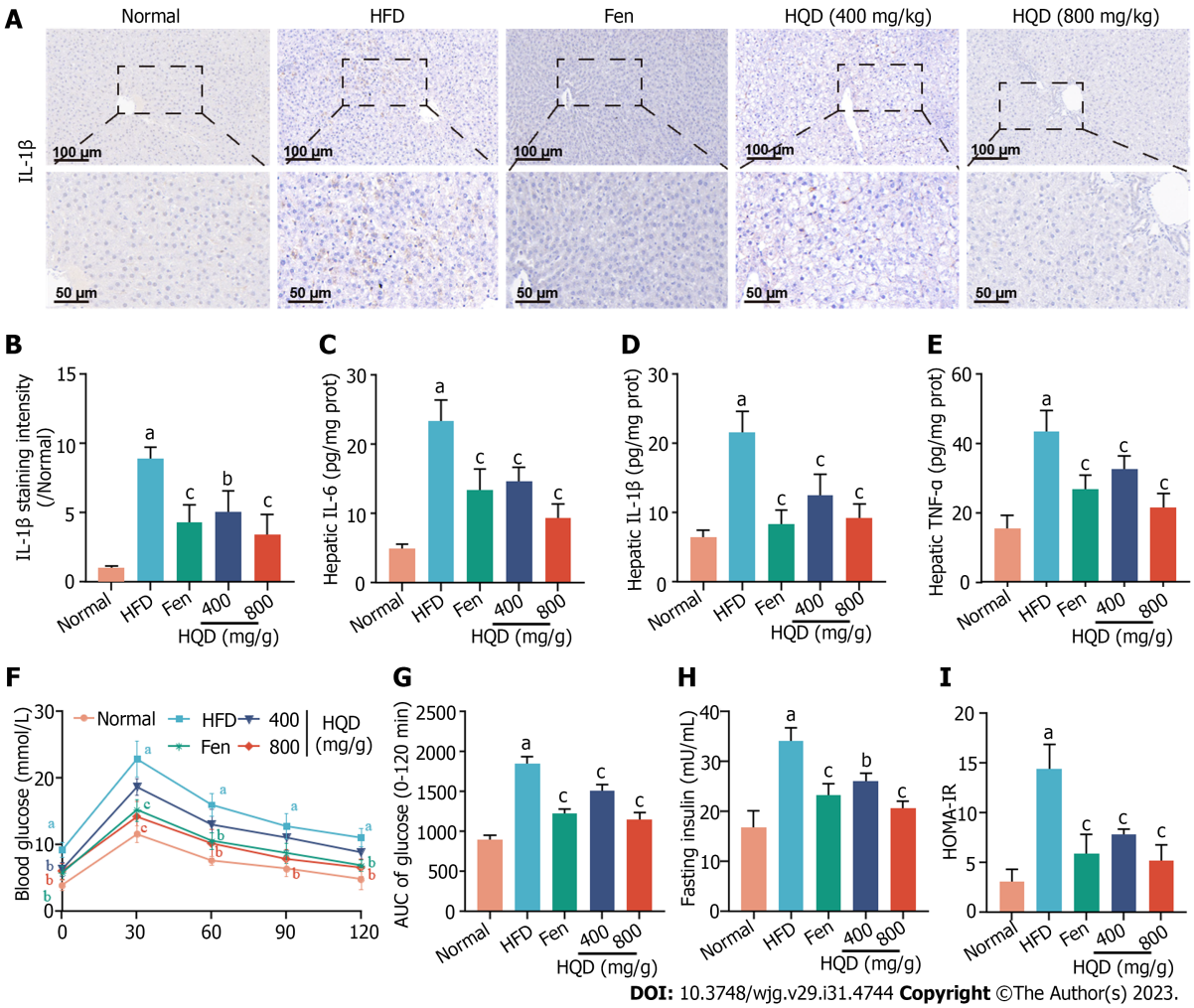

DOI: 10.3748/wjg.v29.i31.4744

Figure 4 Huangqin decoction suppresses hepatic inflammation and insulin resistance in high-fat diet-induced nonalcoholic fatty liver disease rats. Data are presented as mean ± SD (n = 4–8). $^{a}P < 0.01$ *vs* the normal group, $^{b}P < 0.05$ and $^{c}P < 0.01$ *vs* the high-fat diet (HFD) group. A: Representative images of immunohistochemical staining of interleukin (IL)-1β in liver sections; B: Quantitative analysis of staining intensity of IL-1β; C-E: Levels of IL-6 (C), IL-1β (D), and tumor necrosis factor-α (E) in the liver of HFD-fed rats; F: Oral glucose tolerance test (OGTT); G: Area under the curve from OGTT; H: Level of fasting serum insulin; I: Values of homeostasis model assessment of insulin resistance. AUC: Area under the curve; Fen: Fenofibrate; HFD: High-fat diet; HOMA-IR: Homeostasis model assessment of insulin resistance; HQD: Huangqin decoction; IL: Interleukin; TNF: Tumor necrosis factor.

Sirt1 and p-IRS-2, and increased expression of p-NF-κB, SREBP-1, FAS, and CD36 compared with that in the control cells (Figure 7A-G), indicative of inhibition of the Sirt1/NF-B pathway. However, these changes were restored following HQD treatment. To further determine the expression and distribution of Sirt1 and NF-κB, immunofluorescence analyses were performed. Consistently, the intensity of Sirt1 staining in the PA group was clearly lower compared to that in the control group. Furthermore, significantly increased NF-κB nuclear translocation was noted in PA-induced HepG2 cells, which was conspicuously reversed following HQD treatment (Figure 7H). Collectively, these data suggest that HQD protects hepatocytes against PA-induced insults *via* the Sirt1/NF-κB pathway.

To further confirm that the HQD-mediated mitigatory effects on insulin resistance and lipid accumulation occurs *via* the Sirt1/NF-κB pathway, we used a Sirt1 inhibitor, EX-527 to block the pathway. As shown in Figure 8A-G, the ameliorative effects of HQD on lipid accumulation, inflammation, and 2DG uptake were significantly compromised following co-treatment with EX-527. More importantly, EX-527 abolished the regulatory effects of HQD on Sirt1/NF-κB pathway and its downstream-modulated insulin signal transduction- and lipid metabolism-related proteins (Figure 8H-O). In summary, our data indicate that the protective effects of HQD against hepatic lipid accumulation, inflammation, and insulin resistance are mediated through triggering of the Sirt1/NF-κB pathway.

DISCUSSION

NAFLD is the most prevalent chronic liver disease for which no specific effective drug has been approved, making its treatment a top research priority[29]. Unlike synthetic drugs, whose efficacy depends mainly on their action on one target, the efficacy of TCM depends on its holistic effects on multiple targets and pathways. Therefore, TCMs are promising complementary and auxiliary agents for metabolic diseases with multifactorial pathogeneses, such as NAFLD

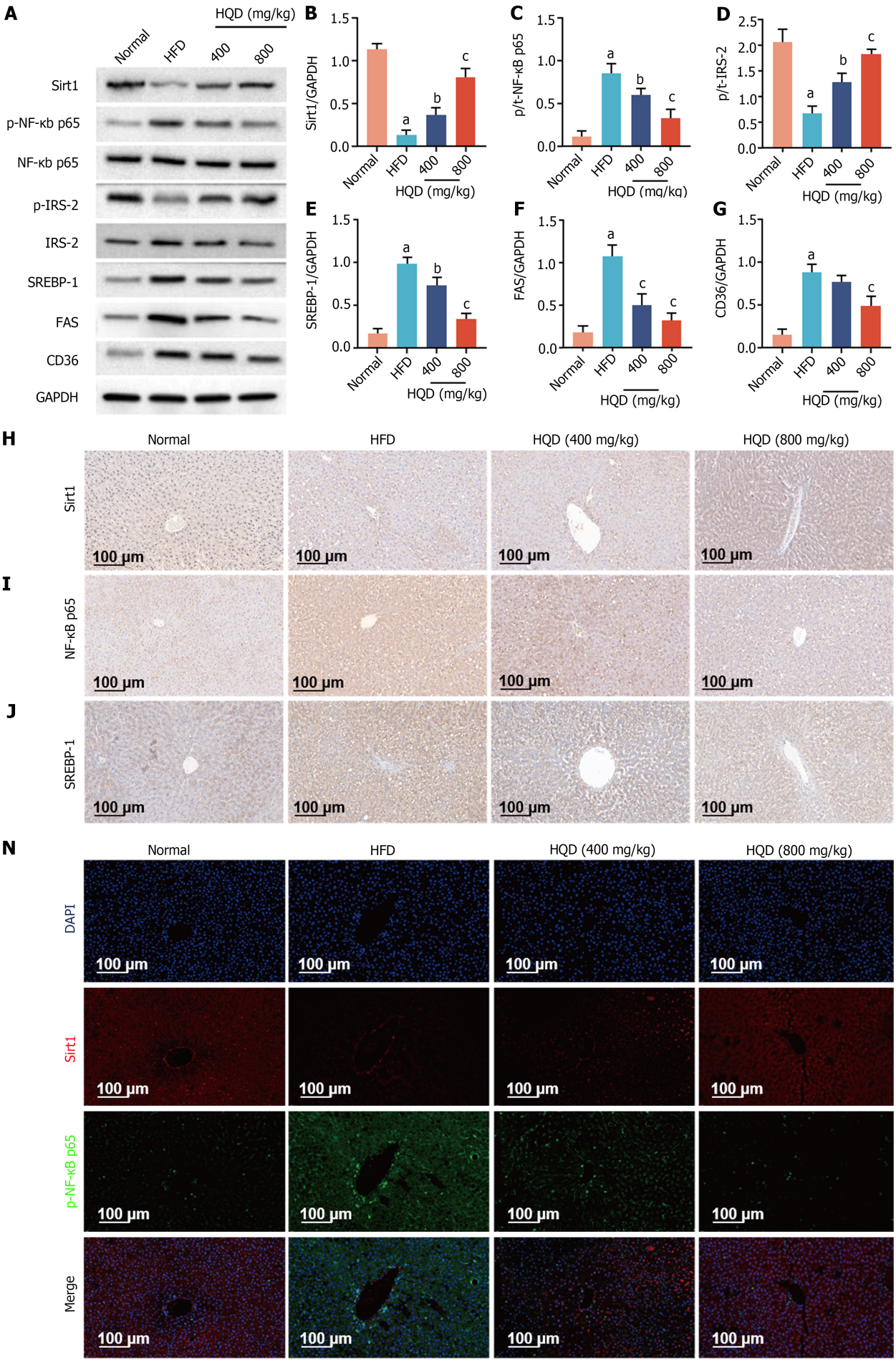
A
HQD (mg/kg)
Normal
HFD
400
800
Sirt1
p-NF-κb p65
NF-κb p65
p-IRS-2
IRS-2
SREBP-1
FAS
CD36
GAPDH
B
Sirt1/GAPDH
C
p/t-NF-κB p65
D
p/t-IRS-2
E
SREBP-1/GAPDH
F
FAS/GAPDH
G
CD36/GAPDH
HQD (mg/kg)
H
Normal
HFD
HQD (400 mg/kg)
HQD (800 mg/kg)
Sirt1
I
NF-κB p65
J
SREBP-1
N
DAPI
Sirt1
p-NF-κB p65
Merge
100 μm

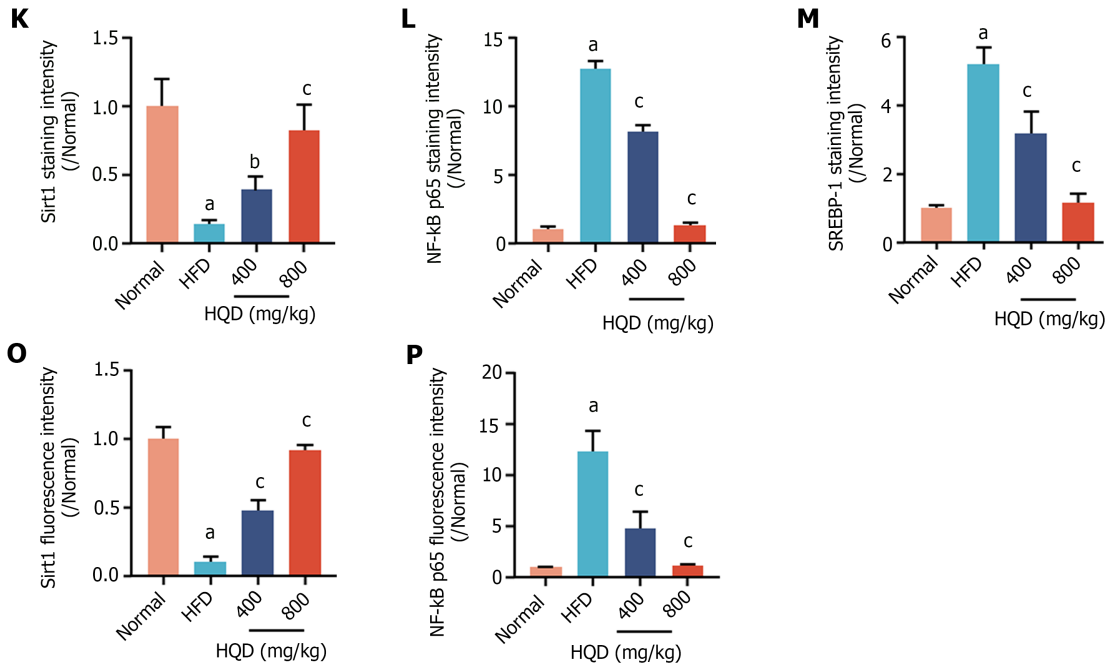

DOI: 10.3748/wjg.v29.i31.4744

Figure 5 Huangqin decoction activates the Sirt1/NF-Kb pathway in high-fat diet-induced nonalcoholic fatty liver disease rats. Data are presented as mean ± SD (n = 3–4). $^{a}P < 0.01$ *vs* the normal group, $^{b}P < 0.05$ and $^{c}P < 0.01$ *vs* the high-fat diet group. A: Expression levels of Sirt1, p-NF-κB/NF-κB, p-IRS-2/IRS-2, sterol regulatory element-binding protein (SREBP)-1c, fatty acid synthase, and cluster of differentiation 36; B-G: Semi-quantitative analysis of these proteins; H-J: Representative images of immunohistochemical staining of Sirt1 (H), NF-κB (I), and SREBP-1c (J) in liver sections; K-M: Quantitative analysis of the staining intensity; N: Representative images of immunofluorescent staining of Sirt1 and NF-κB in liver sections; O and P: Quantitative analysis of the fluorescence intensity. CD36: Cluster of differentiation 36; DAPI: 4',6-diamidino-2-phenylindole; FAS: Fatty acid synthase; GAPDH: Glyceraldehyde-3-phosphate dehydrogenase; HFD: High-fat diet; HQD, Huangqin decoction; SREBP: Sterol regulatory element-binding protein.

[30-32]. HQD, a well-known TCM formula, has emerged as a potentially effective modality for the clinical treatment of liver diseases, including NAFLD. In our study, several constituents of HQD, including gallic acid, paeoniflorin, scutellarin, liquiritin, baicalin, scutellarein, wogonoside, baicalein, wogonin, and chrysin were identified by HPLC analysis. The beneficial effects of these compounds in NAFLD have been reported both *in vivo* and *in vitro*[33-36], which provide the basis for the potential application of HQD in NAFLD therapy. In the present study, using both *in vivo* and *in vitro* experiments, we demonstrated that HQD mitigates insulin resistance and hepatic steatosis by modulating the Sirt1/NF-κB pathway.

Overconsumption of HFD, which is associated with a modern lifestyle, plays a role in the progression of NAFLD[37]. Currently, NAFLD murine models are most commonly developed by long-term consumption of an HFD, resulting in symptoms similar to those observed in patients with NAFLD[37]. PA is an essential fatty acid for TG synthesis in the liver and increased concentrations of PA in hepatocytes accelerate the progression[38]. Typically, the exogenous addition of PA induces hepatocellular lipid accumulation to mimic the pathological process of NAFLD *in vitro*. We used HFD-fed rats and PA-treated HepG2 cells to study the therapeutic effects of HQD on NAFLD. Our results showed that the HFD-fed rats had higher body and liver weights. Histological analysis revealed hepatic steatosis and injuries, which were further supported by aberrant levels of TC, TG, ALT, and AST in the serum and liver. Furthermore, abnormal levels of serum FFA, LDL-c, HDL-c, OGTT, insulin, and HOMA-IR were observed in the HFD-fed rats, indicating the onset of dyslipidemia and insulin resistance. Consistent with these findings, PA-stimulated HepG2 cells exhibited a marked increase in lipid accumulation, intracellular TC and TG levels, and glucose uptake. Notably, all the above mentioned NAFLD symptoms were dose-dependently reversed following HQD treatment, indicating that HQD mitigates lipid metabolism disorders and insulin resistance in NAFLD.

Compromised lipid metabolism contributes to hepatic steatosis, thereby triggering the onset of NAFLD[39,40]. Several studies have confirmed that the activation of *de novo* lipogenesis (DNL) promotes FFA generation and esterification into TG, which are crucial driving factors contributing to lipid metabolism dysfunction[41]. A previous clinical trial revealed that individuals with NAFLD had higher nighttime plasma FFA levels and a threefold increase in DNL[42]. SREBP-1c is a key transcription factor that controls hepatic DNL and lipolysis by modulating the activities of lipogenic enzymes (FAS) and fatty acid importer proteins (CD36) as downstream targets[43-45]. The active state of SREBP-1c directly influences FLD progression in fatty liver[43]. In the present study, rats with HFD-induced NAFLD and PA-treated HepG2 cells showed elevated SREBP-1, FAS, and CD36 Levels, indicating increased DNL and fatty acid uptake. However, oral HQD supplementation effectively reversed these changes. Sirt1 plays a critical role in cellular energy metabolism and deacetylates and inhibits SREBP-1c activity in the regulation of hepatic lipid metabolism; however, it is downregulated in patients with NAFLD[15]. In the rat liver and HepG2 cells, we observed deactivation of Sirt1 following exposure to HFD or PA, whereas HQD treatment increased Sirt1 levels, resulting in NAFLD mitigation.

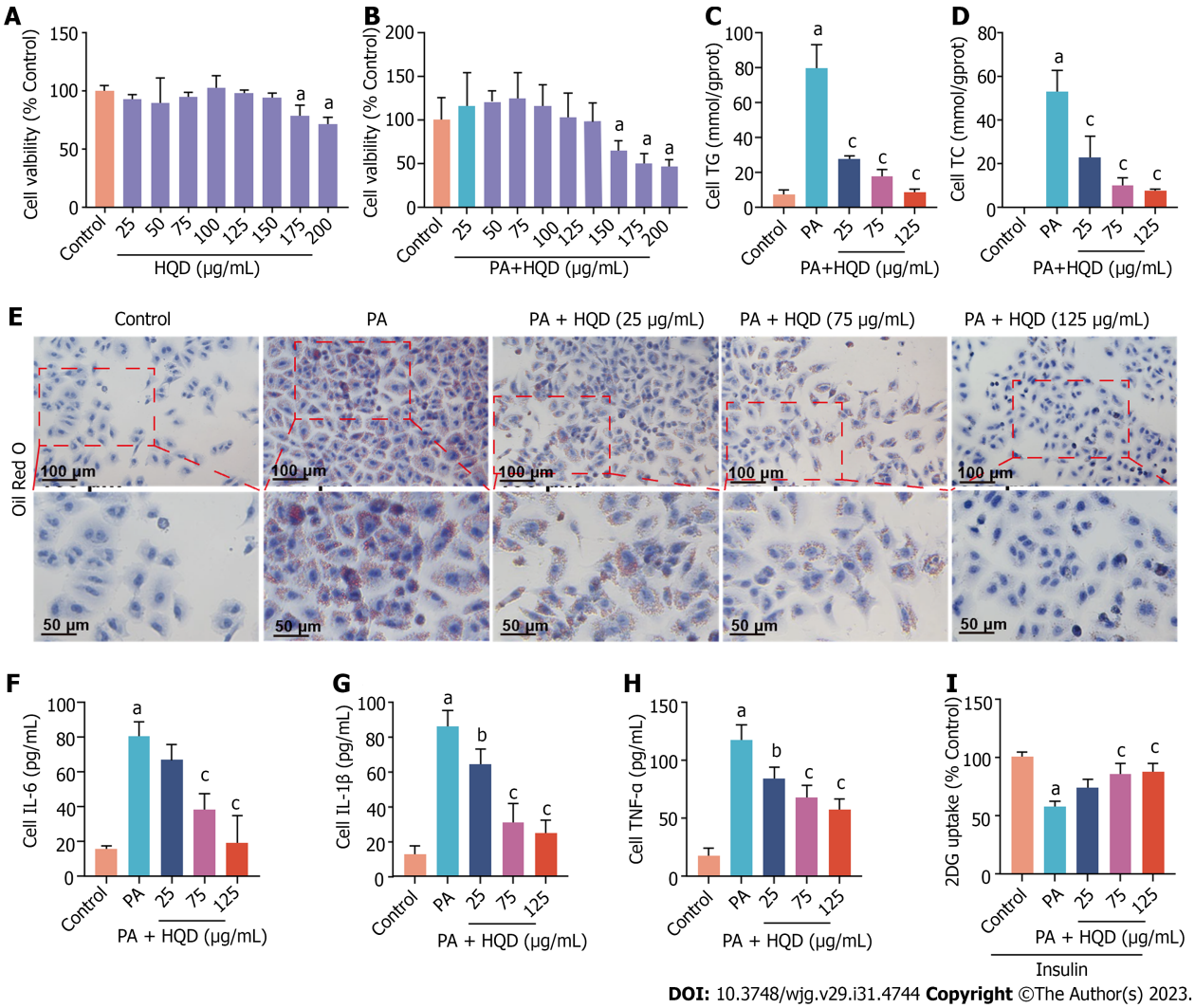

DOI: 10.3748/wjg.v29.i31.4744

Figure 6 Huangqin decoction improves lipotoxicity, inflammation, and insulin resistance in palmitic acid-induced HepG2 cells. Data are presented as mean ± SD of at least three independent experiments. $^{a}P < 0.01$ *vs* the control group, $^{b}P < 0.05$ and $^{c}P < 0.01$ *vs* the palmitic acid (PA) group. A: Viability of HepG2 cells following incubation with different concentrations of Huangqin decoction (HQD); B: Viability of HepG2 cells following co-culture with PA and different concentrations of HQD; C and D: Levels of triacylglycerol and total cholesterol in HepG2 cells; E: Representative micrographs of Oil Red O staining of HepG2 cells; F–H: Levels of interleukin (IL)-6, IL-1β, and tumor necrosis factor-α in HepG2 cells; I: Level of glucose uptake in HepG2 cells. 2DG: 2-deoxydglucose; HQD, Huangqin decoction; IL: Interleukin; TC: Total cholesterol; TG: Triacylglycerol; TNF: Tumor necrosis factor; PA: Palmitic acid.

Insulin resistance is the initial driver of hepatic steatosis in NAFLD[10,11,46]. Moreover, recent studies have suggested that obesity-induced chronic low-grade inflammation exacerbates insulin resistance[26,47]. Specifically, hypertrophic adipocytes promote macrophage infiltration and secrete pro-inflammatory factors including IL-6, IL-1β, and TNF-α, which downregulate insulin signaling molecules by inhibiting the phosphorylation of IRS-2, ultimately promoting insulin resistance[48-50]. NF-κB acts as an inducible transcription factor and induces the production of pro-inflammatory factors [51]. A previous study reported that FFA-induced insulin resistance is strongly associated with the activation of the pro-inflammatory NF-κB pathway[52]. More importantly, Sirt1 can inactivate NF-κB by deacetylating lysine 310, impeding the expression of pro-inflammatory target genes, whereas patients with NAFLD are more susceptible to inactivation of the Sirt1/NF-κB pathway[17,53]. In both, *in vivo* and *in vitro* NAFLD models, phosphorylation of NF-κB was upregulated and accompanied by increased levels of pro-inflammatory factors (IL-1β, TNF-α, and IL-6), whereas phosphorylation of IRS-2 was downregulated, suggesting that Sirt1/NF-κB pathway-mediated insulin resistance occurred in NAFLD. In contrast, the HQD intervention clearly restored these changes. Furthermore, treatment with the Sirt1 inhibitor, EX-527, abolished all HQD-mediated favorable effects in PA-challenged HepG2 cells, confirming that HQD mitigated hepatic steatosis and insulin resistance *via* the Sirt1/NF-κB pathway.

Fen, a peroxisome proliferator-activated receptor α (PPARα) agonist, offers potential therapeutic efficacy against NAFLD by inducing fatty acid oxidation and inhibiting inflammatory gene expression in the liver[54,55]. Clinical studies have shown that Fen may have positive therapeutic outcomes in NAFLD/NASH[56,57]. Herein, we found that HQD achieved therapeutic effects comparable to those of Fen by activating Sirt1. Several studies have shown that Sirt1, a key regulator of PPARα signaling, can trigger PPARα-mediated fatty acid oxidation in the liver, showing favorable effects in NAFLD[9,58,59]. Although HQD and Fen act on different targets, their therapeutic effects could be interpreted from the upstream and downstream regulatory relationships between Sirt1 and PPARα make.

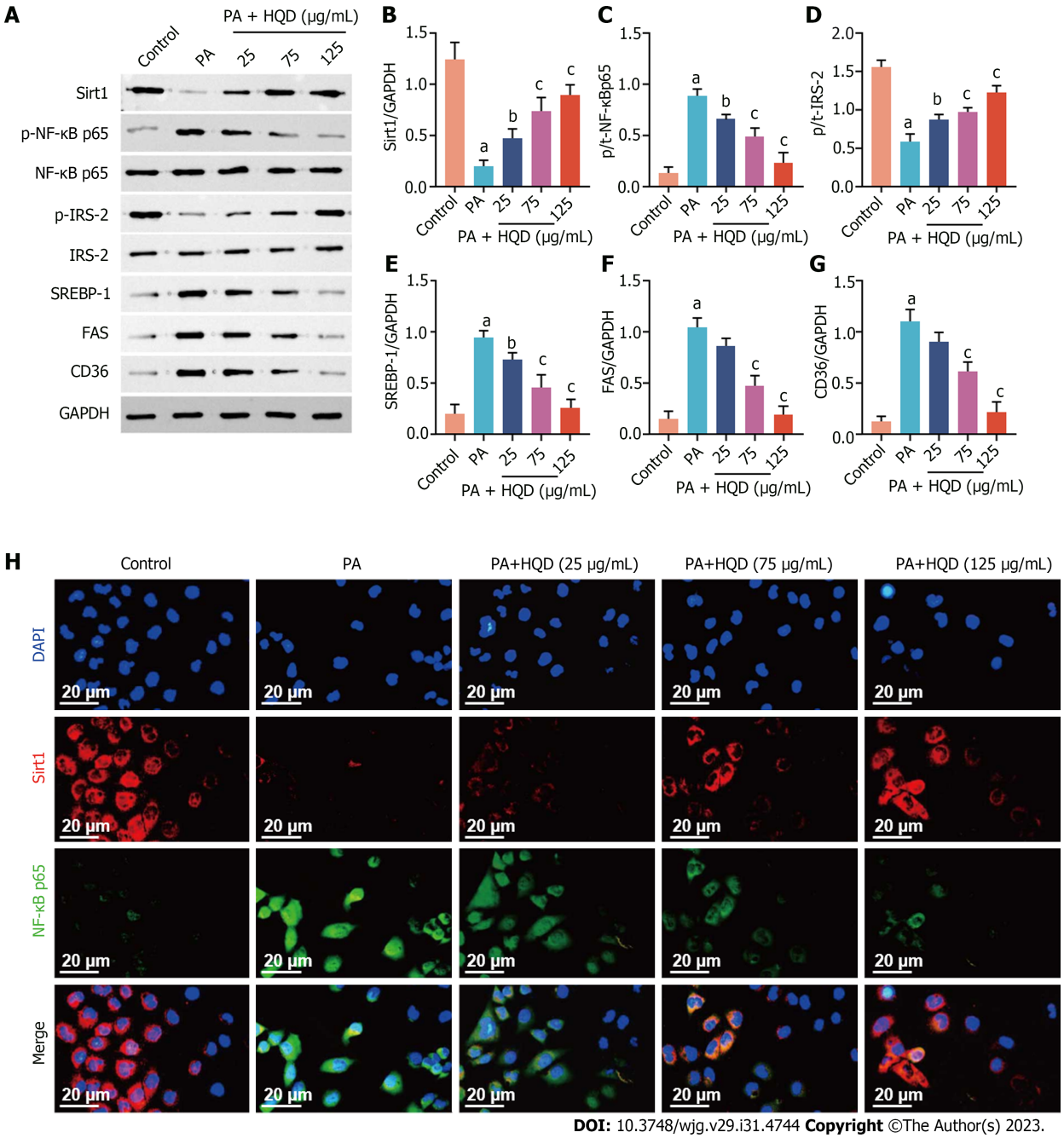

DOI: 10.3748/wjg.v29.i31.4744 **Copyright** ©The Author(s) 2023.

Figure 7 Huangqin decoction activates the Sirt1/NF-κB pathway in palmitic acid-induced HepG2 cells. Data are presented as mean ± SD of at least three independent experiments. $^{a}P < 0.01$ *vs* the control group, $^{b}P < 0.05$ and $^{c}P < 0.01$ *vs* the palmitic acid group. A: Expression levels of Sirt1, p-NF-κB/NF-κB, p-IRS-2/IRS-2, sterol regulatory element-binding protein 1, fatty acid synthase, and cluster of differentiation 36 in HepG2 cells; B–G: Semi-quantitative analysis of these proteins; H: Representative images of immunofluorescent staining of Sirt1 and NF-κB in HepG2 cells. CD36: Cluster of differentiation 36; DAPI: 4',6-diamidino-2-phenylindole; FAS: Fatty acid synthase; GAPDH: Glyceraldehyde-3-phosphate dehydrogenase; HQD, Huangqin decoction; PA: Palmitic acid; SREBP: Sterol regulatory element-binding protein.

CONCLUSION

In summary, we have demonstrated the mitigating effects of HQD on lipid metabolism disorders and insulin resistance. Our investigations revealed that HQD mediates these beneficial effects by modulating lipogenesis and inflammatory responses which trigger the Sirt1/NF-κB pathway (Figure 9). Our study provides strong evidence supporting HQD as a promising agent for NAFLD treatment.

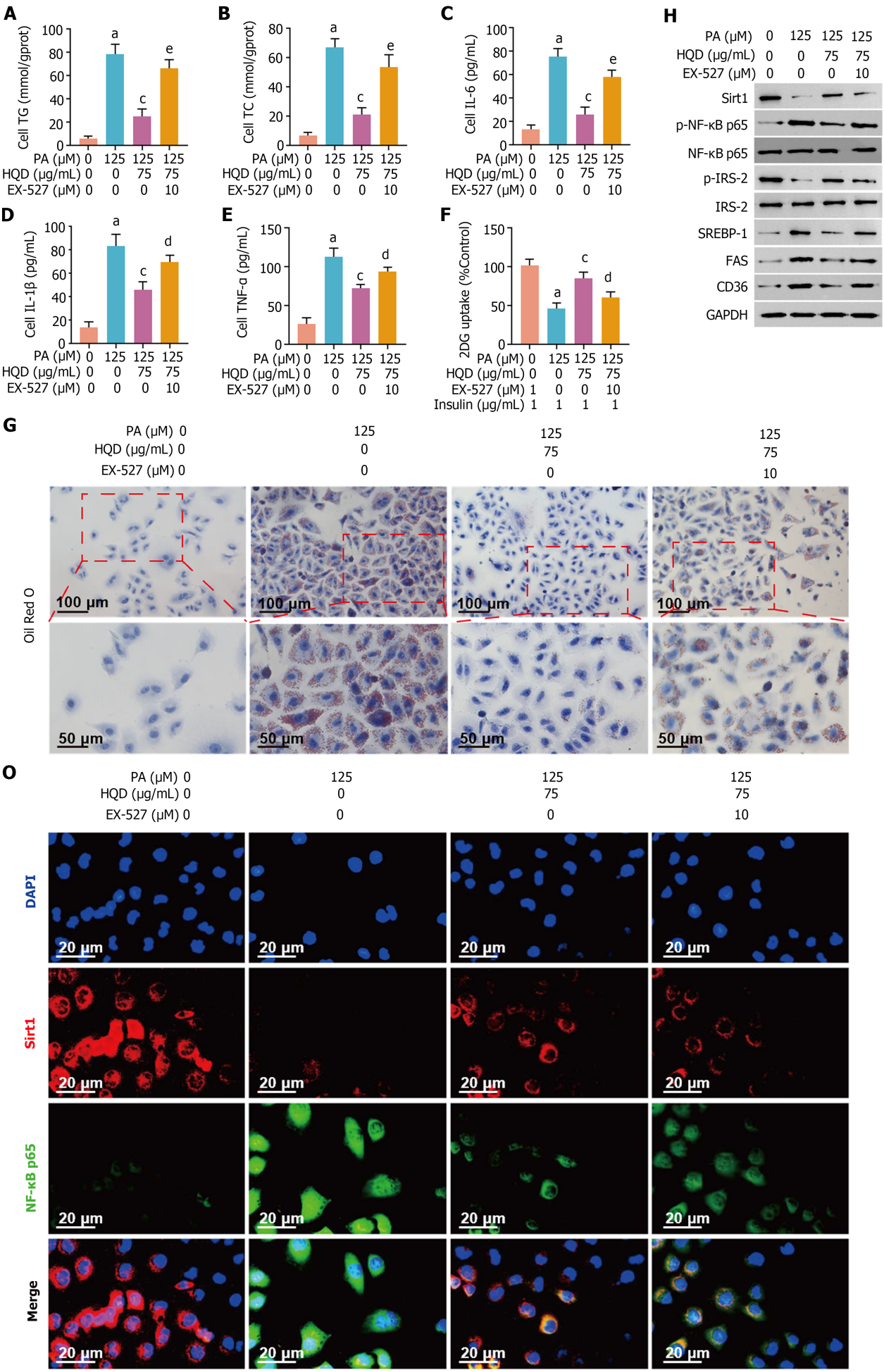
A
Cell TG (mmol/gprot)
B
Cell TC (mmol/gprot)
C
Cell IL-6 (pg/mL)
D
Cell IL-1β (pg/mL)
E
Cell TNF-α (pg/mL)
F
2DG uptake (%Control)
PA (μM) 0 125 125 125
HQD (μg/mL) 0 0 75 75
EX-527 (μM) 0 0 0 10
Insulin (μg/mL) 1 1 1 1
H
Sirt1
p-NF-κB p65
NF-κB p65
p-IRS-2
IRS-2
SREBP-1
FAS
CD36
GAPDH
G
Oil Red O
100 μm
50 μm
O
DAPI
Sirt1
NF-κB p65
Merge
20 μm

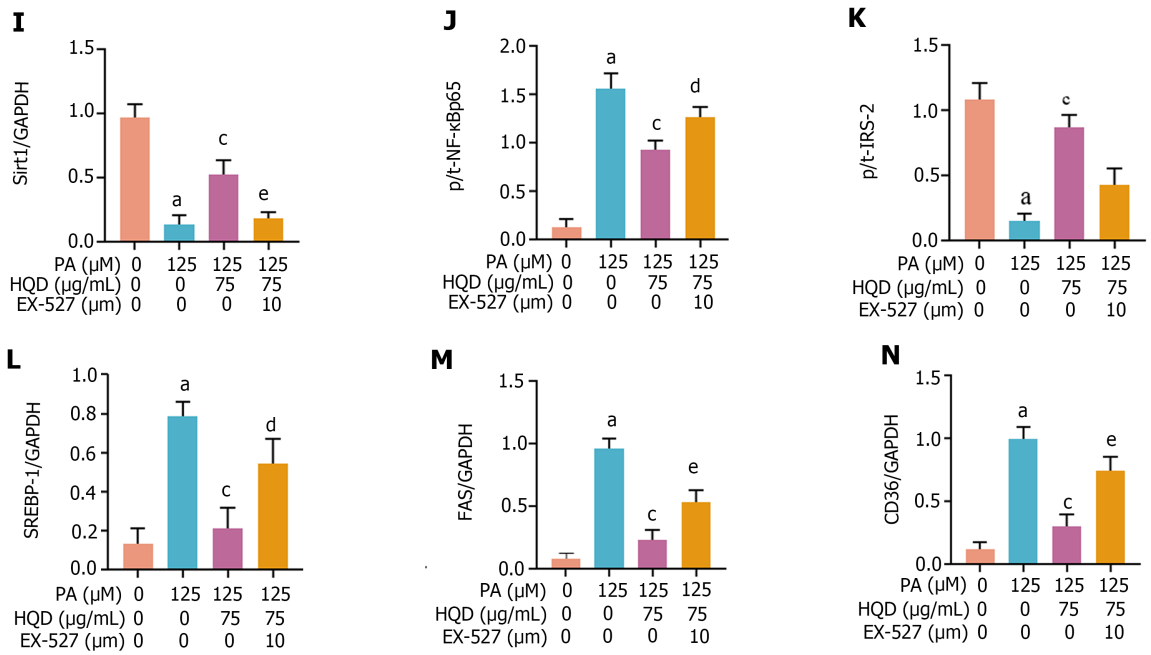

DOI: 10.3748/wjg.v29.i31.4744 **Copyright** ©The Author(s) 2023.

Figure 8 Huangqin decoction protects hepatocytes by triggering Sirt1/NF-κB pathway in palmitic acid-induced HepG2 cells. Data are presented as mean ± SD of at least three independent experiments. [a]*P* < 0.01 *vs* the control group, [b]*P* < 0.05 and [c]*P* < 0.01 *vs* the palmitic acid group, [d]*P* < 0.05 and [e]*P* < 0.01 *vs* the Huangqin decoction group. A and B: Levels of triacylglycerol (A) and total cholesterol (B) in HepG2 cells co-cultured with or without EX-527; C-E: Levels of interleukin (IL)-6, IL-1β, and tumor necrosis factor-α in HepG2 cells co-cultured with or without EX-527; F: Level of glucose uptake in HepG2 cells co-cultured with or without EX-527; G: Representative micrographs of Oil Red O staining of HepG2 cells co-cultured with or without EX-527; H: Expression levels of Sirt1, p-NF-κB/NF-κB, p-IRS-2/IRS-2, sterol regulatory element-binding protein-1c, fatty acid synthase, and cluster of differentiation 36 in HepG2 cells co-cultured with or without EX-527; I-N: Semi-quantitative analysis of these proteins; O: Representative images of immunofluorescent staining of Sirt1 and NF-κB in HepG2 cells co-cultured with or without EX-527. 2DG: 2-deoxydglucose; CD36: Cluster of differentiation 36; DAPI: 4',6-diamidino-2-phenylindole; FAS: Fatty acid synthase; GAPDH: Glyceraldehyde-3-phosphate dehydrogenase; HQD: Huangqin decoction; IL: Interleukin; PA: Palmitic acid; SREBP: Sterol regulatory element-binding protein; TC: Total cholesterol; TG: Triacylglycerol; TNF: Tumor necrosis factor.

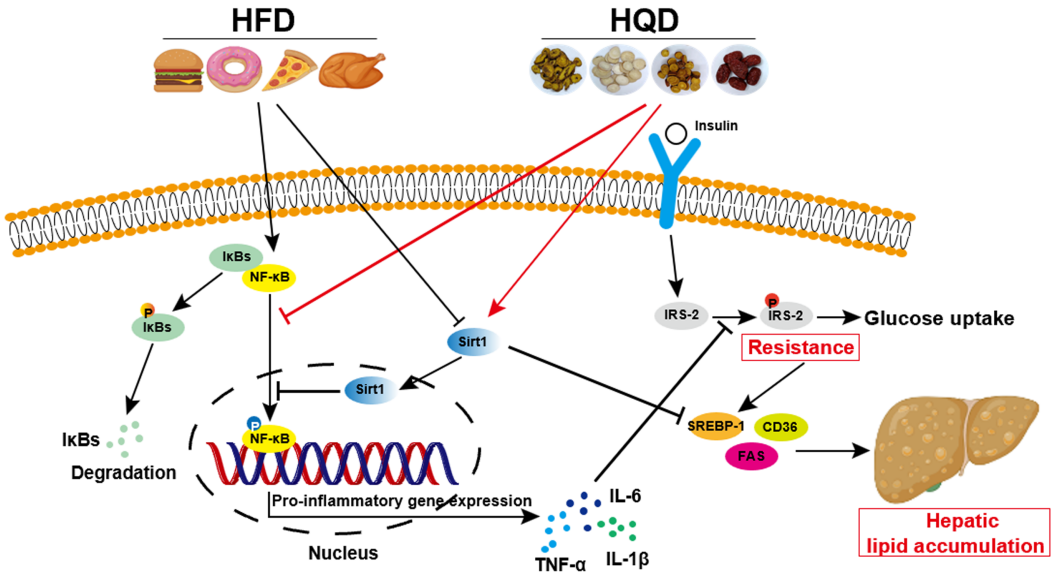

DOI: 10.3748/wjg.v29.i31.4744 **Copyright** ©The Author(s) 2023.

Figure 9 Schematic diagram illustrating the effects of Huangqin decoction on Sirt1/NF-κB pathway-modulated hepatic steatosis and insulin resistance. CD36: Cluster of differentiation 36; FAS: Fatty acid synthase; HFD: High-fat diet; HQD: Huangqin decoction; IL: Interleukin; SREBP: Sterol regulatory element-binding protein; TNF: Tumor necrosis factor.

ARTICLE HIGHLIGHTS

Research background

Non-alcoholic fatty liver disease (NAFLD) is the most common chronic liver disease, for which no effective therapeutic drugs have been approved. Huangqin decoction (HQD), a traditional Chinese medicine, has been widely used to treat liver diseases in clinical practice. Our study confirmed that HQD effectively mitigates high-fat diet (HFD)-induced hepatic inflammation. However, whether HQD has ameliorative effects on lipid metabolism disorders and insulin resistance, as well as the underlying mechanisms, remains unclear.

Research motivation

Convincing evidence for HQD in the clinical treatment of NAFLD is required.

Research objectives

This study aimed to investigate the therapeutic efficacy of HQD on lipid metabolism disorders and insulin resistance and explore the possible molecular mechanisms by focusing on the Sirt1/NF-κB pathway.

Research methods

High-performance liquid chromatography was used to identify the key components of HQD. HFD-induced NAFLD rats and palmitic acid-induced HepG2 cells were treated with HQD to investigate the mitigating effects of HQD on lipid metabolism disorders and insulin resistance. Finally, molecular biology techniques, including western blotting, immunohistochemistry, and immunofluorescence, were applied to explore the protein expression in the Sirt1/NF-κB pathway.

Research results

Ten key components of HQD were identified. The results showed that HQD effectively prevented lipid metabolism disorders in rats and HepG2 cells, inflammatory responses, and insulin resistance. Mechanistic exploration revealed that triggering Sirt1/NF-κB pathway-modulated lipogenesis and inflammation contributed to the favorable effects of HQD, which was further validated by the addition of EX-527 (a Sirt1 antagonist).

Research conclusions

Supported by our previous findings, we strongly believe that HQD is a promising complementary or auxiliary agent for the clinical treatment of NAFLD.

Research perspectives

HQD has been used to treat liver diseases in clinical practice for decades, with positive outcomes. More in-depth and precise research on the molecular mechanisms of HQD could guide and promote the clinical treatment of NAFLD more effectively.

ACKNOWLEDGEMENTS

The authors are grateful to Yue-Tao He (Leishenhe Mechanical and Electrical Equipment Co. Ltd.) for kindly providing high-quality reagents.

FOOTNOTES

Author contributions: Yan BF, Pan LF, and Quan YF contributed equally to this work and performed the research; Liu J and Zheng X designed the research and proofread the manuscript; Sha Q, Zhang JZ, and Zhou LB analyzed the data; Zhang YF carefully revised the manuscript; Qian XL, Gu XM, Li FT, and Wang T interpreted the data; All authors approved the final version of the article.

Supported by the Scientific Research Project of Jiangsu Health Commission, No. Z2022078; the Natural Science Foundation of Jiangsu Province, No. BK20220299.

Institutional review board statement: The study was reviewed and approved by the Institutional Review Board at Jiangsu Health Vocational College.

Institutional animal care and use committee statement: The experimental protocols strictly complied with the European Community criteria and were authorized by the Animal Ethics Committee of Jiangsu Health Vocational College (Permission No. JHVC-IACUC-2022-B007).

Conflict-of-interest statement: The authors declare that they have no competing interests.

Data sharing statement: No additional data are available.

ARRIVE guidelines statement: The authors have read the ARRIVE guidelines, and the manuscript was prepared and revised according to the ARRIVE guidelines.

Country/Territory of origin: China

ORCID number: Xian Zheng 0000-0003-3342-7636.

S-Editor: Lin C
L-Editor: A
P-Editor: Cai YX

REFERENCES

1 **Seval GC**, Kabacam G, Yakut M, Seven G, Savas B, Elhan A, Cinar K, Idilman R. The natural course of non-alcoholic fatty liver disease. *Hepatol Forum* 2020; **1**: 20-24 [PMID: 35949661 DOI: 10.14744/hf.2020.0008]
2 **Rafiq N**, Bai C, Fang Y, Srishord M, McCullough A, Gramlich T, Younossi ZM. Long-term follow-up of patients with nonalcoholic fatty liver. *Clin Gastroenterol Hepatol* 2009; **7**: 234-238 [PMID: 19049831 DOI: 10.1016/j.cgh.2008.11.005]
3 **Dam-Larsen S**, Becker U, Franzmann MB, Larsen K, Christoffersen P, Bendtsen F. Final results of a long-term, clinical follow-up in fatty liver patients. *Scand J Gastroenterol* 2009; **44**: 1236-1243 [PMID: 19670076 DOI: 10.1080/00365520903171284]
4 **McPherson S**, Hardy T, Henderson E, Burt AD, Day CP, Anstee QM. Evidence of NAFLD progression from steatosis to fibrosing-steatohepatitis using paired biopsies: implications for prognosis and clinical management. *J Hepatol* 2015; **62**: 1148-1155 [PMID: 25477264 DOI: 10.1016/j.jhep.2014.11.034]
5 **Yan T**, Yan N, Wang P, Xia Y, Hao H, Wang G, Gonzalez FJ. Herbal drug discovery for the treatment of nonalcoholic fatty liver disease. *Acta Pharm Sin B* 2020; **10**: 3-18 [PMID: 31993304 DOI: 10.1016/j.apsb.2019.11.017]
6 **Targher G**, Day CP, Bonora E. Risk of cardiovascular disease in patients with nonalcoholic fatty liver disease. *N Engl J Med* 2010; **363**: 1341-1350 [PMID: 20879883 DOI: 10.1056/NEJMra0912063]
7 **Younossi Z**, Anstee QM, Marietti M, Hardy T, Henry L, Eslam M, George J, Bugianesi E. Global burden of NAFLD and NASH: trends, predictions, risk factors and prevention. *Nat Rev Gastroenterol Hepatol* 2018; **15**: 11-20 [PMID: 28930295 DOI: 10.1038/nrgastro.2017.109]
8 **Estes C**, Anstee QM, Arias-Loste MT, Bantel H, Bellentani S, Caballeria J, Colombo M, Craxi A, Crespo J, Day CP, Eguchi Y, Geier A, Kondili LA, Kroy DC, Lazarus JV, Loomba R, Manns MP, Marchesini G, Nakajima A, Negro F, Petta S, Ratziu V, Romero-Gomez M, Sanyal A, Schattenberg JM, Tacke F, Tanaka J, Trautwein C, Wei L, Zeuzem S, Razavi H. Modeling NAFLD disease burden in China, France, Germany, Italy, Japan, Spain, United Kingdom, and United States for the period 2016-2030. *J Hepatol* 2018; **69**: 896-904 [PMID: 29886156 DOI: 10.1016/j.jhep.2018.05.036]
9 **Zheng X**, Zhang XG, Liu Y, Zhu LP, Liang XS, Jiang H, Shi GF, Zhao YY, Zhao ZW, Teng Y, Pan K, Zhang J, Yin ZQ. Arjunolic acid from Cyclocarya paliurus ameliorates nonalcoholic fatty liver disease in mice *via* activating Sirt1/AMPK, triggering autophagy and improving gut barrier function. *J Funct Foods* 2021; **86**: 104686 [DOI: 10.1016/j.jff.2021.104686]
10 **Day CP**, James OF. Steatohepatitis: a tale of two "hits"? *Gastroenterology* 1998; **114**: 842-845 [PMID: 9547102 DOI: 10.1016/s0016-5085(98)70599-2]
11 **Mouzaki M**, Loomba R. An update on the role of the microbiome in non-alcoholic fatty liver disease pathogenesis, diagnosis, and treatment. *Curr Treat Options Gastroenterol* 2020; **18**: 270-280 [PMID: 33716495 DOI: 10.1007/s11938-020-00290-2]
12 **Buzzetti E**, Pinzani M, Tsochatzis EA. The multiple-hit pathogenesis of non-alcoholic fatty liver disease (NAFLD). *Metabolism* 2016; **65**: 1038-1048 [PMID: 26823198 DOI: 10.1016/j.metabol.2015.12.012]
13 **Cao Y**, Jiang X, Ma H, Wang Y, Xue P, Liu Y. SIRT1 and insulin resistance. *J Diabetes Complications* 2016; **30**: 178-183 [PMID: 26422395 DOI: 10.1016/j.jdiacomp.2015.08.022]
14 **Li X**. SIRT1 and energy metabolism. *Acta Biochim Biophys Sin (Shanghai)* 2013; **45**: 51-60 [PMID: 23257294 DOI: 10.1093/abbs/gms108]
15 **Wu T**, Liu YH, Fu YC, Liu XM, Zhou XH. Direct evidence of sirtuin downregulation in the liver of non-alcoholic fatty liver disease patients. *Ann Clin Lab Sci* 2014; **44**: 410-418 [PMID: 25361925]
16 **Zhang Y**, Geng C, Liu X, Li M, Gao M, Fang F, Chang Y. Celastrol ameliorates liver metabolic damage caused by a high-fat diet through Sirt1. *Mol Metab* 2017; **6**: 138-147 [PMID: 28123944 DOI: 10.1016/j.molmet.2016.11.002]
17 **de Gregorio E**, Colell A, Morales A, Marí M. Relevance of SIRT1-NF-κB Axis as Therapeutic Target to Ameliorate Inflammation in Liver Disease. *Int J Mol Sci* 2020; **21** [PMID: 32485811 DOI: 10.3390/ijms21113858]
18 **Komeili-Movahhed T**, Bassirian M, Changizi Z, Moslehi A. SIRT1/NFκB pathway mediates anti-inflammatory and anti-apoptotic effects of rosmarinic acid on in a mouse model of nonalcoholic steatohepatitis (NASH). *J Recept Signal Transduct Res* 2022; **42**: 241-250 [PMID: 33787460 DOI: 10.1080/10799893.2021.1905665]
19 **Cobbina E**, Akhlaghi F. Non-alcoholic fatty liver disease (NAFLD) - pathogenesis, classification, and effect on drug metabolizing enzymes and transporters. *Drug Metab Rev* 2017; **49**: 197-211 [PMID: 28303724 DOI: 10.1080/03602532.2017.1293683]
20 **Liu SH**, Cheng YC. Old formula, new Rx: the journey of PHY906 as cancer adjuvant therapy. *J Ethnopharmacol* 2012; **140**: 614-623 [PMID: 22326673 DOI: 10.1016/j.jep.2012.01.047]
21 **Chen Q**, Liu M, Yu H, Li J, Wang S, Zhang Y, Qiu F, Wang T. Scutellaria baicalensis regulates FFA metabolism to ameliorate NAFLD through the AMPK-mediated SREBP signaling pathway. *J Nat Med* 2018; **72**: 655-666 [PMID: 29542003 DOI: 10.1007/s11418-018-1199-5]

22 **Luo Z**, Liu Y, Han X, Yang W, Wang G, Wang J, Jiang X, Sen M, Li X, Yu G, Shi Y. Mechanism of Paeoniae Radix Alba in the Treatment of Non-alcoholic Fatty Liver Disease Based on Sequential Metabolites Identification Approach, Network Pharmacology, and Binding Affinity Measurement. *Front Nutr* 2021; **8**: 677659 [PMID: 34604271 DOI: 10.3389/fnut.2021.677659]

23 **Hajiaghamohammadi AA**, Ziaee A, Samimi R. The efficacy of licorice root extract in decreasing transaminase activities in non-alcoholic fatty liver disease: a randomized controlled clinical trial. *Phytother Res* 2012; **26**: 1381-1384 [PMID: 22308054 DOI: 10.1002/ptr.3728]

24 **Yan BF**, Wang Y, Wang WB, Ding XJ, Wei B, Liu SJ, Fu TM, Chen L, Zhang JZ, Liu J, Zheng X. Huangqin decoction mitigates hepatic inflammation in high-fat diet-challenged rats by inhibiting TLR4/NF-κB/NLRP3 pathway. *J Ethnopharmacol* 2023; **303**: 115999 [PMID: 36509260 DOI: 10.1016/j.jep.2022.115999]

25 **Yan BF**, Chen X, Chen YF, Liu SJ, Xu CX, Chen L, Wang WB, Wen TT, Zheng X, Liu J. Aqueous extract of Paeoniae Radix Alba (Paeonia lactiflora Pall.) ameliorates DSS-induced colitis in mice by tunning the intestinal physical barrier, immune responses, and microbiota. *J Ethnopharmacol* 2022; **294**: 115365 [PMID: 35597411 DOI: 10.1016/j.jep.2022.115365]

26 **Zhu Y**, Wan N, Shan X, Deng G, Xu Q, Ye H, Sun Y. Celastrol targets adenylyl cyclase-associated protein 1 to reduce macrophages-mediated inflammation and ameliorates high fat diet-induced metabolic syndrome in mice. *Acta Pharm Sin B* 2021; **11**: 1200-1212 [PMID: 34094828 DOI: 10.1016/j.apsb.2020.12.008]

27 **Wang Y**, Zhao H, Li X, Li N, Wang Q, Liu Y, Liang Q, Shao Z, Zhang N, Zhao T, Peng L, Li P. Tangshen Formula Alleviates Hepatic Steatosis by Inducing Autophagy Through the AMPK/SIRT1 Pathway. *Front Physiol* 2019; **10**: 494 [PMID: 31105592 DOI: 10.3389/fphys.2019.00494]

28 **Xiao Q**, Zhang S, Yang C, Du R, Zhao J, Li J, Xu Y, Qin Y, Gao Y, Huang W. Ginsenoside Rg1 Ameliorates Palmitic Acid-Induced Hepatic Steatosis and Inflammation in HepG2 Cells *via* the AMPK/NF-κB Pathway. *Int J Endocrinol* 2019; **2019**: 7514802 [PMID: 31467529 DOI: 10.1155/2019/7514802]

29 **Badolati N**, Masselli R, Sommella E, Sagliocchi S, Di Minno A, Salviati E, Campiglia P, Dentice M, Tenore GC, Stornaiuolo M, Novellino E. The Hepatoprotective Effect of Taurisolo, a Nutraceutical Enriched in Resveratrol and Polyphenols, Involves Activation of Mitochondrial Metabolism in Mice Liver. *Antioxidants (Basel)* 2020; **9** [PMID: 32403305 DOI: 10.3390/antiox9050410]

30 **Shi H**, Dong C, Wang M, Liu R, Wang Y, Kan Z, Wang L, Si G. Exploring the mechanism of Yizhi Tongmai decoction in the treatment of vascular dementia through network pharmacology and molecular docking. *Ann Transl Med* 2021; **9**: 164 [PMID: 33569466 DOI: 10.21037/atm-20-8165]

31 **Huo M**, Ma L, Liu G. Exploring the mechanism of Yixinyin for myocardial infarction by weighted co-expression network and molecular docking. *Sci Rep* 2021; **11**: 22567 [PMID: 34799616 DOI: 10.1038/s41598-021-01691-8]

32 **Liu W**, Shang J, Deng Y, Han X, Chen Y, Wang S, Yang R, Dong F, Shang H. Network pharmacology analysis on mechanism of Jian Pi Qing Gan Yin decoction ameliorating high fat diet-induced non-alcoholic fatty liver disease and validated in vivo. *J Ethnopharmacol* 2022; **295**: 115382 [PMID: 35577161 DOI: 10.1016/j.jep.2022.115382]

33 **Chao J**, Cheng HY, Chang ML, Huang SS, Liao JW, Cheng YC, Peng WH, Pao LH. Gallic Acid Ameliorated Impaired Lipid Homeostasis in a Mouse Model of High-Fat Diet-and Streptozotocin-Induced NAFLD and Diabetes through Improvement of β-oxidation and Ketogenesis. *Front Pharmacol* 2020; **11**: 606759 [PMID: 33643038 DOI: 10.3389/fphar.2020.606759]

34 **Li YC**, Qiao JY, Wang BY, Bai M, Shen JD, Cheng YX. Paeoniflorin Ameliorates Fructose-Induced Insulin Resistance and Hepatic Steatosis by Activating LKB1/AMPK and AKT Pathways. *Nutrients* 2018; **10** [PMID: 30081580 DOI: 10.3390/nu10081024]

35 **Zhang X**, Huo Z, Luan H, Huang Y, Shen Y, Sheng L, Liang J, Wu F. Scutellarin ameliorates hepatic lipid accumulation by enhancing autophagy and suppressing IRE1α/XBP1 pathway. *Phytother Res* 2022; **36**: 433-447 [PMID: 34859513 DOI: 10.1002/ptr.7344]

36 **Hu Q**, Zhang W, Wu Z, Tian X, Xiang J, Li L, Li Z, Peng X, Wei S, Ma X, Zhao Y. Baicalin and the liver-gut system: Pharmacological bases explaining its therapeutic effects. *Pharmacol Res* 2021; **165**: 105444 [PMID: 33493657 DOI: 10.1016/j.phrs.2021.105444]

37 **Zheng X**, Zhao MG, Jiang CH, Sheng XP, Yang HM, Liu Y, Yao XM, Zhang J, Yin ZQ. Triterpenic acids-enriched fraction from Cyclocarya paliurus attenuates insulin resistance and hepatic steatosis *via* PI3K/Akt/GSK3β pathway. *Phytomedicine* 2020; **66**: 153130 [PMID: 31790897 DOI: 10.1016/j.phymed.2019.153130]

38 **Araya J**, Rodrigo R, Videla LA, Thielemann L, Orellana M, Pettinelli P, Poniachik J. Increase in long-chain polyunsaturated fatty acid n - 6/n - 3 ratio in relation to hepatic steatosis in patients with non-alcoholic fatty liver disease. *Clin Sci (Lond)* 2004; **106**: 635-643 [PMID: 14720121 DOI: 10.1042/cs20030326]

39 **Park JC**, Jeong WJ, Seo SH, Choi KY. WDR76 mediates obesity and hepatic steatosis *via* HRas destabilization. *Sci Rep* 2019; **9**: 19676 [PMID: 31873167 DOI: 10.1038/s41598-019-56211-6]

40 **Bechmann LP**, Hannivoort RA, Gerken G, Hotamisligil GS, Trauner M, Canbay A. The interaction of hepatic lipid and glucose metabolism in liver diseases. *J Hepatol* 2012; **56**: 952-964 [PMID: 22173168 DOI: 10.1016/j.jhep.2011.08.025]

41 **Tilg H**, Moschen AR, Roden M. NAFLD and diabetes mellitus. *Nat Rev Gastroenterol Hepatol* 2017; **14**: 32-42 [PMID: 27729660 DOI: 10.1038/nrgastro.2016.147]

42 **Lambert JE**, Ramos-Roman MA, Browning JD, Parks EJ. Increased de novo lipogenesis is a distinct characteristic of individuals with nonalcoholic fatty liver disease. *Gastroenterology* 2014; **146**: 726-735 [PMID: 24316260 DOI: 10.1053/j.gastro.2013.11.049]

43 **Song Z**, Xiaoli AM, Yang F. Regulation and Metabolic Significance of De Novo Lipogenesis in Adipose Tissues. *Nutrients* 2018; **10** [PMID: 30274245 DOI: 10.3390/nu10101383]

44 **Horton JD**, Goldstein JL, Brown MS. SREBPs: activators of the complete program of cholesterol and fatty acid synthesis in the liver. *J Clin Invest* 2002; **109**: 1125-1131 [PMID: 11994399 DOI: 10.1172/jci15593]

45 **Manzoor M**, Muroi M, Ogawa N, Kobayashi H, Nishimura H, Chen D, Fasina OB, Wang J, Osada H, Yoshida M, Xiang L, Qi J. Isoquercitrin from Apocynum venetum L. produces an anti-obesity effect on obese mice by targeting C-1-tetrahydrofolate synthase, carbonyl reductase, and glutathione S-transferase P and modification of the AMPK/SREBP-1c/FAS/CD36 signaling pathway in mice in vivo. *Food Funct* 2022; **13**: 10923-10936 [PMID: 36205648 DOI: 10.1039/d2fo02438a]

46 **Tilg H**, Moschen AR. Evolution of inflammation in nonalcoholic fatty liver disease: the multiple parallel hits hypothesis. *Hepatology* 2010; **52**: 1836-1846 [PMID: 21038418 DOI: 10.1002/hep.24001]

47 **Sakurai Y**, Kubota N, Yamauchi T, Kadowaki T. Role of Insulin Resistance in MAFLD. *Int J Mol Sci* 2021; **22** [PMID: 33923817 DOI: 10.3390/ijms22084156]

48 **Zhang HH**, Halbleib M, Ahmad F, Manganiello VC, Greenberg AS. Tumor necrosis factor-alpha stimulates lipolysis in differentiated human adipocytes through activation of extracellular signal-related kinase and elevation of intracellular cAMP. *Diabetes* 2002; **51**: 2929-2935 [PMID: 12351429 DOI: 10.2337/diabetes.51.10.2929]

49 **Hotamisligil GS**, Shargill NS, Spiegelman BM. Adipose expression of tumor necrosis factor-alpha: direct role in obesity-linked insulin resistance. *Science* 1993; **259**: 87-91 [PMID: 7678183 DOI: 10.1126/science.7678183]

50 **Sabio G**, Das M, Mora A, Zhang Z, Jun JY, Ko HJ, Barrett T, Kim JK, Davis RJ. A stress signaling pathway in adipose tissue regulates hepatic insulin resistance. *Science* 2008; **322**: 1539-1543 [PMID: 19056984 DOI: 10.1126/science.1160794]

51 **Zhang JN**, Ma Y, Wei XY, Liu KY, Wang H, Han H, Cui Y, Zhang MX, Qin WD. Remifentanil Protects against Lipopolysaccharide-Induced Inflammation through PARP-1/NF-κB Signaling Pathway. *Mediators Inflamm* 2019; **2019**: 3013716 [PMID: 32082073 DOI: 10.1155/2019/3013716]

52 **Boden G**, She P, Mozzoli M, Cheung P, Gumireddy K, Reddy P, Xiang X, Luo Z, Ruderman N. Free fatty acids produce insulin resistance and activate the proinflammatory nuclear factor-kappaB pathway in rat liver. *Diabetes* 2005; **54**: 3458-3465 [PMID: 16306362 DOI: 10.2337/diabetes.54.12.3458]

53 **Yeung F**, Hoberg JE, Ramsey CS, Keller MD, Jones DR, Frye RA, Mayo MW. Modulation of NF-kappaB-dependent transcription and cell survival by the SIRT1 deacetylase. *EMBO J* 2004; **23**: 2369-2380 [PMID: 15152190 DOI: 10.1038/sj.emboj.7600244]

54 **Yoo J**, Jeong IK, Ahn KJ, Chung HY, Hwang YC. Fenofibrate, a PPARα agonist, reduces hepatic fat accumulation through the upregulation of TFEB-mediated lipophagy. *Metabolism* 2021; **120**: 154798 [PMID: 33984335 DOI: 10.1016/j.metabol.2021.154798]

55 **Mahmoudi A**, Moallem SA, Johnston TP, Sahebkar A. Liver Protective Effect of Fenofibrate in NASH/NAFLD Animal Models. *PPAR Res* 2022; **2022**: 5805398 [PMID: 35754743 DOI: 10.1155/2022/5805398]

56 **El-Haggar SM**, Mostafa TM. Comparative clinical study between the effect of fenofibrate alone and its combination with pentoxifylline on biochemical parameters and liver stiffness in patients with non-alcoholic fatty liver disease. *Hepatol Int* 2015; **9**: 471-479 [PMID: 25956613 DOI: 10.1007/s12072-015-9633-1]

57 **Oscarsson J**, Önnerhag K, Risérus U, Sundén M, Johansson L, Jansson PA, Moris L, Nilsson PM, Eriksson JW, Lind L. Effects of free omega-3 carboxylic acids and fenofibrate on liver fat content in patients with hypertriglyceridemia and non-alcoholic fatty liver disease: A double-blind, randomized, placebo-controlled study. *J Clin Lipidol* 2018; **12**: 1390-1403.e4 [PMID: 30197273 DOI: 10.1016/j.jacl.2018.08.003]

58 **Huang K**, Du M, Tan X, Yang L, Li X, Jiang Y, Wang C, Zhang F, Zhu F, Cheng M, Yang Q, Yu L, Wang L, Huang D, Huang K. PARP1-mediated PPARα poly(ADP-ribosyl)ation suppresses fatty acid oxidation in non-alcoholic fatty liver disease. *J Hepatol* 2017; **66**: 962-977 [PMID: 27979751 DOI: 10.1016/j.jhep.2016.11.020]

59 **Kim TH**, Yang YM, Han CY, Koo JH, Oh H, Kim SS, You BH, Choi YH, Park TS, Lee CH, Kurose H, Noureddin M, Seki E, Wan YY, Choi CS, Kim SG. Gα12 ablation exacerbates liver steatosis and obesity by suppressing USP22/SIRT1-regulated mitochondrial respiration. *J Clin Invest* 2018; **128**: 5587-5602 [PMID: 30300140 DOI: 10.1172/jci97831]

World Journal of Gastroenterology

Submit a Manuscript: https://www.f6publishing.com

World J Gastroenterol 2023 August 21; 29(31): 4763-4773

DOI: 10.3748/wjg.v29.i31.4763

ISSN 1007-9327 (print) ISSN 2219-2840 (online)

ORIGINAL ARTICLE

Retrospective Cohort Study

Gastric cancer incidence based on endoscopic Kyoto classification of gastritis

Osamu Toyoshima, Toshihiro Nishizawa, Shuntaro Yoshida, Tatsuya Matsuno, Gota Fujisawa, Akira Toyoshima, Hirotoshi Ebinuma, Mitsuhiro Fujishiro, Yutaka Saito, Hidekazu Suzuki

Specialty type: Gastroenterology and hepatology

Provenance and peer review: Unsolicited article; Externally peer reviewed.

Peer-review model: Single blind

Peer-review report's scientific quality classification

Grade A (Excellent): 0
Grade B (Very good): B
Grade C (Good): C
Grade D (Fair): 0
Grade E (Poor): 0

P-Reviewer: Ma L, China; Senchukova M, Russia

Received: June 3, 2023
Peer-review started: June 3, 2023
First decision: July 10, 2023
Revised: July 20, 2023
Accepted: July 28, 2023
Article in press: July 28, 2023
Published online: August 21, 2023

Osamu Toyoshima, Shuntaro Yoshida, Tatsuya Matsuno, Gota Fujisawa, Department of Gastroenterology, Toyoshima Endoscopy Clinic, Tokyo 157-0066, Japan

Toshihiro Nishizawa, Hirotoshi Ebinuma, Department of Gastroenterology and Hepatology, International University of Health and Welfare, Narita Hospital, Narita 286-8520, Japan

Akira Toyoshima, Department of Colorectal Surgery, Japanese Red Cross Medical Center, Tokyo 150-8935, Japan

Mitsuhiro Fujishiro, Department of Gastroenterology, Graduate School of Medicine, The University of Tokyo, Tokyo 113-8655, Japan

Yutaka Saito, Division of Endoscopy, National Cancer Center Hospital, Tokyo 104-0045, Japan

Hidekazu Suzuki, Division of Gastroenterology and Hepatology, Department of Internal Medicine, Tokai University School of Medicine, Isehara 259-1193, Japan

Corresponding author: Toshihiro Nishizawa, MD, PhD, Professor, Department of Gastroenterology and Hepatology, International University of Health and Welfare, Narita Hospital, Hatakeda 852, Narita, Chiba, Narita 286-8520, Japan. nisizawa@kf7.so-net.ne.jp

Abstract

BACKGROUND

Gastric cancer (GC) incidence based on the endoscopic Kyoto classification of gastritis has not been systematically investigated using time-to-event analysis.

AIM

To examine GC incidence in an endoscopic surveillance cohort.

METHODS

This study was retrospectively conducted at the Toyoshima Endoscopy Clinic. Patients who underwent two or more esophagogastroduodenoscopies were enrolled. GC incidence was based on Kyoto classification scores, such as atrophy, intestinal metaplasia (IM), enlarged folds (EFs), nodularity, diffuse redness (DR), and total Kyoto scores. Hazard ratios (HRs) adjusted for age and sex were calculated using a Cox hazard model.

RESULTS

A total of 6718 patients were enrolled (median age 54.0 years; men 44.2%). During the follow-up period (max 5.02 years; median 2.56 years), GC developed in 34 patients. The average frequency of GCs per year was 0.19%. Kyoto atrophy scores 1 [HR with score 0 as reference: 3.66, 95% confidence interval (CI): 1.06 to 12.61], 2 (11.60, 3.82-35.27), IM score 2 (9.92, 4.37-22.54), EF score 1 (4.03, 1.63-9.96), DR scores 1 (6.22, 2.65-14.56), and 2 (10.01, 3.73-26.86) were associated with GC incidence, whereas nodularity scores were not. The total Kyoto scores of 4 (HR with total Kyoto scores 0-1 as reference: 6.23, 95%CI: 1.93 to 20.13, $P = 0.002$) and 5-8 (16.45, 6.29-43.03, $P < 0.001$) were more likely to develop GC, whereas the total Kyoto scores 2-3 were not. The HR of the total Kyoto score for developing GC per 1 rank was 1.75 (95%CI: 1.46 to 2.09, $P < 0.001$).

CONCLUSION

A high total Kyoto score (≥ 4) was associated with GC incidence. The endoscopy-based diagnosis of gastritis can stratify GC risk.

Key Words: Gastric cancer; Gastritis; Endoscopy; Atrophy; Intestinal metaplasia; Kyoto classification

Core Tip: A high total Kyoto score (≥ 4) was associated with gastric cancer (GC) incidence. Adjusted hazard ratios (HRs) for the total Kyoto scores of 4 and 5-8 were high at 6.23 and 16.45, respectively, compared to the total Kyoto scores of 0-1. The HR of the total Kyoto score for developing GC per 1 rank was 1.75.

Citation: Toyoshima O, Nishizawa T, Yoshida S, Matsuno T, Fujisawa G, Toyoshima A, Ebinuma H, Fujishiro M, Saito Y, Suzuki H. Gastric cancer incidence based on endoscopic Kyoto classification of gastritis. *World J Gastroenterol* 2023; 29(31): 4763-4773
URL: https://www.wjgnet.com/1007-9327/full/v29/i31/4763.htm
DOI: https://dx.doi.org/10.3748/wjg.v29.i31.4763

INTRODUCTION

Gastric cancer (GC) is a global health problem and the third most common cause of cancer-related deaths worldwide[1]. *Helicobacter pylori* (*H. pylori*) infection is estimated to account for 89% of GC cases, and *H. pylori*-related gastritis is a precursor of GC[2-6]. Evaluation of *H. pylori*-related gastritis is clinically important because it allows for the risk stratification of GC[2,7-9]. Endoscopy detects early GCs and precisely diagnoses gastritis. Periodic endoscopic screening can reduce deaths from GC[10]. Recent advances in endoscopic technology allow for more accurate endoscopic diagnosis of gastritis[11,12].

The endoscopy-based Kyoto classification of gastritis was advocated by the Japan Society for Gastrointestinal Endoscopy in 2013. This classification aims to ensure that the endoscopic diagnosis of gastritis is unified and matched with the histopathology[13]. Recently, the Kyoto classification has been widely used in clinical practice and vigorously studied worldwide[14,15]. To assess GC risk, the Kyoto classification individually scores five *H. pylori*-related gastritis findings, such as atrophy, intestinal metaplasia (IM), enlarged fold (EF), nodularity, and diffuse redness (DR), and defines their sum as the total Kyoto score.

Several investigations have clarified that not only individual Kyoto scores but also the total Kyoto score are associated with *H. pylori* infection and GC risks[14]. For example, the total Kyoto score was associated with *H. pylori* infection, presence of GC[16-19], and GC risk indicators, such as serum pepsinogen titer, serum *H. pylori* antibody titer, histological distribution of neutrophil infiltration in the gastric mucosa, and genotype of the single nucleotide polymorphism. Collectively, total Kyoto scores of 0, ≥ 2, and ≥ 4 indicated a normal stomach, *H. pylori*-infected gastritis, and gastritis at risk for GC, respectively[14].

To date, GC incidence based on the Kyoto classification scores has not been systematically investigated using time-to-event analysis. Therefore, we examined GC incidence according to the five individual Kyoto scores and the total Kyoto score in the endoscopic surveillance cohort and verified the GC risks of endoscopic gastritis in Japan, which is a high GC morbidity area.

MATERIALS AND METHODS

Study design and overview

This cohort study was retrospectively conducted at the Toyoshima Endoscopy Clinic. We obtained data from the Toyoshima Endoscopy Clinic Database. This study was approved by the institutional review board of the Yoyogi Mental Clinic (approval no. RKK227). Written informed consent was obtained from patients at the time of esophagogastroduodenoscopy (EGD) to use their data for research purposes. The study's protocol was published on our institute's website (

www.ichou.com) so that patients could opt out of the study. All clinical investigations were conducted in accordance with the ethical guidelines of the Declaration of Helsinki.

Patients

This study enrolled patients who underwent two or more EGDs at the Toyoshima Endoscopy Clinic, an urban area in Tokyo, Japan, between April 2017 and April 2022. We excluded patients with a previous surgical gastrectomy at baseline and those who underwent the last EGD within one month after the index EGD. The indications for the index EGD included screening, surveillance for gastritis or other upper gastrointestinal diseases, and examination for symptoms or abnormal findings on other tests. *H. pylori* status was determined using serum anti-*H. pylori* antibodies, urea breath test, histology, and/or endoscopy.

Kyoto classification score

In the Kyoto classification, the total Kyoto score was developed as a GC risk score[14]. The total Kyoto score is calculated as the sum of the following five Kyoto scores: Atrophy, IM, EF, nodularity, and DR, and ranges from 0 to 8 (Supplementary Table 1). Atrophy was classified based on the extent of mucosal atrophy using the Kimura-Takemoto classification[20]. Non-atrophy and Closed I, Closed II and III, and Open I to III were scored as atrophy scores of 0, 1, and 2, respectively. The IM commonly appears as a grayish-white, slightly elevated patch. IM scores of 0, 1, and 2 were defined as the absence of IM, IM limited to the antrum, and IM extending into the corpus, respectively. EF was defined as a width of ≥ 5 mm in the greater curvature of the corpus, which was not flattened by stomach insufflation. The absence and presence of EF were scored as 0 and 1, respectively. Nodularity was identified by a miliary pattern resembling "goose flesh", which was typically located in the antrum. The absence and presence of nodularity were scored 0 and 1, respectively. DR indicated uniform redness observed in the non-atrophic mucosa, mainly in the greater curvature of the corpus. The regular arrangement of collecting venules (RAC) in the corpus appears as numerous dots, which are starfish-like shapes in close view. DR scores of 0, 1, and 2 were defined as the absence of DR, mild DR and/or DR with partial RAC, and severe DR without RAC, respectively[14].

EGD

EGDs were performed by gastrointestinal endoscopists using the Olympus' (Tokyo, Japan) endoscopic system (EVIS X1 or LUCERA ELITE) and endoscope (GIF-XZ1200, GIF-1200N, GIF-HQ290, GIF-H290Z, or GIF-XP290N). The T-File System (STS-MEDIC Inc., Tokyo, Japan) was used to file endoscopic images and document endoscopic findings.

The Kyoto classification scores were assessed using white light imaging without magnification. The endoscopists diagnosed the Kyoto classification scores on-site during EGD, and it was retrospectively reviewed by experienced endoscopists. Endoscopists performed EGDs after learning from textbooks and journal articles on the Kyoto classification of gastritis[14,21].

GC

GC was histologically diagnosed based on biopsy or resected specimens. GC morphology and histology were classified based on the Japanese classification of gastric carcinoma[22] and Lauren's classification[23], respectively.

Outcomes

This cohort study evaluated GC incidence based on patients' age, sex, *H. pylori* status, and endoscopic Kyoto classification scores of gastritis, such as atrophy, IM, EF, nodularity, DR, and total Kyoto scores. The primary outcome was GC incidence according to the total Kyoto score. We performed a time-to-event analysis with the start time as the date of index EGD. Data were censored on the date of the last EGD. The effects of Kyoto classification scores on GC development were estimated. The total Kyoto scores were categorized into 4 (*i.e.*, 0-1, 2-3, 4, and 5-8) based on the frequency of GC increasing stepwise with the total Kyoto scores of 0-1, 2-3, and ≥ 4 in a cross-sectional study[24] and the number of patients in this study. The secondary outcomes were GC incidence according to the Kyoto atrophy, IM, EF, nodularity, and DR scores.

Statistical analysis

Baseline characteristics were compared between GC and non-GC groups using binomial logistic regression model. Kaplan-Meier curves were constructed according to patient age, sex, *H. pylori* status, and Kyoto classification scores (*i.e.*, atrophy, IM, EF, nodularity, DR, and the total Kyoto scores). Statistical differences were estimated using the log-rank tests. The average frequency of GCs per year was calculated by dividing the number of events by the total person-years of observation. Hazard ratios (HRs) with 95% confidence intervals (CIs) for GC development were estimated using the Cox proportional hazards regression model. In multivariate analysis, HRs were adjusted for patient age and sex. A P value < 0.05 (two-sided) was defined as statistically significant. Statistical analysis was conducted using BellCurve for Excel version 4.03 (Social Survey Research Information Co., Ltd., Tokyo, Japan).

RESULTS

Patient enrollment

A total of 30585 EGDs in 16969 patients were performed during the study period. Six thousand seven hundred forty-four

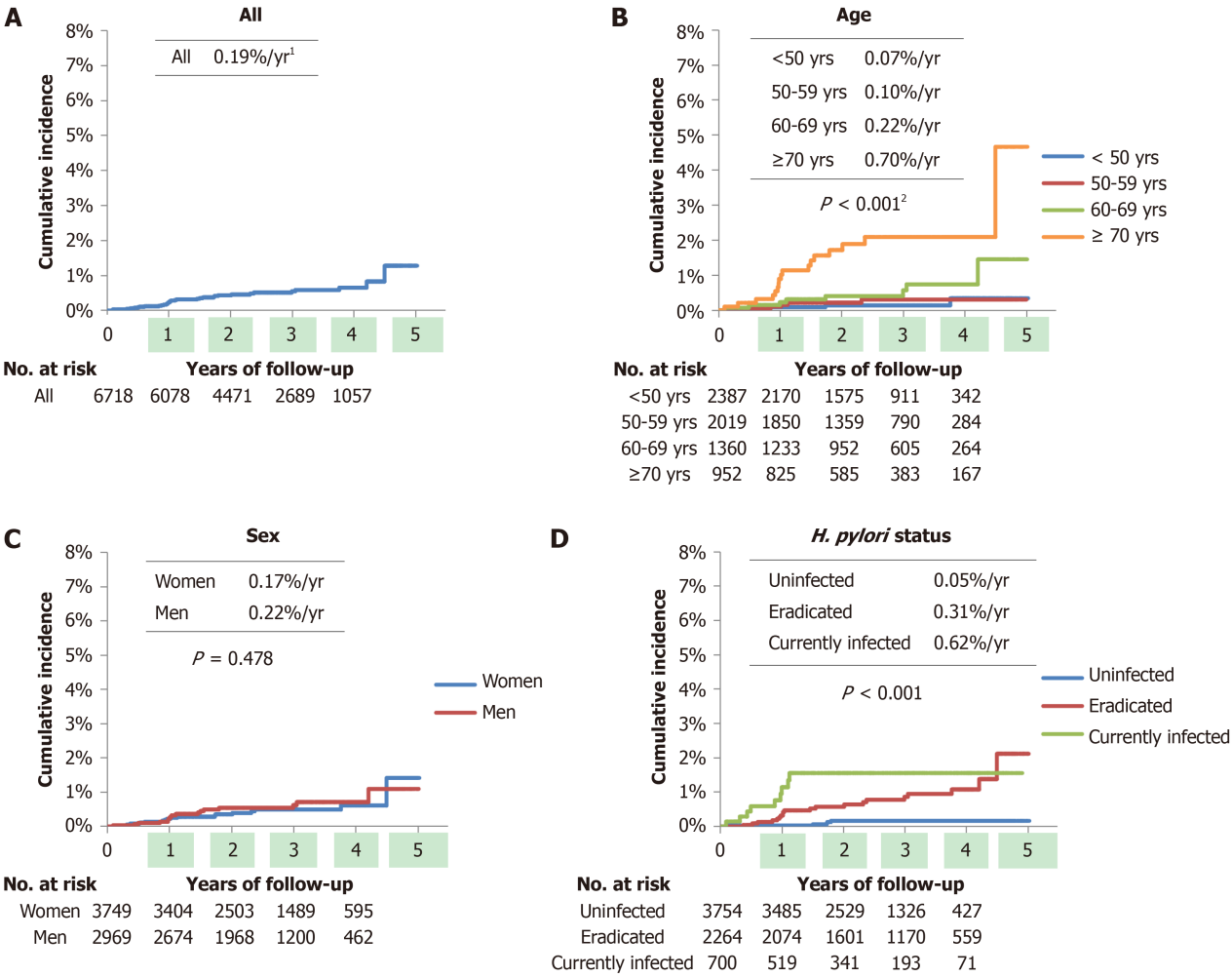

DOI: 10.3748/wjg.v29.i31.4763

Figure 1 Cumulative incidence of gastric cancer according to patient demographic characteristics. A-D: Kaplan-Meier curves of gastric cancer development for all patients (A), according to age (B), sex (C), and *Helicobacter pylori* status (D). [1]The average frequency of gastric cancer per year. [2]*P* values were calculated using a log-rank test.

patients underwent two or more EGDs. Of these, 19 patients with a previous surgical gastrectomy and 7 with a follow-up period of less than 1 mo were excluded. A total of 6718 patients were enrolled.

The baseline patient characteristics are shown in Table 1. The median age of the patients was 54 years with the interquartile range (IQR) of 46-64 years. Men accounted for 44.2% of the cases. The proportion of patients with *H. pylori* status of uninfected, eradicated, and currently infected was 55.9%, 33.7%, and 10.4%, respectively. Patients were followed up for up to 5.02 years (median 2.56 years, IQR 1.74-3.64 years). The median (IQR) of Kyoto classification scores were 0 (0-1) for atrophy; 0 (0-0) for IM, EF, nodularity, and DR; and 0 (0-2) for total Kyoto. Supplementary Table 2 is shown with the mean and standard deviation. During the follow-up period, 37 GCs occurred in 34 patients. The characteristics of GCs are presented in Table 2. All GCs were superficial and within the submucosal depth. Lauren's intestinal type made up 89.1% of GCs.

GC incidence

Kaplan-Meier curves of GC development according to patient demographic characteristics are shown in Figure 1. In this study, the average frequency of GCs was 0.19%/year. Age and *H. pylori* status were associated with GC incidence (both $P < 0.001$), whereas sex was not.

Figures 2A-E show the cumulative incidence using the Kaplan-Meier method for each Kyoto classification score. Atrophy, IM, EF, and DR scores were associated with GC development (all $P < 0.001$), whereas nodularity was not. The average frequencies of GCs per year were 0.04%, 0.17%, and 0.73% for atrophy scores of 0, 1, and 2; 0.07%, 0.25%, and 1.10% for IM scores of 0, 1, and 2; 0.17% and 0.92% for EF scores of 0 and 1; and 0.06%, 0.55%, and 0.74% for DR scores of 0, 1, and 2, respectively. The total Kyoto score was associated with GC development ($P < 0.001$), as shown in Figure 2F. The average frequencies of GCs were 0.05, 0.07, 0.47, and 1.27% per year for the total Kyoto scores of 0-1, 2-3, 4, and 5-8, respectively.

Table 1 Demographic characteristics and endoscopic findings of the patient at baseline

	All	Gastric cancer	Non-gastric cancer	*P* value[1]
No.	6718	34	6684	
Age, median (IQR), yr	54 (46-64)	69.5 (57.8-73.8)	54 (46-64)	< 0.001
Male sex, No. (%)	2969 (44.2)	17 (50.0)	2952 (44.2)	0.495
H. pylori status, No. (%)				< 0.001
Uninfected	3754 (55.9)	5 (14.7)	3749 (56.1)	
Eradicated	2264 (33.7)	20 (58.8)	2244 (33.6)	
Currently infected	700 (10.4)	9 (26.5)	691 (10.3)	
Duration of follow up, median (IQR), yr	2.56 (1.74-3.64)	1.03 (0.85-1.78)	2.57 (1.76-3.64)	< 0.001
No. EGD per patient, median (IQR)	2 (2-4)	2 (2-3)	2 (2-4)	0.652
Kyoto classification score, median (IQR)				
Atrophy	0 (0-1)	2 (1-2)	0 (0-1)	< 0.001
Intestinal metaplasia	0 (0-0)	2 (0-2)	0 (0-0)	< 0.001
Enlarged folds	0 (0-0)	0 (0-0)	0 (0-0)	< 0.001
Nodularity	0 (0-0)	0 (0-0)	0 (0-0)	0.916
Diffuse redness	0 (0-0)	1 (1-1)	0 (0-0)	< 0.001
Total Kyoto	0 (0-2)	5 (4-5)	0 (0-2)	< 0.001

[1]*P* values were calculated using binomial logistic regression model.
IQR: Interquartile range; EGD: Esophagogastroduodenoscopy; *H. pylori*: *Helicobacter pylori*.

Table 2 Characteristics of gastric cancers

	n
Gastric cancer patient	34
Gastric cancer lesion	37
Morphological type[1]	
Superficial elevated (0-IIa)	7
Superficial flat (0-IIb)	5
Superficial depressed (0-IIc)	25
Depth	
Mucosa	33
Submucosa	4
Lauren's histological type	
Diffuse	4
Intestinal	33

[1]According to the Japanese classification of gastric carcinoma[22].

Multivariate analysis of GC incidence

Table 3 provides the crude and adjusted HRs for GC development according to Kyoto classification scores. Multivariate analysis showed that atrophy scores 1 (adjusted HR with score 0 as reference: 3.66, 95%CI: 1.06 to 12.61), 2 (11.60, 3.82-35.27), IM score 2 (9.92, 4.37-22.54), EF score 1 (4.03, 1.63-9.96), DR scores 1 (6.22, 2.65-14.56), and 2 (10.01, 3.73-26.86) were significantly associated with GC incidence, independent of patient age and sex, whereas nodularity score was not.

The total Kyoto scores of 4 (adjusted HR with total Kyoto scores 0-1 as reference: 6.23, 95%CI: 1.93 to 20.13, $P = 0.002$) and 5-8 (16.45, 6.29-43.03, $P < 0.001$) were more likely to develop GC, whereas the total Kyoto scores of 2-3 were not. In

Table 3 Univariate and multivariate analysis of gastric cancer development

	GC patients, No.	Non-GC patients, No.	Crude HR[1]	95%CI	*P* value	Adjusted HR[1,2]	95%CI	*P* value
Age (yr)								
< 50	4	2383	Reference					
50-59	5	2014	1.48	0.40-5.50	0.562			
60-69	8	1352	3.37	1.01-11.19	0.047			
≥ 70	17	935	10.75	3.62-31.96	< 0.001			
Sex								
Women	17	3732	Reference					
Men	17	2952	1.27	0.65-2.48	0.488			
H. pylori status								
Uninfected	5	3749	Reference			Reference		
Eradicated	20	2244	6.00	2.25-16.05	< 0.001	3.81	1.40-10.38	0.009
Currently infected	9	691	11.60	3.88-34.64	< 0.001	9.53	3.17-28.65	< 0.001
Atrophy								
0	4	3992	Reference			Reference		
1	7	1508	4.40	1.29-15.06	0.018	3.66	1.06-12.61	0.040
2	23	1184	19.02	6.56-55.12	< 0.001	11.60	3.82-35.27	< 0.001
Intestinal metaplasia								
0	10	5516	Reference			Reference		
1	3	473	3.42	0.94-12.44	0.062	2.25	0.60-8.43	0.228
2	21	695	16.01	7.52-34.05	< 0.001	9.92	4.37-22.54	< 0.001
Enlarged folds								
0	28	6429	Reference			Reference		
1	6	255	5.41	2.23-13.10	< 0.001	4.03	1.63-9.96	0.003
Nodularity								
0	33	6507	Reference			Reference		
1	1	177	1.18	0.16-8.62	0.872	2.51	0.33-18.86	0.372
Diffuse redness								
0	8	5058	Reference			Reference		
1	18	1187	9.05	3.92-20.85	< 0.001	6.22	2.65-14.56	< 0.001
2	8	439	12.26	4.60-32.68	< 0.001	10.01	3.73-26.86	< 0.001
Total Kyoto								
0-1	6	4615	Reference			Reference		
2-3	2	1008	1.48	0.30-7.34	0.631	1.12	0.22-5.63	0.887
4	6	473	9.54	3.07-29.62	< 0.001	6.23	1.93-20.13	0.002
5-8	20	588	25.58	10.25-63.84	< 0.001	16.45	6.29-43.03	< 0.001

[1]Hazard ratios were calculated using the Cox proportional hazards model.
[2]Hazard ratios were adjusted for age and sex.
GC: Gastric cancer; HR: Hazard ratio; CI: Confidence interval; *H. pylori*: *Helicobacter pylori*.

per 1 rank analysis, an adjusted HR of the total Kyoto score for developing GC was 1.75 (95%CI: 1.46 to 2.09, $P < 0.001$).

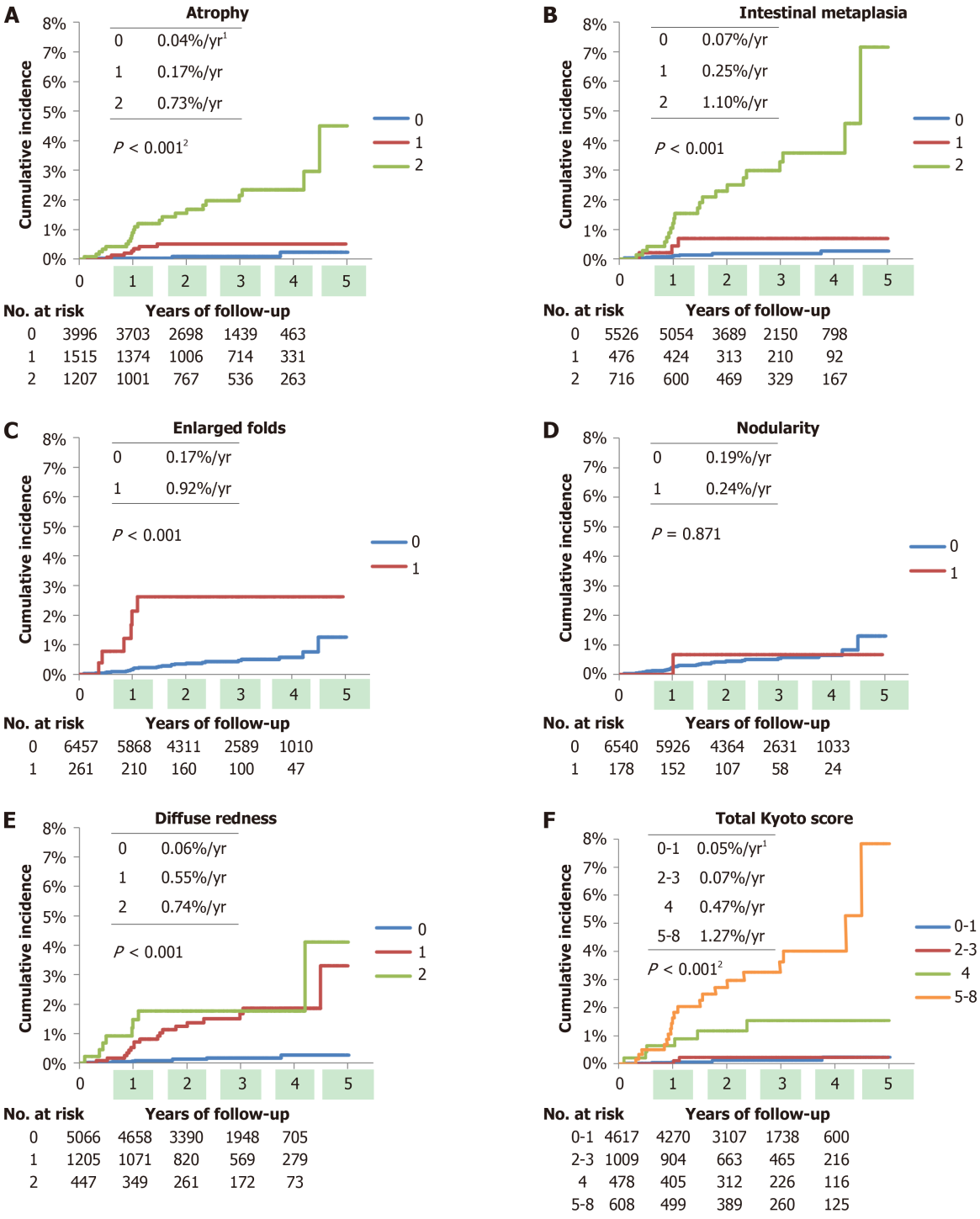

DOI: 10.3748/wjg.v29.i31.4763

Figure 2 Cumulative incidence of gastric cancer according to the Kyoto classification scores. A-E: Kaplan-Meier curves of gastric cancer development according to atrophy (A), intestinal metaplasia (B), enlarged folds (C), nodularity (D), and diffuse redness (E) scores, respectively; F: Kaplan-Meier curves of gastric cancer development according to total Kyoto scores. [1]The average frequency of gastric cancer per year. [2]*P* values were calculated using a log-rank test.

DISCUSSION

We found that high total Kyoto scores, especially ≥ 4, were associated with GC incidence. The adjusted HR of the total Kyoto score for GC development was 1.75 per 1 rank analysis. Additionally, adjusted HRs for the total Kyoto scores of 4 and 5-8 were high at 6.23 and 16.45, respectively, compared to the total Kyoto scores of 0-1. The total Kyoto score was associated with the cumulative incidence of GC ($P < 0.001$). The average frequencies of GCs per year increased with the total Kyoto score (0.05%, 0.07%, 0.47%, and 1.27% for the total Kyoto scores of 0-1, 2-3, 4, and 5-8, respectively). This is the first report that shows that high total Kyoto scores represent GC risks in a time-to-event analysis. This finding is consistent with those of several previous studies. In cross-sectional studies, we and Lin *et al*[19] reported that the odds

ratios of the total Kyoto score for GC were 1.6 and 1.5 per 1 rank, respectively[18]. Liu *et al*[24] indicated an increased trend of GC frequency in patients with total Kyoto scores of 0-1, 2-3, and ≥ 4. Some investigators showed that the mean total Kyoto scores of the patients with GC, *H. pylori*-infected GC, and *H. pylori*-eradicated GC were 4.0-4.6, 4.8-5.6, and 4.2, respectively[18,25,26]. Taken together, a total Kyoto score ≥ 4 was available for determining GC risks.

This cohort study demonstrated that patients with endoscopy-based atrophy, IM, EF, and DR are more likely to develop GC. In contrast, nodularity was not associated with GC incidence. Endoscopic atrophy has been shown to be a predictor of GC development. Shichijo *et al*[27] described a significantly higher adjusted HR of severe atrophy for developing GC as 9.3, while we identified significantly higher adjusted HRs of Kyoto atrophy scores 1 and 2 as 3.7 and 11.6, respectively. Several cohort studies have shown that severe endoscopic atrophy is associated with a high incidence of GC, especially in patients who have undergone *H. pylori* eradication[9,27,28]. These studies revealed that the average frequencies of GCs per year for non-to-mild, moderate, and severe atrophy were 0.06%-0.15%, 0.12%-0.34%, and 0.31%-1.60%, respectively. Similarly, our study showed that the average frequencies of GCs per year for total Kyoto scores of 0, 1, and 2 were 0.04%, 0.17%, and 0.73%, respectively. Since more than half of the study patients were uninfected with *H. pylori*, our study may present a lower GC incidence in patients with a Kyoto atrophy score of 0. Two meta-analyses also showed that a high Kyoto atrophy score provided a high-risk ratio of 2.8-8.0[29,30]. Thus, our study results are in line with those of previous studies.

Although the risk of GC in histological IM has been well studied[2,8,27,31,32], few studies have examined GC risks associated with endoscopic IM. A high Kyoto IM score has been identified as a risk factor for GC, especially multiple GC [14,18]. This study revealed that endoscopic corpus IM was associated with GC development (adjusted HR: 9.92), which is supported by Sakitani *et al*[33], who clarified histological corpus IM as a predictor of GC. The consistency of IM between endoscopy and histology has been demonstrated[13]; we successfully verified endoscopic IM as a risk factor for GC using event history analysis.

Watanabe *et al*[34] provided an adjusted HR of EF for GC development as high as 43.3, whereas our study's adjusted HR was 4.03. These results are similar; however, the difference in HRs between them may be attributed to the inclusion of many *H. pylori*-uninfected individuals in the study population. However, whether nodularity is a risk factor for GC remains controversial. Nodularity has been reported to be a juvenile and histologically diffuse-type GC risk[35,36], whereas we have shown in a cross-sectional study that the odds ratio for GC of nodularity is low at 0.5[18]. After adjusting for age and sex, no association between nodularity and GC was observed. Although nodularity decreases with age[37], the risk of intestinal-type GC increases with age. Furthermore, intestinal-type cancers are more common than diffuse-type cancers. Therefore, age offsets the association of nodularity with GC, especially in older generations, although nodularity is associated with diffuse-type GC in the young generation[35]. As the association between nodularity and the risk of developing GC is still debated, nodularity might be listed separately. For example, the total Kyoto classification score for atrophy 1, IM 0, EF 1, nodularity 1, and DR 1 might be reported as 3 + 1 instead of 4.

Several studies have reported that DR is strongly associated with *H. pylori* infection[15,38-40], but little is known about the association between DR and GC incidence. This study identified Kyoto DR scores of 1 and 2 as indicators of GC incidence (adjusted HRs: 6.22 and 10.01, respectively). Since DR presents inflammatory cell infiltration caused by *H. pylori* [13] and *H. pylori* infection is a definite risk factor for GC[2,3], DR is expressed as a GC risk. Additionally, since the Kyoto DR score includes RAC as a negative factor and RAC is inversely associated with GC development[41], a high Kyoto DR score may be associated with high GC incidence.

This study has some limitations. First, this was a single-center, retrospective cohort study. Although the endoscopy data were well-organized, multi-center, prospective studies are warranted. Second, this study was conducted only in areas with a high GC prevalence in Asia. Therefore, studies in Western countries are warranted. Third, the total Kyoto score has shortcomings in the scoring design, which simply adds five individual Kyoto scores[14]. IM is associated with a high risk of intestinal-type GC but a low risk of diffuse-type GC[18]. In addition, EF and nodularity are high risks for diffuse-type GC but low risks for intestinal-type GC. Therefore, the evaluation of GC risk using a scoring system that individually predicts the risks of intestinal- and diffuse-type GCs is needed.

CONCLUSION

In conclusion, a high total Kyoto score of ≥ 4 was associated with GC incidence in a cohort study. The endoscopy-based diagnosis of gastritis can stratify GC risk.

ARTICLE HIGHLIGHTS

Research background

The Japan Gastroenterological Endoscopy Society advocated the Kyoto classification, a new grading system for endoscopic gastritis in 2013.

Research motivation

Although a high Kyoto score is believed to reflect an increased gastric cancer (GC) risk, it has not been systematically investigated using time-to-event analysis.

Research objectives
We examined GC incidence according to the total Kyoto score in the endoscopic surveillance cohort and verified the GC risks of endoscopic gastritis.

Research methods
Patients who underwent two or more esophagogastroduodenoscopies were enrolled. GC incidence was based on Kyoto classification scores. Hazard ratios (HRs) adjusted for age and sex were calculated using a Cox hazard model.

Research results
A total of 6718 patients were enrolled. The annual incidence rate of GC was 0.19%. The total Kyoto scores of 4 [HR with total Kyoto scores 0-1 as reference: 6.23, 95% confidence interval (CI): 1.93 to 20.13, $P = 0.002$] and 5-8 (16.45, 6.29-43.03, $P < 0.001$) were more likely to develop GC, whereas the total Kyoto scores 2-3 were not. The HR of the total Kyoto score for developing GC per 1 rank was 1.75 (95%CI: 1.46 to 2.09, $P < 0.001$).

Research conclusions
A total Kyoto score ≥ 4 could predict GC risk. The endoscopic Kyoto classification of gastritis can stratify GC risk.

Research perspectives
This was a single-center, retrospective cohort study, and multi-center, prospective studies are warranted.

ACKNOWLEDGEMENTS

We would like to thank Shido Inc. (www.Shido.co.jp) for consulting the statistical analysis. We would like to thank clinical laboratory engineer Tadahiro Yamakawa for managing the endoscopy database of the Toyoshima Endoscopy Clinic.

FOOTNOTES

Author contributions: Toyoshima O, Nishizawa T, Yoshida S, Matsuno T, Fujisawa G, and Toyoshima A contributed to the conception of article; Toyoshima O drafted the article; Toyoshima O, Nishizawa T, Yoshida S, and Matsuno T involved in the review of endoscopic images; Toyoshima O contributed to the statistical analysis; Nishizawa T edited the article; Toyoshima O, Nishizawa T, Yoshida S, Matsuno T, Fujisawa G, Toyoshima A, Ebinuma H, Fujishiro M, Saito Y, and Suzuki H contributed to the critical review; and all authors approved the final manuscript.

Institutional review board statement: This study was approved by the institutional review board of the Yoyogi Mental Clinic (approval no. RKK227).

Informed consent statement: Written informed consent was obtained from patients at the time of esophagogastroduodenoscopy to use their data for research purposes. The study's protocol was published on our institute's website (www.ichou.com) so that patients could opt out of the study.

Conflict-of-interest statement: All the authors report no relevant conflicts of interest for this article.

Data sharing statement: No additional data are available.

STROBE statement: The authors have read the STROBE Statement-checklist of items, and the manuscript was prepared and revised according to the STROBE Statement-checklist of items.

Country/Territory of origin: Japan

ORCID number: Osamu Toyoshima 0000-0002-6953-6079; Toshihiro Nishizawa 0000-0003-4876-3384; Shuntaro Yoshida 0000-0002-9437-9132; Tatsuya Matsuno 0000-0002-1935-3506; Gota Fujisawa 0000-0002-0218-200X; Akira Toyoshima 0000-0002-5697-6251; Hirotoshi Ebinuma 0000-0001-6604-053X; Mitsuhiro Fujishiro 0000-0002-4074-1140; Yutaka Saito 0000-0003-2296-8373; Hidekazu Suzuki 0000-0002-8994-6163.

S-Editor: Wang JJ
L-Editor: A
P-Editor: Xu ZH

REFERENCES

1 **Bray F**, Ferlay J, Soerjomataram I, Siegel RL, Torre LA, Jemal A. Global cancer statistics 2018: GLOBOCAN estimates of incidence and mortality worldwide for 36 cancers in 185 countries. *CA Cancer J Clin* 2018; **68**: 394-424 [PMID: 30207593 DOI: 10.3322/caac.21492]

2 **Uemura N**, Okamoto S, Yamamoto S, Matsumura N, Yamaguchi S, Yamakido M, Taniyama K, Sasaki N, Schlemper RJ. Helicobacter pylori infection and the development of gastric cancer. *N Engl J Med* 2001; **345**: 784-789 [PMID: 11556297 DOI: 10.1056/NEJMoa001999]

3 **Plummer M**, Franceschi S, Vignat J, Forman D, de Martel C. Global burden of gastric cancer attributable to Helicobacter pylori. *Int J Cancer* 2015; **136**: 487-490 [PMID: 24889903 DOI: 10.1002/ijc.28999]

4 **Sugano K**. Effect of Helicobacter pylori eradication on the incidence of gastric cancer: a systematic review and meta-analysis. *Gastric Cancer* 2019; **22**: 435-445 [PMID: 30206731 DOI: 10.1007/s10120-018-0876-0]

5 **Choi Y**, Kim N, Yun CY, Choi YJ, Yoon H, Shin CM, Park YS, Ahn SH, Joong Park D, Lee HS, Kim JW, Lee KW, Chang W, Park JH, Lee YJ, Lee KH, Kim YH, Lee DH, Kim HH. Effect of Helicobacter pylori eradication after subtotal gastrectomy on the survival rate of patients with gastric cancer: follow-up for up to 15 years. *Gastric Cancer* 2020; **23**: 1051-1063 [PMID: 32361784 DOI: 10.1007/s10120-020-01076-2]

6 **Takahashi Y**, Yamamichi N, Kubota D, Shimamoto T, Nagao S, Sakuma N, Sakaguchi Y, Yakabi S, Tsuji Y, Wada R, Mitsushima T, Ichinose M, Fujishiro M. Risk factors for gastric cancer in Japan in the 2010s: a large, long-term observational study. *Gastric Cancer* 2022; **25**: 481-489 [PMID: 35067826 DOI: 10.1007/s10120-021-01273-7]

7 **Song H**, Ekheden IG, Zheng Z, Ericsson J, Nyrén O, Ye W. Incidence of gastric cancer among patients with gastric precancerous lesions: observational cohort study in a low risk Western population. *BMJ* 2015; **351**: h3867 [PMID: 26215280 DOI: 10.1136/bmj.h3867]

8 **Pimentel-Nunes P**, Libânio D, Marcos-Pinto R, Areia M, Leja M, Esposito G, Garrido M, Kikuste I, Megraud F, Matysiak-Budnik T, Annibale B, Dumonceau JM, Barros R, Fléjou JF, Carneiro F, van Hooft JE, Kuipers EJ, Dinis-Ribeiro M. Management of epithelial precancerous conditions and lesions in the stomach (MAPS II): European Society of Gastrointestinal Endoscopy (ESGE), European Helicobacter and Microbiota Study Group (EHMSG), European Society of Pathology (ESP), and Sociedade Portuguesa de Endoscopia Digestiva (SPED) guideline update 2019. *Endoscopy* 2019; **51**: 365-388 [PMID: 30841008 DOI: 10.1055/a-0859-1883]

9 **Take S**, Mizuno M, Ishiki K, Kusumoto C, Imada T, Hamada F, Yoshida T, Yokota K, Mitsuhashi T, Okada H. Risk of gastric cancer in the second decade of follow-up after Helicobacter pylori eradication. *J Gastroenterol* 2020; **55**: 281-288 [PMID: 31667586 DOI: 10.1007/s00535-019-01639-w]

10 **Hamashima C**, Shabana M, Okada K, Okamoto M, Osaki Y. Mortality reduction from gastric cancer by endoscopic and radiographic screening. *Cancer Sci* 2015; **106**: 1744-1749 [PMID: 26432528 DOI: 10.1111/cas.12829]

11 **Shah SC**, Piazuelo MB, Kuipers EJ, Li D. AGA Clinical Practice Update on the Diagnosis and Management of Atrophic Gastritis: Expert Review. *Gastroenterology* 2021; **161**: 1325-1332.e7 [PMID: 34454714 DOI: 10.1053/j.gastro.2021.06.078]

12 **Takeda T**, Asaoka D, Nojiri S, Nishiyama M, Ikeda A, Yatagai N, Ishizuka K, Hiromoto T, Okubo S, Suzuki M, Nakajima A, Nakatsu Y, Komori H, Akazawa Y, Nakagawa Y, Izumi K, Matsumoto K, Ueyama H, Sasaki H, Shimada Y, Osada T, Hojo M, Kato M, Nagahara A. Linked Color Imaging and the Kyoto Classification of Gastritis: Evaluation of Visibility and Inter-Rater Reliability. *Digestion* 2020; **101**: 598-607 [PMID: 31302654 DOI: 10.1159/000501534]

13 **Toyoshima O**, Nishizawa T, Yoshida S, Matsuno T, Odawara N, Toyoshima A, Sakitani K, Watanabe H, Fujishiro M, Suzuki H. Consistency between the endoscopic Kyoto classification and pathological updated Sydney system for gastritis: A cross-sectional study. *J Gastroenterol Hepatol* 2022; **37**: 291-300 [PMID: 34569096 DOI: 10.1111/jgh.15693]

14 **Toyoshima O**, Nishizawa T. Kyoto classification of gastritis: Advances and future perspectives in endoscopic diagnosis of gastritis. *World J Gastroenterol* 2022; **28**: 6078-6089 [PMID: 36483157 DOI: 10.3748/wjg.v28.i43.6078]

15 **Wang K**, Zhao J, Jin H, Meng L, Fan Y, Zhou Y, Ye C, Li M, Ma P, Zhu L, Ye Y, Lyu B. Establishment of a modified Kyoto classification scoring model and its significance in the diagnosis of Helicobacter pylori current infection. *Gastrointest Endosc* 2023; **97**: 684-693 [PMID: 36403805 DOI: 10.1016/j.gie.2022.11.008]

16 **Shichijo S**, Hirata Y, Niikura R, Hayakawa Y, Yamada A, Koike K. Association between gastric cancer and the Kyoto classification of gastritis. *J Gastroenterol Hepatol* 2017; **32**: 1581-1586 [PMID: 28217843 DOI: 10.1111/jgh.13764]

17 **Sugimoto M**, Ban H, Ichikawa H, Sahara S, Otsuka T, Inatomi O, Bamba S, Furuta T, Andoh A. Efficacy of the Kyoto Classification of Gastritis in Identifying Patients at High Risk for Gastric Cancer. *Intern Med* 2017; **56**: 579-586 [PMID: 28321054 DOI: 10.2169/internalmedicine.56.7775]

18 **Toyoshima O**, Nishizawa T, Yoshida S, Aoki T, Nagura F, Sakitani K, Tsuji Y, Nakagawa H, Suzuki H, Koike K. Comparison of endoscopic gastritis based on Kyoto classification between diffuse and intestinal gastric cancer. *World J Gastrointest Endosc* 2021; **13**: 125-136 [PMID: 34046150 DOI: 10.4253/wjge.v13.i5.125]

19 **Lin J**, Su H, Zhou Q, Pan J, Zhou L. Predictive value of nomogram based on Kyoto classification of gastritis to diagnosis of gastric cancer. *Scand J Gastroenterol* 2022; **57**: 574-580 [PMID: 34994675 DOI: 10.1080/00365521.2021.2023626]

20 **Kimura K**, Takemoto T. An endoscopic recognition of the atrophic border and its significance in chronic gastritis. *Endoscopy* 1969; **1**: 87-97 [DOI: 10.1055/S-0028-1098086]

21 **Haruma K**, Kato M, Inoue K, Murakami K, Kamada T. Kyoto Classification of Gastritis. 1st Edition. Tokyo Japan: Nihon Medical Center, 2017

22 **Japanese Gastric Cancer Association**. Japanese classification of gastric carcinoma: 3rd English edition. *Gastric Cancer* 2011; **14**: 101-112 [PMID: 21573743 DOI: 10.1007/s10120-011-0041-5]

23 **Lauren P**. The two histological main types of gastric carcinoma: Diffuse and so-called intestinal-type carcinoma. an attempt at a histo-clinical classification. *Acta Pathol Microbiol Scand* 1965; **64**: 31-49 [PMID: 14320675 DOI: 10.1111/apm.1965.64.1.31]

24 **Liu XM**, Ma XY, Liu F, Liu ZL, Tang XY, Ji MZ, Zheng JX. Gastric Cancer Screening Methods: A Comparative Study of the Chinese New Gastric Cancer Screening Score and Kyoto Classification of Gastritis. *Gastroenterol Res Pract* 2022; **2022**: 7639968 [PMID: 35309108 DOI: 10.1155/2022/7639968]

25 **Ohno A**, Miyoshi J, Kato A, Miyamoto N, Yatagai T, Hada Y, Kusuhara M, Jimbo Y, Ida Y, Tokunaga K, Okamoto S, Hisamatsu T. Endoscopic severe mucosal atrophy indicates the presence of gastric cancer after Helicobacter pylori eradication -analysis based on the Kyoto classification. *BMC Gastroenterol* 2020; **20**: 232 [PMID: 32689949 DOI: 10.1186/s12876-020-01375-z]

26 **Sugimoto M**, Kawai Y, Morino Y, Hamada M, Iwata E, Niikura R, Nagata N, Koyama Y, Fukuzawa M, Itoi T, Kawai T. Efficacy of high-vision transnasal endoscopy using texture and colour enhancement imaging and narrow-band imaging to evaluate gastritis: a randomized

controlled trial. *Ann Med* 2022; **54**: 1004-1013 [PMID: 35441573 DOI: 10.1080/07853890.2022.2063372]

27 **Shichijo S**, Hirata Y, Niikura R, Hayakawa Y, Yamada A, Ushiku T, Fukayama M, Koike K. Histologic intestinal metaplasia and endoscopic atrophy are predictors of gastric cancer development after Helicobacter pylori eradication. *Gastrointest Endosc* 2016; **84**: 618-624 [PMID: 26995689 DOI: 10.1016/j.gie.2016.03.791]

28 **Kaji K**, Hashiba A, Uotani C, Yamaguchi Y, Ueno T, Ohno K, Takabatake I, Wakabayashi T, Doyama H, Ninomiya I, Kiriyama M, Ohyama S, Yoneshima M, Koyama N, Takeda Y, Yasuda K. Grading of Atrophic Gastritis is Useful for Risk Stratification in Endoscopic Screening for Gastric Cancer. *Am J Gastroenterol* 2019; **114**: 71-79 [PMID: 30315306 DOI: 10.1038/s41395-018-0259-5]

29 **Sui Z**, Chen J, Li P, Shao L, Ye J, Lu X, Cai J. Risk for gastric cancer in patients with gastric atrophy: a systematic review and meta-analysis. *Transl Cancer Res* 2020; **9**: 1618-1624 [PMID: 35117509 DOI: 10.21037/tcr.2020.01.54]

30 **Xiao S**, Fan Y, Yin Z, Zhou L. Endoscopic grading of gastric atrophy on risk assessment of gastric neoplasia: A systematic review and meta-analysis. *J Gastroenterol Hepatol* 2021; **36**: 55-63 [PMID: 32656803 DOI: 10.1111/jgh.15177]

31 **Yue H**, Shan L, Bin L. The significance of OLGA and OLGIM staging systems in the risk assessment of gastric cancer: a systematic review and meta-analysis. *Gastric Cancer* 2018; **21**: 579-587 [PMID: 29460004 DOI: 10.1007/s10120-018-0812-3]

32 **Na YS**, Kim SG, Cho SJ. Risk assessment of metachronous gastric cancer development using OLGA and OLGIM systems after endoscopic submucosal dissection for early gastric cancer: a long-term follow-up study. *Gastric Cancer* 2023; **26**: 298-306 [PMID: 36609936 DOI: 10.1007/s10120-022-01361-2]

33 **Sakitani K**, Hirata Y, Watabe H, Yamada A, Sugimoto T, Yamaji Y, Yoshida H, Maeda S, Omata M, Koike K. Gastric cancer risk according to the distribution of intestinal metaplasia and neutrophil infiltration. *J Gastroenterol Hepatol* 2011; **26**: 1570-1575 [PMID: 21575058 DOI: 10.1111/j.1440-1746.2011.06767.x]

34 **Watanabe M**, Kato J, Inoue I, Yoshimura N, Yoshida T, Mukoubayashi C, Deguchi H, Enomoto S, Ueda K, Maekita T, Iguchi M, Tamai H, Utsunomiya H, Yamamichi N, Fujishiro M, Iwane M, Tekeshita T, Mohara O, Ushijima T, Ichinose M. Development of gastric cancer in nonatrophic stomach with highly active inflammation identified by serum levels of pepsinogen and Helicobacter pylori antibody together with endoscopic rugal hyperplastic gastritis. *Int J Cancer* 2012; **131**: 2632-2642 [PMID: 22383377 DOI: 10.1002/ijc.27514]

35 **Kamada T**, Tanaka A, Yamanaka Y, Manabe N, Kusunoki H, Miyamoto M, Tanaka S, Hata J, Chayama K, Haruma K. Nodular gastritis with helicobacter pylori infection is strongly associated with diffuse-type gastric cancer in young patients. *Dig Endosc* 2007; **19**: 180-184 [DOI: 10.1111/j.1443-1661.2007.00750.x]

36 **Nishikawa I**, Kato J, Terasoma S, Matsutani H, Tamaki H, Tamaki T, Kuwashima F, Nakata H, Tomeki T, Matsunaka H, Ibata Y, Yamashita Y, Maekita T, Higashi K, Ichinose M. Nodular gastritis in association with gastric cancer development before and after Helicobacter pylori eradication. *JGH Open* 2018; **2**: 80-86 [PMID: 30483568 DOI: 10.1002/jgh3.12049]

37 **Nishizawa T**, Sakitani K, Suzuki H, Yoshida S, Kataoka Y, Nakai Y, Ebinuma H, Kanai T, Toyoshima O, Koike K. Clinical features of cardiac nodularity-like appearance induced by Helicobacter pylori infection. *World J Gastroenterol* 2020; **26**: 5354-5361 [PMID: 32994693 DOI: 10.3748/wjg.v26.i35.5354]

38 **Yoshii S**, Mabe K, Watano K, Ohno M, Matsumoto M, Ono S, Kudo T, Nojima M, Kato M, Sakamoto N. Validity of endoscopic features for the diagnosis of Helicobacter pylori infection status based on the Kyoto classification of gastritis. *Dig Endosc* 2020; **32**: 74-83 [PMID: 31309632 DOI: 10.1111/den.13486]

39 **Zhao J**, Xu S, Gao Y, Lei Y, Zou B, Zhou M, Chang D, Dong L, Qin B. Accuracy of Endoscopic Diagnosis of Helicobacter pylori Based on the Kyoto Classification of Gastritis: A Multicenter Study. *Front Oncol* 2020; **10**: 599218 [PMID: 33344250 DOI: 10.3389/fonc.2020.599218]

40 **Fiuza F**, Maluf-Filho F, Ide E, Furuya CK Jr, Fylyk SN, Ruas JN, Stabach L, Araujo GA, Matuguma SE, Uemura RS, Sakai CM, Yamazaki K, Ueda SS, Sakai P, Martins BC. Association between mucosal surface pattern under near focus technology and Helicobacter pylori infection. *World J Gastrointest Endosc* 2021; **13**: 518-528 [PMID: 34733412 DOI: 10.4253/wjge.v13.i10.518]

41 **Kawamura M**, Uedo N, Koike T, Kanesaka T, Hatta W, Ogata Y, Oikawa T, Iwai W, Yokosawa S, Honda J, Asonuma S, Okata H, Ohyauchi M, Ito H, Abe Y, Ara N, Kayaba S, Shinkai H, Shimokawa T. Kyoto classification risk scoring system and endoscopic grading of gastric intestinal metaplasia for gastric cancer: Multicenter observation study in Japan. *Dig Endosc* 2022; **34**: 508-516 [PMID: 34415621 DOI: 10.1111/den.14114]

World Journal of Gastroenterology

Submit a Manuscript: https://www.f6publishing.com

World J Gastroenterol 2023 August 21; 29(31): 4774-4782

DOI: 10.3748/wjg.v29.i31.4774

ISSN 1007-9327 (print) ISSN 2219-2840 (online)

ORIGINAL ARTICLE

Observational Study

Dental evaluation is helpful in the differentiation of functional heartburn and gastroesophageal reflux disease

Krisztina Helle, Anna Zsófia Árok, Georgina Ollé, Márk Antal, András Rosztóczy

Specialty type: Gastroenterology and hepatology

Provenance and peer review: Unsolicited article; Externally peer reviewed.

Peer-review model: Single blind

Peer-review report's scientific quality classification

Grade A (Excellent): 0
Grade B (Very good): B
Grade C (Good): C
Grade D (Fair): 0
Grade E (Poor): 0

P-Reviewer: Montasser IF, Egypt; Wang ZF, China

Received: June 20, 2023
Peer-review started: June 20, 2023
First decision: July 10, 2023
Revised: July 19, 2023
Accepted: July 27, 2023
Article in press: July 27, 2023
Published online: August 21, 2023

Krisztina Helle, Georgina Ollé, András Rosztóczy, Department of Internal Medicine, Division of Gastroenterology, University of Szeged, Szeged 6725, Hungary

Anna Zsófia Árok, Márk Antal, Department of Operative and Esthetic Dentistry, University of Szeged, Szeged 6725, Hungary

Corresponding author: András Rosztóczy, MD, PhD, Associate Professor, Department of Internal Medicine, Division of Gastroenterology, University of Szeged, 57 Kálvária Sugárút, Szeged 6725, Hungary. rosztoczy.andras@med.u-szeged.hu

Abstract

BACKGROUND

Heartburn is identically the key symptom of both, gastroesophageal reflux disease (GERD) and functional heartburn (FHB), making the differential diagnosis resource-intensive. Oral manifestations of GERD can be easily examined; therefore, their exploration might be a cheap, widely available, and useful tool in the differentiation of GERD and FHB.

AIM

To evaluate the prevalence of dental erosions (DE) and periodontal diseases (PD) in patients with heartburn and their association with GERD and FHB.

METHODS

A total of 116 [M/F: 51/65, mean age: 54 (17-80) years] consecutive patients with heartburn were enrolled for detailed esophageal function and orodental examinations.

RESULTS

Dental disorders were detected in 89% (103/116). Patients with PD + DE had significantly more often pathologic reflux (90.0% *vs* 27.8%; $P < 0.05$), higher esophagitis scores (1.8 *vs* 0.9; $P < 0.05$), and a significantly different mean impedance curve ($P = 0.04$) than those without any dental diseases. The opposite approach established that patients with GERD had significantly higher prevalence of DE and PD, especially if both were present (28.9% *vs* 2.0%; $P < 0.01$), more severe PD (1.5 *vs* 1.0; $P < 0.01$), and longer history of heartburn (15 years *vs* 9 years; $P < 0.01$) than those with FHB.

CONCLUSION

The dental evaluation of patients with heartburn seems to be useful in the differential diagnosis of GERD and FHB. Among the studied parameters, the co-appearance of DE and PD seems to be the best predictor of GERD, whereas the absence of dental disorders was mostly observed in FHB.

Key Words: Gastroesophageal reflux disease; Gastric acid; Heartburn; Differential diagnosis; Epidemiology; Oral manifestations; Prevalence; Risk factors; Dental erosion; Periodontal diseases

Core Tip: Heartburn is identically the key symptom of gastroesophageal reflux disease (GERD) and functional heartburn (FHB), making the differential diagnosis resource-intensive. Oral manifestations of GERD can be easily examined to differentiate GERD and FHB. A total of 116 consecutive patients with heartburn were enrolled to evaluate the prevalence of dental erosions (DE) and periodontal diseases (PD). The dental evaluation of patients with heartburn seems to be useful in the differential diagnosis of GERD and FHB. The co-appearance of DE and PD seems to be the best predictor of GERD, while the absence of dental disorders was mostly observed in FHB.

Citation: Helle K, Árok AZ, Ollé G, Antal M, Rosztóczy A. Dental evaluation is helpful in the differentiation of functional heartburn and gastroesophageal reflux disease. *World J Gastroenterol* 2023; 29(31): 4774-4782
URL: https://www.wjgnet.com/1007-9327/full/v29/i31/4774.htm
DOI: https://dx.doi.org/10.3748/wjg.v29.i31.4774

INTRODUCTION

Heartburn is mostly considered a typical symptom of gastroesophageal reflux disease (GERD) and has a global prevalence of 11.9%. However, it cannot be diagnosed without performing detailed esophageal function tests based on the symptom of patients with functional heartburn (FHB)[1].

According to the Montreal definition, GERD may be associated with supraesophageal manifestations, including oropharyngeal symptoms[2]. Among various oropharyngeal symptoms (salivation, mouth burning, and tongue burning), dental erosion (DE) is considered to have a proven correlation with GERD. The association between DE and GERD was apparently first reported in 1933[3]. By definition, DE is a progressive loss of tough tissues of the teeth due to the action of extrinsic or intrinsic acids. Its median prevalence has been reported to be 24% in all patients with GERD and 32.5% in adult patients with GERD[4]. However, DE can be accompanied by other disorders, such as bulimia, rumination, and the consumption of acidic foods or drinks.

Much less data are available regarding other oral symptoms, especially periodontal diseases (PD), which have recently been suggested to be associated with GERD[5]. PD, which represent a group of oral inflammatory conditions caused by oral pathogens, lead to the destruction of tooth-supporting soft tissues. DE and PD may be considered as cumulative lesions, representing the long-term consequences of gastroesophageal reflux.

To the best of our knowledge, currently, no studies have been performed to assess hard and soft tissue injuries (DE and PD), and their relationship has never been investigated from dental and gastroenterological perspectives. Moreover, there are no studies about the possibility to distinguish GERD from FHB on the basis of oral manifestations.

Therefore, we aimed to obtain data on the prevalence of DE and PD in patients with heartburn and evaluate their association with GERD.

MATERIALS AND METHODS

One-hundred and sixteen consecutive patients (M/F: 51/65, mean age: 54.00 years ± 15.62 years) with heartburn were enrolled in our tertiary center for detailed esophageal function testing, including upper gastrointestinal endoscopy, high-resolution esophageal manometry [medical measurement systems (MMS) solar with a 22-channel, water-perfused catheter], and 24-h multi-channel intra-esophageal pH-impedance monitoring (MMS Ohmega®, with a pHersaflex Z61A pH probe). Any medications with any effect on gastrointestinal motility or gastric secretion were suspended one month before the esophageal testing. For gastroscopy, Olympus GIF-Q165 endoscopes were used, and the procedure was carried out under local, topical anesthesia. The presence of esophageal manifestations was recorded. Esophagitis was classified per the Los Angeles criteria[6]. On this basis, the following scoring system (no erosion = 0, LA-A = 1, LA-B = 2, LA-C = 3, LA-D = 4) was applied for quantitative comparison of the degree of esophagitis. Esophagogastric junction outflow obstruction and other major motility disorders were excluded *via* high-resolution esophageal manometry according to the Chicago classification 3.0[7]. During pH-impedance monitoring, the pH sensor was placed 5 cm above the lower esophageal sphincter as determined *via* manometry.

The significance of GERD was judged by the Lyon consensus[8]. The diagnosis of FHB was established according to the Rome IV criteria[9], including < 4% acid exposure time in the esophagus and the independence of symptoms of acidic and non-acidic reflux episodes. The occurrence of reflux hypersensitivity was also evaluated, but none of the studied patients fulfilled the accepted Rome IV criteria of this disease. Moreover, baseline impedance values were above 2000 Ω in this patient group[10]. We also calculated the mean 24-h impedance in all channels, the impedance values of the six channels during the 24-h measurement were exported to a .csv file and averaged.

Before dental examinations, general personal data, social and dental habits, and the presence, frequency, and appearance of typical and atypical reflux symptoms were assessed using standardized questionnaires that were collected by an interviewer (medical doctor and student). Among the enrolled subjects, 116 patients [M/F: 51/65, mean age: 56 (22-82) years] with heartburn were participating in further oral and dental examinations. Oral evaluations were carried out by a dentist who was blinded to the results of the esophageal function tests. The tooth wear index was evaluated and scored using the Smith and Knight's criteria, while the clinical staging of periodontitis was performed according to some study[11,12]. To quantitatively compare the severity of periodontitis, the following score system was used: No sign = 0, mild = 1, moderate = 2, severe = 3). The plaque index was calculated *via* percentage of plaque area in relation to total area.

Based on the presence of DE and/or PD, subgroups were formed.

Statistical analyses (one-way analysis of variance, chi-squared test, and unpaired *t*-test) were performed using R program; the significance level was set at $P = 0.05$. Data are expressed using the mean ± SD. This study was approved by the Regional Human Research Ethics Committee of the University of Szeged (Ethical approval No. 4564).

RESULTS

Detailed esophageal testing identified 66 patients with GERD (56.9%) and 50 patients with FHB (43.1%) among the 116 enrolled patients. Dental disorders were detected in 89% (103/116) of the enrolled patients with heartburn. The global prevalence of DE among the enrolled patients was 23.3%. In the group of subjects with GERD, the mean DeMeester score (DMS) was 29.84 ± 27.06. In contrast, in the other group, the mean DMS was 3.34 ± 2.94. Fourteen subjects were diagnosed with Barrett's esophagus. Among patients with GERD, LA-A in 12 (18.2%), LA-B in 15 (22.7%), LA-C in 20 (30.3%), and LA-D in 4 cases (6.1%) were detected, and 15 (22.7%) of them had no sign of esophagitis. In the group with FHB, there was no esophagitis on gastroscopy. Based on the results of pH-impedance monitoring, proximal reflux was found in 41 cases. Dental erosions were significantly more common among patients with GERD (66/116) than among those with FHB (21/66, 31.8% *vs* 6/50, 12.0%; $P = 0.0312$). The mean body mass index (BMI) in the GERD group was 27.8 kg/m^2 ± 4.45 kg/m^2 while that in the FHB group was 26.2 kg/m^2 ± 4.53 kg/m^2 ($P = 0.0192$). Eleven patients were toothless. Furthermore, we established significantly more severe periodontal problems in patients with GERD ($P = 0.0253$). However, instead of the fact that neither only DE nor only PD was significantly more common in any of the study groups, PD and DE together were significantly more prevalent among patients with GERD ($P = 0.00008$). DEs alone were less common among patients with GERD (3/8, 37.5%) than among those with FHB (5/8, 62.5%). Moreover, more patients were toothless in the GERD group (8/11, 72.7%). However, the most prominent difference is the presence of DE and PD together: 19/20 (95%) in the group of patients with GERD and 1/20 (5%) in the control group. The mean plaque index was 52 (0-100) in both groups. Fewer teeth were detected in the GERD group; however, the difference was not statistically significant (18 *vs* 21; $P = 0.098$). Patients with GERD had a longer history of symptoms than those with FHB (15 years *vs* 9 years, $P = 0.0041$) (Table 1).

Mean impedance values were compared between the two study groups and found to be significantly lower among patients with GERD than among those with FHB, and a characteristic tendency of GERD was detected (Figure 1).

In the entire study population, the periodontal examination was possible in only 105 patients because 11 of them were toothless. Among the examined subjects, 17/105 (16.2%) had DE alone, 24/105 (22.9%) had PD alone, 10/105 (9.5%) had both, and 54/105 (51.4%) had neither. Patients with DE alone had no more pathologic reflux than those with intact teeth (41.2% *vs* 27.8%). Among patients with both PD and DE, pathologic reflux was significantly more prevalent (27.8% and 90.0%; $P = 0.03$) than among patients without DE and PD. Furthermore, patients with PD and DE had higher esophagitis scores (1.8 *vs* 0.9; $P = 0.05$) than those without any dental diseases, and there was a tendency for more proximal reflux ($P = 0.08$). The presence of PD causing tooth loss was more common than the presence of DE or both (18 *vs* 22 and 24, $P = 0.11$) On the other hand, the mean plaque index was significantly higher among patients with PD than among patients without PD and/or DE (72 *vs* 49, $P < 0.0001$; Table 2). Other oral, atypical symptoms were not significant in the studied group, such as burning sensation of the mouth and tongue, sore throat, bad breath, sour taste, and ageusia.

Evaluating the mean impedance values, the tendency in patients with DE and PD was similar to that in patients with GERD (Figure 2).

Besides the abovementioned risk factors, no other ones were detected in the study. Furthermore, there was no difference between the four groups in terms of smoking ($P = 0.36$), alcohol consumption ($P = 0.59$), and coffee consumption ($P = 0.86$). There was also no significant difference in different habits resulting in DEs, such as drinking carbonated drinks ($P = 0.58$), teeth grinding ($P = 0.71$), and eating sour foods ($P = 0.23$).

DISCUSSION

The complete symptom similarity of GERD and FHB makes the differential diagnosis of heartburn complicated and resource-intensive. According to the Rome IV classification, it is not possible to differentiate the role of acid and

Table 1 Comparison of parameters between patients with gastroesophageal reflux disease and those with functional heartburn

		GERD (*n* = 66)	FHB (*n* = 50)	*P* value
Gender (male/female)		32 (48.5%)/34 (51.5%)	19 (38%)/31 (62%)	NS
Age, yr (min-max)		57 (22-82)	51 (25-79)	NS
BMI, kg/m^2 (min-max)		28 (16-37)	26 (17-39)	< 0.05
Mean DMS		29.84	3.34	< 0.0001
Mean impedance ± SD		2175 ± 650	2489 ± 731	< 0.05
Number of teeth (min-max)		18.3 (0-32)	20.7 (0-32)	NS
Toothless		8 (12.1%)	3 (6%)	NS
DE all		22 (33.3%)	6 (12%)	< 0.01
DE only		3 (4.5%)	5 (10%)	NS
PD all		52 (78.8%)	32 (64%)	NS
PD only		33 (50%)	31 (62%)	NS
DE and PD		19 (28.9%)	1 (2%)	< 0.01
Neither DE, nor PD		3 (4.5%)	10 (20%)	< 0.01
Periodontal scores (mean ± SD)		1.45 ± 0.85	0.97 ± 0.84	< 0.01
Drinking carbonated drinks	Nowadays	8 (12.2%)	10 (20%)	NS
	Previously	22 (33.3%)	15 (30%)	
	Never	36 (54.5%)	25 (50%)	
Eating sour foods	Nowadays	15 (22.7%)	9 (18%)	NS
	Previously	13 (19.7%)	9 (18%)	
	Never	38 (57.6%)	32 (64%)	
Bruxism/teeth grinding		9 (13.6%)	8 (16%)	NS
Total duration of heartburn, mean years (range)		15 (0-64)	9 (0-35)	< 0.01
Duration of heartburn until diagnosis, mean years (range)		5.3 (0-49)	2.9 (0-30)	NS

GERD: Gastroesophageal reflux disease; FHB: Functional heartburn; BMI: Body mass index; DMS: DeMeester score; PD: Periodontal disease; DE: Dental erosion; DE all: All the patients who had DE, and some of them have associated PD as well; DE only: Such patients have only DE and have not PD; PD all: All the patients who had PD, and some of them have associated DE as well; PD only: Such patients have only PD and have not DE; SD: Standard deviation; NS: Not significant.

hypersensitivity in the development of heartburn on the basis of the frequency and subjective severity of heartburn symptom. To confirm the diagnosis, detailed esophageal examinations are mandatory. That is why the necessity of comparative studies was also raised in the latest Rome IV criteria[13]; however, such studies had not been carried out. To the best of our knowledge, this study attempted the first differentiation between FHB and GERD based on oral manifestations. The rationale behind the use of oral evaluation is based on its low cost, wide availability, and the fact that the suggested parameters are not temporary symptoms but long-term consequences of GERD.

In the literature, there are many studies on the association between GERD and DE or PD. However, to the best of our knowledge, studies assessing the hard and soft tissue injuries, namely DE and PD, together have not been conducted yet. Furthermore, none of the previous studies examined their relations from both dental and gastroenterological perspectives.

Several studies discussed and concluded a clear but variable relationship between DE and GERD[14,15]. The proposed pathogenesis of DEs is attributed the direct contact of acid and the enamel, resulting in dissolution of the enamel crystals and destruction of the interprismatic matrix and subsequently, the dentin[16-19].

As a result of our research, 41.2% of those with DE had reflux, which did not prove to be a significant result. However, this result differed from the findings recorded in the literature. Pace *et al*[4] published a recent systematic review involving 17 eligible studies, mainly observational and case-control studies on GERD and DE, in which they reported a strong association between the two conditions. The median prevalence of DE among all patients with GERD was 24%, and the median prevalence of GERD among adults with DEs was 32.5% (21.0%-83.0%) However, in this population, there were wide percentage ranges and degrees of tooth tissue loss, and not all studies and evaluations of patients included esophageal endoscopy and/or 24 h esophageal pH-metry[4].

Table 2 Comparison of parameters between patients with or without dental erosion and periodontal disease

		DE (*n* = 17)	PD (*n* = 24)	Both (*n* = 10)	Neither (*n* = 54)	*P* value
Gender (male/female)		7 (41.2%)/10 (58.8%)	12 (50%)/12 (50%)	7 (70%)/3 (30%)	21 (38.9%)/33 (61.1%)	NS
Age, yr (min-max)		50 (24-79)	60 (41-82)	62 (40-71)	53 (22-80)	NS
BMI, kg/m^2 (min-max)		27 (17-35)	28 (16-39)	29 (26-35)	26 (18-37)	NS
Heartburn		17 (100%)	24 (100%)	10 (100%)	54 (100%)	NS
Nausea		12 (70.6%)	9 (37.5%)	7 (70%)	23 (42.6%)	NS
Vomiting		4 (23.6%)	5 (20.8%)	5 (50%)	9 (16.7%)	NS
Dysphagia		11 (64.7%)	10 (41.7%)	5 (50%)	21 (38.9%)	NS
Regurgitation		15 (88.2%)	15 (62.5%)	8 (80%)	39 (72.2%)	NS
Drinking carbonated drinks	Nowadays	2 (11.8%)	5 (20.8%)	2 (20%)	8 (14.8%)	NS
	Previously	6 (35.3%)	10 (41.7%)	1 (10%)	17 (31.5%)	
	Never	9 (52.9%)	9 (37.5%)	7 (70%)	29 (53.7%)	
Eating sour foods	Nowadays	5 (29.4%)	6 (25%)	0 (0%)	11 (20.4%)	NS
	Previously	2 (11.8%)	6 (25%)	4 (40%)	7 (13%)	
	Never	10 (58.8%)	12 (50%)	6 (60%)	36 (66.7%)	
Bruxism (teeth grinding)		4 (23.6%)	4 (16.7%)	2 (20%)	7 (13%)	NS
Number of teeth (min-max)		24 (13-31)	18 (1-30)	21 (13-28)	22 (2-32)	NS
Plaque Index (min-max)		58 (15-100)	72 (32-100)	67 (35-97)	49 (0-94)	< 0.01
Esophagitis score (mean ± SD)		1.6 ± 1.4	1.5 ± 1.4	1.8 ± 1.2	0.9 ± 1.1	0.05
Mean DMS		23.11	17.5	26.91	13.94	NS
Mean impedance ± SD		2390 ± 878	2393 ± 714	1708 ± 249	2427 ± 690	NS
Pathological reflux		7 (41.2%)	9 (37.5%)	9 (90%)	15 (27.8%)	< 0.01
Any proximal reflux		8 (47.1%)	9 (37.5%)	7 (70%)	19 (35.2%)	NS
Distal reflux		11 (64.7%)	13 (54.2%)	10 (100%)	21 (38.9%)	< 0.01

PD: Periodontal disease; DE: Dental erosion; BMI: Body mass index; DMS: DeMeester score; SD: Standard deviation; NS: Not significant.

Another systematic review was carried out and used different references since 2007. From a total of 273 articles, the mean prevalence values of DE were 48.8% in GERD patients and 20.5% in non-GERD controls. The prevalence of DE among adults with GERD was 38.9%, compared to 98.1% among children with GERD[20].

The total prevalence of DE (23.3%) in all subjects was less than the known global prevalence of DE. It can be stated that in the patient group we examined, the prevalence of DEs was found to be significantly higher among patients with GERD (33.1%) than among patients with FHB (12.0%) ($P < 0.01$). Our findings differ from those of studies conducted in different parts of the world.

A recent study conducted in China in 2016, reported a 60.8% presence of DE among patients diagnosed with GERD [21]. Another study carried out in Italy could not establish a significant co-appearance in the association between GERD and DE[22].

Previous studies have confirmed the association between DE and GERD. However, other manifestations (xerostomia, halitosis, oral burning, altered taste, bruxism, and soft tissue injuries, such as mucositis/stomatitis, aphthous-like ulcerations, gingivitis, and periodontal disease) are less likely to be investigated. The relationship between these diseases and GERD could either be direct or indirect[23].

In the literature, the presence of extrinsic factors resulting in DE was uncertain. According to a cross-sectional study, there was a clear relationship between DE and extrinsic dietary factors in patients with GERD[24]. This result was supported by a systematic review that highlighted the etiological complexity of DE (dietary habits, lifestyle, abrasion, bruxism, *etc*.), and the importance of taking a detailed medical history[25]. In contrast, based on an Indian cross-sectional study, extrinsic factors were not related to DE in GERD. In our study, there was no significant difference between the different habits resulting in DE ($P = 0.23$)[26].

In contrast to Song *et al*[27], our results could not confirm a close association between GERD and such manifestations except PD. The mechanism by which PD develops in GERD is mainly attributed to the direct action of acid on the mucosa, although hyposalivation is also suggested to play a role[28,29]. Watanabe *et al*[30] reported significant presence of soft tissue symptoms (stinging, bad breath, and burning sensation), oral cavity symptoms (sour/sour taste sensation),

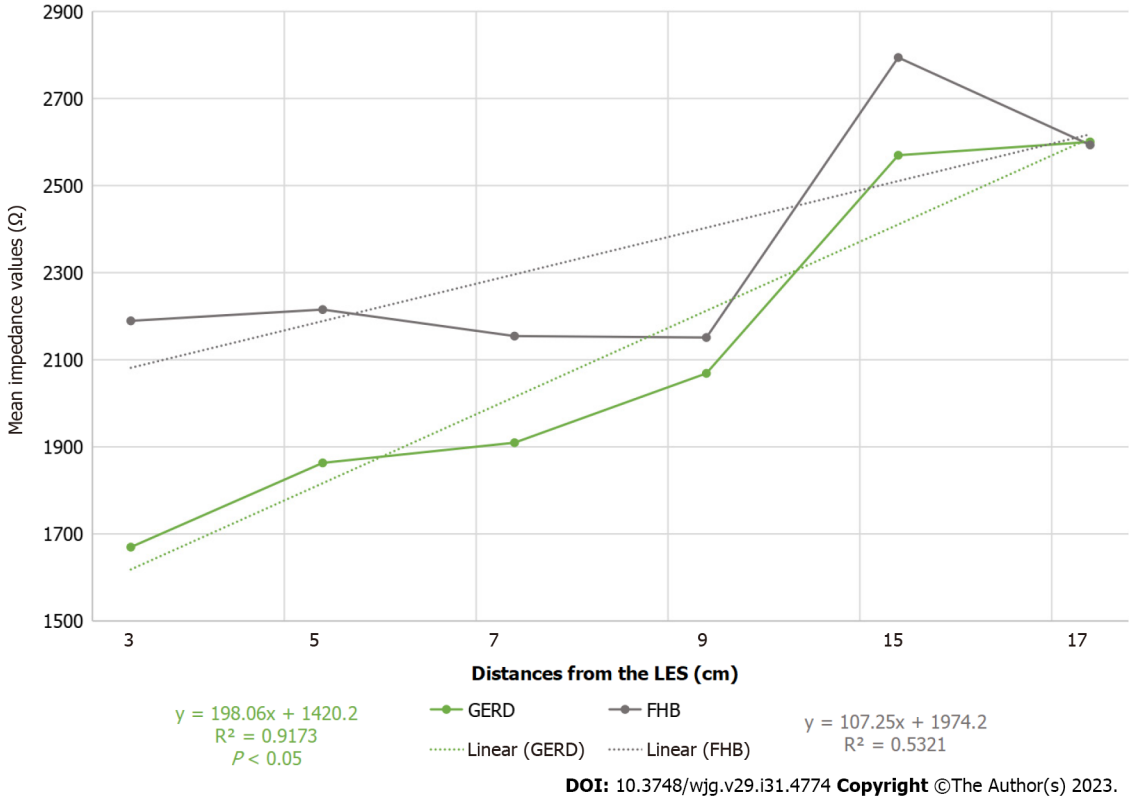

DOI: 10.3748/wjg.v29.i31.4774

Figure 1 Mean impedance values in patients with gastroesophageal reflux disease and those with functional heartburn. GERD: Gastroesophageal reflux disease; FHB: Functional heartburn; LES: Lower esophageal sphincter.

and the presence of GERD.

Di Fede *et al*[22] assessed the occurrence of oral pathological changes and symptoms in patients with GERD. Two hundred patients with GERD and 100 matched healthy controls were enrolled and studied. Univariate analyses revealed that xerostomia, oral burning sensation, subjective halitosis, and soft, hard palate mucosa, and uvula erythema were more common among patients with GERD than among matched controls ($P < 0.05$). The main outcome of this study was that no significant association between GERD and DEs was found, whereas some other symptoms or objective oral mucosal changes were found to be significantly associated with GERD[22]. In contrast, based on the responses of the patients we interviewed and examined, we did not find any data indicating a significant occurrence of oral complaints (such as the mouth and tongue burning, unpleasant breath, taste perception problems, inflammation of the mucous membrane, hypersensitivity, and sensations of sour taste).

A Chinese study found that periodontal factors were significantly associated with the risk of GERD in the studied 50183 patients. Severe periodontitis (OR = 1.40, $P < 0.001$) and lower frequency of tooth brushing (OR = 2.01, $P < 0.001$) were significantly associated with GERD[31].

In our study, neither DE nor PD alone was predictive of the presence of pathological reflux. There is not significantly more reflux in these cases. However, if both are present, the simultaneous presence of pathological reflux is more likely, as evidenced by the characteristic impedance deviations following the reflux pattern.

Increased BMI is commonly mentioned as a predictor of GERD. In their population-based study, Locke *et al*[31] found a significant relationship between higher BMI and the presence of GERD compared to subjects without reflux disease. Conversely, Watanabe *et al*[30] failed to establish a significant correlation between an increase in BMI and the presence of GERD. Our results seem to support the suggested association because our patients with GERD had significantly higher BMI than those with FHB. However, the observed difference is not significant enough to allow the prediction of GERD on the basis of this parameter alone.

In our study, higher esophagitis scores were detected in patients with DE and PD together than those without any dental diseases. This result suggests that there is more severe esophagitis in case of DE and PD than in the other groups. The correlation between the degree of DE and the severity of esophagitis was barely studied. A study conducted among the Mexican population found that 3/4 of the patients with mild grade DE had normal esophageal mucosa or LA-A esophagitis, whereas patients with severe DE were associated with a higher frequency of esophagitis LA-C and -D ($P = 0.021$)[32].

There are limitations to our study: First, the study was carried out in a single tertiary referral center; therefore, the prevalence of GERD phenotypes is different from the values of the general population. Second, during the process of pH-MII, inpatients were examined under standard conditions that do not correspond to their everyday conditions at home. DEs could be considered as cumulative lesions, representing the long-term consequences of reflux. Therefore, the dental status does not necessarily correlate with the current reflux state, since the bolus exposure time is not always the same, and it may significantly vary day by day, especially in the proximal part of the esophagus.

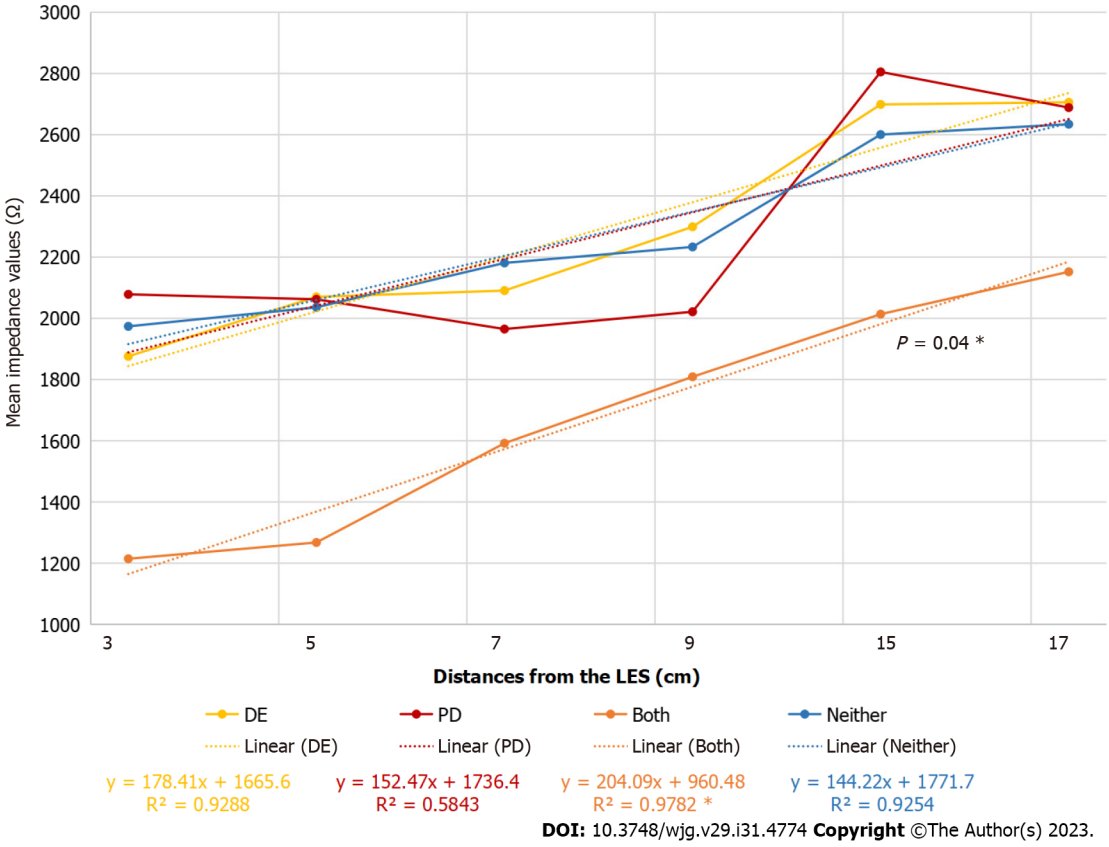

DOI: 10.3748/wjg.v29.i31.4774

Figure 2 Mean impedance values in patients with or without dental erosion and periodontal disease. The asterisk (*) the curve of "Both" group is significantly different from the others, and similar to the one in patients with gastroesophageal reflux disease. PD: Periodontal disease; DE: Dental erosion; LES: Lower esophageal sphincter.

CONCLUSION

The dental evaluation of patients with heartburn seems to be useful in the differential diagnosis of GERD and FHB. The co-appearance of dental erosions and periodontal diseases was present mostly in patients with GERD, whereas DE or PD (especially its mild forms) alone were not predictive for the disease. In contrast, the absence of dental disorders in patients with heartburn was predictive of FHB.

ARTICLE HIGHLIGHTS

Research background

Heartburn is a typical symptom of gastroesophageal reflux disease (GERD) and other functional gastrointestinal diseases. To diagnose them, detailed esophageal function tests are required. Oral manifestations are also common in patients with GERD. The dental evaluation is cheap and widely available.

Research motivation

This study raised the hypothesis that dental evaluation (dental erosions, periodontal diseases) in patients with heartburn may be useful in the differential diagnosis of GERD and functional heartburn (FHB).

Research objectives

To evaluate the prevalence of oral manifestations in patients with heartburn and their association with GERD and FHB.

Research methods

We enrolled 116 [M/F: 51/65, mean age: 54 (17-80) years] consecutive patients with heartburn for detailed esophageal function tests and dental evaluation.

Research results

The prevalence of dental diseases in patients with heartburn was about 89%. Compared with heartburn patients without any dental diseases, heartburn patients with both DE and PD had more significant pathological reflux, higher grade of

esophagitis, and significantly different mean impedance curves. Compared to FHB, GERD had a higher prevalence of DE and PD, especially when they coexisted. When evaluating the mean impedance curve, the trend of patients with both PD and DE was similar to those with GERD. The results of the study confirmed the abovementioned hypothesis experimentally.

Research conclusions

The co-existence of PD and DE is more likely to have pathological reflux, and the severity of esophagitis is higher than that of other groups. This study provides a new, inexpensive, widely available, and useful method for the differential diagnosis of GERD and FHB.

Research perspectives

On the one hand, our aim is to expand the study multicentrally in the direction of patients with heartburn presenting in primary care, and thereby reach a larger number of cases. On the other hand, this would probably also enable the inclusion of patients with reflux hypersensitivity, which is defined as a special borderline area between GERD and FHB in the Rome IV criteria system, which may help to decide whether this group of patients is more similar to patients GERD or FHB based on the oral status.

FOOTNOTES

Author contributions: Antal M and Rosztóczy A contributed tools and further data; Ollé G contributed help in the research; Rosztóczy A designed the research study; Árok AZ and Helle K performed the research; Helle K analyzed the data and wrote the manuscript; and all authors have read and approved the final manuscript.

Supported by the University of Szeged Open Access Fund, No. 6373.

Institutional review board statement: The study was reviewed and approved by the Institutional Review Board of the University of Szeged.

Informed consent statement: All study participants, or their legal guardian, provided informed written consent prior to study enrollment.

Conflict-of-interest statement: The authors have no conflict of interest to disclose.

Data sharing statement: No additional data are available.

STROBE statement: The authors have read the STROBE Statement—checklist of items, and the manuscript was prepared and revised according to the STROBE Statement—checklist of items.

Country/Territory of origin: Hungary

ORCID number: Krisztina Helle 0000-0002-5477-2618; Georgina Ollé 0000-0003-1726-8436; Márk Antal 0000-0002-4109-9356; András Rosztóczy 0000-0002-8597-8934.

S-Editor: Chen YL
L-Editor: A
P-Editor: Yuan YY

REFERENCES

1 **Moraes-Filho JP**, Chinzon D, Eisig JN, Hashimoto CL, Zaterka S. Prevalence of heartburn and gastroesophageal reflux disease in the urban Brazilian population. *Arq Gastroenterol* 2005; **42**: 122-127 [PMID: 16127569 DOI: 10.1590/s0004-28032005000200011]

2 **Vakil N**, van Zanten SV, Kahrilas P, Dent J, Jones R; Global Consensus Group. The Montreal definition and classification of gastroesophageal reflux disease: a global evidence-based consensus. *Am J Gastroenterol* 2006; **101**: 1900-20; quiz 1943 [PMID: 16928254 DOI: 10.1111/j.1572-0241.2006.00630.x]

3 **Bodecker CF**. Dental erosion: its possible causes and treatment. *Dental Cosmos* 1933; **75**: 1056-1062 [DOI: 10.14219/jada.archive.1938.0134]

4 **Pace F**, Pallotta S, Tonini M, Vakil N, Bianchi Porro G. Systematic review: gastro-oesophageal reflux disease and dental lesions. *Aliment Pharmacol Ther* 2008; **27**: 1179-1186 [PMID: 18373634 DOI: 10.1111/j.1365-2036.2008.03694.x]

5 **Boyapati R**, Vudathaneni VKP, Nadella SB, Bollepalli AC, Marella Y, Adurty C. Reflex Gastroesophageal Disorders and Functional Dyspepsia: Potential Confounding Variables for the Progression of Chronic Periodontitis: A Clinical Study. *Int J Prev Med* 2020; **11**: 138

[PMID: 33088466 DOI: 10.4103/ijpvm.IJPVM_141_19]

6 **Lundell LR**, Dent J, Bennett JR, Blum AL, Armstrong D, Galmiche JP, Johnson F, Hongo M, Richter JE, Spechler SJ, Tytgat GN, Wallin L. Endoscopic assessment of oesophagitis: clinical and functional correlates and further validation of the Los Angeles classification. *Gut* 1999; **45**: 172-180 [PMID: 10403727 DOI: 10.1136/gut.45.2.172]

7 **Kahrilas PJ**, Bredenoord AJ, Fox M, Gyawali CP, Roman S, Smout AJ, Pandolfino JE; International High Resolution Manometry Working Group. The Chicago Classification of esophageal motility disorders, v3.0. *Neurogastroenterol Motil* 2015; **27**: 160-174 [PMID: 25469569 DOI: 10.1111/nmo.12477]

8 **Gyawali CP**, Kahrilas PJ, Savarino E, Zerbib F, Mion F, Smout AJPM, Vaezi M, Sifrim D, Fox MR, Vela MF, Tutuian R, Tack J, Bredenoord AJ, Pandolfino J, Roman S. Modern diagnosis of GERD: the Lyon Consensus. *Gut* 2018; **67**: 1351-1362 [PMID: 29437910 DOI: 10.1136/gutjnl-2017-314722]

9 **Palsson OS**, Whitehead WE, van Tilburg MA, Chang L, Chey W, Crowell MD, Keefer L, Lembo AJ, Parkman HP, Rao SS, Sperber A, Spiegel B, Tack J, Vanner S, Walker LS, Whorwell P, Yang Y. Rome IV Diagnostic Questionnaires and Tables for Investigators and Clinicians. *Gastroenterology* 2016 [PMID: 27144634 DOI: 10.1053/j.gastro.2016.02.014]

10 **Zhong C**, Duan L, Wang K, Xu Z, Ge Y, Yang C, Han Y. Esophageal intraluminal baseline impedance is associated with severity of acid reflux and epithelial structural abnormalities in patients with gastroesophageal reflux disease. *J Gastroenterol* 2013; **48**: 601-610 [PMID: 23076541 DOI: 10.1007/s00535-012-0689-6]

11 **Smith BG**, Knight JK. An index for measuring the wear of teeth. *Br Dent J* 1984; **156**: 435-438 [PMID: 6590081 DOI: 10.1038/sj.bdj.4805394]

12 **Eke PI**, Page RC, Wei L, Thornton-Evans G, Genco RJ. Update of the case definitions for population-based surveillance of periodontitis. *J Periodontol* 2012; **83**: 1449-1454 [PMID: 22420873 DOI: 10.1902/jop.2012.110664]

13 **Aziz Q**, Fass R, Gyawali CP, Miwa H, Pandolfino JE, Zerbib F. Functional Esophageal Disorders. *Gastroenterology* 2016 [PMID: 27144625 DOI: 10.1053/j.gastro.2016.02.012]

14 **Bartlett D**. Intrinsic causes of erosion. *Monogr Oral Sci* 2006; **20**: 119-139 [PMID: 16687891 DOI: 10.1159/000093359]

15 **Ranjitkar S**, Kaidonis JA, Smales RJ. Gastroesophageal reflux disease and tooth erosion. *Int J Dent* 2012; **2012**: 479850 [PMID: 22194748 DOI: 10.1155/2012/479850]

16 **Hannig C**, Hannig M, Attin T. Enzymes in the acquired enamel pellicle. *Eur J Oral Sci* 2005; **113**: 2-13 [PMID: 15693823 DOI: 10.1111/j.1600-0722.2004.00180.x]

17 **Meurman JH**, Frank RM. Scanning electron microscopic study of the effect of salivary pellicle on enamel erosion. *Caries Res* 1991; **25**: 1-6 [PMID: 2070377 DOI: 10.1159/000261335]

18 **Lussi A**, Jäggi T, Schärer S. The influence of different factors on in vitro enamel erosion. *Caries Res* 1993; **27**: 387-393 [PMID: 8242676 DOI: 10.1159/000261569]

19 **Cairns AM**, Watson M, Creanor SL, Foye RH. The pH and titratable acidity of a range of diluting drinks and their potential effect on dental erosion. *J Dent* 2002; **30**: 313-317 [PMID: 12554112 DOI: 10.1016/s0300-5712(02)00044-1]

20 **Picos A**, Badea ME, Dumitrascu DL. Dental erosion in gastro-esophageal reflux disease. A systematic review. *Clujul Med* 2018; **91**: 387-390 [PMID: 30564013 DOI: 10.15386/cjmed-1017]

21 **Li W**, Liu J, Chen S, Wang Y, Zhang Z. Prevalence of dental erosion among people with gastroesophageal reflux disease in China. *J Prosthet Dent* 2017; **117**: 48-54 [PMID: 27616724 DOI: 10.1016/j.prosdent.2016.04.029]

22 **Di Fede O**, Di Liberto C, Occhipinti G, Vigneri S, Lo Russo L, Fedele S, Lo Muzio L, Campisi G. Oral manifestations in patients with gastro-oesophageal reflux disease: a single-center case-control study. *J Oral Pathol Med* 2008; **37**: 336-340 [PMID: 18284539 DOI: 10.1111/j.1600-0714.2008.00646.x]

23 **Mahajan R**, Kulkarni R, Stoopler ET. Gastroesophageal reflux disease and oral health: A narrative review. *Spec Care Dentist* 2022; **42**: 555-564 [PMID: 35605234 DOI: 10.1111/scd.12726]

24 **Ortiz AC**, Fideles SOM, Pomini KT, Buchaim RL. Updates in association of gastroesophageal reflux disease and dental erosion: systematic review. *Expert Rev Gastroenterol Hepatol* 2021; **15**: 1037-1046 [PMID: 33571021 DOI: 10.1080/17474124.2021.1890030]

25 **Chauhan N**, Manjunath BC, Malhotra P, Yadav V, Kumar JS, Muppalla L, Bhukal S. Dietary Practices as a Potential Predictor for Dental Erosion among Patients Having Gastroesophageal Reflux Disease: An Analytical Cross-sectional Study. *J Int Soc Prev Community Dent* 2022; **12**: 583-589 [PMID: 36777015 DOI: 10.4103/jispcd.JISPCD_95_22]

26 **Liu Z**, Gao X, Liang L, Zhou X, Han X, Yang T, Huang K, Lin Y, Deng S, Wang Z, Wang C. Prevalence, General and Periodontal Risk Factors of Gastroesophageal Reflux Disease in China. *J Inflamm Res* 2023; **16**: 235-244 [PMID: 36691403 DOI: 10.2147/JIR.S395777]

27 **Song JY**, Kim HH, Cho EJ, Kim TY. The relationship between gastroesophageal reflux disease and chronic periodontitis. *Gut Liver* 2014; **8**: 35-40 [PMID: 24516699 DOI: 10.5009/gnl.2014.8.1.35]

28 **Hauk L**. Laparoscopic Roux-en-Y gastric bypass. *AORN J* 2018; **107**: P12-P14 [PMID: 29486072 DOI: 10.1002/aorn.12107]

29 **Jajam M**, Bozzolo P, Niklander S. Oral manifestations of gastrointestinal disorders. *J Clin Exp Dent* 2017; **9**: e1242-e1248 [PMID: 29167716 DOI: 10.4317/jced.54008]

30 **Watanabe M**, Nakatani E, Yoshikawa H, Kanno T, Nariai Y, Yoshino A, Vieth M, Kinoshita Y, Sekine J. Oral soft tissue disorders are associated with gastroesophageal reflux disease: retrospective study. *BMC Gastroenterol* 2017; **17**: 92 [PMID: 28784097 DOI: 10.1186/s12876-017-0650-5]

31 **Locke GR 3rd**, Talley NJ, Fett SL, Zinsmeister AR, Melton LJ 3rd. Risk factors associated with symptoms of gastroesophageal reflux. *Am J Med* 1999; **106**: 642-649 [PMID: 10378622 DOI: 10.1016/s0002-9343(99)00121-7]

32 **Roesch-Ramos L**, Roesch-Dietlen F, Remes-Troche JM, Romero-Sierra G, Mata-Tovar Cde J, Azamar-Jácome AA, Barranca-Enríquez A. Dental erosion, an extraesophageal manifestation of gastroesophageal reflux disease. The experience of a center for digestive physiology in Southeastern Mexico. *Rev Esp Enferm Dig* 2014; **106**: 92-97 [PMID: 24852734 DOI: 10.4321/S1130-01082014000200004]

World Journal of Gastroenterology

Submit a Manuscript: https://www.f6publishing.com

World J Gastroenterol 2023 August 21; 29(31): 4783-4796

DOI: 10.3748/wjg.v29.i31.4783

ISSN 1007-9327 (print) ISSN 2219-2840 (online)

ORIGINAL ARTICLE

Randomized Controlled Trial

Poly(A)-specific ribonuclease protein promotes the proliferation, invasion and migration of esophageal cancer cells

Fu-Wei Zhang, Xiao-Wei Xie, Meng-Hua Chen, Jian Tong, Qun-Qing Chen, Jing Feng, Feng-Ti Chen, Wen-Qi Liu

Specialty type: Gastroenterology and hepatology

Provenance and peer review: Unsolicited article; Externally peer reviewed.

Peer-review model: Single blind

Peer-review report's scientific quality classification

Grade A (Excellent): 0
Grade B (Very good): B
Grade C (Good): C
Grade D (Fair): 0
Grade E (Poor): 0

P-Reviewer: Arigami T, Japan; Luyer MDP, Netherlands

Received: April 4, 2023
Peer-review started: April 4, 2023
First decision: April 12, 2023
Revised: April 29, 2023
Accepted: July 27, 2023
Article in press: July 27, 2023
Published online: August 21, 2023

Fu-Wei Zhang, Jian Tong, Qun-Qing Chen, Jing Feng, Department of Thoracic Surgery, Zhujiang Hospital, Southern Medical University, Guangzhou 510282, Guangdong Province, China

Xiao-Wei Xie, Meng-Hua Chen, Feng-Ti Chen, Wen-Qi Liu, Department of Radiation Oncology, The Second Affiliated Hospital of Guangxi Medical University, Nanning 530000, Guangxi Zhuang Autonomous Region, China

Corresponding author: Wen-Qi Liu, PhD, Chief Doctor, Doctor, Department of Radiation Oncology, The Second Affiliated Hospital of Guangxi Medical University, No. 166 East University Road, Nanning 530000, Guangxi Zhuang Autonomous Region, China.
liuwenqigx@163.com

Abstract

BACKGROUND

Bioinformatics analysis showed that the expression of the poly(A)-specific ribonuclease (PARN) gene in gastric cancer, head and neck squamous cell carcinoma, melanoma, cervical cancer and lung squamous cell carcinoma tissues was significantly higher than that in normal tissues and was associated with high stage and poor prognosis. The expression of the PARN gene in esophageal cancer (EC) tissue is also significantly higher than that in normal tissues, but the effect of PARN on the proliferation, migration and invasion of EC cells remains unclear.

AIM

To investigate the relationship between PARN and the proliferation, migration and invasion of EC cells.

METHODS

The EC tissues of 91 patients after EC surgery and 63 paired precancerous healthy tissues were collected. PARN mRNA levels were measured using a tissue microarray, and the PARN expression level was evaluated using immunohistochemistry to analyze the relationship between PARN expression and clinicopathologic features as well as the survival and prognosis of patients. In addition, the effects of PARN gene knockout on tumor cell proliferation, invasion and migration were studied by using shRNA during the *in vitro* culture of EC cell lines Eca-109 and TE-1, and the effects of the PARN gene on tumor growth *in vivo* were verified by a xenotransplantation nude mice model.

RESULTS

The expression of PARN in EC tissues was higher than that in adjacent normal tissues, and the level of PARN expression was significantly positively correlated with lymphatic metastasis. Patients with high PARN levels had poor overall survival. BIM, IGFBP-5 and p21 levels were significantly increased in the PARN knockout group, while the expression levels of the antiapoptotic proteins Survivin and sTNF-R1 were significantly decreased in the apoptotic antibody array data. In addition, the expression levels of Akt, p-Akt, PIK3CA and CCND1 in the downstream signaling pathway regulating EC progression were significantly decreased. The culture of EC cell lines confirmed that the apoptosis rate of EC cells was significantly increased, the growth and proliferation of tumor cells were significantly inhibited, and the invasion and migration ability of tumor cells were significantly decreased after PARN gene knockout. *In vivo* experiments of BALB/c nude mice transfected with Eca-109 cells expressing control shRNA (sh-NC) and PARN shRNA (sh-PARN) showed that the tumor volume and weight of nude mice treated with sh-PARN were significantly decreased compared with those of nude mice treated with sh-NC, indicating that PARN knockdown significantly inhibited tumor growth *in vivo*.

CONCLUSION

PARN has antiapoptotic effects on EC cells and promotes their proliferation, invasion and migration, which is associated with the development of EC and poor patient prognosis. PARN may become a potential target for the diagnosis, prognosis prediction and treatment of EC.

Key Words: Poly(A)-specific ribonuclease; Esophageal cancer; Apoptotic; Phosphatidylinositol 3-kinase/protein kinase B

Core Tip: Bioinformatics analysis showed that the expression of the poly(A)-specific ribonuclease (PARN) gene in gastric cancer, head and neck squamous cell carcinoma, melanoma, cervical cancer and lung squamous cell carcinoma tissues was significantly higher than that in normal tissues and was associated with high stage and poor prognosis. The expression of the PARN gene in esophageal cancer (EC) tissue is also significantly higher than that in normal tissues, but the effect of PARN on the proliferation, migration and invasion of EC cells remains unclear. This study investigated the relationship between PARN and the proliferation, migration and invasion of EC cells.

Citation: Zhang FW, Xie XW, Chen MH, Tong J, Chen QQ, Feng J, Chen FT, Liu WQ. Poly(A)-specific ribonuclease protein promotes the proliferation, invasion and migration of esophageal cancer cells. *World J Gastroenterol* 2023; 29(31): 4783-4796
URL: https://www.wjgnet.com/1007-9327/full/v29/i31/4783.htm
DOI: https://dx.doi.org/10.3748/wjg.v29.i31.4783

INTRODUCTION

Esophageal cancer (EC) is one of the most common malignancies in the world and the sixth leading cause of cancer-related mortality worldwide[1]. The main pathological types of esophageal carcinoma include esophageal squamous cell carcinoma (ESCC) and esophageal adenocarcinoma. In contrast to Europe and America, Asia has the most ESCC cases, which account for the vast majority of EC cases[2,3]. Currently, the main treatments for EC include surgery, radiotherapy and chemotherapy[4]. Since the clinical symptoms of early EC are not obvious, more than half of patients are in the advanced stage at the time of detection, and only 20% of patients with EC can be treated with surgery. Inoperable EC patients can only use radiotherapy, chemotherapy and other comprehensive treatments. Since it is highly invasive and has a high recurrence and metastasis rate, the prognosis for ESCC patients remains poor despite the use of multidisciplinary therapies[5]. The overall 5-year survival rate for ESCC patients is only 30%-40%. Patients with advanced or metastatic EC have a worse prognosis, with a 5-year overall survival of less than 15 years[2,4,5].

Increasing evidence shows that the resistance of some ECs to radiotherapy and chemotherapy is the cause of relapse and metastasis. Obviously, it is necessary to study the molecular mechanism of EC progression through genomics and proteomics and explore effective cancer biomarkers to predict treatment efficacy and EC patient prognosis.

Bioinformatics analysis from The Cancer Genome Atlas (TCGA) database showed that the expression of the PARN gene in breast cancer, head and neck squamous cell carcinoma, skin cancer, testicular cancer, thymic carcinoma and lung cancer tissues was significantly higher than that in normal tissues and was positively correlated with high stage and poor prognosis. In addition, the expression of the PARN gene in EC tissues in the TCGA database was also significantly higher than that in adjacent tissues. However, the effect of PARN on the proliferation, migration and invasion of EC cells is not clear and is worth further discussion.

Poly(A)-specific ribonuclease (PARN) is a deadenylase enzyme that is present in mammalian cells[6,7]. As a deadenylase, PARN interacts with the cap and the poly(A) tail of mRNA to control the length of the poly(A) tail and regulate gene expression. Therefore, it plays a role in mRNA degradation in the nucleus and cytoplasm[8,9]. Interference

in RNA stability is closely related to tumorigenesis and tumor development, and factors that affect RNA stability may become new targets for the treatment of malignant tumors[10]. Recent studies have shown that RNA-degrading enzymes, called RNases, are involved in the development of malignant tumors, so the regulation of mRNA turnover is a promising mechanism[11].

However, the biological function of PARN and its basic molecular mechanism in the carcinogenesis of the esophagus are still unclear and are worthy of further investigation. In the present study, EC tissues and adjacent normal tissues were immunohistochemically stained and analyzed to detect PARN expression. Moreover, we also investigated the clinicopathological characteristics of PARN and explored the value of PARN expression in predicting prognosis. In addition, we investigated the role of PARN knockdown in the biological characteristics of EC cells *in vitro* and *in vivo*.

MATERIALS AND METHODS

Online databases used in this study

Data on PARN expression in EC cell lines were obtained from the Cancer Cell Line Encyclopedia (CCLE) (www.broadinstitute.org/ccle). Mutation data were obtained from cBioPortal (https://www.cbioportal.org/). The mRNA expression level data of EC patients were downloaded from TCGA Portal (https://tcga-data.nci.nih.gov/tcga/).

Clinical samples

Ninety-one EC tissues and 63 healthy mucosa tissues were taken from EC patients who underwent resection at the Second Affiliated Hospital of Guangxi Medical University and the Affiliated Zhujiang Hospital of Southern Medical University from 2017 to 2018. The study ethics were approved by the Research Ethics Committee of the Second Affiliated Hospital of Guangxi Medical University and Zhujiang Hospital Affiliated to Southern Medical University, and written patient consent was obtained from all patients.

Immunohistochemistry

Immunohistochemistry (IHC) was conducted as previously described[12]. Briefly, the unstained tissue sections were deparaffinized by xylene and then rehydrated with a graded alcohol series. The sections were placed in EDTA buffer (pH = 8.0) buffer at 95-100 °C for 20 min to retrieve antigens. Then, the sections were incubated with rabbit anti-human PARN primary antibodies at 4 °C (1:100; Abcam, ab188333) overnight and then incubated with secondary antibodies for 1 h at room temperature.

Tissue microarray

The mRNA transcription levels of PARN in tumor tissues and adjacent normal mucosal tissues were measured using a tissue microarray (TMA).

Construction of a protein-protein interaction network and enrichment of functions and pathways

In this research, we obtained the protein-protein interaction by using an online tool, the String Database (STRING, https://string-db.org/). Then, the protein-protein interaction (PPI) we obtained was analyzed by using the software CytoScape (https://cytoscape.org/) and its plug-ins ClueGO and CluePedia. Then, Gene Ontology and Kyoto Encyclopedia of Genes and Genomes analyses were performed. The results of the PPI network and functional and pathway enrichment analyses are shown in Figures 1A and B.

Human apoptosis antibody array

The *Homo sapiens* apoptosis antibody array kit was purchased from Abcam (ab134001). Total protein samples were prepared as described above and incubated with the array according to the kit instructions. After the addition of chemiluminescence detection reagent, a signal proportional to the protein binding amount was detected. After RNA interference with the PARN gene in Eca-109 cells, the expression levels of apoptosis signaling pathway-related genes and proteins BIM, IGFBP-5 and p21 were evaluated.

Cell culture and transfection

We purchased human EC cell lines (Eca-109 and TE-1) from the Chinese Academy of Sciences Cell Bank (Shanghai, China). We cultured all cells in RPMI 1640 (Gibco, Grand Island, NY, United States) supplemented with 10% fetal bovine serum and maintained all cells in a humidified chamber at 37 °C with 5% CO_2. Control shRNA, shPARN-1, shPARN-2, and shPARN-3 were constructed by our group (the list of shRNA sequences is shown in Table 1). Viral transduction and selection of stable transfectants were carried out as mentioned above.

Western blot assay and antibodies

We collected cells and lysed them in RIPA lysis buffer. Aliquots of protein were then loaded and separated on SDS-PAGE gels and transferred to a polyvinylidene difluoride membrane. After blocking, the membrane was incubated with the appropriate primary antibody, followed by incubation with the corresponding secondary antibody. The primary antibodies and dilution factors were as follows: Rabbit anti-PARN (ab1883331, 1:1000 dilution; Abcam, United States), rabbit anti-CDK1 (ab133327, 1:3000 dilution, Abcam, United States), rabbit anti-PIK3CA (ab40776, 1:1000 dilution, Abcam, United States), rabbit anti-AKT [4685, 1:1000 dilution, Cell Signaling Technology (CST), United States], rabbit anti-

Table 1 Poly(A)-specific ribonuclease shRNA target sequence

Target number	Target sequence
Human-PARN-1	TATGACACAGCCTCTGAACA
Human-PARN-2	TGGATACTAAATTGATGGCCA
Human-PARN-3	CAACACATCCCTTGCGGAATT

PARN: Poly(A)-specific ribonuclease.

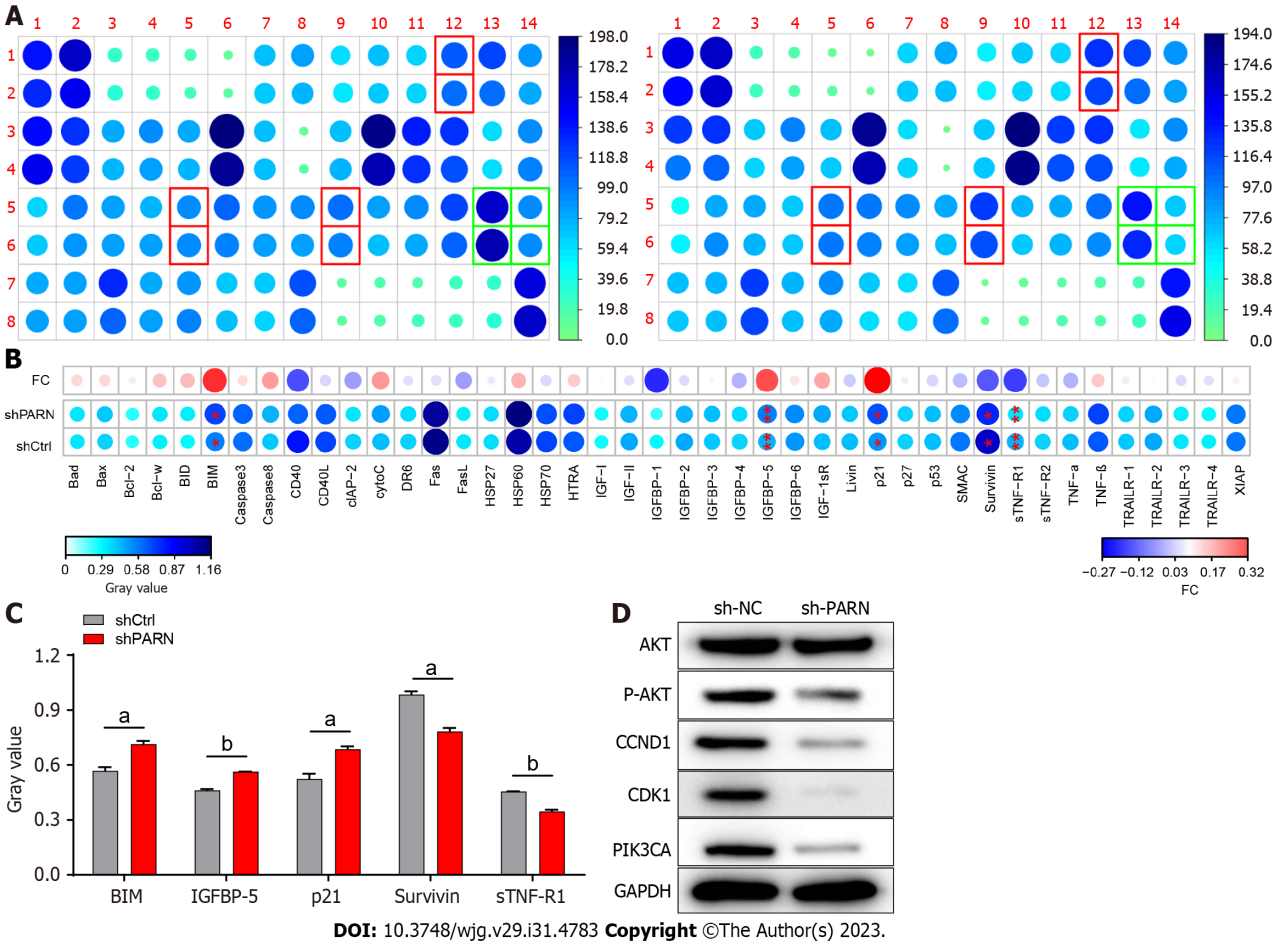

DOI: 10.3748/wjg.v29.i31.4783

Figure 1 Exploration of the downstream molecular mechanism of poly(A)-specific ribonuclease in esophageal cancer cells. A: Human apoptosis antibody array analysis was performed in Eca-109 cells transfected with control shRNA or poly(A)-specific ribonuclease shRNA; B: Differences in the human apoptotic antibody array were visualized; C: Densitometry analysis was performed, and the gray values of differentially expressed proteins are shown; D: The expression of the target protein pathway in Eca-109 cells was observed by western blot. The data are expressed as the mean ± SD, $^{a}P < 0.05$, $^{b}P < 0.01$. sh PARN: Poly(A)-specific ribonuclease shRNA; sh-NC: Control shRNA.

CCND1 (2978, 1:1000 dilution, CST, United States), rabbit anti-P-AKT (AF887-sp, 1:500 dilution, R&D Systems, United States), and rabbit anti-GAPDH (AP0063, 1:3000 dilution, Bioworld, United States).

Quantitative real-time polymerase chain reaction

Total RNA was isolated using TRIzol (Sigma-Aldrich, T9424-100 m), and cDNA was obtained with HiScript Q RT SuperMix for quantitative real-time polymerase chain reaction qRT-PCR (+gDNA wiper) (Vazyme, R123-01). PCRs were performed on an ABI 7500 qRT-PCR machine. GAPDH was used as an endogenous control. We assessed the qualified expression by employing the $2^{-\Delta\Delta Ct}$ formula, while statistical analysis was conducted by using the fold change. All primer sequences used in this research are available in Table 2.

Cell viability assay

The cell viability of the TE-1 and Eca-109 cell lines was calculated using the Celigo cell counting assay after transfection. Logarithmic-phase transfected cells were collected, and cell suspensions were obtained by trypsin digestion. Then, we

Table 2 Primer sequences

Gene		Sequence (5'-3')	Tm (°C)
GAPDH	Forward primer	GAAAGCCTGCCGGTGACTAA	60.32
	Reverse primer	GCCCAATACGACCAAATCAGAG	59.39
PARN	Forward primer	GCCGCGGAATTCGATTTTAAG	58.63
	Reverse primer	ATCGATGGCGAAGAAGTCGG	60.25

PARN: Poly(A)-specific ribonuclease.

seeded the cell suspensions (2000 cells/well) into 96-well plates and cultured them for 5 d. The cell number was recorded, and the cell growth curve was plotted.

Apoptosis and cell cycle assay

Apoptosis and cell cycle analyses were performed by flow cytometry. As mentioned above, transfected TE-1 and Eca-109 cells were cultured in 6-well plates and then collected, washed with D-Hanks buffer and incubated with 1 × binding buffer. The cells were centrifuged and resuspended in 200 μL 1 × binding buffer, and an additional 10 μL Annexin V from the Annexin V Apoptosis Detection kit APC (cat. no. 88-8007; eBioscience; Thermo Fisher Scientific, Inc.) was added. Then, the cells were incubated in the dark for 15 min. The cell cycle distribution phases were detected based on propidium iodide (PI; Sigma, P4170) staining. The samples were analyzed on an easy Cyte HT flow cytometer (Merck Millipore).

Wound healing assay

In this study, we detected cell migratory abilities by using a wound healing assay. Cells were seeded into 96-well plates (5.0×10^4) and cultured to 90% confluence. Confluent monolayer cells were scratched gently with a 96 Wounding Replicator (VP scientific, VP408FH), and images were captured using a Cellomics ArrayScan VTI (Thermo Scientific) at 0 h, 4 h, 8 h, 24 h and 72 h. The wound area was quantified using a Cellomics ArrayScan HCS Reader (Thermo Scientific).

Migration assay

Transwell plates (Corning, 3422) were used for migration assays, which were carried out according to the manufacturer's protocol. Cells were seeded in transwell inserts (100 μL, 6.0×10^4/inserts), and RPMI 1640 medium with 30% foetal bovine serum (600 μL) was added to the bottom chamber. Following incubation for 24 h, the inserts were removed and stained with crystal violet. Photos were obtained using an inverted microscope (Olympus I × 73) and analyzed by ImageJ software.

BALB/c nude mouse xenograft model

This study was approved by the Guangxi Medical University Ethics Committee. All BALB/c nude mice (male; 4 wk old) were purchased from Charles River (Beijing, China). All BALB/c nude mice (male; 4 wk old) were maintained in a specific-pathogen-free environment. Cells were collected and suspended in D-Hanks solution (1×10^7 cells/mL) and then subcutaneously injected into the right front limb of 20 nude mice (n = 10 for each group). After injection, the size of the tumor was measured with calipers every 4 d for 23 d. On day 23 after injection, the mice were deeply anesthetized with isoflurane gas, and tumor growth and metastases were visualized and analyzed using a whole-body fluorescence imaging system (Berthold Technologies, LB983). After the live imaging experiment, mice were sacrificed by cervical dislocation under anesthesia. Additionally, the tumors were isolated, weighed and photographed. Tumor tissues were saved for further experimentation.

Statistical analysis

In this study, data are reported as the mean ± SD, and statistical analysis was carried out using GraphPad Prism 8.3 and SPSS 23.0. The Kaplan-Meier log rank test was used for survival curve analysis. Unpaired student's t test was used to assess statistically significant differences between two groups, and one-way ANOVA with Dunnett's posttest was used to compare the differences among three or more groups. P values < 0.05 represented a statistically significant difference.

RESULTS

Cancer data and bioinformatics analysis

Analysis of EC datasets from TCGA demonstrated that PARN mRNA levels were significantly increased in EC tissues compared with adjacent nontumor tissues (Figure 2B). Then, we extended the detailed annotation process of the preclinical human cancer model by compiling CCLE data and proved that PARN was abnormally upregulated in EC cell lines (Figures 2D and E). We found that PARN expression was upregulated in various EC cell lines, including Eca-109,

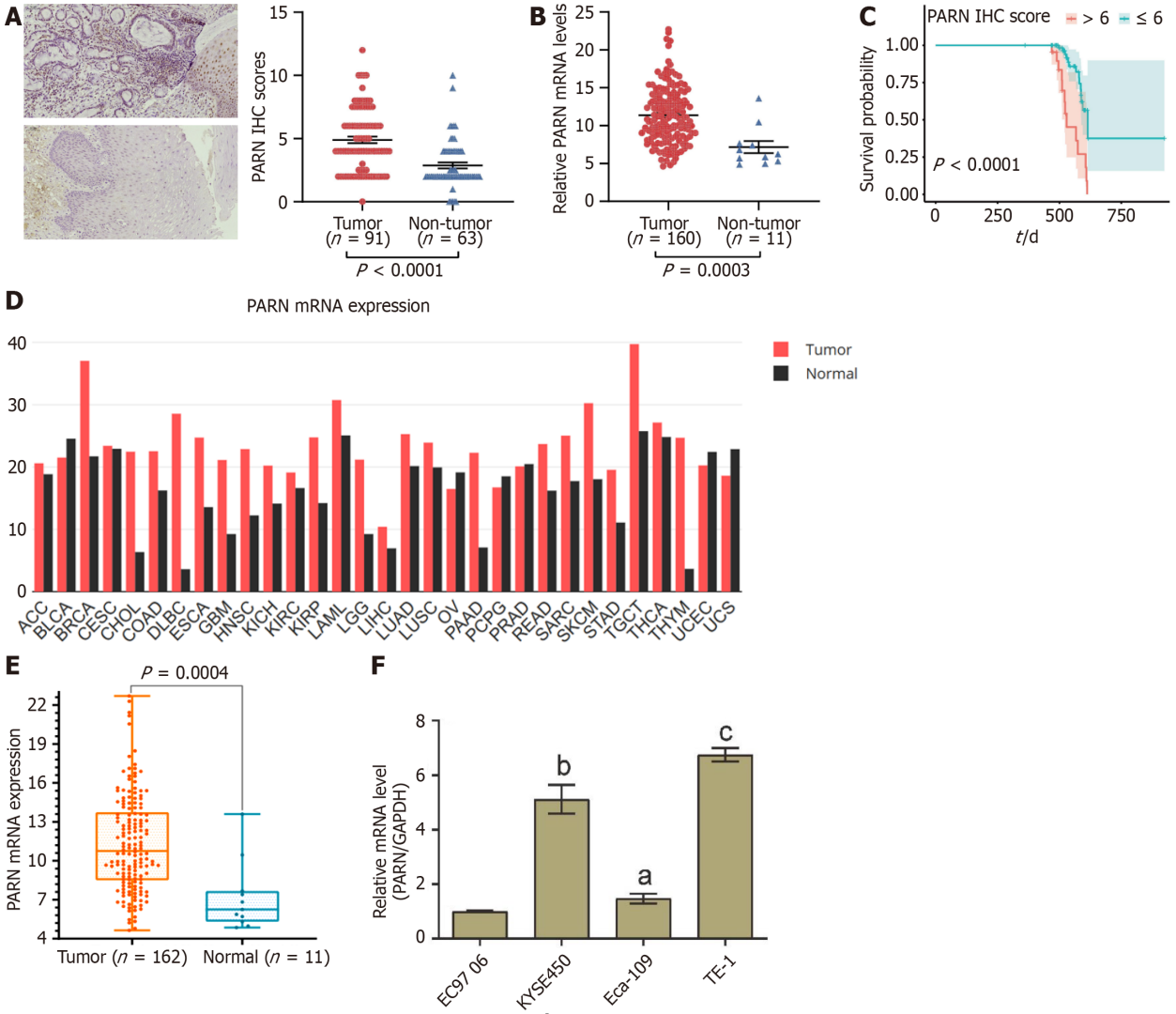

DOI: 10.3748/wjg.v29.i31.4783

Figure 2 Poly(A)-specific ribonuclease protein expression was upregulated in both esophageal cancer tissue and cell lines and correlated with poor prognosis in esophageal cancer patients. A: Left panel: Representative immunohistochemistry (IHC) staining images of poly(A)-specific ribonuclease (PARN) in esophageal cancer tissue specimens (magnification × 400, bar = 50 μm). Right panel: Summary of IHC staining of PARN in esophageal cancer tissues (n = 91) and adjacent normal tissues (n = 63) in an esophageal tissue microarray; B: PARN mRNA levels were significantly increased in esophageal cancer tissue (n = 160) compared with adjacent normal tissues (n = 11). The data were obtained from The Cancer Genome Atlas; C: Kaplan-Meier survival analysis showed that high expression of PARN was correlated with poor prognosis in esophageal cancer patients (the PARN IHC score criteria: Table 5); D and E: Exploration of PARN gene expression in various malignant tumors using TCGA database, and the expression of PARN gene in EC was significantly higher than that in adjacent tissues in the TCGA database, P = 0.0004; F: PARN mRNA levels in esophageal cancer cell lines. $^{a}P < 0.05$, $^{b}P < 0.01$, $^{c}P < 0.001$, mean ± SD is shown. PARN: Poly(A)-specific ribonuclease; IHC: Immunohistochemistry.

KYSE450 and TE-1 cells (Figure 2F). In this study, we observed PARN mutations in < 2% of EC patients based on the cBioportal datasets, suggesting that gene mutation is not a major mechanism contributing to the frequent upregulation of PARN in EC patients (Supplementary Figure 1).

IHC and TMA of clinical samples

The IHC staining and the TMA assay results indicated that PARN protein expression is exceedingly upregulated in EC tissues compared with nontumor tissues (Figure 2A). Additionally, to assess the clinical significance of PARN expression in EC, we investigated the relationship between PARN expression and clinicopathologic data in 91 EC patients (Table 3). After statistical analysis, we found that PARN expression was correlated with lymphatic metastasis (P = 0.028). The expression of PARN was positively correlated with tumor lymph node metastasis (N value). With increasing tumor malignancy, the expression levels of PARN increased (Table 4). However, PARN expression was not correlated with tumor size (P = 0.110), T cell infiltration (P = 0.680) or stage (P = 0.336). To determine the relationship between PARN expression and EC patient clinical prognosis, we performed survival analysis using the survival data of 91 EC patients. The Kaplan-Meier analysis results indicated that high PARN levels were linked with poor survival (Figure 2C and Table 5). In summary, the above results demonstrated that high PARN expression may be implicated in the progression and metastasis of EC and that high PARN expression may predict a worse prognosis.

Table 3 Relationship between poly(A)-specific ribonuclease expression and tumor characteristics in patients with esophageal cancer

Features	No. of patients	PARN expression		*P* value
		Low	High	
All patients	91	48	43	
Age (yr)				0.758
< 65	45	23	22	
≥ 65	46	25	21	
Gender				0.433
Male	73	40	33	
Female	18	8	10	
Tumor size				0.110
≤ 5 cm	46	28	18	
> 5 cm	35	15	20	
T Infiltrate				0.680
T0	1	1	0	
T1	3	1	2	
T2	15	8	7	
T3	39	22	17	
T4	10	4	6	
Lymphatic metastasis (*n*)				0.028[a]
N0	31	20	11	
N1	18	10	8	
N2	11	4	7	
N3	8	2	6	
Stage				0.336
I	3	2	1	
II	30	18	12	
III	33	14	19	
IV	2	2	0	
Lymphoid positive number				0.164
< 1	43	26	17	
≥ 1	46	21	25	
Grade				0.516
I	7	4	3	
II	49	25	24	
III	26	16	10	

[a]$P < 0.05$.

The high expression group: Poly(A)-specific ribonuclease immunohistochemistry scores > 6; the low expression group: Poly(A)-specific ribonuclease immunohistochemistry scores ≤ 6. PARN: Poly(A)-specific ribonuclease.

Construction of a PPI network, enrichment analyses and human apoptosis antibody array results

Functional and pathway enrichment and differential gene analysis showed that PARN plays a role in tumor apoptosis. To further identify the potential mechanism by which PARN induces apoptosis, a Human Apoptosis Antibody Array kit (ab134001), including 43 human apoptosis-related proteins, was used to investigate the mechanisms of PARN knockdown treatment-induced apoptosis. Among all detected proteins, BIM, IGFBP-5 and p21 were found to be significantly

Table 4 Relationship between poly(A)-specific ribonuclease expression and tumor characteristics (lymphatic metastasis) in patients with esophageal cancer (Spearman's correlation coefficient for ranked data)

		PARN
Lymphatic metastasis (N)	Spearman correlation analysis	0.269
	Significance (two-tailed)	0.027[a]
	N	68

[a]$P < 0.05$.
PARN: Poly(A)-specific ribonuclease.

Table 5 Immunohistochemistry scoring criteria

Score type	Score point	Score
Positive cell score	No positive signal	0 (negative)
	0% < the proportion of positive cells < 25%	1
	25% ≤ the proportion of positive cells < 50%	2
	50% ≤ the proportion of positive cells < 75%	3
	75% ≤ the proportion of positive cells	4
Staining intensity score (the staining intensity of cytoplasm, membrane or nucleus)	No signal color	0 (negative)
	Pale yellow	1
	Brown yellow	2
	Dark brown	3

The positive cell score × staining color intensity score was used to judge the immunohistochemistry results, and the higher the score, the higher the antibody expression (score 0: Negative, score 1-4: Positive, score 5-8: Positive ++, score 9-12: Positive +++).

upregulated in the PARN knockdown group, while knockdown of PARN significantly downregulated the expression of the antiapoptotic proteins Surviving and sTNF-R1 (Figures 1A-C). Changes in apoptosis-associated proteins strongly demonstrated that PARN is involved in preventing apoptosis of EC cells by regulating these apoptotic proteins. The original figures of the Human Apoptosis Antibody Array in this study are provided (Supplementary Figure 2). Furthermore, the expression of Akt, p-Akt, CCND1, CDK1 and PIK3CA was downregulated in the sh-PARN group compared with the sh-NC group (Figure 1D).

Effects of PARN on the proliferation, apoptosis and cell cycle of tumor cells in vitro

To investigate the effect of PARN on the biological characteristics of esophageal tumor cells, TE-1 and Eca-109 cells were transfected with sh-NC, shPARN-1, shPARN-2, and shPARN-3. The knockdown efficiency of PARN was validated by RT-qPCR. The results showed that shPARN-1 achieved the most efficient knockdown of PARN (Figure 3A), and thereafter, it was used to represent PARN knockdown in all follow-up experiments. The knockdown efficiency was verified at the protein level by western blotting (Figure 3B). The potential effect of PARN on the proliferation of Eca-109 and TE-1 cells was evaluated using the Celigo cell counting method. The results showed that the proliferation rate of Eca-109 and TE-1 cells infected with sh-PARN was significantly reduced compared with that of control cells (Figure 3C). It was confirmed that PARN knockout could significantly inhibit the proliferation of tumor cells. Apoptosis was analyzed by flow cytometry with Annexin V staining and showed a significantly increased percentage of apoptotic cells in sh-PARN-infected TE-1 and Eca-109 cells compared to sh-NC cells (Figure 3G). These results suggest that PARN knockout inhibits cell proliferation by inducing apoptosis. It was also found that compared with the sh-NC group, the sh-PARN group exhibited a significantly increased percentage of cells in the G2/M phase (Figure 3F), suggesting that PARN affects the proliferation of TE-1 and Eca-109 cells by regulating the cell cycle. Together, these findings confirm that PARN promotes EC cell proliferation by blocking cell cycle arrest and apoptosis.

Wound healing assay and transwell invasion assay

In the wound healing assay, the migration rates were significantly decreased in the sh-PARN group compared to the sh-NC group after lentivirus transfection. The migration abilities of Eca-109 cells in the sh-PARN group (72 h) were 47% lower than those in the sh-NC group ($P < 0.001$). In TE-1 cells, migration abilities in the sh-PARN group (8 h) were reduced by 40% ($P < 0.001$). (Figures 3D and E). Transwell invasion assays showed that after lentivirus transfection, the invasion ability of Eca-109 cells in the sh-PARN group was reduced by 73% compared with that in the sh-NC group ($P <$

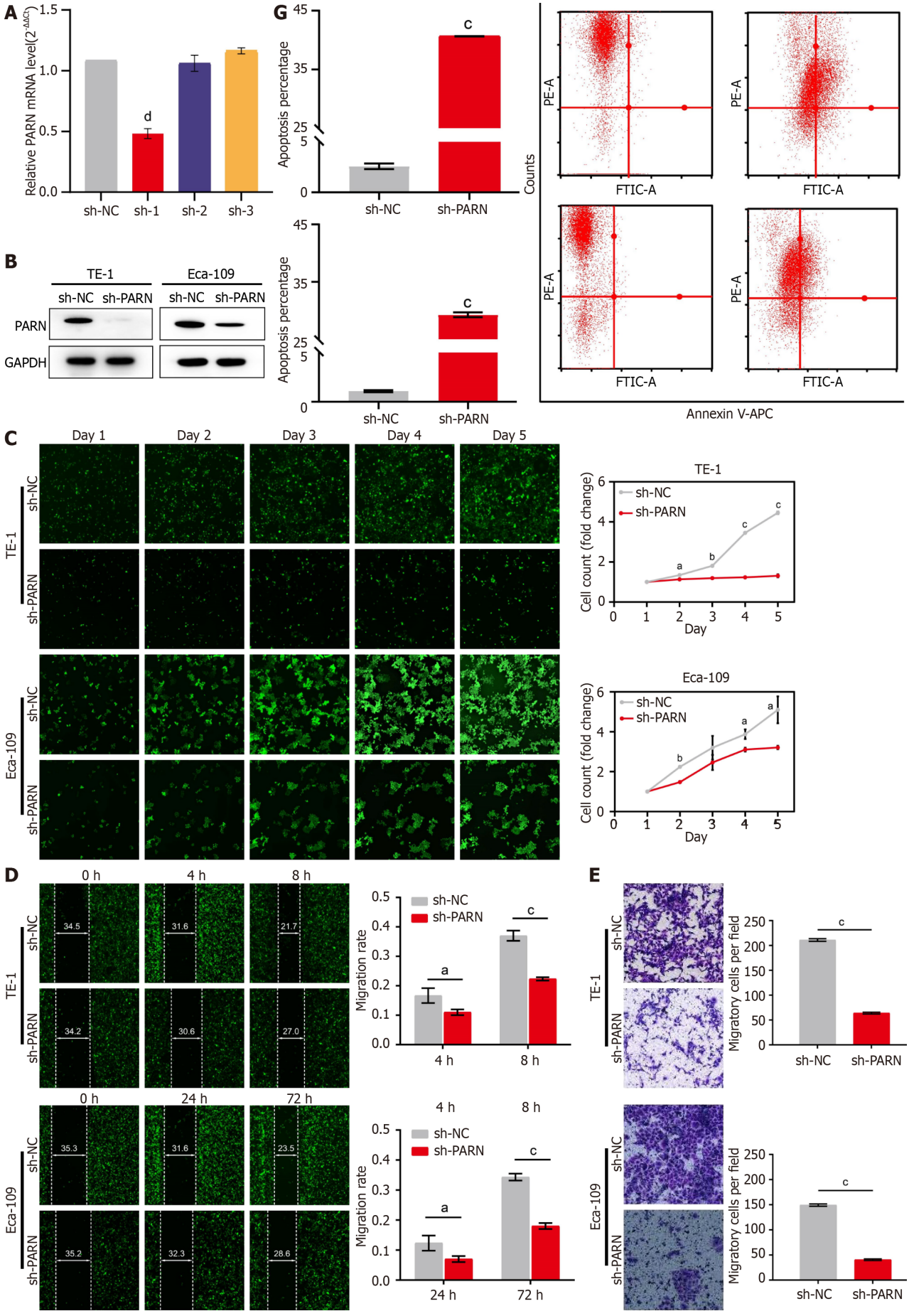
A
Relative PARN mRNA level(2^-ΔΔCt)
1.5
1.0
0.5
0.0
d
sh-NC
sh-1
sh-2
sh-3
B
TE-1
Eca-109
sh-NC
sh-PARN
sh-NC
sh-PARN
PARN
GAPDH
G
Apoptosis percentage
45
35
25
5
0
c
sh-NC
sh-PARN
Apoptosis percentage
45
35
25
5
0
c
sh-NC
sh-PARN
Counts
PE-A
FTIC-A
PE-A
FTIC-A
PE-A
FTIC-A
PE-A
FTIC-A
Annexin V-APC
C
Day 1
Day 2
Day 3
Day 4
Day 5
TE-1
sh-NC
sh-PARN
Eca-109
sh-NC
sh-PARN
TE-1
sh-NC
sh-PARN
Cell count (fold change)
Day
Eca-109
sh-NC
sh-PARN
Cell count (fold change)
Day
D
0 h
4 h
8 h
TE-1
sh-NC
sh-PARN
34.5
31.6
21.7
34.2
30.6
27.0
Migration rate
sh-NC
sh-PARN
4 h
8 h
0 h
24 h
72 h
Eca-109
sh-NC
sh-PARN
35.3
31.6
23.5
35.2
32.3
28.6
Migration rate
sh-NC
sh-PARN
4 h
8 h
24 h
72 h
E
TE-1
sh-NC
sh-PARN
Migratory cells per field
sh-NC
sh-PARN
Eca-109
sh-NC
sh-PARN
Migratory cells per field
sh-NC
sh-PARN

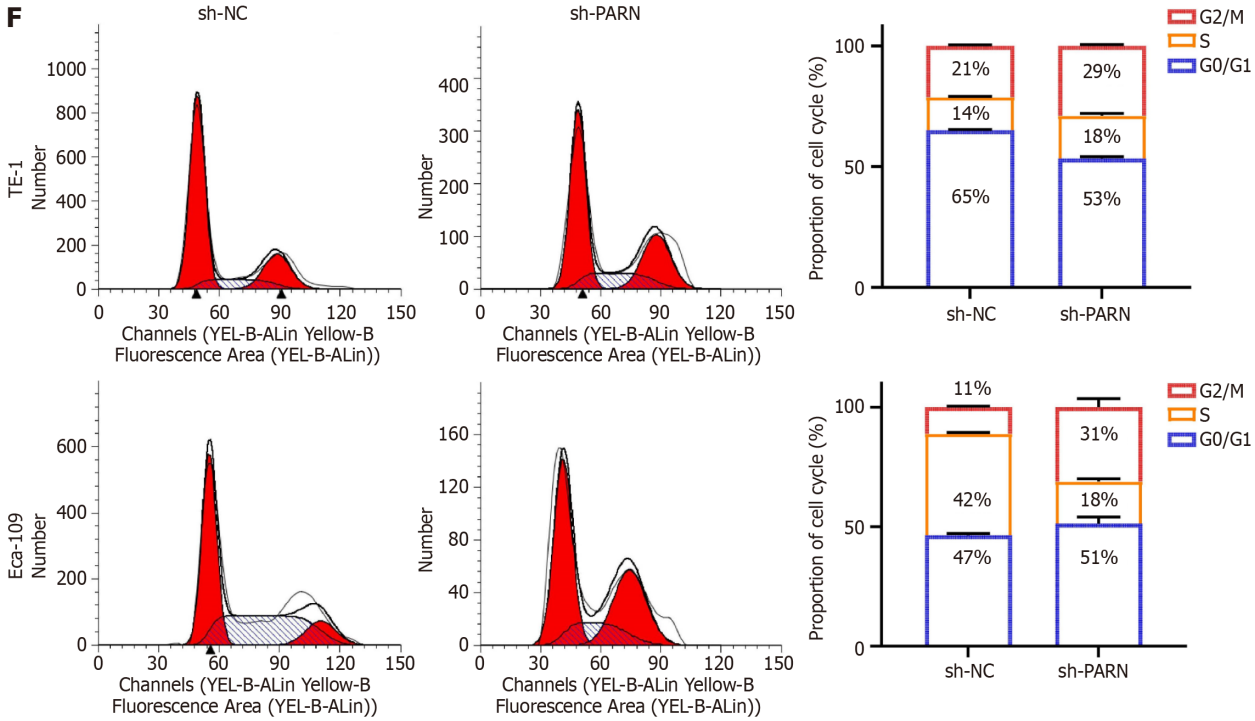

DOI: 10.3748/wjg.v29.i31.4783

Figure 3 Effect of poly(A)-specific ribonuclease on esophageal cancer cell proliferation, migration and invasion, cell cycle, and cell apoptosis *in vitro*. A and B: The interference efficiency of poly(A)-specific ribonuclease (PARN) *via* shRNA; C: Representative images of the Celigo cell count assay (magnification, × 100) and cumulative data of cell numbers in TE-1 and Eca-109 cells transfected with control shRNA or PARN shRNA; D: Representative images and statistical analysis of the wound healing assay; E: Representative images and statistical analysis of the transwell assay; F and G: Representative images and statistical analysis of flow cytometry analysis of TE-1 and Eca-109 cells after transfection. Cell cycle analysis revealed that PARN affected TE-1 and Eca-109 cell proliferation (F), and cell apoptosis analysis showed that PARN affected the apoptosis of TE-1 and Eca-109 cells (G). $^{a}P < 0.05$, $^{b}P < 0.01$, $^{a}P < 0.0001$, $^{c}P < 0.001$, means ± SDs are shown. sh PARN: Poly(A)-specific ribonuclease shRNA; sh-NC: Control shRNA.

0.001). In TE-1 cells, cell invasion was 70% lower in the sh-PARN group than in the sh-NC group ($P < 0.001$).

PARN facilitates tumor growth in vivo

The above results showed that knockdown of PARN inhibits cell proliferation and promotes cell apoptosis *in vitro*. We next wanted to examine the tumor suppression effects of PARN *in vivo*. To establish the xenograft tumor model, Eca-109 cells that were stably transfected with sh-NC and sh-PARN were subcutaneously implanted into BALB/c nude mice. Tumor weight and volume in the shPARN group were significantly reduced compared with those in the sh-NC-treated group (Figures 4A-C). Additionally, bioluminescence imaging suggested that tumor growth in the sh-PARN group was substantially suppressed (Figures 4D and E), which was similar to the results presented above. The sh-PARN group exhibited significantly repressed tumor development *in vivo*, suggesting that the tumor-forming capacity of Eca-109 cells in nude mice was significantly accelerated by PARN downregulation. Additionally, Ki67 staining was used to examine the proliferative cells in tumors. IHC data of tumor tissue showed that the number of Ki-67-positive tumor cells in the sh-PARN group markedly declined in comparison to that in the sh-NC group (Figure 4F). These *in vivo* results confirmed the *in vitro* results and showed that PARN significantly accelerated EC formation in nude mice.

DISCUSSION

Tumor progression is a complicated process, and increasing the degradation rate of homologous mRNAs affects the expression of dominant oncogenes, dysfunctional trans-acting factors and/or destruction of specific tumor suppressor genes. Therefore, precise control of mRNA levels is important for the regulation of gene expression[13,14].

As an RNA-processing enzymes, PARN may have an important role in tumor development and progression[15-17]. Currently, there is little evidence indicating a correlation between PARN expression and EC. Our study found that PARN expression levels in EC tissues are clearly higher than those in adjacent normal tissues and are significantly correlated with lymph node metastasis and poor patient survival. Since PARN expression has potential clinical implications in EC, the investigation of its regulatory mechanisms attracted our attention.

The main function of PARN is to cut the mRNA poly(A) tail and produce AMP in the process. The shortening of the eukaryotic poly(A) mRNA tail inhibits mRNA translation and induces transcript renewal; the deregulation of this process is common in cancer. A shortened poly(A) tail destabilizes mRNA and induces degradation. Thus, PARN is considered to be one of the important posttranscriptional regulators in cells. Previous studies have reported that the poly(A) tail of

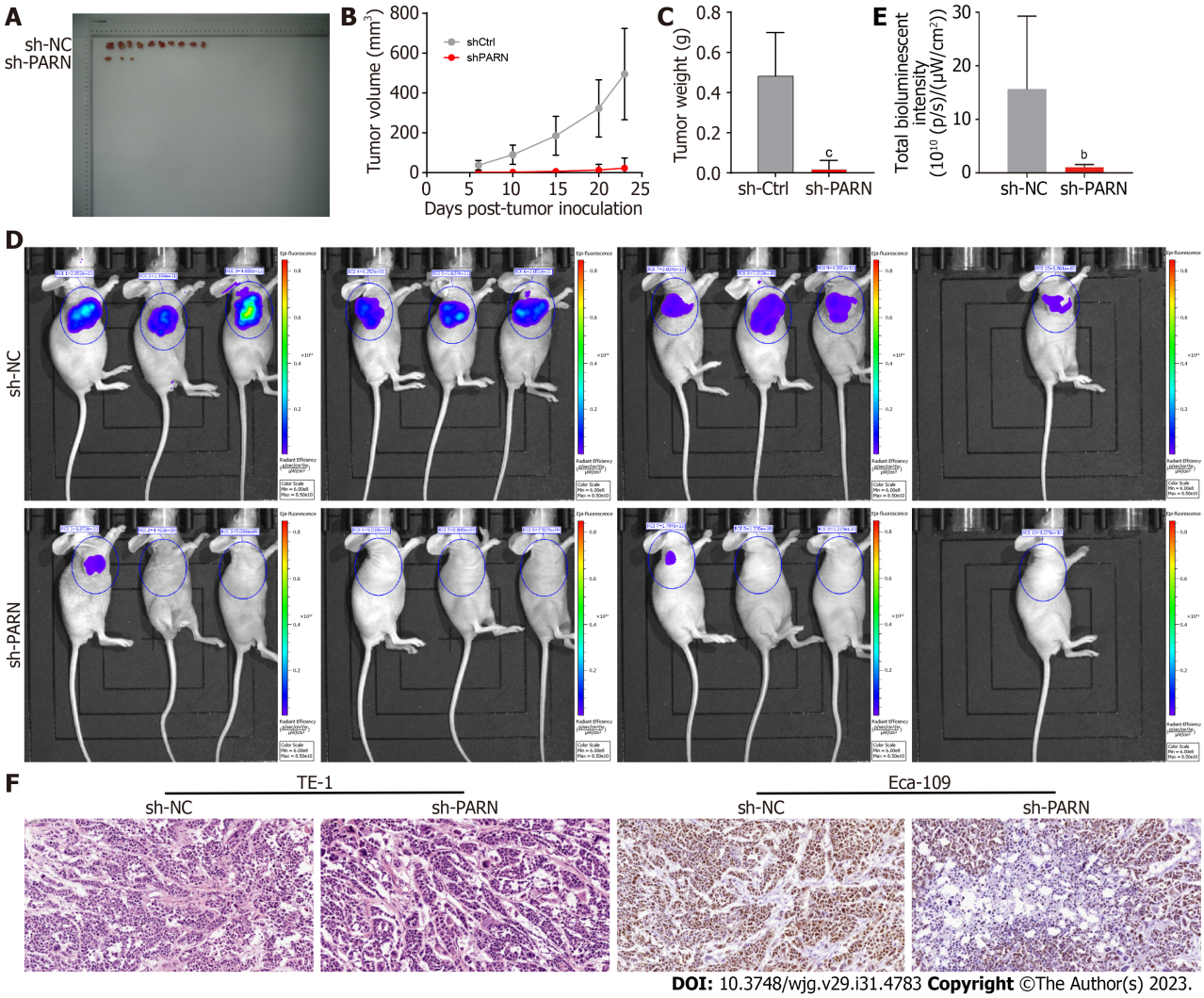

DOI: 10.3748/wjg.v29.i31.4783

Figure 4 Poly(A)-specific ribonuclease promotes tumor growth *in vivo*. A: Representative image of tumors separated from nude mice; B and C: Tumor volume and weight were measured in nude mice; D and E: Representative bioluminescence imaging (BLI) images and quantification of BLI in the tumor regions of nude mice; F: Representative images of Ki-67 staining in tumors isolated from the nude mice. Scale bars are indicated in the upper left corner of the picture (Bar = 50 μm). Assays were conducted in triplicate. °$P < 0.001$, mean ± SD is shown. sh PARN: Poly(A)-specific ribonuclease shRNA; sh-NC: Control shRNA.

mRNA transcripts is removed by 3′ to 5′ exonucleases (deadenylases), and this process is referred to as the rate-limiting step of mRNA degradation[9,18-21]. After mRNA transcript degradation, the protein expression levels also change accordingly. The levels of these mRNAs are low under normal conditions due to deadenylase activity[22-24].

In our study, compared with normal tissues, EC tissues exhibited significantly increased mRNA levels of PARN, and we also observed this trend in EC cell lines. Interestingly, we found that high PARN expression predicted a poor prognosis in EC patients.

Furthermore, compared with the those of the respective control cell lines, the growth and proliferation of EC cells were significantly inhibited after PARN knockdown. In contrast, it was confirmed that high PARN levels can promote the growth and proliferation of EC cells.

In addition, it was also found that compared with the sh-NC group, the sh-PARN group exhibited a significantly increased percentage of cells in the G2/M phase, suggesting that PARN affects the proliferation of carcinoma cells by regulating the cell cycle.

Escape from apoptosis is beneficial for malignant cell survival and thus could be one of the important mechanisms in cancer pathogenesis[25,26]. Apoptosis involves many biochemical processes that are induced by multiple signaling pathways[27,28]. In our study, PARN knockdown significantly downregulated multiple apoptosis-related proteins (for example, the antiapoptotic proteins Surviving and sTNF-R1) and promoted apoptosis. Therefore, knockdown of the PARN gene promotes apoptosis by regulating apoptotic proteins. In addition, PARN knockdown not only affects the apoptosis rate but also regulates a wide range of downstream signaling factors, including Akt, p-Akt, PIK3CA and CCND1. There has been much evidence suggesting that the PI3K/Akt pathway is one of the most important signaling pathways for cell proliferation, survival, apoptosis and malignant transformation[29,30]. These results suggest that PARN may inhibit tumor cell apoptosis and promote tumor proliferation through the PI3K/Akt pathway in EC. Subsequent wound healing tests and transwell invasion tests confirmed the promoting effect of PARN on the migration and invasion of EC cells. In a BALB/c nude mouse xenograft model, the apoptosis ratio of Eca-109 and TE-1 cells was significantly

increased after PARN knockout, and the cell proliferation rate was significantly decreased, as well as the percentage of cells in G2/M phase arrest. It has been confirmed that PARN promotes tumor cell proliferation by blocking cell cycle arrest and apoptosis in EC.

CONCLUSION

Our study preliminarily concluded that PARN may inhibit in EC cell apoptosis and cell cycle arrest through the PI3K/Akt pathway, thus promoting tumor proliferation, invasion and migration and further accelerating the progression of EC. Therefore, PARN can be used as a prognostic marker and therapeutic target for the diagnosis and treatment of EC.

ARTICLE HIGHLIGHTS

Research background

Esophageal cancer (EC) is a common malignant cancer type and the sixth leading cause of cancer-related mortality worldwide. The main treatment options for esophageal squamous cell carcinoma (ESCC) include surgery, radiotherapy, and chemotherapy. Due to its high invasiveness and high recurrence and metastasis rates, the prognosis of ESCC patients remains poor despite the use of multidisciplinary treatment. The 5-year overall survival rate of ESCC patients is only 30%-40%. However, the prognosis of patients with advanced or metastatic EC is even worse, with a 5-year overall survival rate of less than 15%.

Research motivation

Poly(A)-specific ribonuclease (PARN) is a multifunctional enzyme that plays a crucial role in the occurrence and development of a variety of cancer types. The aim of this study was to explore the relationship between PARN and the proliferation, metastasis and invasion of EC cells to evaluate whether PARN could be a potential biomarker and drug target for the treatment of EC.

Research objectives

The objects of this study are as follows: (1) EC tissues and paired adjacent normal tissues were obtained from 91 patients with EC after surgery; (2) EC lines Eca-109 and TE-1; and (3) Nude mice.

Research methods

The expression of PARN mRNA was measured using a tissue microarray, and the expression of PARN was also detected using immunohistochemistry. The relationship between PARN expression and clinicopathological features and the survival prognosis of patients was analyzed. The effect of PARN on the proliferation, invasion and migration of Eca-109 and TE-1 EC cells was investigated *in vitro* by knocking down PARN using shRNA. The effect of PARN on tumor growth *in vivo* was verified by a nude mouse xenograft model.

Research results

Our study found that PARN expression in EC tissues is clearly higher than that in adjacent healthy tissues and is significantly correlated with lymph node metastasis and poor survival. It was confirmed that PARN can promote the growth and proliferation of EC cells. Compared with the control shRNA group, the PARN shRNA group exhibited a significantly increased percentage of cells in the G2/M phase, suggesting that PARN affects the proliferation of carcinoma cells by regulating their cell cycle. Knockdown of the PARN gene promoted apoptosis by regulating apoptotic proteins. Wound healing tests and transwell invasion tests confirmed the promoting effect of PARN on the migration and invasion of EC cells. In the BALB/c nude mouse xenograft model, the apoptosis ratio of Eca-109 and TE-1 cells was significantly increased after PARN knockout, and the cell proliferation rate was significantly decreased, as well as the percentage of cells in G2/M phase arrest.

Research conclusions

Our study preliminarily concluded that PARN may inhibit EC cell apoptosis and cell cycle arrest through the PI3K/Akt pathway, thus promoting tumor cell proliferation, invasion and migration and further accelerating the progression of EC.

Research perspectives

PARN can be used as a prognostic marker and therapeutic target for the diagnosis and treatment of EC.

FOOTNOTES

Author contributions: Zhang FW and Liu WQ contributed to the conceptualization of this manuscript; Tong J, Chen QQ, and Feng J collected and curated the data and contributed to the supervision of this study; Xie XW contributed to the experiments; Tong J contributed to the data analysis; Zhang FW wrote the original draft; Liu WQ contributed to the writing, review and editing of this article;

and all authors reviewed, discussed, and agreed with manuscript.

Institutional review board statement: The study was reviewed and approved by the Second Affiliated Hospital of Guangxi Medical University Ethics Committee.

Clinical trial registration statement: Our study was not a prospective, randomized, controlled clinical trial and did not give a population one or more pre-defined interventions. Our study was a retrospective study of postoperative tissue samples from patients who had completed treatment. Cell experiments and animal experiments were conducted according to the results of clinical specimens. Therefore, our study should not apply the registration policy and should not require registration for clinical studies.

Informed consent statement: Written patient consent was obtained from all patients.

Conflict-of-interest statement: All the authors report no relevant conflicts of interest for this article.

Data sharing statement: No additional data are available.

CONSORT 2010 statement: The authors have read the CONSORT 2010 statement, and the manuscript was prepared and revised according to the CONSORT 2010 statement.

Country/Territory of origin: China

ORCID number: Wen-Qi Liu 0000-0003-4986-1234.

S-Editor: Wang JJ
L-Editor: A
P-Editor: Zhao S

REFERENCES

1 **Kashyap MK**, Abdel-Rahman O. Expression, regulation and targeting of receptor tyrosine kinases in esophageal squamous cell carcinoma. *Mol Cancer* 2018; **17**: 54 [PMID: 29455652 DOI: 10.1186/s12943-018-0790-4]
2 **van den Ende T**, Ter Veer E, Mali RMA, van Berge Henegouwen MI, Hulshof MCCM, van Oijen MGH, van Laarhoven HWM. Prognostic and Predictive Factors for the Curative Treatment of Esophageal and Gastric Cancer in Randomized Controlled Trials: A Systematic Review and Meta-Analysis. *Cancers (Basel)* 2019; **11** [PMID: 31013858 DOI: 10.3390/cancers11040530]
3 **Tepper J**, Krasna MJ, Niedzwiecki D, Hollis D, Reed CE, Goldberg R, Kiel K, Willett C, Sugarbaker D, Mayer R. Phase III trial of trimodality therapy with cisplatin, fluorouracil, radiotherapy, and surgery compared with surgery alone for esophageal cancer: CALGB 9781. *J Clin Oncol* 2008; **26**: 1086-1092 [PMID: 18309943 DOI: 10.1200/JCO.2007.12.9593]
4 **Sjoquist KM**, Burmeister BH, Smithers BM, Zalcberg JR, Simes RJ, Barbour A, Gebski V; Australasian Gastro-Intestinal Trials Group. Survival after neoadjuvant chemotherapy or chemoradiotherapy for resectable oesophageal carcinoma: an updated meta-analysis. *Lancet Oncol* 2011; **12**: 681-692 [PMID: 21684205 DOI: 10.1016/S1470-2045(11)70142-5]
5 **van Hagen P**, Hulshof MC, van Lanschot JJ, Steyerberg EW, van Berge Henegouwen MI, Wijnhoven BP, Richel DJ, Nieuwenhuijzen GA, Hospers GA, Bonenkamp JJ, Cuesta MA, Blaisse RJ, Busch OR, ten Kate FJ, Creemers GJ, Punt CJ, Plukker JT, Verheul HM, Spillenaar Bilgen EJ, van Dekken H, van der Sangen MJ, Rozema T, Biermann K, Beukema JC, Piet AH, van Rij CM, Reinders JG, Tilanus HW, van der Gaast A; CROSS Group. Preoperative chemoradiotherapy for esophageal or junctional cancer. *N Engl J Med* 2012; **366**: 2074-2084 [PMID: 22646630 DOI: 10.1056/NEJMoa1112088]
6 **Balatsos NA**, Maragozidis P, Anastasakis D, Stathopoulos C. Modulation of poly(A)-specific ribonuclease (PARN): current knowledge and perspectives. *Curr Med Chem* 2012; **19**: 4838-4849 [PMID: 22834816 DOI: 10.2174/092986712803341539]
7 **Dejene EA**, Li Y, Showkatian Z, Ling H, Seto E. Regulation of poly(a)-specific ribonuclease activity by reversible lysine acetylation. *J Biol Chem* 2020; **295**: 10255-10270 [PMID: 32457045 DOI: 10.1074/jbc.RA120.012552]
8 **Delis C**, Krokida A, Tomatsidou A, Tsikou D, Beta RA, Tsioumpekou M, Moustaka J, Stravodimos G, Leonidas DD, Balatsos NA, Papadopoulou KK. AtHESPERIN: a novel regulator of circadian rhythms with poly(A)-degrading activity in plants. *RNA Biol* 2016; **13**: 68-82 [PMID: 26619288 DOI: 10.1080/15476286.2015.1119363]
9 **Virtanen A**, Henriksson N, Nilsson P, Nissbeck M. Poly(A)-specific ribonuclease (PARN): an allosterically regulated, processive and mRNA cap-interacting deadenylase. *Crit Rev Biochem Mol Biol* 2013; **48**: 192-209 [PMID: 23496118 DOI: 10.3109/10409238.2013.771132]
10 **Dehan E**, Ben-Dor A, Liao W, Lipson D, Frimer H, Rienstein S, Simansky D, Krupsky M, Yaron P, Friedman E, Rechavi G, Perlman M, Aviram-Goldring A, Izraeli S, Bittner M, Yakhini Z, Kaminski N. Chromosomal aberrations and gene expression profiles in non-small cell lung cancer. *Lung Cancer* 2007; **56**: 175-184 [PMID: 17258348 DOI: 10.1016/j.lungcan.2006.12.010]
11 **Valles I**, Pajares MJ, Segura V, Guruceaga E, Gomez-Roman J, Blanco D, Tamura A, Montuenga LM, Pio R. Identification of novel deregulated RNA metabolism-related genes in non-small cell lung cancer. *PLoS One* 2012; **7**: e42086 [PMID: 22876301 DOI: 10.1371/journal.pone.0042086]
12 **Yu K**, Ahrens S, Zhang X, Schiff H, Ramakrishnan C, Fenno L, Deisseroth K, Zhao F, Luo MH, Gong L, He M, Zhou P, Paninski L, Li B. The

central amygdala controls learning in the lateral amygdala. *Nat Neurosci* 2017; **20**: 1680-1685 [PMID: 29184202 DOI: 10.1038/s41593-017-0009-9]

13 **Audic Y**, Hartley RS. Post-transcriptional regulation in cancer. *Biol Cell* 2004; **96**: 479-498 [PMID: 15380615 DOI: 10.1016/j.biolcel.2004.05.002]

14 **Tang Y**, Shu G, Yuan X, Jing N, Song J. FOXA2 functions as a suppressor of tumor metastasis by inhibition of epithelial-to-mesenchymal transition in human lung cancers. *Cell Res* 2011; **21**: 316-326 [PMID: 20820189 DOI: 10.1038/cr.2010.126]

15 **Maragozidis P**, Karangeli M, Labrou M, Dimoulou G, Papaspyrou K, Salataj E, Pournaras S, Matsouka P, Gourgoulianis KI, Balatsos NA. Alterations of deadenylase expression in acute leukemias: evidence for poly(a)-specific ribonuclease as a potential biomarker. *Acta Haematol* 2012; **128**: 39-46 [PMID: 22614729 DOI: 10.1159/000337418]

16 **Maragozidis P**, Papanastasi E, Scutelnic D, Totomi A, Kokkori I, Zarogiannis SG, Kerenidi T, Gourgoulianis KI, Balatsos NA. Poly(A)-specific ribonuclease and Nocturnin in squamous cell lung cancer: prognostic value and impact on gene expression. *Mol Cancer* 2015; **14**: 187 [PMID: 26541675 DOI: 10.1186/s12943-015-0457-3]

17 **Zhang LN**, Yan YB. Depletion of poly(A)-specific ribonuclease (PARN) inhibits proliferation of human gastric cancer cells by blocking cell cycle progression. *Biochim Biophys Acta* 2015; **1853**: 522-534 [PMID: 25499764 DOI: 10.1016/j.bbamcr.2014.12.004]

18 **Funakoshi Y**, Doi Y, Hosoda N, Uchida N, Osawa M, Shimada I, Tsujimoto M, Suzuki T, Katada T, Hoshino S. Mechanism of mRNA deadenylation: evidence for a molecular interplay between translation termination factor eRF3 and mRNA deadenylases. *Genes Dev* 2007; **21**: 3135-3148 [PMID: 18056425 DOI: 10.1101/gad.1597707]

19 **Nousch M**, Techritz N, Hampel D, Millonigg S, Eckmann CR. The Ccr4-Not deadenylase complex constitutes the main poly(A) removal activity in C. elegans. *J Cell Sci* 2013; **126**: 4274-4285 [PMID: 23843623 DOI: 10.1242/jcs.132936]

20 **Wilson T**, Treisman R. Removal of poly(A) and consequent degradation of c-fos mRNA facilitated by 3' AU-rich sequences. *Nature* 1988; **336**: 396-399 [PMID: 3194021 DOI: 10.1038/336396a0]

21 **Wolf J**, Passmore LA. mRNA deadenylation by Pan2-Pan3. *Biochem Soc Trans* 2014; **42**: 184-187 [PMID: 24450649 DOI: 10.1042/BST20130211]

22 **Cevher MA**, Zhang X, Fernandez S, Kim S, Baquero J, Nilsson P, Lee S, Virtanen A, Kleiman FE. Nuclear deadenylation/polyadenylation factors regulate 3' processing in response to DNA damage. *EMBO J* 2010; **29**: 1674-1687 [PMID: 20379136 DOI: 10.1038/emboj.2010.59]

23 **Devany E**, Zhang X, Park JY, Tian B, Kleiman FE. Positive and negative feedback loops in the p53 and mRNA 3' processing pathways. *Proc Natl Acad Sci U S A* 2013; **110**: 3351-3356 [PMID: 23401530 DOI: 10.1073/pnas.1212533110]

24 **Moraes KC**, Wilusz CJ, Wilusz J. CUG-BP binds to RNA substrates and recruits PARN deadenylase. *RNA* 2006; **12**: 1084-1091 [PMID: 16601207 DOI: 10.1261/rna.59606]

25 **Chen T**, Dai X, Dai J, Ding C, Zhang Z, Lin Z, Hu J, Lu M, Wang Z, Qi Y, Zhang L, Pan R, Zhao Z, Lu L, Liao W, Lu X. AFP promotes HCC progression by suppressing the HuR-mediated Fas/FADD apoptotic pathway. *Cell Death Dis* 2020; **11**: 822 [PMID: 33009373 DOI: 10.1038/s41419-020-03030-7]

26 **Zhivotovsky B**, Kroemer G. Apoptosis and genomic instability. *Nat Rev Mol Cell Biol* 2004; **5**: 752-762 [PMID: 15340382 DOI: 10.1038/nrm1443]

27 **Fuchs Y**, Steller H. Live to die another way: modes of programmed cell death and the signals emanating from dying cells. *Nat Rev Mol Cell Biol* 2015; **16**: 329-344 [PMID: 25991373 DOI: 10.1038/nrm3999]

28 **Jeong SY**, Seol DW. The role of mitochondria in apoptosis. *BMB Rep* 2008; **41**: 11-22 [PMID: 18304445 DOI: 10.5483/bmbrep.2008.41.1.011]

29 **Downward J**. Mechanisms and consequences of activation of protein kinase B/Akt. *Curr Opin Cell Biol* 1998; **10**: 262-267 [PMID: 9561851 DOI: 10.1016/s0955-0674(98)80149-x]

30 **Duan C**, Bauchat JR, Hsieh T. Phosphatidylinositol 3-kinase is required for insulin-like growth factor-I-induced vascular smooth muscle cell proliferation and migration. *Circ Res* 2000; **86**: 15-23 [PMID: 10625300 DOI: 10.1161/01.res.86.1.15]

World Journal of Gastroenterology

Submit a Manuscript: https://www.f6publishing.com

World J Gastroenterol 2023 August 21; 29(31): 4797-4808

DOI: 10.3748/wjg.v29.i31.4797

ISSN 1007-9327 (print) ISSN 2219-2840 (online)

META-ANALYSIS

Circulating copeptin level and the clinical prognosis of patients with chronic liver disease

Hao-Qian Tan, Ming Zhao, Zan Huang, Yang Liu, Han Li, Long-Hui Ma, Jun-Ying Liu

Specialty type: Gastroenterology and hepatology

Provenance and peer review: Unsolicited article; Externally peer reviewed.

Peer-review model: Single blind

Peer-review report's scientific quality classification

Grade A (Excellent): A
Grade B (Very good): B
Grade C (Good): 0
Grade D (Fair): 0
Grade E (Poor): 0

P-Reviewer: El-Shabrawi MH, Egypt; Rodrigues AT, Brazil

Received: June 15, 2023
Peer-review started: June 15, 2023
First decision: July 14, 2023
Revised: July 21, 2023
Accepted: July 28, 2023
Article in press: July 28, 2023
Published online: August 21, 2023

Hao-Qian Tan, Department of Gastroenterology, Zhoukou Central Hospital Affiliated to Xinxiang Medical University, Zhoukou 466000, Henan Province, China

Ming Zhao, Yang Liu, Han Li, Jun-Ying Liu, Department of Gastroenterology, Zhoukou Central Hospital, Zhoukou 466000, Henan Province, China

Zan Huang, Long-Hui Ma, Department of Teaching and Research, Zhoukou Central Hospital, Zhoukou 466000, Henan Province, China

Corresponding author: Jun-Ying Liu, MD, Director, Department of Gastroenterology, Zhoukou Central Hospital, No. 26 Renmin Road East Section, Chuanhui District, Zhoukou 466000, Henan Province, China. liujunying781025@163.com

Abstract

BACKGROUND

The relationship between copeptin and the severity of circulatory dysfunction and systemic stress response in patients with chronic liver disease (CLD) has been established. Nevertheless, the potential of serum copeptin levels to predict the prognosis of CLD patients remains unclear.

AIM

To conduct a systematic review and meta-analysis to investigate the correlation between serum copeptin and transplant-free survival (TFS) in this population.

METHODS

To achieve the objective of the meta-analysis, PubMed, Embase, the Cochrane Library, and the Web of Science were searched to identify observational studies with longitudinal follow-up. The Cochrane *Q* test was utilized to assess between-study heterogeneity, and the I^2 statistic was estimated. Random-effects models were employed to combine the outcomes, taking into account the potential influence of heterogeneity.

RESULTS

Ten datasets including 3133 patients were involved. The follow-up durations were 1 to 48 mo (mean: 12.5 mo). Overall, it was shown that a high level of serum copeptin was associated with a poor TFS [risk ratio (RR): 1.82, 95% confidence interval: 1.52-2.19, $P < 0.001$; $I^2 = 0\%$]. In addition, sensitivity analysis by omitting one dataset at a time showed consistent results (RR: 1.73-2.00, $P < 0.05$). Finally, subgroup analyses according to study country, study design, patient diagnosis,

cutoff of copeptin, follow-up duration, and study quality score also showed similar results (*P* for subgroup difference all > 0.05).

CONCLUSION
Patients with CLD who have high serum copeptin concentrations may be associated with a poor clinical prognosis.

Key Words: Chronic liver disease; Liver cirrhosis; Copeptin; Prognosis; Mortality; Meta-analysis

Core Tip: Serum copeptin has been related to the severity of circulatory dysfunction and systemic stress response in patients with chronic liver disease (CLD). However, little is known about the relationship between serum copeptin and the prognosis of patients with CLD. In this systematic review and meta-analysis, evidence from ten datasets including 3133 patients were integrated. The results showed that a high level of serum copeptin was associated with a poor transplant-free survival in these patients. These findings support the use of serum copeptin as a prognostic biomarker for patients with CLD.

Citation: Tan HQ, Zhao M, Huang Z, Liu Y, Li H, Ma LH, Liu JY. Circulating copeptin level and the clinical prognosis of patients with chronic liver disease. *World J Gastroenterol* 2023; 29(31): 4797-4808
URL: https://www.wjgnet.com/1007-9327/full/v29/i31/4797.htm
DOI: https://dx.doi.org/10.3748/wjg.v29.i31.4797

INTRODUCTION

Chronic liver disease (CLD) patients are more likely to develop complications associated with the progression of the disease, such as portal hypertension, ascites, spontaneous bacterial peritonitis, gastroesophageal varices, and hepatic encephalopathy[1,2]. For those with advanced CLD (ACLD), the clinical prognosis is generally poor, which has become a substantial cause of morbidity and mortality worldwide[3,4]. Accumulating evidence suggests that patients with ACLD may have multiple features of circulatory dysfunction, such as incremental intrahepatic vascular resistance, decrease of portal blood flow, and a reduced systemic vascular resistance[5,6], all of which could subsequently activate the neurohormonal system for counter regulation, including the upregulated systemic arginine vasopressin (AVP)[7,8]. As a biomarker of disease progression, the AVP increment in patients with CLD has been hypothesized as a predictor of poor prognosis[9]. However, as a small peptide of nine amino acids, the blood level of AVP is difficult to quantitatively analyze due to its short half-life[10]. Copeptin is a 39-amino-acid glycopeptide which contains the C-terminus of AVP precursor, making it an effective surrogate marker for AVP release[11,12]. As a result of osmotic stress and osmotic stimulation, a high level of copeptin has been demonstrated in patients with ACLD[13,14]. However, it remains unknown whether the serum level of copeptin may predict the prognosis of patients with CLD. Therefore, in this study, we conducted a systematic review and meta-analysis to investigate the potential association between serum copeptin and clinical outcomes in this patient population.

MATERIALS AND METHODS

Throughout the process of planning, conducting, and reporting the study, the Preferred Reporting Items for Systematic Reviews and Meta-Analyses statement[15,16] and Cochrane Handbook[17] were followed.

Search of databases

We searched electronic databases including PubMed, Embase, the Cochrane Library, and Web of Science, starting from inception and ending April 21st, 2023, for studies that had been published up to that date. The search was performed with terms related to our study including: (1) "Copeptin" OR "C-terminal provasopressin"; and (2) "cirrhosis" OR "cirrhotic" OR "liver" OR "hepatic" OR "hepatitis". There was no limitation on the language of the publication in the search for human studies. As part of our manual screening process, references from relevant original and review articles were screened for possible relevant studies.

Inclusion and exclusion criteria of studies

Inclusion criteria were developed in accordance with PICOS recommendations and according to the aim of the meta-analysis.

P (patients): Adult patients (18 years or older) with a confirmed diagnosis of CLD; I (exposure): Patients with a high serum concentration of copeptin at baseline. Methods for measuring serum copeptin and cutoffs for defining high serum copeptin were consistent with those of the original studies; C (control): Patients with a low serum concentration of

copeptin at baseline; O (outcomes): Incidence of transplant-free survival (TFS) compared between CLD patients with high *vs* low serum levels of copeptin at baseline. S (study design): Studies with longitudinal follow-up, including cohort and case-control studies, as well as post-hoc analyses of clinical trials.

Excluded from the meta-analysis were reviews, editorials, preclinical studies, and studies that did not involve patients with CLD, failed to measure serum copeptin, or did not report the relevant outcome. In instances where there was a patient population overlap, the study with the greatest sample size was incorporated into the meta-analysis.

Data extraction and quality evaluation

Two of the authors conducted literature searches, data collection, and assessments of study quality independently. In instances where discrepancies arose, a third author was consulted for discussion, and a consensus was reached. The analysis of studies included the collection of information pertaining to study information, design characteristics, patient diagnosis, demographic factors, measuring methods, serum copeptin cutoffs, follow-up durations, and adjusted variables for the evaluation of the association between serum copeptin levels and TFS in patients with CLD. In terms of quality, the study was scored using the Newcastle-Ottawa Scale[18] based on the criteria for participant selection, the comparability of the groups, and the validity of the outcomes. There were nine stars on the scale, with a larger number of stars representing a higher quality study.

Statistics

Risk ratios (RRs) and corresponding 95% confidence interval (CI) were used as the variables to indicate the association between serum concentration of copeptin and the survival of patients with CLD. A logarithmical transformation was performed on the RR and its corresponding standard error from each study to stabilize and normalize its variance[19]. In order to estimate between-study heterogeneity, the Cochrane Q test and the I^2 statistic[20] were used. An $I^2 > 50\%$ indicates that there is significant heterogeneity between studies. The utilization of a random-effects model was employed to amalgamate the findings, as it has been acknowledged to encompass the impact of potential heterogeneity[17]. In order to assess the impact of individual studies on the meta-analysis outcomes, sensitivity analyses were conducted by eliminating one dataset at a time[21]. To ascertain the effect of study characteristics on the outcome, subgroup analyses were executed based on the study country, design, patient diagnosis, cutoffs of copeptin, follow-up duration, and study quality scores. The subgroups were defined based on the medians of continuous variables. A funnel plot was used to estimate publication bias based on visual judgments of symmetry, along with Egger's regression asymmetry test[22]. The statistical analyses were carried out with RevMan (Version 5.1; Cochrane Collaboration, Oxford, United Kingdom) and Stata software (version 12.0; Stata Corporation, College Station, TX, United States).

RESULTS

Database search and study retrieval

Figure 1 shows the process of the literature search and study retrieval. Initially, 253 records were obtained from the database, and 77 duplicate entries were removed. After screening the titles and abstracts, a further 159 studies were removed as they did not fit the meta-analysis' objectives. Following full-text reviews of 17 studies, eight were excluded because of the reasons listed in Figure 1. Accordingly, 9 studies were obtained for subsequent meta-analysis[23-31].

Study characteristics

One of the studies reported two datasets from two cohort studies[26], and these datasets were independently incorporated into the meta-analysis. Overall, ten datasets from nine cohort studies[23-31], which included 3133 patients with CLD, were used for the meta-analysis. The characteristics of the included studies are summarized in Table 1. These studies were published between 2013 and 2021, and performed in European and Asian countries. As for the study design, four cohorts were prospective[23,25,26,29], and six were retrospective[24,26-28,30,31]. Patients with cirrhosis were included in six cohorts of the included studies[23-27], while patients with various CLD were included in the other four cohorts[28-31]. The mean ages of the patients were 49.0 years to 67.3 years, and the proportions of men were 58.2% to 83.4%. Serum copeptin was measured with the Kryptor immunoassay in eight cohorts[23-28,30], while other methods such as enzyme-linked immunosorbent assay and the automated copeptin immunofluorescent assay were used in the other two studies[29,31]. A high serum level of copeptin was defined according to receiver operating characteristic analysis in four cohorts[24,25,27,31], medians in three cohorts[26,29], tertiles in two cohorts[23,28], and the upper limit of normal level in one cohort[30]. The follow-up durations were 1 mo to 48 mo (mean: 12.5 mo). Multivariate regression analyses were applied in all of the included studies when the association between serum copeptin and TFS of patients with CLD were estimated, and factors including age, sex, and scores for hepatic dysfunction were adjusted, such as the Child-Pugh score, the Model for End-Stage Liver Disease score, and the albumin-bilirubin score. Among the included studies, all had quality scores between seven and nine stars, indicating that they were of good quality (Table 2).

Meta-analysis results

Overall, pooled results of ten datasets from nine cohort studies showed that a high level of serum copeptin at baseline was associated with a poor TFS (RR: 1.82, 95%CI: 1.52-2.19, $P < 0.001$; Figure 2) with no evidence of significant heterogeneity (P for Cochrane Q test = 0.54, $I^2 = 0\%$). In addition, sensitivity analysis by omitting one dataset at a time showed consistent results (RR: 1.73-2.00, $P < 0.05$). Finally, subgroup analyses showed that the association between serum

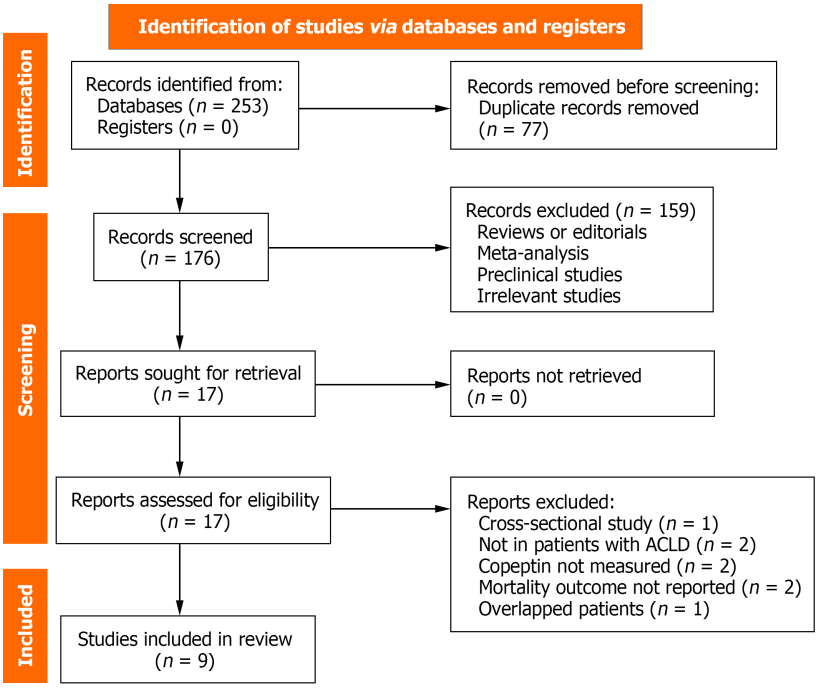

DOI: 10.3748/wjg.v29.i31.4797

Figure 1 Flowchart of database search and study inclusion. ACLD: Advanced chronic liver diseases.

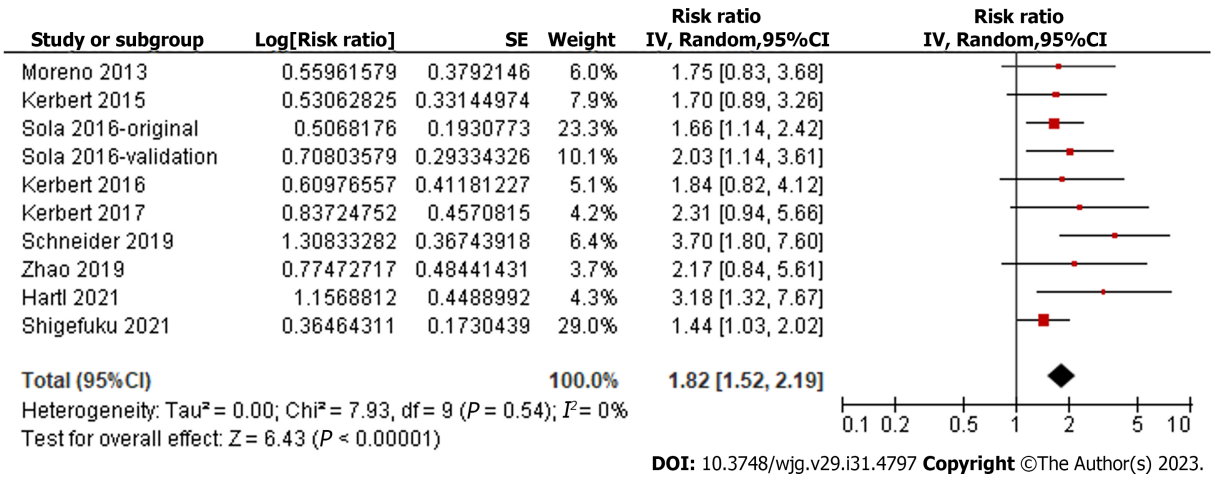

DOI: 10.3748/wjg.v29.i31.4797

Figure 2 Forest plots for the overall meta-analyses regarding the association between serum copeptin and transplant-free survival of patients with chronic liver diseases. 95%CI: 95% confidence interval.

copeptin and poor TFS was consistent between European and Asian studies (*P* for subgroup difference = 0.16, Figure 3A), between prospective and retrospective cohorts (*P* for subgroup difference = 0.48, Figure 3B), between studies of patients with cirrhosis and all CLD (*P* for subgroup difference = 0.42, Figure 4A), between studies with cutoffs for copeptin < and ≥ 15 pmol/L (P for subgroup difference = 0.17, Figure 4B), between studies with mean follow-up durations < and ≥ 1 year (*P* for subgroup difference = 0.29, Figure 5A), and between studies with different quality scores (*P* for subgroup difference = 0.14, Figure 5B).

Publication bias

The funnel plots for the meta-analysis of the association between copeptin and TFS in patients with CLD are shown in Figure 6. Based on visual examination, the plots are symmetrical, suggesting that publication bias is low. Additionally, Egger's regression tests indicated a low likelihood of publication bias (*P* = 0.47).

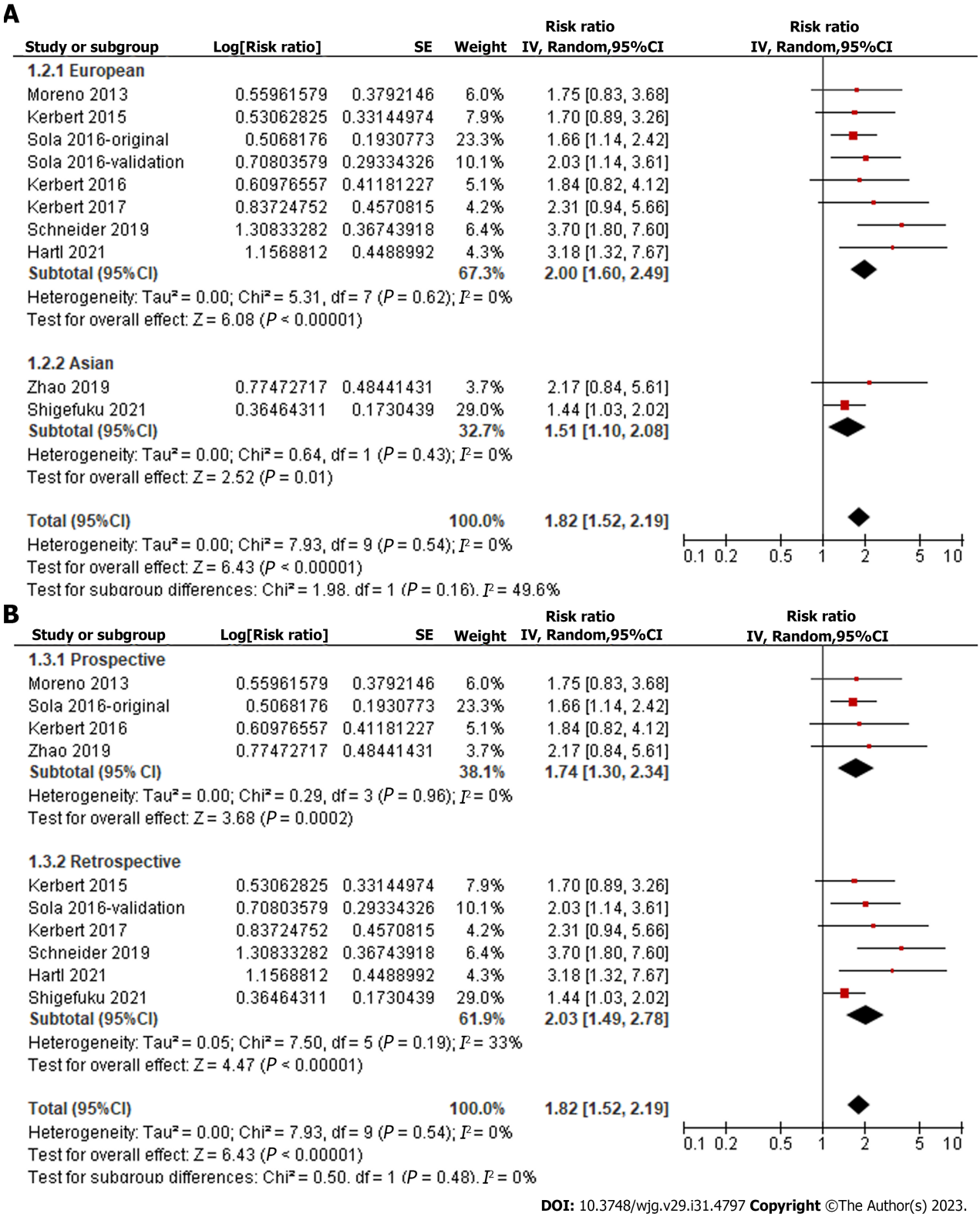

DOI: 10.3748/wjg.v29.i31.4797

Figure 3 Forest plots for the subgroup analyses regarding the association between serum copeptin and transplant-free survival of patients with chronic liver diseases. A: subgroup analysis according to study country; B: Subgroup analysis according to study design. 95%CI: 95% confidence interval.

DISCUSSION

This systematic review and meta-analysis synthesized data from ten cohort studies to investigate the association between serum copeptin concentration and poor TFS in patients with CLD. Our findings indicate that patients with a high serum copeptin level at baseline are at a greater risk of experiencing poor TFS during follow-up, compared to those with a low serum copeptin concentration. The robustness of our results was confirmed through sensitivity analyses that excluded

Table 1 Characteristics of the included studies

Ref.	Country	Design	Diagnosis	Patient number	Mean age (yr)	Male (%)	CP class C (%)	Methods for copeptin measuring	Copeptin analysis	Median follow-up duration (mo)	Variables adjusted
Moreno *et al*[23], 2013	France	PC	Cirrhosis (alcohol 84.2%)	125	58	69	33.7	Kryptor immunoassay	13 pmol/L, T3:T1-2	11	Age, sex, CP Class, and CRP
Kerbert *et al*[24], 2015	The Netherlands	RC	Cirrhosis (alcohol 34.4%, viral 18%)	61	54	75.4	31.1	Kryptor immunoassay	21.9 pmol/L, ROC analysis	12	Age, sex, and MELD score
Sola 2016-original	Spain	PC	Cirrhosis (alcohol 43%, HCV 34%)	265	60	66	NR	Kryptor immunoassay	14 pmol/L, median	3	Age, sex, MELD score, and leukocyte count
Sola 2016-validation	Multiple European countries	RC	Cirrhosis (alcohol 51%, HCV 19%)	120	57	72	NR	Kryptor immunoassay	19 pmol/L, median	3	Age, sex, and MELD score
Kerbert *et al*[25], 2016	The Netherlands and France	PC	Cirrhosis (alcohol 70.1%, viral 11.4%)	184	55.7	70.7	21.2	Kryptor immunoassay	12.3 pmol/L, ROC analysis	12	Age, sex, CP class, and CRP
Kerbert *et al*[27], 2017	Multiple European countries	RC	Acute decompensated cirrhosis (alcohol 61%, HCV 31.9%, and HBV 5.7%)	779	58	65.7	NR	Kryptor immunoassay	13.6 pmol/L, ROC analysis	3	Age, sex, WBC, sodium, and MELD score
Schneider *et al*[28], 2019	Germany	RC	End-stage liver disease (alcohol 63.4%, viral 8.5%)	615	57.2	61.9	NR	Kryptor immunoassay	16.3 pmol/L, T3:T1-2	9.3	Age, sex, and MELD-Na score
Zhao *et al* [29], 2019	China	PC	HBV related ACLF	151	49	83.4	NR	ELISA	18.7 pmol/L, median	1	Age, sex, and MELD score
Hartl *et al* [30], 2021	Austria	RC	ACLD (alcohol 36.2%, viral 35.9%)	663	56.6	68.2	16.5	Kryptor immunoassay	11.4 pmol/L, ULN	26.2	Age, sex, MELD score, HVPG, albumin, sodium, and presence of HCC
Shigefuku *et al*[36], 2021	Japan	RC	CLD (alcohol 45.9%, viral 57.0%), cirrhosis 66.5%	170	67.3	58.2	NR	Automated copeptin immuno-fluorescent assay	4.8 pmol/L, ROC analysis	48	Age, sex, eGFR, ALBI score, and presence of HCC

CP: Child-Pugh; PC: Prospective cohort; RC: Retrospective cohort; HBV: Hepatitis B virus; HCV: Hepatitis C virus; ACLF: Acute-on-chronic liver failure; ACLD: Advanced chronic liver diseases; CLD: Chronic liver diseases; NR: Not Reported; ELISA: Enzyme-linked immunosorbent assay; T: Tertile; ROC: Receiver operating characteristic; ULN: Upper limit of normal; CRP: C-reactive protein; MELD: Model for end-stage liver disease; WBC: White blood cell; HVPG: Hepatic venous pressure gradient; HCC: Hepatocellular carcinoma; ALBI: Albumin-bilirubin; eGFR: Estimated glomerular infiltrating rate.

individual datasets and subgroup analyses based on various study characteristics, including country, design, patient diagnosis, copeptin cutoffs, follow-up duration, and study quality scores. These findings demonstrate that a high serum copeptin level may be a useful index which is associated with poor prognosis for patients with CLD.

To the best of our knowledge, this is the first meta-analysis investigating the potential role of serum copeptin concentration as a prognostic factor of patients with CLD. Several advantages in meta-analysis methodologies deserve to be noticed. For example, we performed a comprehensive literature search in four commonly used databases, which could provide current evidence regarding the relationship of serum copeptin and TFS of patients with CLD. Furthermore, it is noteworthy that all of the studies incorporated in this analysis were cohort studies, implying a potential longitudinal correlation between elevated serum copeptin levels and diminished transplant-free survival among individuals with

Table 2 Quality evaluation of the included studies *via* the Newcastle-Ottawa scale

Ref.	Representativeness of the exposed cohort	Selection of the non-exposed cohort	Ascertainment of exposure	Outcome not present at baseline	Control for age and sex	Control for other confounding factors	Assessment of outcome	Suitable follow-up duration	Adequacy of follow-up of cohorts	Total
Moreno *et al*[23], 2013	1	1	1	1	1	1	1	0	1	8
Kerbert *et al*[24], 2015	0	1	1	1	1	1	1	1	1	8
Sola 2016-original	1	1	1	1	1	1	1	0	1	8
Sola 2016-validation	0	1	1	1	1	1	1	0	1	7
Kerbert *et al*[25], 2016	1	1	1	1	1	1	1	1	1	9
Kerbert *et al*[27], 2017	0	1	1	1	1	1	1	0	1	7
Schneider *et al*[28], 2019	0	1	1	1	1	1	1	0	1	7
Zhao *et al* [29], 2019	1	1	1	1	1	1	1	0	1	8
Hartl *et al* [30], 2021	0	1	1	1	1	1	1	1	1	8
Shigefuku *et al*[36], 2021	1	1	1	1	1	1	1	1	1	9

CLD. Additionally, the utilization of multivariate regression analysis in all of the studies included in this review indicates that the relationship between heightened serum copeptin levels and reduced TFS in this population may be autonomous of potential confounding factors, such as age, gender, and hepatic dysfunction scores. Ultimately, multiple sensitivity and subgroup analyses were executed, and the uniform outcomes reinforced the durability and stability of the conclusions. Collectively, these conclusions substantiate that elevated serum levels of copeptin in individuals with CLD may serve as an indicator of unfavorable prognosis.

There may be multiple mechanisms underlying the relationship between a high serum copeptin level and a poor survival outcome in patients with CLD. Previous studies have shown that a high copeptin level in patients with cirrhosis was correlated to the risk of various complications that may lead to a poor prognosis of these patients, such as gastrointestinal hemorrhage due to portal hypertension, hepatorenal syndrome, hepatic encephalopathy, and larger amounts of ascites[32,33]. Pathophysiologically, as a surrogate marker of AVP, increased copeptin may reflect the enhanced systemic release of AVP in these patients[34]. A high AVP in patients with cirrhosis may deteriorate the status of vasoconstriction, water retention, and hyponatremia, which have all been recognized as key risk factors for poor survival of these patients[35]. The role of copeptin in the pathogenesis and progression of CLD should be further investigated, either as a simple biomarker or an active participant in the disease.

This study is subject to certain limitations. Firstly, the meta-analysis results were predominantly influenced by studies involving patients with ACLD, including those with decompensated cirrhosis and other end-stage liver diseases. The efficacy of copeptin as a prognostic factor in patients with early CLD requires further validation in future research. Additionally, despite the utilization of multivariate regression analyses across all the studies included, the potential for residual factors to confound the association between copeptin and TFS cannot be entirely ruled out. For example, serum copeptin may predict the response to tolvaptan in patients with decompensated cirrhosis[36]. Accordingly, use of treatments such as tolvaptan may confound the association between copeptin and TFS. Furthermore, the determination of an optimal serum copeptin cutoff for predicting the survival of patients with CLD remains elusive, necessitating further investigation. Moreover, the absence of a causal association between elevated copeptin levels and unfavorable TFS in CLD patients is attributable to the reliance on observational studies in the meta-analysis.

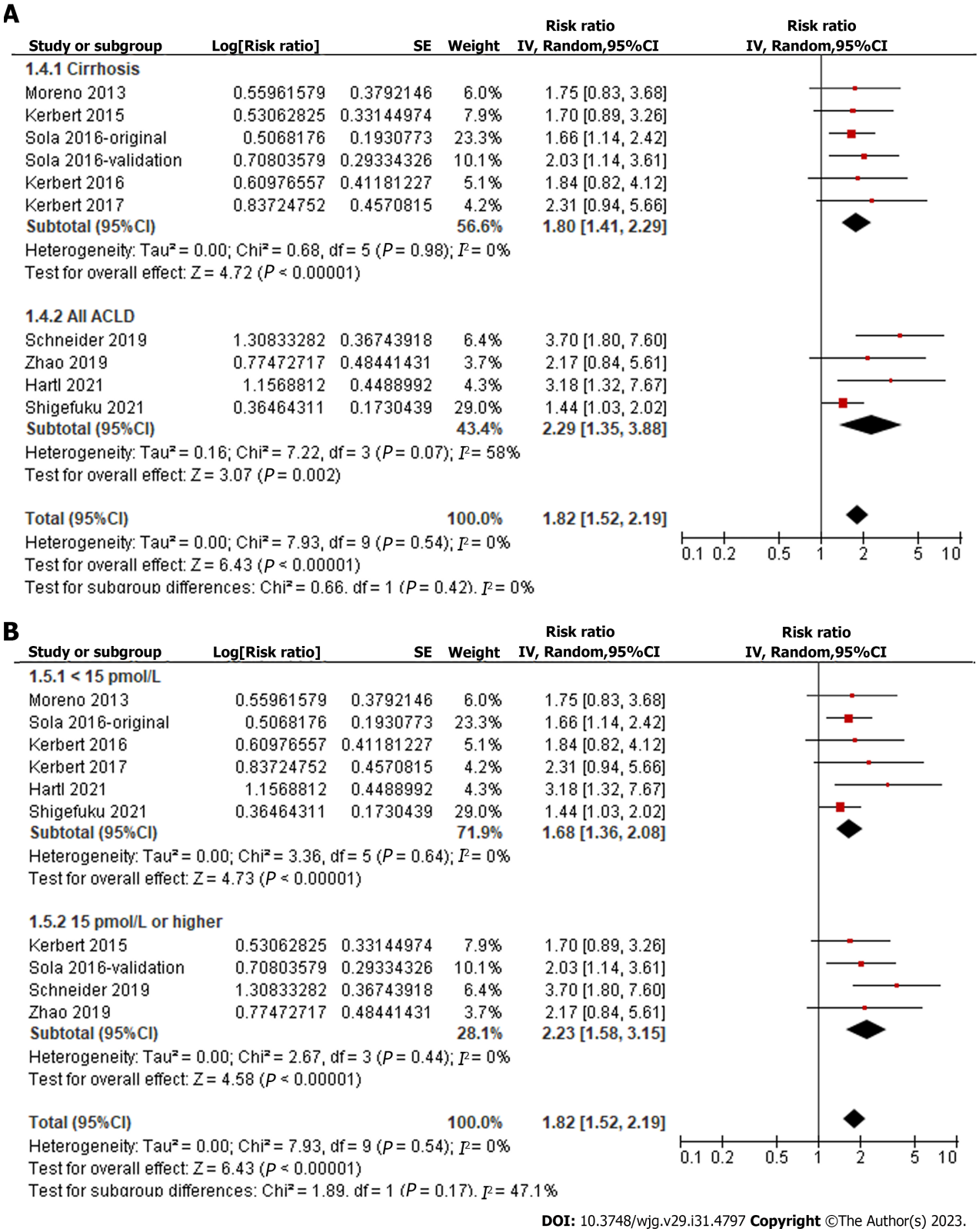

DOI: 10.3748/wjg.v29.i31.4797

Figure 4 Forest plots for the subgroup analyses regarding the association between serum copeptin and transplant-free survival of patients with chronic liver diseases. A: Subgroup analysis according to the diagnosis of the patients; B: Subgroup analysis according to the cutoffs of serum copeptin. 95%CI: 95% confidence interval.

CONCLUSION

The findings of the meta-analysis indicate that an elevated serum copeptin concentration in individuals with CLD is linked to unfavorable TFS. The assessment of serum copeptin levels may hold significance in the stratification of risk among CLD patients. Furthermore, it is imperative to investigate whether the reduction of copeptin levels in these patients is correlated with a better clinical outcome, particularly in those with ACLD.

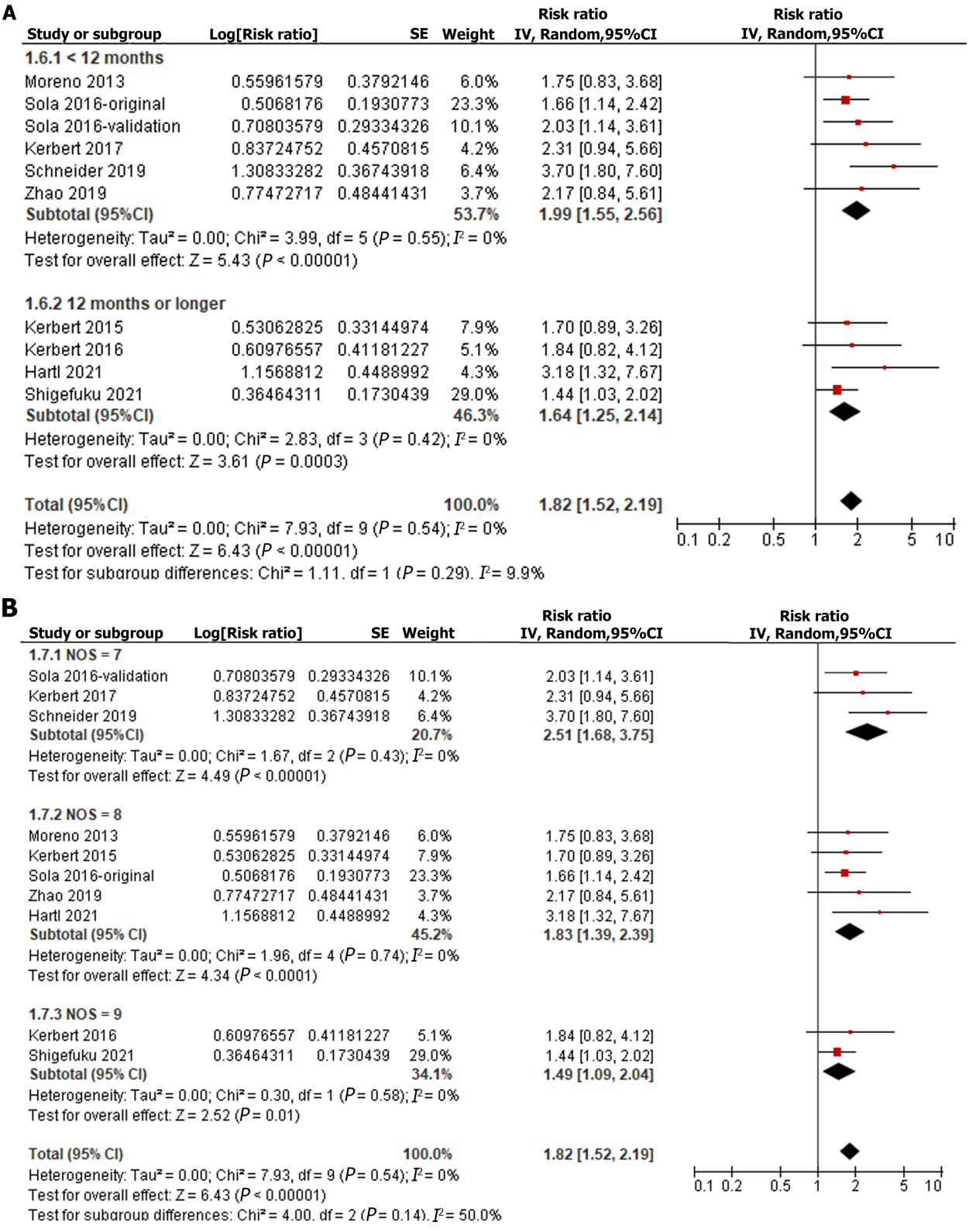

DOI: 10.3748/wjg.v29.i31.4797

Figure 5 Forest plots for the subgroup analyses regarding the association between serum copeptin and transplant-free survival of patients with chronic liver diseases. A: Subgroup analysis according to the follow-up durations; B: Subgroup analysis according to the study quality scores. 95%CI: 95% confidence interval.

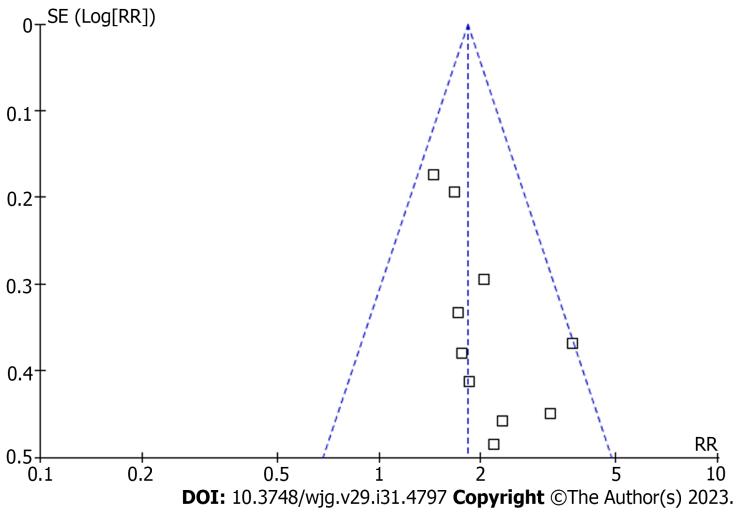

Figure 6 Funnel plots for the publication bias underlying the meta-analysis regarding the association between serum copeptin and transplant-free survival of patients with chronic liver diseases. RR: Risk ratio.

ARTICLE HIGHLIGHTS

Research background

Patients with chronic liver disease (CLD) will develop various complications with the progression of the disease. Upregulated systemic arginine vasopressin (AVP) has been observed in patients with advanced CLD. However, measuring AVP is clinically challenging due to the short half-life. Copeptin is a C-terminus of AVP precursor, which may be of importance for prognostic prediction in patients with CLD.

Research motivation

Identifying biomarkers that predict the prognosis of patients with CLD is clinically important. Although there are pilot studies aiming to correlate copeptin with survival of patients with CLD, the results are not always consistent. In this regard, a systematic review with meta-analysis is particularly useful.

Research objectives

To investigate the correlation between serum copeptin and transplant-free survival (TFS) in patients with CLD with a systematic review and meta-analysis.

Research methods

Studies were obtained by search of PubMed, Embase, the Cochrane Library, and Web of Science. Two authors independently screened the studies, assessed the study quality with Newcastle-Ottawa Scale, and extracted the data. Risk ratios and corresponding 95% confidence intervals were used as the variables to indicate the association between serum concentration of copeptin and the survival of patients with CLD. The RevMan and Stata software were used for the statistical analyses.

Research results

This meta-analysis enrolled ten datasets involving 3133 patients, who were followed for 1 to 48 mo (mean: 12.5 mo). We found that a high level of serum copeptin was associated with a poor TFS, with a risk ratio of 1.82. Additionally, sensitivity analysis retrieved similar results by omitting one dataset at a time. The robustness of the finding was further evidenced by consistent results of subgroup analyses according to study country, study design, patient diagnosis, cutoff of copeptin, follow-up duration, and study quality score.

Research conclusions

High serum concentration of copeptin may be associated with a poor clinical prognosis in patients with CLD. These findings were not significantly affected by either of the included studies and were not influenced by multiple study characteristics within the subgroup analysis.

Research perspectives

In view of the standard methods for the measuring copeptin in clinical practice, as well as the finding of the meta-analysis, evaluating serum copeptin may be considered at the initial management of patients with CLD, which may provide prognostic significance.

FOOTNOTES

Author contributions: Tan HQ and Liu JY conceived and designed the study; Tan HQ, Zhao M, Huang Z, and Liu Y performed database search, data collection, and study quality evaluation; Tan HQ, Li H, and Ma LH performed statistical analysis; Tan HQ, Zhao M, Huang Z, and Liu JY interpreted the results; Tan HQ wrote the initial draft; all authors revised the manuscript, read and approved the final version of the manuscript.

Conflict-of-interest statement: The authors have no conflicts of interest to declare.

PRISMA 2009 Checklist statement: The authors have read the PRISMA 2009 Checklist, and the manuscript was prepared and revised according to the PRISMA 2009 Checklist.

Country/Territory of origin: China

ORCID number: Hao-Qian Tan 0000-0001-5349-0507; Ming Zhao 0009-0005-8792-0612; Zan Huang 0009-0000-6942-212X; Yang Liu 0009-0003-8587-2800; Han Li 0009-0001-6171-8783; Long-Hui Ma 0009-0003-4569-2346; Jun-Ying Liu 0009-0002-8058-6197.

S-Editor: Chen YL
L-Editor: A
P-Editor: Cai YX

REFERENCES

1 **Br VK**, Sarin SK. Acute-on-chronic liver failure: Terminology, mechanisms and management. *Clin Mol Hepatol* 2023; **29**: 670-689 [PMID: 36938601 DOI: 10.3350/cmh.2022.0103]
2 **Huang DQ**, Terrault NA, Tacke F, Gluud LL, Arrese M, Bugianesi E, Loomba R. Global epidemiology of cirrhosis - aetiology, trends and predictions. *Nat Rev Gastroenterol Hepatol* 2023; **20**: 388-398 [PMID: 36977794 DOI: 10.1038/s41575-023-00759-2]
3 **Moon AM**, Singal AG, Tapper EB. Contemporary Epidemiology of Chronic Liver Disease and Cirrhosis. *Clin Gastroenterol Hepatol* 2020; **18**: 2650-2666 [PMID: 31401364 DOI: 10.1016/j.cgh.2019.07.060]
4 **Younossi ZM**, Wong G, Anstee QM, Henry L. The Global Burden of Liver Disease. *Clin Gastroenterol Hepatol* 2023; **21**: 1978-1991 [PMID: 37121527 DOI: 10.1016/j.cgh.2023.04.015]
5 **Engelmann C**, Clària J, Szabo G, Bosch J, Bernardi M. Pathophysiology of decompensated cirrhosis: Portal hypertension, circulatory dysfunction, inflammation, metabolism and mitochondrial dysfunction. *J Hepatol* 2021; **75** Suppl 1: S49-S66 [PMID: 34039492 DOI: 10.1016/j.jhep.2021.01.002]
6 **Møller S**, Bendtsen F. The pathophysiology of arterial vasodilatation and hyperdynamic circulation in cirrhosis. *Liver Int* 2018; **38**: 570-580 [PMID: 28921803 DOI: 10.1111/liv.13589]
7 **Tapper EB**, Parikh ND. Diagnosis and Management of Cirrhosis and Its Complications: A Review. *JAMA* 2023; **329**: 1589-1602 [PMID: 37159031 DOI: 10.1001/jama.2023.5997]
8 **Wagener G**, Bakker J. Vasopressin in cirrhosis and sepsis: physiology and clinical implications. *Minerva Anestesiol* 2015; **81**: 1377-1383 [PMID: 25384691]
9 **Rondon-Berrios H**, Velez JCQ. Hyponatremia in Cirrhosis. *Clin Liver Dis* 2022; **26**: 149-164 [PMID: 35487602 DOI: 10.1016/j.cld.2022.01.001]
10 **Leng G**, Sabatier N. Measuring Oxytocin and Vasopressin: Bioassays, Immunoassays and Random Numbers. *J Neuroendocrinol* 2016; **28** [PMID: 27467712 DOI: 10.1111/jne.12413]
11 **Bankir L**, Bichet DG, Morgenthaler NG. Vasopressin: physiology, assessment and osmosensation. *J Intern Med* 2017; **282**: 284-297 [PMID: 28649750 DOI: 10.1111/joim.12645]
12 **Szmygin H**, Szydełko J, Matyjaszek-Matuszek B. Copeptin as a novel biomarker of cardiometabolic syndrome. *Endokrynol Pol* 2021; **72**: 566-571 [PMID: 34378786 DOI: 10.5603/EP.a2021.0072]
13 **Di Martino V**, Weil D, Cervoni JP, Thevenot T. New prognostic markers in liver cirrhosis. *World J Hepatol* 2015; **7**: 1244-1250 [PMID: 26019739 DOI: 10.4254/wjh.v7.i9.1244]
14 **Mookerjee RP**. Prognosis and Biomarkers in Acute-on-Chronic Liver Failure. *Semin Liver Dis* 2016; **36**: 127-132 [PMID: 27172354 DOI: 10.1055/s-0036-1583200]
15 **Page MJ**, Moher D, Bossuyt PM, Boutron I, Hoffmann TC, Mulrow CD, Shamseer L, Tetzlaff JM, Akl EA, Brennan SE, Chou R, Glanville J, Grimshaw JM, Hróbjartsson A, Lalu MM, Li T, Loder EW, Mayo-Wilson E, McDonald S, McGuinness LA, Stewart LA, Thomas J, Tricco AC, Welch VA, Whiting P, McKenzie JE. PRISMA 2020 explanation and elaboration: updated guidance and exemplars for reporting systematic reviews. *BMJ* 2021; **372**: n160 [PMID: 33781993 DOI: 10.1136/bmj.n160]
16 **Page MJ**, McKenzie JE, Bossuyt PM, Boutron I, Hoffmann TC, Mulrow CD, Shamseer L, Tetzlaff JM, Akl EA, Brennan SE, Chou R, Glanville J, Grimshaw JM, Hróbjartsson A, Lalu MM, Li T, Loder EW, Mayo-Wilson E, McDonald S, McGuinness LA, Stewart LA, Thomas J, Tricco AC, Welch VA, Whiting P, Moher D. The PRISMA 2020 statement: an updated guideline for reporting systematic reviews. *BMJ* 2021; **372**: n71 [PMID: 33782057 DOI: 10.1136/bmj.n71]
17 **Higgins J**, Thomas J, Chandler J, Cumpston M, Li T, Page M, Welch V. Cochrane Handbook for Systematic Reviews of Interventions version 6.2. 2021. [cited 5 July 2023]. Available from: https://training.cochrane.org/handbook

18 **Wells GA**, Shea B, O'Connell D, Peterson J, Welch V, Losos M, Tugwell P. The Newcastle-Ottawa Scale (NOS) for assessing the quality of nonrandomised studies in meta-analyses. 2010. [cited 5 July 2023]. Available from: https://www.semanticscholar.org/paper/The-Newcastle-Ottawa-Scale-(NOS)-for-Assessing-the-Wells-Wells/c293fb316b6176154c3fdbb8340a107d9c8c82bf

19 **Higgins J**, Green S. Cochrane Handbook for Systematic Reviews of Interventions Version 5.1.0. 2011. [cited 5 July 2023]. Available from: http://handbook-5-1.cochrane.org/

20 **Higgins JP**, Thompson SG. Quantifying heterogeneity in a meta-analysis. *Stat Med* 2002; **21**: 1539-1558 [PMID: 12111919 DOI: 10.1002/sim.1186]

21 **Patsopoulos NA**, Evangelou E, Ioannidis JP. Sensitivity of between-study heterogeneity in meta-analysis: proposed metrics and empirical evaluation. *Int J Epidemiol* 2008; **37**: 1148-1157 [PMID: 18424475 DOI: 10.1093/ije/dyn065]

22 **Egger M**, Davey Smith G, Schneider M, Minder C. Bias in meta-analysis detected by a simple, graphical test. *BMJ* 1997; **315**: 629-634 [PMID: 9310563]

23 **Moreno JP**, Grandclement E, Monnet E, Clerc B, Agin A, Cervoni JP, Richou C, Vanlemmens C, Dritsas S, Dumoulin G, Di Martino V, Thevenot T. Plasma copeptin, a possible prognostic marker in cirrhosis. *Liver Int* 2013; **33**: 843-851 [PMID: 23560938 DOI: 10.1111/liv.12175]

24 **Kerbert AJ**, Verbeke L, Chiang FW, Laleman W, van der Reijden JJ, van Duijn W, Nevens F, Wolterbeek R, van Hoek B, Verspaget HW, Coenraad MJ. Copeptin as an Indicator of Hemodynamic Derangement and Prognosis in Liver Cirrhosis. *PLoS One* 2015; **10**: e0138264 [PMID: 26378453 DOI: 10.1371/journal.pone.0138264]

25 **Kerbert AJ**, Weil D, Verspaget HW, Moréno JP, van Hoek B, Cervoni JP, Di Martino V, Coenraad MJ, Thevenot T. Copeptin is an independent prognostic factor for transplant-free survival in cirrhosis. *Liver Int* 2016; **36**: 530-537 [PMID: 26502363 DOI: 10.1111/liv.12992]

26 **Solà E**, Kerbert AJ, Verspaget HW, Moreira R, Pose E, Ruiz P, Cela R, Morales-Ruiz M, López E, Graupera I, Solé C, Huelin P, Navarro AA, Ariza X, Jalan R, Fabrellas N, Benten D, de Prada G, Durand F, Jimenez W, van der Reijden JJ, Fernandez J, van Hoek B, Coenraad MJ, Ginès P. Plasma copeptin as biomarker of disease progression and prognosis in cirrhosis. *J Hepatol* 2016; **65**: 914-920 [PMID: 27422752 DOI: 10.1016/j.jhep.2016.07.003]

27 **Kerbert AJC**, Verspaget HW, Navarro ÀA, Jalan R, Solà E, Benten D, Durand F, Ginès P, van der Reijden JJ, van Hoek B, Coenraad MJ; CANONIC Study Investigators of the EASL-CLIF Consortium. Copeptin in acute decompensation of liver cirrhosis: relationship with acute-on-chronic liver failure and short-term survival. *Crit Care* 2017; **21**: 321 [PMID: 29268760 DOI: 10.1186/s13054-017-1894-8]

28 **Schneider C**, Remmler J, Netto J, Seehofer D, Engelmann C, Berg T, Thiery J, Kaiser T. Copeptin - a biomarker of short-term mortality risk (7 days) in patients with end-stage liver disease. *Clin Chem Lab Med* 2019; **57**: 1897-1905 [PMID: 31199758 DOI: 10.1515/cclm-2019-0023]

29 **Zhao R**, Wu W, Zhou Z, Zheng X, Sun W, Shi Y, Yu H, Wang F, Zhao H, Sun S, Jin L, Sheng J. Prognostic utility of novel biomarkers in acute-on-chronic liver failure (ACLF) associated with hepatitis B: A multicenter prospective study. *Hepatol Res* 2019; **49**: 42-50 [PMID: 30246902 DOI: 10.1111/hepr.13251]

30 **Hartl L**, Jachs M, Desbalmes C, Schaufler D, Simbrunner B, Paternostro R, Schwabl P, Bauer DJM, Semmler G, Scheiner B, Bucsics T, Eigenbauer E, Marculescu R, Szekeres T, Peck-Radosavljevic M, Kastl S, Trauner M, Mandorfer M, Reiberger T. The differential activation of cardiovascular hormones across distinct stages of portal hypertension predicts clinical outcomes. *Hepatol Int* 2021; **15**: 1160-1173 [PMID: 34021479 DOI: 10.1007/s12072-021-10203-9]

31 **Shigefuku R**, Iwasa M, Eguchi A, Tamai Y, Yoshikawa K, Sugimoto R, Takei Y. Serum copeptin level is a biomarker associated with ascites retention and the formation of a portosystemic shunt in chronic liver disease. *J Gastroenterol Hepatol* 2021; **36**: 1006-1014 [PMID: 32790956 DOI: 10.1111/jgh.15215]

32 **Tawfik AK**, Helmy A, Yousef M, Abou-Saif S, Kobtan A, Asaad E, Abd-Elsalam S. Copeptin as a novel marker predicting prognosis of liver cirrhosis and its major complications. *Hepat Med* 2018; **10**: 87-93 [PMID: 30214326 DOI: 10.2147/HMER.S174267]

33 **Abudeif A**, Hashim MS, Ahmed NM, Ahmed AO. Serum copeptin is associated with major complications of liver cirrhosis and spontaneous bacterial peritonitis. *Clin Exp Hepatol* 2023; **9**: 71-78 [PMID: 37064833 DOI: 10.5114/ceh.2023.125970]

34 **Glavaš M**, Gitlin-Domagalska A, Dębowski D, Ptaszyńska N, Łęgowska A, Rolka K. Vasopressin and Its Analogues: From Natural Hormones to Multitasking Peptides. *Int J Mol Sci* 2022; **23** [PMID: 35328489 DOI: 10.3390/ijms23063068]

35 **Alukal JJ**, John S, Thuluvath PJ. Hyponatremia in Cirrhosis: An Update. *Am J Gastroenterol* 2020; **115**: 1775-1785 [PMID: 33156095 DOI: 10.14309/ajg.0000000000000786]

36 **Shigefuku R**, Iwasa M, Eguchi A, Tempaku M, Tamai Y, Suzuki T, Takei Y. Serum Copeptin and Zinc-α2-glycoprotein Levels Are Novel Biomarkers of Tolvaptan Treatment in Decompensated Cirrhotic Patients with Ascites. *Intern Med* 2021; **60**: 3359-3368 [PMID: 34719623 DOI: 10.2169/internalmedicine.7291-21]

World Journal of Gastroenterology

Submit a Manuscript: https://www.f6publishing.com

World J Gastroenterol 2023 August 21; 29(31): 4809-4814

DOI: 10.3748/wjg.v29.i31.4809

ISSN 1007-9327 (print) ISSN 2219-2840 (online)

CASE REPORT

Inherited CHEK2 p.H371Y mutation in solitary rectal ulcer syndrome among familial patients: A case report

Cheng-Cheng He, Shan-Ping Wang, Pei-Rong Zhou, Zhi-Jun Li, Na Li, Ming-Song Li

Specialty type: Gastroenterology and hepatology

Provenance and peer review: Unsolicited article; Externally peer reviewed.

Peer-review model: Single blind

Peer-review report's scientific quality classification

Grade A (Excellent): 0
Grade B (Very good): B
Grade C (Good): C, C
Grade D (Fair): 0
Grade E (Poor): 0

P-Reviewer: Choi YS, South Korea; Zamani M, Iran

Received: June 5, 2023
Peer-review started: June 5, 2023
First decision: July 7, 2023
Revised: July 18, 2023
Accepted: July 31, 2023
Article in press: July 31, 2023
Published online: August 21, 2023

Cheng-Cheng He, Shan-Ping Wang, Pei-Rong Zhou, Zhi-Jun Li, Na Li, Ming-Song Li, Department of Gastroenterology, The Third Affiliated Hospital of Guangzhou Medical University, Guangzhou 510150, Guangdong Province, China

Corresponding author: Ming-Song Li, MD, PhD, Chief Physician, Professor, Department of Gastroenterology, The Third Affiliated Hospital of Guangzhou Medical University, No. 63 Duobao Road, Liwan District, Guangzhou 510150, Guangdong Province, China.
2020683127@gzhmu.edu.cn

Abstract

BACKGROUND

Solitary rectal ulcer syndrome (SRUS) is a rare rectal disease with unknown etiology. Data on the genetic background in SRUS is lacking.

CASE SUMMARY

Here, we report the first case of SRUS in a mother-son relationship. Gene sequencing was conducted on the whole family, which revealed an inherited CHEK2 p.H371Y mutation. The experiment preliminarily revealed that the CHEK2 mutation did not affect the expression of CHEK2 protein, but affected the function of CHEK2, resulting in the expression level changes of downstream genes such as CDC25A.

CONCLUSION

SRUS is a genetic susceptibility disease where CHEK2 p.H371Y mutation may play a crucial role in the development and prognosis of SRUS.

Key Words: Solitary rectal ulcer syndrome; CHEK2 mutation; CDC25A; Genetic background; Gene sequencing; Case report

Core Tip: Solitary rectal ulcer syndrome (SRUS) is a rare rectal disease with unknown etiology. Data on the genetic background in SRUS is lacking. Here, we present the first case of SRUS in a mother-son relationship. Gene sequencing and experiment preliminarily indicate that SRUS may serve as a genetic susceptibility disease in which CHEK2 p.H371Y mutation may play a crucial role in the development and prognosis of SRUS. This case may offer some new insights into the virulence genes and genetic background of SRUS.

Citation: He CC, Wang SP, Zhou PR, Li ZJ, Li N, Li MS. Inherited CHEK2 p.H371Y mutation in solitary rectal ulcer syndrome among familial patients: A case report. *World J Gastroenterol* 2023; 29(31): 4809-4814
URL: https://www.wjgnet.com/1007-9327/full/v29/i31/4809.htm
DOI: https://dx.doi.org/10.3748/wjg.v29.i31.4809

INTRODUCTION

Solitary rectal ulcer syndrome (SRUS) is a chronic rectal disease characterized by difficulty in defecation, mucous hematochezia, and anal pain, and bulging. SRUS is a rare disease with unknown etiology that was proposed by Rutter in 1975[1]. We have a detailed understanding of the clinical, endoscopy, pathology and images characteristics based on recent reports about SRUS, but data about the etiology, especially the virulence genes and genetic background, are limited[2,3]. Herein, we present the first case that describes a Chinese female patient with SRUS and one of her sons diagnosed with SRUS. Her daughter and the other son demonstrated healthy gastrointestinal tracts. Next-generation sequencing of family inheritance results indicated an inherited CHEK2 p.H371Y mutation may contributes to SRUS.

CASE PRESENTATION

Chief complaints

A 63-year-old female patient was admitted to the Third Affiliated Hospital of Guangzhou Medical University for abdominal pain, anal irritation, and repeated hematochezia. Her 31-year-old son was previously diagnosed with SRUS and underwent an inpatient examination.

History of present illness

Her symptoms started 1 year before the presentation of abdominal pain, anal irritation, and repeated hematochezia. Additionally, her 31-year-old son started to present with repeated diarrhea and intermittent hematochezia at the age of 26. He suffered from chronic diarrhea of up to 30 times a day, with the worst demonstrating fecal incontinence. He was subsequently diagnosed with SRUS 3 years ago and underwent surgical removal. The surgical pathology was consistent with the pathological features of SRUS (Supplementary Figure 1). Hematochezia disappeared postoperatively, but his diarrhea remained. Chronic diarrhea causes his anxiety because his symptoms worsen as his mood changed.

History of past illness

The patients were healthy before the SRUS incidence.

Personal and family history

The patient has two sons and one daughter. Notably, one of her sons was diagnosed with SRUS before her diagnosis and underwent partial rectal resection. The other son was healthy. Additionally, she and her son with SRUS like to eat mixed and coarse grains, and they have high-fiber eating habits and a sedentary lifestyle. Moreover, they are accustomed to squatting for a long time to defecate. Furthermore, they were healthy before the SRUS incidence, but are prone to anxious behaviors in life.

Physical examination

A physical examination upon admission revealed no obvious abnormality in both patients.

Laboratory examinations

Laboratory tests of the female patient revealed high triglyceride (2.11 mmol/L), while others were all within normal ranges. Further, Epstein-Barr virus, and cytomegalovirus were negative. Blood routine, coagulation function and autoimmune tests were within normal ranges. Additionally, laboratory tests of the male patient upon admission revealed no obvious abnormality.

Imaging examinations

Her total digestive tract endoscopy results revealed a rectal solitary ulcer (Figure 1A), the indicarmine dyeing demonstrated a clear boundary (Figure 1B), and pathological results indicated the fibrous tissue hyperplasia in the lamina

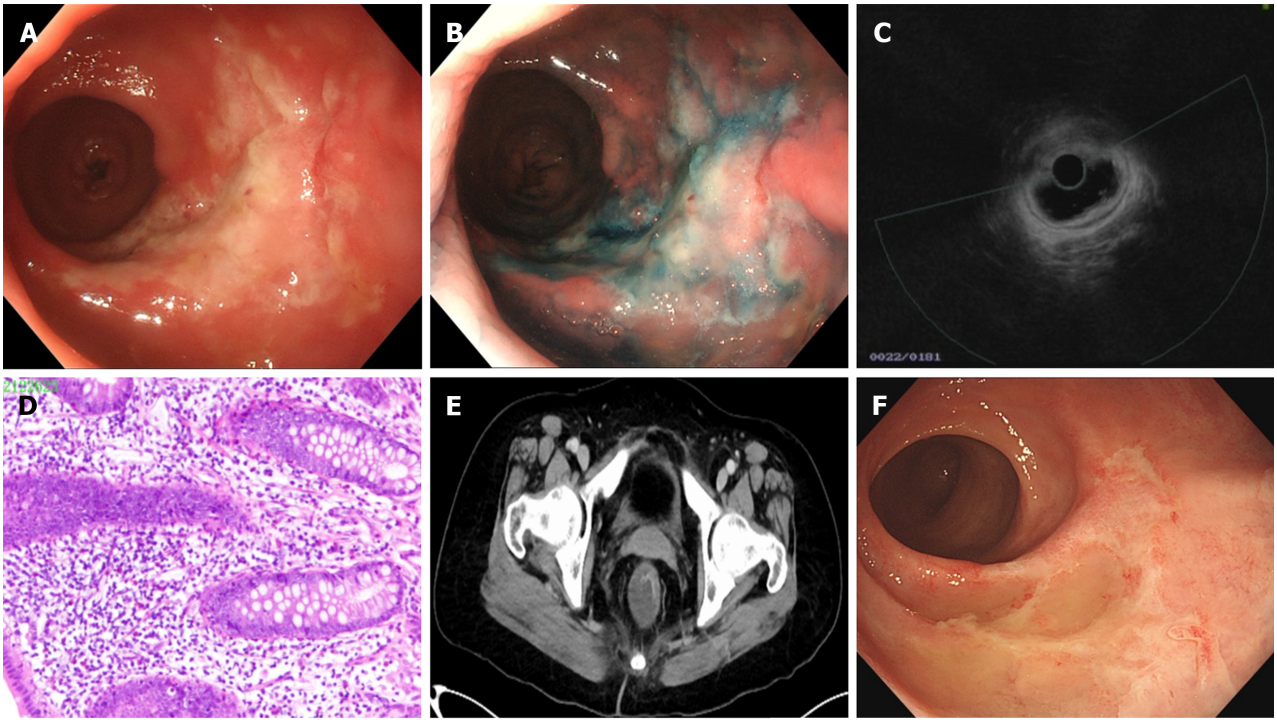

DOI: 10.3748/wjg.v29.i31.4809 **Copyright** ©The Author(s) 2023.

Figure 1 Clinical features of the female patient with solitary rectal ulcer syndrome. A: Colonoscopy image upon her admission; B: Chromoendoscopy result upon her admission using the Indicarmine dyeing; C: Ultrasonic endoscopy was used for solitary rectal ulcer observation; D: Pathological results of the solitary rectal ulcer; E: Imaging of the solitary rectal ulcer, using the intestine computed tomography enhancement; F: Colonoscopy image upon her reexamination after therapy.

propria layer as well as glands destruction (Figure 1D). Ultrasonic endoscopy revealed clearly demarcated mucosal layers, missing ulcerative mucosa and submucosa layers, and intact and thickened muscularis propria (Figure 1C). Moreover, the intestinal computed tomography enhancement revealed segmental rectal wall thickening (Figure 1E). The anorectal function test demonstrated a low resting pressure of the anal canal and normal contractile response and anorectal inhibition reflex but with increased anorectal sensitivity. Further, a colonoscopy of the male patient showed that the mucosa of his rectal anastomosis was smooth without any erosion or ulcer (Supplementary Figure 1).

Further diagnostic work-up

Whereas their complicate family history and next-generation sequencing of heritage whole exome sequencing was then conducted with their consent. The results (Figure 2) exhibited a CHEK2 gene (c.1111C>T, p.His371Tyr) missense mutation in the patient and her son with SRUS, but not in the other son and the daughter. The CHEK2 p.H371Y mutation was reported as a kind of pathologic mutation[4]. Then we conduct the immunohistochemical staining (IHC) to analyze the expression and function of CHEK2 (Antibody: CHEK2, CST#3440, 1:1600; p-CHEK2, CST#82263, 1:500; CDC25A, CST#3652, 1:100; p-P53, CST#9287, 1:100), which revealed a normal CHEK2 protein level but an impaired downstream gene protein level. As shown in Figure 2, CHEK2 protein levels and autophosphorylation CHEK2 protein levels showed no significant difference among the healthy control, inflammatory bowel diseases, rectal cancer and SRUS groups (including familial and sporadic cases). In contrast, the downstream gene of CHEK2, such as CDC25A and p-P53 (Ser 20), exhibit differential expression among these groups. CDC25A and p-p53 protein expression levels were the highest and the lowest in the SRUS group, while the differences between the SRUS and rectal cancer groups do not reach significance.

The SRUS groups contain familial patients in our case and non-familial cases (sporadic cases). The IHC results revealed that the CHEK2 mutation did not affect the expression of CHEK2 protein whether in familial SRUS cases or sporadic SRUS cases, but it would affect CHEK2 functions to different degrees. CDC25A expression level variations are more significant in familial SRUS cases, while p-p53 expression level changes are more pronounced in sporadic SRUS cases.

FINAL DIAGNOSIS

Both patients with a mother-son relationship were diagnosed with SRUS based on the above-mentioned results.

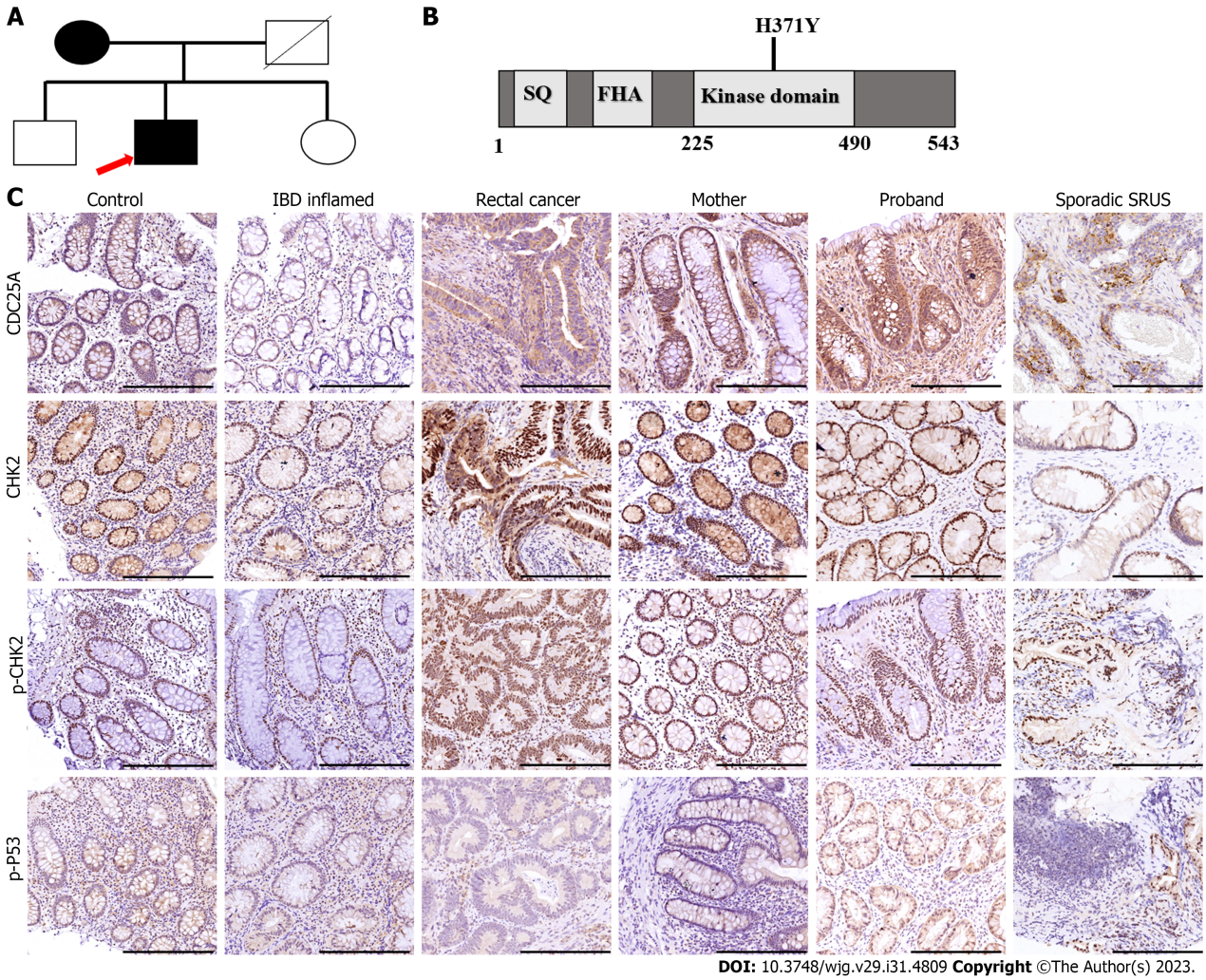

DOI: 10.3748/wjg.v29.i31.4809

Figure 2 Genetic background of the patients with solitary rectal ulcer syndrome patients in a mother-son relationship. A: Family tree of the familial patients with solitary rectal ulcer syndrome. Squares indicate male family members; circles indicate female family members; black indicate affected patients; white indicate healthy family members; slashes indicate deceased family members; arrow indicate the first diagnosed patient of the family; B: Schematic diagram of the CHEK2 protein; C: The differential expressions of CHEK2 and the downstream genes among the healthy control, and patients with inflammatory bowel diseases, rectal cancer, and solitary rectal ulcer syndrome, using the immunohistochemical staining; scale bars, 100 μm. IBD: Inflammatory bowel diseases; SRUS: Solitary rectal ulcer syndrome.

TREATMENT

SRUS treatment should be comprehensive and aimed at restoring the patient's normal bowel pattern, including behavior modification, medication, biofeedback, and surgery. Initially, we guided patient's lifestyles and eating habits and advised them to change their sedentary habits and appropriately reduce the amount of dietary fiber in their food. Simultaneously, we guided them to develop good defecation habits, avoid forceful defecation, set defecation time and body position, and artificially limit defecation frequency. Then, we provide psychological care to patients and encourage them to appropriately participate in social activities to vent their bad emotions. Concurrently, biofeedback, which can limit the change of toilet frequency in patients with frequent bowel movements, was recommended as an effective treatment. Biofeedback training can help resolve symptoms, especially in patients who remain symptomatic postoperatively. Finally, we advise patients to use thalidomide and mesalazine for rapid improvement of inflammation, considering the long medical history of the patient, especially frequent diarrhea in the male patients. Mesalazine is a commonly used drug for SRUS and thalidomide is used for anti-inflammation and its side effects of constipation and improved sleeping happen to help patients relieve diarrhea and help them sleep.

OUTCOME AND FOLLOW-UP

Changes in eating and living habits need to be maintained for a long time. Patients are advised to undergo re-examination 3 mo after drug treatment and biofeedback adjuvant therapy. A significant improvement can be maintained for a long time under the condition of monitoring drug side effects. Additionally, the medication regimen was adjusted

following the patient's symptoms during the follow-up. Patients' symptoms were significantly improved under the comprehensive treatment. The reexamination results after 3 mo indicated a significantly relieved mucosa (Figure 1F). Patients remain under regular follow-up and treatment annually.

DISCUSSION

Previous studies have reported the relevance of rectal mucosal prolapse, ischemia, or injury to SRUS pathogens. These main SRUS features include the following clinical manifestations: defecation difficulty with mucous blood stools and lower abdominal pain, normal general physical examination condition, colonoscopy revealing an isolated rectal ulcer, ultrasound colonoscopy showing proliferative mucosal lesions, pathological results demonstrating mucosal myometrium hyperplasia and fibrosis, dynamic examination indicating abnormal rectal and pelvic floor dynamics, normal blood and inflammatory markers, and negative tumor markers[5].

SRUS has no specific clinical manifestation, thus it is frequently misdiagnosed because its clinical diagnosis mainly depends on endoscopy and histopathology. Current SRUS treatment includes medical, surgical treatment, and biofeedback therapy. Drug therapy aims to inhibit inflammatory response and proliferation. Literature reports revealed a similar treatment plan to ulcerative colitis (UC), which can be used orally with mesalazine and locally with rectal administration. This disease has a long treatment period, causing a non-exact therapeutic effect, although biofeedback therapy aims to harmonize and improve pelvic floor muscle function. However, biofeedback therapy may be effective for patients with pelvic floor dysfunction[6]. Surgical treatment is an alternative option, but it is only effective for some patients and has a risk of recurrence postoperatively. Hence, surgical treatment should not be the first therapeutic choice.

To the best of our knowledge, this is the first case of two patients with SRUS in a mother-son relationship. Thus, this is the first study to indicate a possible genetic background for SRUS. The mother in our cases had a very late onset although SRUS was rarely reported in patients over 60 years old. Meanwhile, the symptoms of both patients have commonalities and differences. Her ulcer and symptom significantly improved after medication, while her young son's symptoms did not improve much even with surgery, although a follow-up colonoscopy revealed no further rectal mucosa damage and anastomosis. Concurrently, long-term diarrhea caused psychologically abnormalities, specifically anxiety, in the young male thereby aggravating diarrhea symptoms. Therefore, surgery may be not available for all patients. Most importantly, the psychological symptoms of the disease should also be considered an important treatment scheme aspect.

Genetic data on SRUS is limited. Genes, heritage data, and features need to be explored for a better understanding of the SRUS pathogen and mechanism. Our cases demonstrated that CHEK2 p.H371Y mutation may be relevant to SRUS development and prognosis. CHEK2 is a cell cycle checkpoint regulator, and it plays an essential role in DNA damage repair. Phosphorylation of p53/TP53 at "Ser-20" by CHEK2 is required for the accumulation of active TP53. When activated, the encoded CHEK2 is known to inhibit CDC25A through phosphorylation of CDC25A and cause its degradation[7]. The CHEK2 p.H371Y mutation was reported as a pathogenic mutation causing decreased kinase activity because p.H371Y is located within the activation region of the CHEK2 protein kinase domain. Here, we performed a series of clinical specimens, which revealed no changes in the CHEK2 expression level while the downstream gene expression was significantly modified, exhibiting an impaired CHEK2 protein function. Both familial and sporadic SRUS cases showed weakened function in CHEK2 protein, and familial SRUS cases are mainly characterized by changes in CDC25A of CHEK2 downstream, while sporadic SRUS cases are mainly characterized by variations in p-p53 of CHEK2 downstream. We speculate similarities and differences in the pathogenesis and prognosis between familial SRUS and non-familial SRUS.

Previous studies have revealed that CHEK2 is associated with inflammation and functions through the kinase mechanism to down-regulate the nuclear factor kappa-light-chain-enhancer of activated B cells (NF-κB) pathway in macrophages to alleviate *Staphylococcus aureus*-induced pneumonia in mice. Additionally, phospho-CHEK2 was associated with high macrophage infiltration in UC[8]. Moreover, SRUS is a manifestation of inflammation and CHEK2 mutation may contribute to the development of SRUS *via* effects on inflammatory pathways, such as the NF-κB pathway [9]. Furthermore, the CHEK2 gene is associated with rectal cancer and inflammatory bowel diseases (IBD). SRUS is closely correlated with rectal cancer and IBD, thus it is difficult to differentiate the diagnosis between SRUS from IBD, especially through UC[10]. Rectal cancer is the most important aspect of SRUS prognostic follow-up, but whether the CHEK2 gene is a pathological gene causing SRUS or a gene for assessing the SRUS prognosis or a potential cause of rectal cancer remains uncertain, as well as the exact role of CHEK2 p.H371Y mutation in familial SRUS.

Limitations related to a small-cohort study and the patient heterogeneity exist. The following possible drawbacks may occur in our study. Firstly, this is a single case report and a retrospective study, and the role of CHEK2 mutation in SRUS pathogenesis needs further investigation. Secondly, this study did not involve the detailed mechanism of CHEK2 mutation causing SRUS. Therefore, subsequent verification of large samples and more detailed experimental verification should be prepared.

CONCLUSION

In summary, this is the first study to report two patients with SRUS in a mother-son relationship with an inherited CHEK2 p.H371Y mutation, which provides insights that SRUS may serve as a genetic susceptibility disease, and CHEK2 p.H371Y mutation may play a crucial role in the development and prognosis of SRUS.

ACKNOWLEDGEMENTS

The authors thank Wei Zhang, BS, from the Department of Pathology in The Third Affiliated Hospital of Guangzhou Medical University for the histology slides and for providing helpful advice.

FOOTNOTES

Author contributions: He CC wrote the manuscript and designed the study; Wang SP performed the experiments; Li ZJ and Li N helped to collect the data; Zhou PR and Li MS supervised the study; All authors have read and approved the final manuscript.

Supported by This work was supported by the Guangdong Basic and Applied Basic Research Fund, No. 2022A1515111193; and the Guangzhou Science and technology plan project, No. 2023A04J0581.

Informed consent statement: Collection and usage of clinical specimens were approved by The Third Affiliated Hospital of Guangzhou Medical University's Ethical Committee Board (Approval number: EN-2022010). All patients were informed of sample collection and usage.

Conflict-of-interest statement: All the authors declare that they have no competing financial or other interests to disclose.

CARE Checklist (2016) statement: The authors have read the CARE Checklist (2016), and the manuscript was prepared and revised according to the CARE Checklist (2016).

Country/Territory of origin: China

ORCID number: Cheng-Cheng He 0000-0001-8176-8588; Shan-Ping Wang 0000-0003-1313-369X; Pei-Rong Zhou 0000-0002-6799-6792; Zhi-Jun Li 0009-0000-8528-6498; Na Li 0009-0003-7703-8285; Ming-Song Li 0000-0003-2115-5928.

S-Editor: Liu JH
L-Editor: A
P-Editor: Cai YX

REFERENCES

1 **Rutter KR**. Solitary rectal ulcer syndrome. *Proc Royal Soc Med* 1975; **68**: 22-26 [PMID: 1863712 DOI: 10.1177/003591577506800110]
2 **Gouriou C**, Siproudhis L, Chambaz M, Ropert A, Wallenhorst T, Merlini-l'Héritier A, Carlo A, Bouguen G, Brochard C. Solitary rectal ulcer syndrome in 102 patients: Do different phenotypes make sense? *Dig Liver Dis* 2021; **53**: 190-195 [PMID: 33199231 DOI: 10.1016/j.dld.2020.10.041]
3 **Felt-Bersma RJF**. Solitary rectal ulcer syndrome. *Curr Opin Gastroenterol* 2021; **37**: 59-65 [PMID: 33060396 DOI: 10.1097/MOG.0000000000000689]
4 **Bartek J**, Falck J, Lukas J. CHK2 kinase--a busy messenger. *Nat Rev Mol Cell Biol* 2001; **2**: 877-886 [PMID: 11733767 DOI: 10.1038/35103059]
5 **Abusharifah O**, Bokhary RY, Mosli MH, Saadah OI. Solitary rectal ulcer syndrome in children and adolescents: a descriptive clinicopathologic study. *Int J Clin Exp Pathol* 2021; **14**: 399-407 [PMID: 33936361]
6 **Forootan M**, Shekarchizadeh M, Farmanara H, Esfahani ARS, Esfahani MS. Biofeedback efficacy to improve clinical symptoms and endoscopic signs of solitary rectal ulcer syndrome. *Eur J Transl Myol* 2018; **28**: 7327 [PMID: 29686820 DOI: 10.4081/ejtm.2018.7327]
7 **Xu X**, Tsvetkov LM, Stern DF. Chk2 activation and phosphorylation-dependent oligomerization. *Mol Cell Biol* 2002; **22**: 4419-4432 [PMID: 12024051 DOI: 10.1128/MCB.22.12.4419-4432.2002]
8 **Xie F**, Chen R, Zhao J, Xu C, Zan C, Yue B, Tian W, Yi W. Cell cycle kinase CHEK2 in macrophages alleviates the inflammatory response to Staphylococcus aureus-induced pneumonia. *Exp Lung Res* 2022; **48**: 53-60 [PMID: 35075953 DOI: 10.1080/01902148.2022.2029625]
9 **Sohn JJ**, Schetter AJ, Yfantis HG, Ridnour LA, Horikawa I, Khan MA, Robles AI, Hussain SP, Goto A, Bowman ED, Hofseth LJ, Bartkova J, Bartek J, Wogan GN, Wink DA, Harris CC. Macrophages, nitric oxide and microRNAs are associated with DNA damage response pathway and senescence in inflammatory bowel disease. *PLoS One* 2012; **7**: e44156 [PMID: 22970173 DOI: 10.1371/journal.pone.0044156]
10 **Abid S**, Khawaja A, Bhimani SA, Ahmad Z, Hamid S, Jafri W. The clinical, endoscopic and histological spectrum of the solitary rectal ulcer syndrome: a single-center experience of 116 cases. *BMC Gastroenterol* 2012; **12**: 72 [PMID: 22697798 DOI: 10.1186/1471-230X-12-72]

Published by **Baishideng Publishing Group Inc**
7041 Koll Center Parkway, Suite 160, Pleasanton, CA 94566, USA
Telephone: +1-925-3991568
E-mail: bpgoffice@wjgnet.com
Help Desk: https://www.f6publishing.com/helpdesk
https://www.wjgnet.com